UDK 66:54(05) CODEN HMIDA 8 ISSN 0367–598 X

1 Hemijska industrija

Vol. 68

Časopis Saveza hemijskih inženjera

Chemical Industry

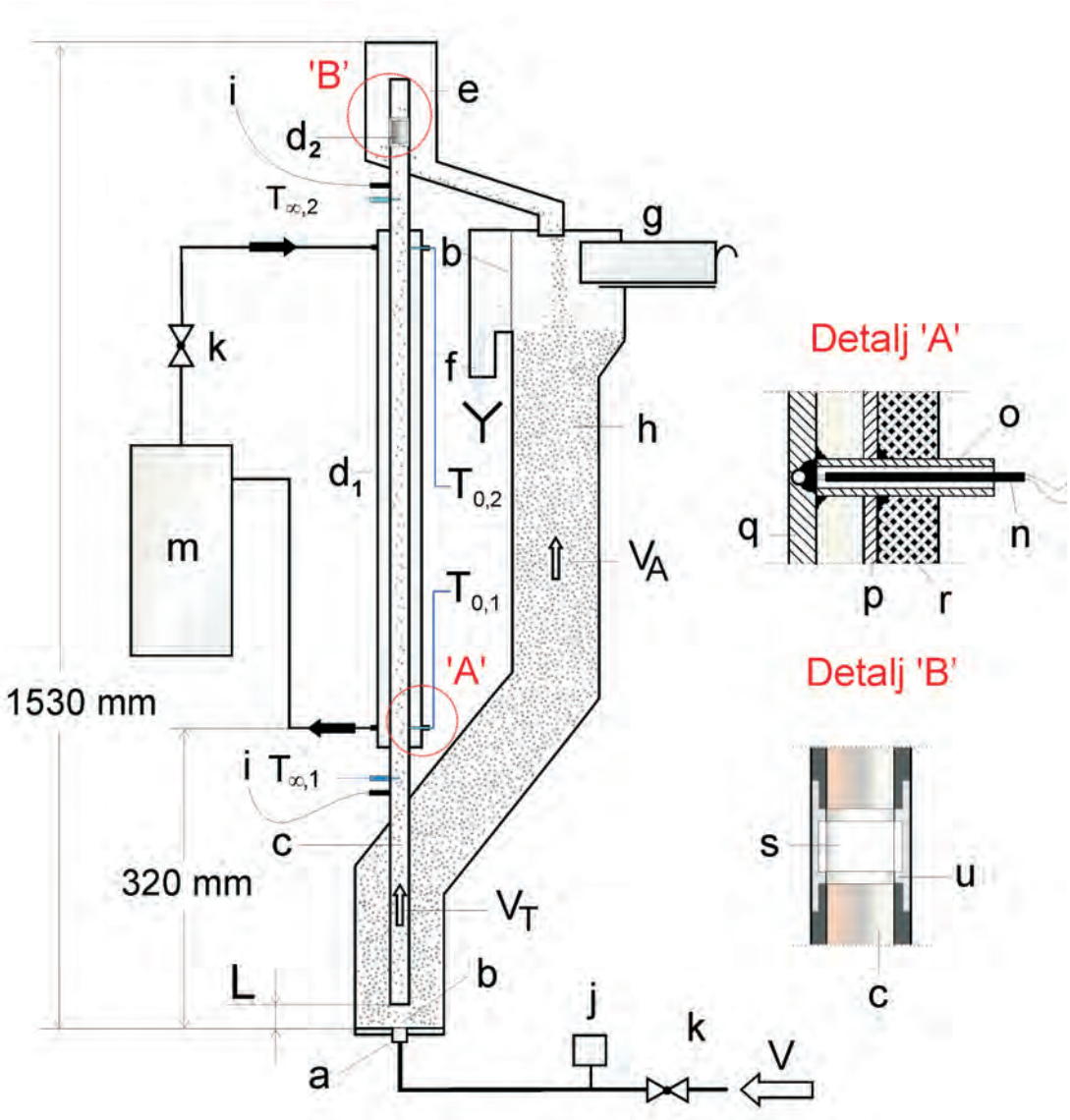

GENERALNI POKROVITELJ

Hemofarm

HEMOFARM KONCERN

VRŠAC, Beogradski put bb, tel. 013/821-345, 821-027, 821-129
BEOGRAD, Prote Mateje 70, tel. 011/344-26-63, faks: 344-17-87
E-pošta: info@hemofarm.com

IZDAVANJE ČASOPISA POMOGLA JE:

INŽENJERSKA KOMORA SRBIJE
Bulevar vojvode Mišića 37
11000 Beograd

SUIZDAVAČI

Tehnološko-metalurški fakultet
Univerziteta u Beogradu, Beograd

Prirodno-matematički fakultet Univerziteta
u Novom Sadu, Novi Sad

Hemijski fakutet
Univerziteta u Beogradu
Beograd

ITNMS
Institut za tehnologiju nuklearnih i drugih
mineralnih sirovina, Beograd

HIP PETROHEMIJA
HIP Petrohemija a.d. Pančevo

Tehnološki fakultet Univerziteta
u Novom Sadu, Novi Sad

NU Institut za hemiju,
tehnologiju i metalurgiju
Univerziteta u Beogradu,
Beograd

nevena
„Nevena Color“ d.o.o.
Leskovac

Tehnološki fakultet Univerziteta
u Nišu, Leskovac

dcp-hemigal
DCP Hemigal, Leskovac

SHI Beograd Srbija

Chemical Industry
Химическая промышленность

Hemijska industrija

Časopis Saveza hemijskih inženjera Srbije
Journal of the Association of Chemical Engineers of Serbia
Журнал Союза химических инженеров Сербии

VOL. 68 **Beograd, januar–februar 2014** **Broj 1**

Izdavač
Savez hemijskih inženjera Srbije
Beograd, Kneza Miloša 9/I

Glavni urednik
Branko Bugarski

Zamenica glavnog i odgovornog urednika
Nevenka Bošković-Vragolović

Urednici
Katarina Jeremić, Ivana Banković-Ilić, Maja Obradović, Dušan Mijin

Članovi uredništva
Milorad Cakić, Željko Čupić, Željko Grbavčić, Katarina Jeremić, Miodrag Lazić, Slobodan Petrović, Milovan Purenović, Aleksandar Spasić, Dragoslav Stoiljković, Radmila Šećerov-Sokolović, Slobodan Šerbanović, Nikola Nikačević, Svetomir Milojević

Članovi uredništva iz inostranstva
Dragomir Bukur (SAD), Jiri Hanika (Češka Republika), Valerij Meshalkin (Rusija), Ljubiša Radović (SAD), Constantinos Vayenas (Grčka)

Likovno-grafičko rešenje naslovne strane
Milan Jovanović

Redakcija
11000 Beograd, Kneza Miloša 9/I
Tel/fax: 011/3240-018
E-pošta: shi@yubc.net
www.ache.org.rs

Izlazi dvomesečno, rukopisi se ne vraćaju

Za izdavača
Tatijana Dudukoviċ

Sekretar redakcije
Slavica Desnica

Izdavanje časopisa pomaže
Republika Srbija, Ministarstvo prosvete, nauke i tehnološkog razvoja

Uplata pretplate i oglasnog prostora vrši se na tekući račun Saveza hemijskih inženjera Srbije, Beograd, broj 205-2172-71, Komercijalna banka a.d., Beograd

Kompjuterska priprema
Vladimir Panić

Štampa
Razvojno-istraživački centar grafičkog inženjerstva, Tehnološko-metalurški fakultet, Univerzitet u Beogradu, Karnegijeva 4, 11000 Beograd

Indeksiranje
Radovi koji se publikuju u časopisu *Hemijska Industrija* ideksiraju se preko *Thompson Reuters Scietific®* servisa *Science Citation Index - Expanded™* i *Journal Citation Report* (*JCR*), kao i domaćeg *SCIndeks* servisa Centra za evaluaciju u obrazovanju i nauci

SADRŽAJ

SADRŽAJ nastavak

CONTENTS

CONTENTS Continued

Microwave-assisted synthesis of 2-pyridone and 2-pyridone-based compounds

Dušan Ž. Mijin, Jelena M. Marković, Danijela V. Brković, Aleksandar D. Marinković

Faculty of Technology and Metallurgy, University of Belgrade, Belgrade, Serbia

Abstract

2-Pyridones are important heterocyclic compounds that are widely used in medical chemistry, and their various derivatives have significant biological and medical applications. In this paper, the synthesis of 2-pyridones as well as 2-pyridone-based compounds, such as 2-quinolones, using microwave assisted organic chemistry is reviewed. The review is divided in three parts. In the first part, microwave synthesis of 2-pyridones according to the type of condensation is discussed. In the second part, microwave assisted synthesis of 2-quionolones is listed. At the end of the review several examples of microwave synthesis of other 2-pyridone based compounds (ring fused *N*-substituted 2-pyridones) are given.

Keywords: heterocyclic compounds, medical chemistry, microwave assisted organic chemistry, 2-quinolone ring fused *N*-substituted 2-pyridones.

Available online at the Journal website: http://www.ache.org.rs/HI/

REVIEW PAPER

UDC 61:54]:547.7/.8:547.824

Hem. Ind. **68** (1) 1–14 (2014)

doi: 10.2298/HEMIND121204021M

Aromatic heterocyclic compounds represent an important group of compounds due to their biological and medical applications. The six-member heterocyclic rings containing nitrogen (*e.g.*, pyridine, pyridone, pyrimidine, piperidine and piperazine) are used in medicine since they possess certain pharmacological properties. Among them, 2-pyridone compounds are particularly significant (Figure 1).

2-Pyridone derivatives are especially interesting because the 2-pyridone structure is present in many compounds of natural origin [1], many of which possess biological activity. Most of these compounds possess antibacterial [2,3], antifungal [4], anti-inflammatory [5], antiviral [6,7], antitumor [8] and antiplatelet [9,10] properties. 2-Pyridone derivatives are used in the manufacturing of paints [11], pigments, additives for fuels and lubricants, acid-base indicators, stabilizers for polymers and coatings [12]. Due to a variety of pharmacological properties, the 2-pyridone structure is important in the pharmaceutical industry [13]. Many medications contain 2-pyridone structure: cardiotonics (milrinone (Figure 1a) and amrinone (Figure 1b) used for the treatment of heart failure [14,15]; and antibiotics (pilicides (Figure 1c) and curlicides) which treat bacterial infections caused by Gram-negative bacteria [16,17]. A derivative of *N*-phenyl-2-pyridone, perampanel (Figure 1d), acts as a non-competitive and selective antagonist of α-amino-3-hydroxy-5-methyl-4-isoxazolepropionic acid receptor, and improves motor symptoms in animal models of Parkinson's disease [18].

Correspondence: D. Mijin, Faculty of Technology and Metallurgy, University of Belgrade, Karnegijeva 4, P.O. Box 3503, 11120 Belgrade, Serbia.

E-mail: kavur@tmf.bg.ac.rs

Paper received: 4 December, 2012

Paper accepted: 25 January, 2013

It should be noted that 4-pyridone, isomer of 2-pyridone, due to mesogenic properties, is used in the synthesis of liquid crystals [19]. It has antioxidant properties and is used in the treatment of hyperglycemia [20]. 4-pyridone also has the capability of complexation and can be used for the preparation of supramolecular structures [21]. Methylated *N*-4-pyridone derivatives are used as intermediates for the synthesis of pharmaceuticals, pesticides, insecticides, fungicides, etc. *N*-Methyl-4-pyridone is used in the production of compounds that are used to produce images [22].

Due to the many applications of the compounds that contain 2-pyridone structure, a number of procedures for their synthesis was developed [23,24]. A general procedure for obtaining substituted 2-pyridones is the Guareschi-Thorpe condensation reaction of 1,3-dicarbonyl compounds with cyanoacetamide [25,26], which was used for the synthesis of large number of pyridones [27–29]. Cyclization of cyanoacetamide with 1,3-dicarbonyl compounds belongs to the 3-2 type of condensation that leads to the formation of pyridone ring. The mechanism of the reaction is complex and involves Knoevenagel reaction, addition of Michael or Perkin reaction, whereby the degree of enolyzation of dioxo compounds determines the participation of Michael addition [30,31]. Also, this type of reaction is used to obtain arylazo pyridone dyes [32–37]. Unlike conventional conditions (high temperature, polar organic solvents), the newer approach, enzymatically catalyzed synthesis of 2-pyridones, carried under mild reaction conditions, is characterized by high regio- and stereo-selectivity, high purity and final yield of the obtained products [38,39].

The conventional way of performing organic synthesis involves heating by external heat sources (*e.g.*, oil bath). In this way, heat is transferred by conduction,

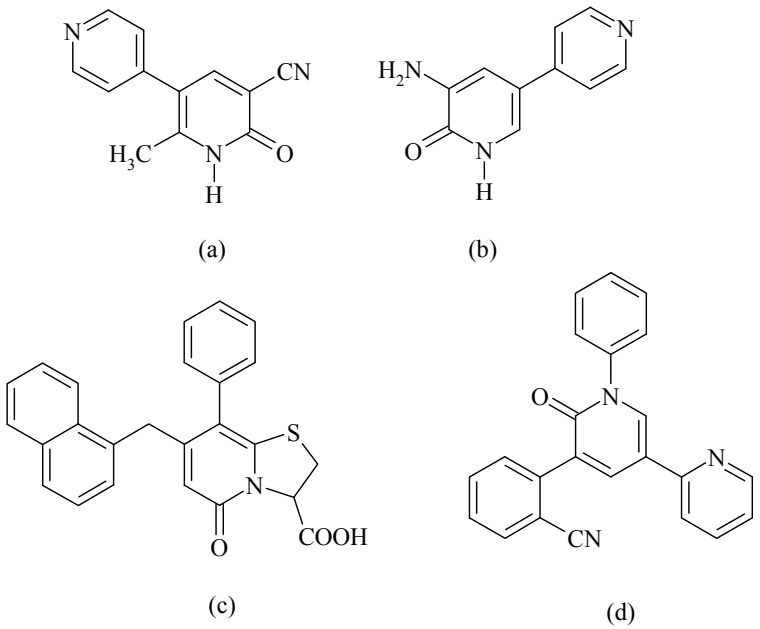

Figure 1. 2-Pyridone compounds which possess physiological activity: a) milrinone, b) amrinone, c) ring fused pyridone with pilicide activity and d) perampanel.

which is a slow and inefficient method of energy transfer, because it depends on the thermal conductivity of the materials and the reactor temperature is higher than the temperature of the reaction mixture. On the other hand, microwave irradiation is an efficient way of heating where energy is transmitted directly through interaction with polar molecules present in the reaction mixture [40,41].

Microwave irradiation is not ionizing and does not belong to harmful radiation. Microwaves have a frequency between 0.3 GHz and 300 GHz, corresponding to wavelengths between 1 cm and 1 m [42]. The main advantages of microwave-assisted organic chemistry are the increase of product yields and the reduction of reaction time [43,44]. The short reaction time and the increasing number of microwave assisted reactions lead to the application of this technique in the various fields of industry. For example, the modern pharmaceutical industry requires the creation of a growing number of new molecules, forcing chemists to conduct a number of experiments in a short period of time [45]. Also, the microwave technique is used in the food industry as well as in the pyrolysis of waste materials [46], the preparation of samples for analysis [47], extraction of natural products [48] and hydrolysis of proteins and peptides [49].

Microwave synthesis is among methods that respect the principles of the so-called "green chemistry" which is one more reason for performing this type of synthesis [50].

In this paper, the synthesis of the certain 2-pyridones and 2-pyridone based compounds using microwave irradiation will be discussed. We will point out the advantages of microwave assisted synthesis in comparison to conventional heating. First, we will discuss the microwave synthesis of 2-pyridones. In the second part, microwave assisted synthesis of 2-quionolones will be given. At the end of the review, examples of microwave synthesis of ring fused *N*-substituted 2-pyridones will be discussed.

MICROWAVE SYNTHESIS OF 2-PYRIDONE

The application of microwave techniques in the synthesis of organic compounds has inevitably led to the microwave synthesis of compounds with the 2-pyridone ring. In the beginning, the synthesis was performed using conventional microwave ovens. Due to the problems associated with the use of these ovens in the synthesis (reproducibility, controllability and safety), dedicated microwave reactors were introduced. The basic principles of synthesis of heterocyclic molecules used in conventional synthesis were applied to microwave synthesis [51]. Thus conducted synthetic route yield pyridone ring from fragments containing different numbers of carbon atoms. Different combinations of fragments were used: 4-1, 3-2, 1-3-1, 2-2-1 and 2-1-2. Condensation of type 4-1 means that the condensation involves two acyclic systems one of which has four and the other only one carbon atom. Nitrogen can be a part of one of the fragments, or be introduced as a separate fragment.

A good example of such a combination is given in a paper by Gorobets *et al.* [1], in which different carbonyl building blocks were reacted with *N*,*N*-dimethyl-

formamide dimethyl acetal (DMFDMA) to obtain enaminones in high yields (the reaction is carried out in the absence of solvent and at elevated temperature). The obtained enaminones, without purification, react with different methylene nitriles at 100 °C for 5 min in 2-propanol and in the presence of a catalytic amount of piperidine (base). In this way, the authors were able to isolate 18 different 2-pyridones of 80 possible with yields varying from 27 to 96%, while some products were obtained in pure form after simple filtration. This synthesis is given in Figure 2.

An example of 3-2 type condensation of 3-cyano-2--pyridones is shown in Figure 3 [28]. *N*-substituted 4,6--dimethyl-3-cyano-2-pyridones were obtained from acetylacetone and the corresponding *N*-substituted cyanoacetamide using conventional and microwave synthesis in the presence of piperidine as a catalyst. Conventional synthesis was performed by heating the reaction mixture under reflux (solvent mixture water/ /ethanol). Microwave synthesis was performed using a conventional microwave oven in the absence of solvent. The products were obtained in high yields and in a short reaction time (up to 7 min), while the conventional method of synthesis required up to 4 h with lower yields (Figure 4).

6-Hydroxy-3-cyano-4-methyl-2-pyridone was also synthesized using microwave technique (condensation type 3-2). The first microwave synthesis was reported in 1994 in the German patent [52]. Compared to the conventional synthesis which takes 16.5 h with a yield of 80%, microwave synthesis is carried out for 5 min with a yield of 96%. In this synthesis, product was obtained starting from cyanoacetamide, ethyl cyanoacetate and ethylamine. This pyridone can also be

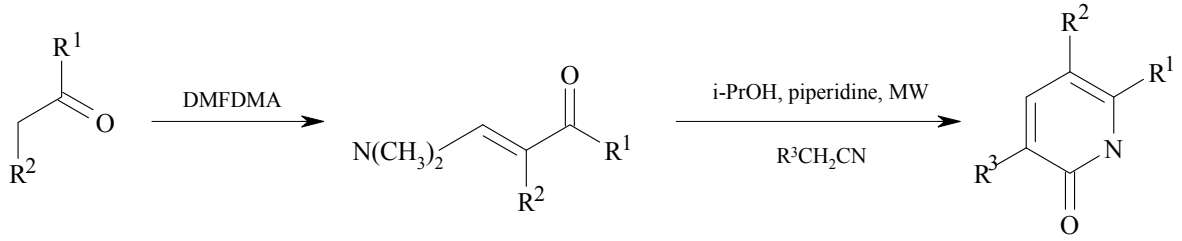

Figure 2. Microwave synthesis of substituted 2-pyridones from enaminones.

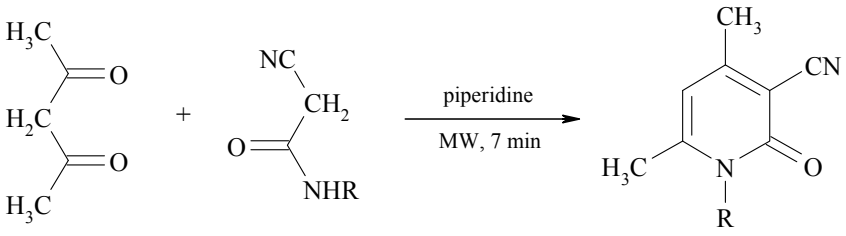

Figure 3. Synthesis of N-substituted 4,6-dimethyl-3-cyano-2-pyridones.

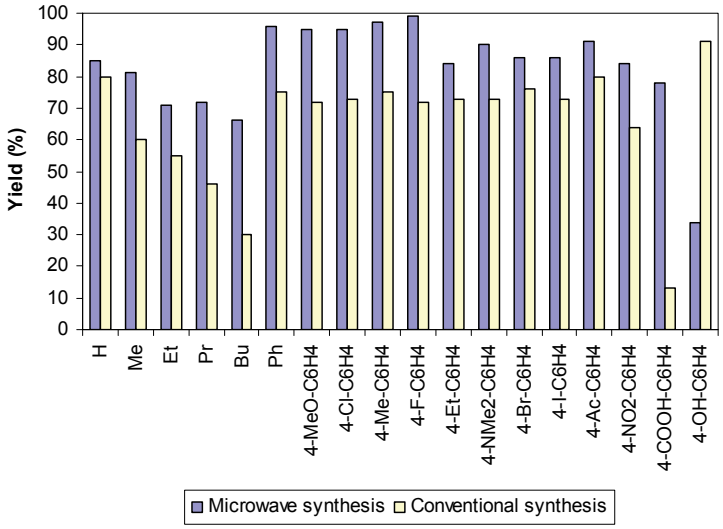

Figure 4. N-Substituted 4,6-dimethyl-3-cyano-2-pyridones yields obtained by microwave and conventional synthesis.

obtained using conventional synthesis with potassium hydroxide as a catalyst [27,53]. Reaction times varied from 1 to 8 h, with yields ranging from 40–60%. Recently, a synthesis of this pyridone was published, using microwave irradiation in a conventional microwave oven, in the absence of solvent starting from ethyl cyanoacetate and cyanoacetamide, using powdered potassium hydroxide as a catalyst (Figure 5). The isolated yield was 60%, after only 4 min of irradiation [54].

Dave *et al*. reported on microwave synthesis of 4,6-diaryl-3-cyano-2-pyridones starting from cyanoacetamide and 1,3-diarylpropen-1-ones in the presence of powdered potassium hydroxide, with phenyl or substituted phenyl groups in positions 4 and 6 [55]. The authors have reported yields that ranged from 74 to 81% with high purity of compounds after only 1–2 min of irradiation (Figure 6).

Microwave synthesis of arylazo pyridone dyes [56] is based on the previously described 3-2 type of condensation. This type of synthesis involves the reaction of phenylazo carbonyl compounds and cyanoacetamide using KOH as base and ethanol as solvent in a dedicated microwave reactor. Synthesis of 5-phenylazo-4,6-dimethyl-3-cyano-2-pyridones and 5-phenylazo-4,6-diphenyl-3-cyano-2-pyridone are shown in Figure 7. The synthesized derivatives of 4,6-dimethyl-3-cyano-2-pyridone (Table 1, entries 1–6) were obtained in nearly quantitative yield, while the derivatives of 4,6-diphenyl-3-cyano-2-pyridones (Table 1, entries 7–9) were obtained in lower yields. Synthesis of 5-phenylazo-4,6-dimethyl-3-cyano-2-pyridone in the conventional manner [35] also takes place in the presence of a base in ethanol, except that this synthesis lasted for 3 h with somewhat lower yields (70–80%).

Similarly, the synthesis of the 5-phenylazo-2-hydroxy-4-methyl-3-cyano-2-pyridones starting from β-phenylazo ketoesters under the same conditions was performed (Figure 7, Table 1, entries 10–13). In addition to these products a derivative of 2-hydroxy-4-phenyl-3-cyano-2-pyridones was also obtained (Table 1, entry 14). In comparison to derivatives of dialkyl 2-pyridone, lower yields were obtained as a result of lower reactivity of β-keto esters compared to 1,3-diketones [56], in which is still higher yield compared to conventional synthesis (30–60%) [32].

Synthesis of substituted 3-cyano-2-pyridones at positions 4 and 6 was also carried out using microwave irradiation (1-2-2 type condensation) [57], and under conventional conditions [58] (Figure 8). By applying microwave irradiation (dedicated microwave reactor) yields of 90–95% over 5–7 min were obtained, while

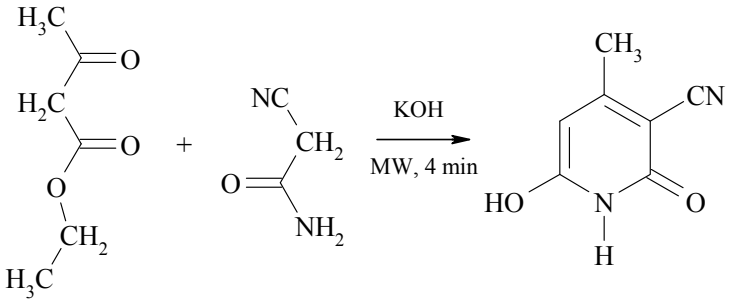

Figure 5. Synthesis of 4-methyl-6-hydroxy-3-cyano-2-pyridones.

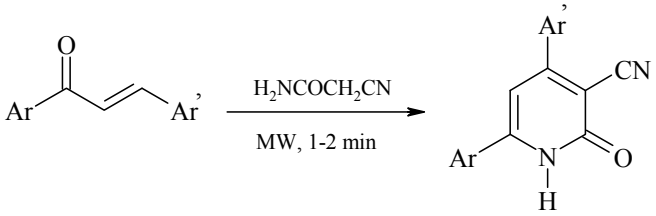

Figure 6. Synthesis of 4,6-diaryl-3-cyano-2-pyridones.

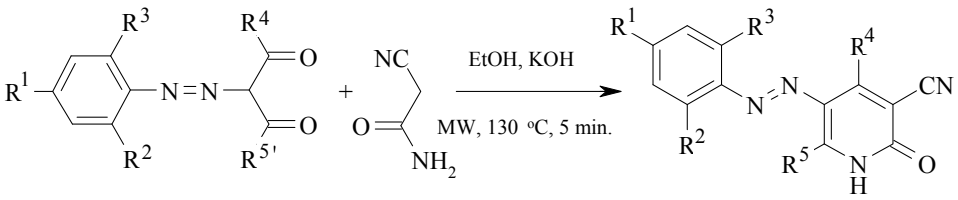

Figure 7. Microwave synthesis of arylazo 4,6-dimethyl- and 4,6-diphenyl-3-cyano-2-pyridone dyes.

Table 1. Synthesized arylazo 4,6-dimethyl- and 4,6-diphenyl-3-cyano-2-pyridone dyes with their yields

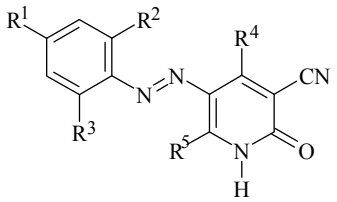

Entry	R^1	R^2	R^3	R^4	R^5	Yield, %
1	H	H	H	Me	Me	99
2	H	H	NO_2	Me	Me	100
3	Br	H	H	Me	Me	92
4	Br	Me	Me	Me	Me	100
5	H	Me	Me	Me	Me	100
6	H	H	I	Me	Me	100
7	H	H	H	Ph	Ph	72
8	Br	Me	Me	Ph	Ph	72
9	H	Me	Me	Ph	Ph	83
10	H	H	H	Me	OH	47
11	Br	H	H	Me	OH	93
12	Br	Me	Me	Me	OH	80
13	H	Me	Me	Me	OH	50
14	H	H	H	Ph	OH	78

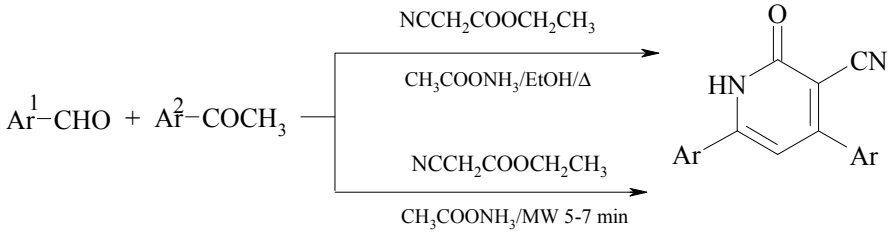

Figure 8. Conventional and microwave synthesis of substituted 3-cyano-2-pyridones.

the conventional method of synthesis lasted for 6 h and gave lower yields (67–85%).

Another example of microwave synthesis of 2-2-1 condensing type of 2-pyridones is shown in Figure 9 [59]. The synthesis of 3,5-dicyano-2-pyridone is carried out in aqueous solution starting from aldehydes and malononitrile in the presence of sodium hydroxide as a base. The advantage of this synthesis is short reaction time, efficiency and use of water instead of organic solvents which have a favorable impact on the environment. The method is applicable not only to aromatic aldehydes with electron-donor and electron-acceptor groups, but also to heterocyclic and aliphatic aldehydes.

Syntheses were performed at 100 °C both in the conventional and the microwave method. The reaction time of microwave synthesis was 2–3 min while conventional synthesis took 2–3 h. On the other hand, reaction yields increased from 25–37% (conventional) to 40–49% (microwave synthesis).

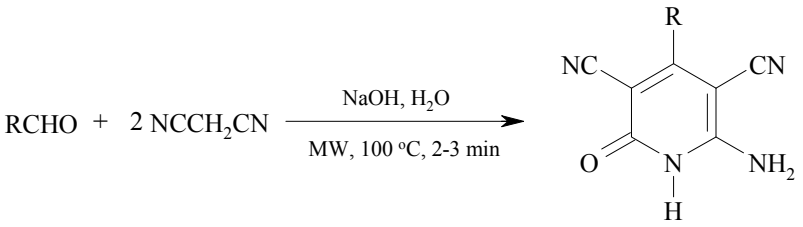

Figure 9. Synthesis of 4-substituted 6-amino-3,5-dicyano-2-pyridones in aqueous media under microwave irradiation.

4-Aryl substituted 5-alkoxycarbonyl-6-methyl-3,4--dihydropyridones were prepared by the reaction of Meldrum's acid, methyl acetoacetate and appropriate benzaldehyde in the presence of ammonium acetate (2-2-1 condensation type, Figure 10) [60–62]. Microwave assisted synthesis, performed in a dedicated microwave reactor, produced pure products in high yields (81–91%), while the conventional synthesis gave yields lower by 17–28%.

Synthesis of 2-pyridone based bifunctional compounds (1,4-dihydropyridines) by the condensation of dialdehyde, Meldrum's acid, acetoacetic acid and ammonium acetate is another example of 2-2-1 type condensation of pyridones (Figure 11) [63]. This synthesis was achieved by heating the reaction mixture in a conventional microwave oven for 8 min using small amounts of glycol as an energy transfer reagent (yield 83%).

MICROWAVE SYNTHESIS OF RING FUSED 2-PYRIDONE DERIVATIVES

Synthesis of 2-quinolones

The most widely used procedure for the synthesis of 2-quinolones is the reaction of aniline with malonic acid esters. However, this reaction is conducted at high temperatures (250–350 °C) that are difficult to achieve by conventional heating methods. The reaction of aniline with malonic acid esters produces two moles of ethanol, which affect the equilibrium between the reactants and the reaction products (Figure 12). There-

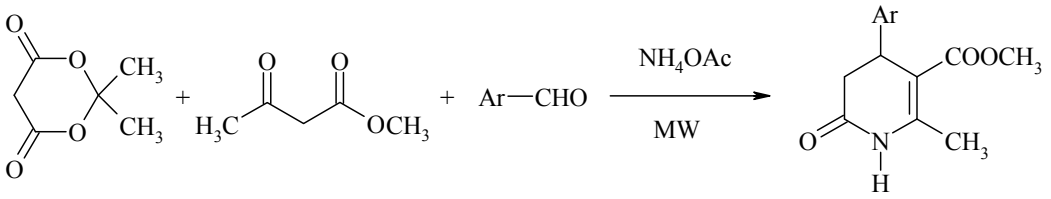

Figure 10. Synthesis of 4-aryl substituted 5-alkoxycarbonyl-6-methyl-3,4-dihydropyridones.

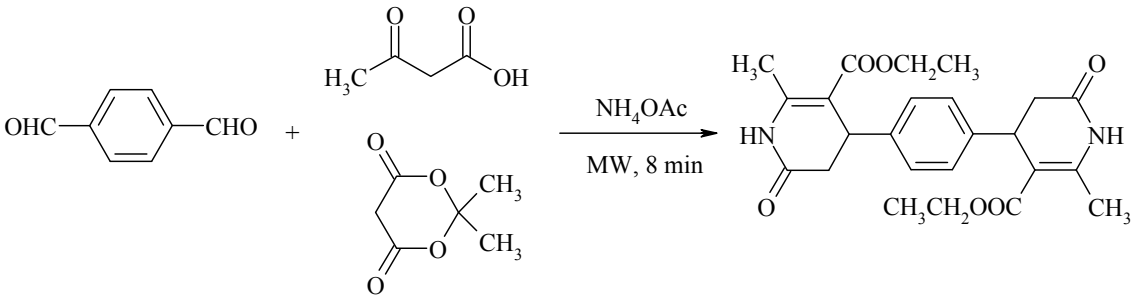

Figure 11. Synthesis of bifuncional 2-pyridone.

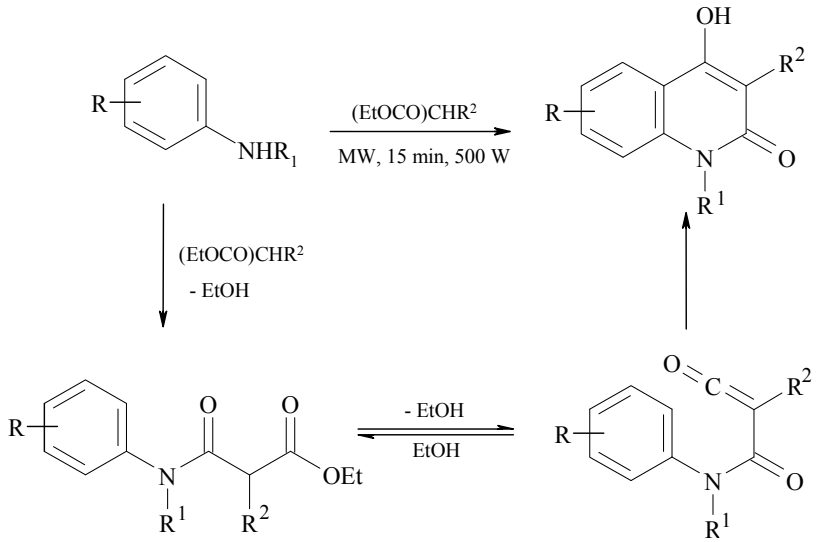

Figure 12. Formation of 3-substituted 4-hydroxy-2-quinolones in the reaction between anilines and substituted malonic esters.

fore, it is essential, if the reaction is carried out in a closed reactor, to maintain the volume and concentration of reactants low, in order to shift the equilibrium towards the products. On the other hand, the reaction can be carried out in an open vessel even on a larger scale without such demands [64]. It was found that the synthesis of 4-hydroxy-2-quinolones proceeds best when an electron-donor group (R) is substituent in aniline. The nucleophilicity of the nitrogen is increased and therefore both reactions, the condensation with the malonic ester and the ring closing acylation proceed faster (Figure 5). The presence of R^2-aryl group provides additional conjugation and stability of the product, which is reflected in the high product yield (up to 94%) [64].

This method cannot be applied in cases where an electron-acceptor group (*e.g.*, trifluoromethyl group) is substituent in aniline. In this case, malondianilide was treated with Eaton's reagent (7.7% phosphorus pentoxide in methanesulfonic acid) and resulted in high yield products (80–90%, Figure 13) [65,66].

In addition to Eaton's reagent, *p*-toluenesulfonic acid can be used in the microwave synthesis of 2-quinolones. 2-Quinolones can be obtained from substituted aniline and diethyl malonate with a yield of 89––96% in only 6 min [67]. Instead of *p*-toluenesulfonic acid, silica gel or aluminum oxide can be used, but yields were lower with longer reaction times. Also, malonic acid can be used. Microwave synthesis of 2-quinolones can be achieved in a conventional microwave oven by irradiation of a mixture of aniline and malonic acid in the presence of dimethylformamide for 3–5 min (yield 85–94%) [68].

Instead of diethyl malonate/malonic acid, acetoacetic ester can be used. In this manner, carbostyril analogues can be synthesized (Figure 14). The synthesis is favored by electron-donor groups in the aniline ring and electron-acceptor groups in electrophilic compounds [69]. Microwave synthesis reduces the reaction time from 18–58 h to just 80 min giving products of high purity and in higher yield (58%).

In a similar way, 2-quinolones can be obtained from *o*-aminoarylketones and acetoacetic ester using microwave synthesis (4–6 min at 160 °C in the presence of a catalyst ($CeCl_3 \cdot 7H_2O$) – yields 85–95%) (Figure 15) [70]. In comparison to conventional synthesis, microwave reactor synthesis shows that the reaction is 5 or more times faster using microwave technique.

2-Quinolones can also be obtained by intramolecular Heck cyclizations of heteroarylamide [71]. Conventionally Heck cyclizations are achieved with *N*,*N*-dimethylacetamide (DMA) as a solvent, potassium acetate and $Pd(PPh_3)_4$ as a catalyst at 120 °C for 24 h with yields from 56 to 89%. Microwave irradiation often has a positive effect on the metal-catalyzed reactions [72–75] and in this case 2-quinolones were

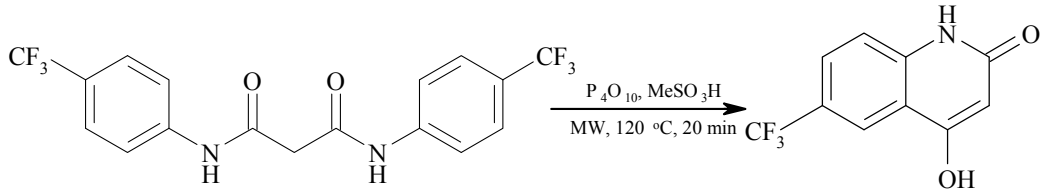

Figure 13. Synthesis of 2-quinolones from 1,3-dicarbonyl compounds.

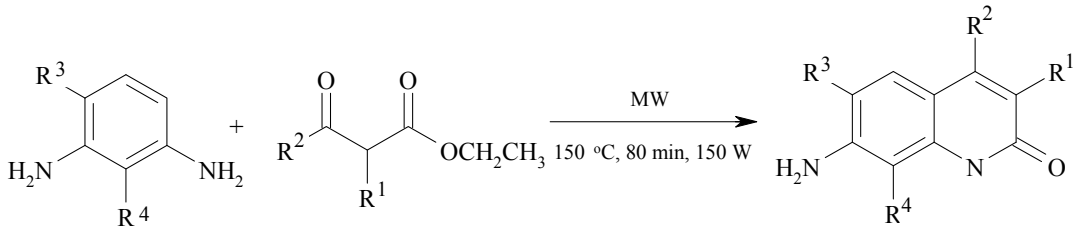

Figure 14. Synthesis of carbostyril analogues of 2-quinolones from 1,3-dicarbonyl compounds.

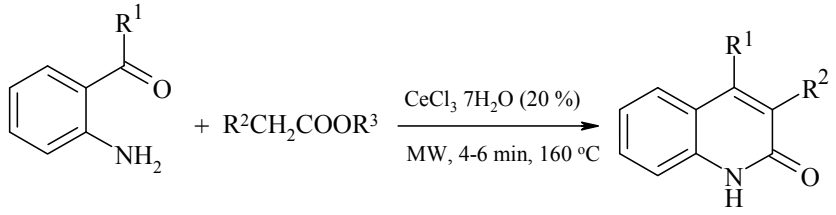

Figure 15. Synthesis of 2-quinolones by the $CeCl_3$-catalysed reaction.

obtained in 90–96% yields during 12-30 min in DMA (Figure 16).

Stadler *et al*. [76] applied successfully the microwave technique in the synthesis of 4-hydroxy-2-quinolone (Figure 17). The reaction was performed in 1,2--dichlorobenzene, in which the reactants are soluble, but the product of the reaction is not. The product, of high purity, can be obtained from the reaction mixture by simple filtration. The reaction can be also performed by applying solvent-free microwave irradiation conditions.

2-Quinolone derivative, needed for the synthesis of cryptotackieine and cryptosanguinolentine, compounds which display various biological properties, can also be obtained from *o*-vinylsubstituted isocyanate by microwave heating [77]. 3-Aryl substituted 2-quinolones were synthesized in yields of 80% by heating the reaction mixture in a dedicated microwave reactor at 150 °C for 12 min in nitrobenzene as a solvent (Figure 18).

It should be noted that 4-quinolones can be obtained from substituted aniline and diethyl (etoxymethylene) malonate in a conventional microwave oven. Although the synthesized compounds (ethyl esters of 4-oxo-1,4-dihydroquiniline-3-carboxylic acid) were obtained in a yield of about 50%, the reaction times were from 0.4 to 5 min [78].

Synthesis of other ring fused 2-pyridone derivatives

In the last part of this review, the synthesis of condensed derivatives of 2-pyridone (ring fused *N*-sub-

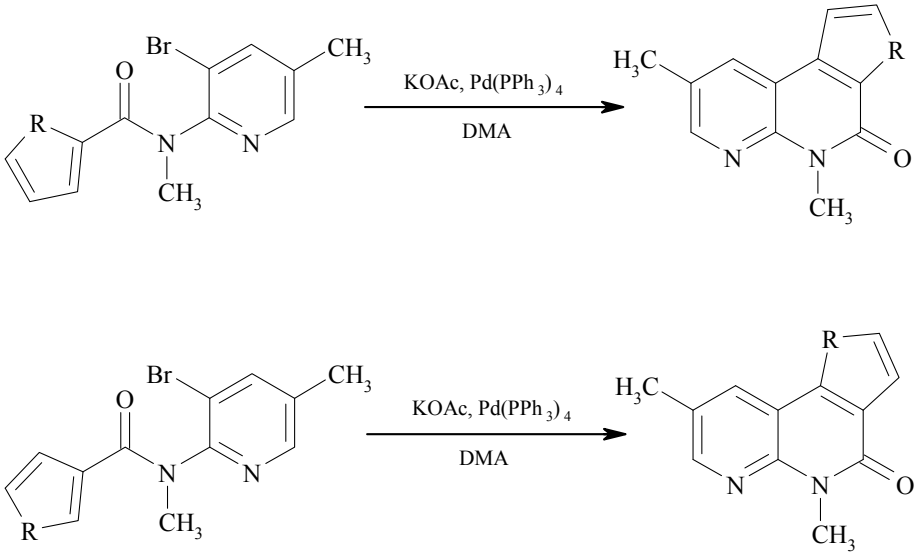

Figure 16. Synthesis of heterocyclic derivatives of 2-quinolones using intramolecular Heck coupling.

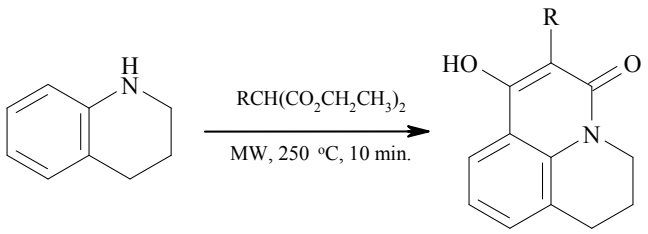

Figure 17. Microwave synthesis of 2-quinolones.

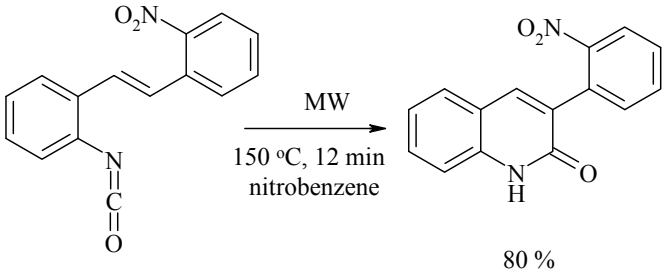

Figure 18. Microwave synthesis of 2-quinolones from o-vinyl substituted isocyanates.

stituted 2-pyridones) will be presented. The optically active bicyclo-2-pyridone was obtained by the reaction of acyl-ketenes with substituted Δ^2-thiazolines by microwave heating at 140 °C for 2 min with the yield of 73 to 95% (Figure 19). The thiazolines were prepared from iminoethers and cysteine while the acyl-ketenes were generated *in situ* from acyl Meldrum's acid derivatives [79]. This type of synthesis leads to the preparation of pilicide and curlicide compounds, based on the same peptidomimetic scaffold, that target bacterial virulence factors in Gram-negative bacteria [16,17].

It was demonstrated that the sulfur in the pilicide scaffold could be exchanged for oxygen with an almost retained pilicide activity. Dihydrooxazolo and dihydrothiazolo ring fused 2-pyridones were prepared using microwave assisted organic synthesis in good yields and high enantiomeric purity. Trifluoro acetic acid (TFA), tosic acid and pyridinium *p*-toluenesulfonate were used to optimize reaction conditions. Reactions were performed in 1,2-dichloroethane (DCE) at 120 °C for 140 s [80].

The above mentioned reactions were carried out in the presence of solvents [81] and in the solid state [82] using the conventional synthesis. However, the use of microwave irradiation has a number of advantages over both conventional methods: the reaction is carried out in two steps by reducing the reaction time from 2 days (conventional method) to 8±2 min with yields up to 79%. Microwave synthesis requires less acid which results in milder reaction conditions. Instead of Δ^2-thiazoline, imines can be used, thus making possible synthesis of multiple ring fused 2-pyridones (Figure 20) [83]. TFA was used as a proton source reducing the formation of byproducts and increasing the isolated yields.

Condensed 2-pyridone derivatives can also be obtained from aminopropenoate obtained from dimethylformamide diethyl acetal (DMFDEA) and CH-acidic carbonyl compounds. Microwave technology is used in both synthetic steps. Disubstituted quinalozines were obtained by reaction of intermediates (aminopropenoate) with bident C,N nucleophiles (Figure 21) in yields of up to 92% [84]. Synthesis can be also performed in the solid phase.

In addition, condensed 2-pyridone can be obtained by the reaction of 1,3-dicarbonyl compounds and substituted benzaldehydes or phenylendialdehide in the presence of ammonium acetate using microwave irradiation in the absence of a solvent, as previously described for the synthesis of 2-pyridones [61–63].

It should be pointed out that a significant number of papers on the reactions of functionalization of 2-pyridone ring exist. One such review was published by Pemberton *et al*. which summarized papers published until 2006 [85]. This issue requires special attention and is beyond the scope of this paper.

CONCLUSION

2-Pyridone and 2-pyridone-based compounds, such as 2-quinolones, are known for having specific pharmacological properties and are widely used in medicine. Because of the various applications of compounds that contain 2-pyridone structure a number of procedures for their synthesis was developed. Besides the conventional synthesis, microwave assisted syntheses were also developed. Synthesis of 2-pyridone and compounds based on 2-pyridones under microwave irradiation has certain advantages over conventional methods of synthesis primarily in terms of higher

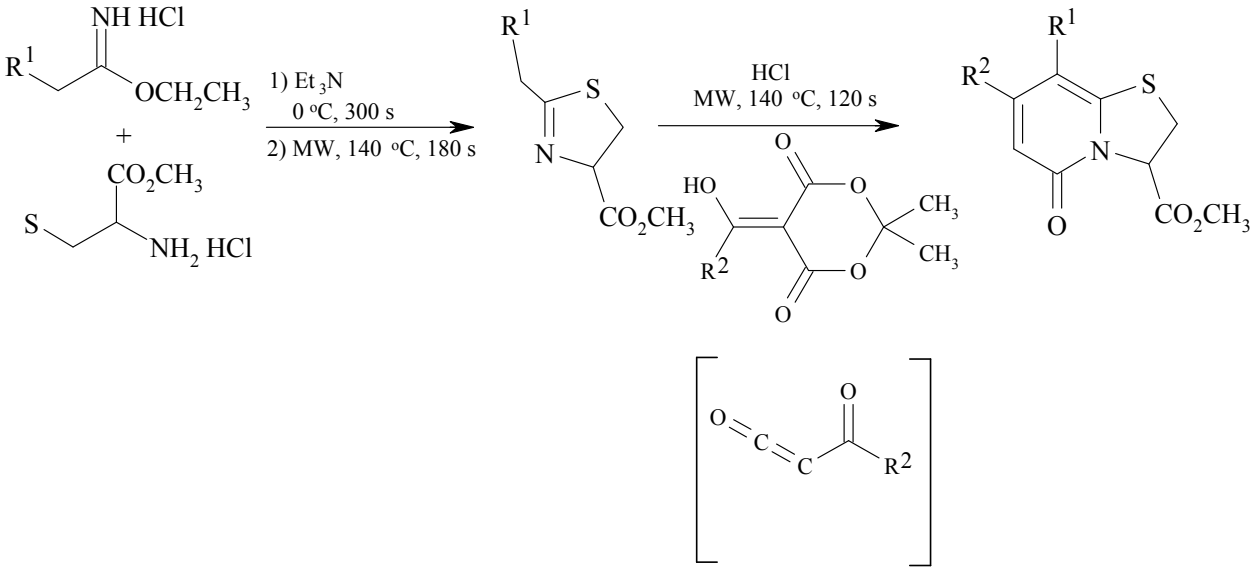

Figure 19. Synthesis of chiral bicyclic 2-pyridones via acyl-ketenes and Δ^2-thiazolines.

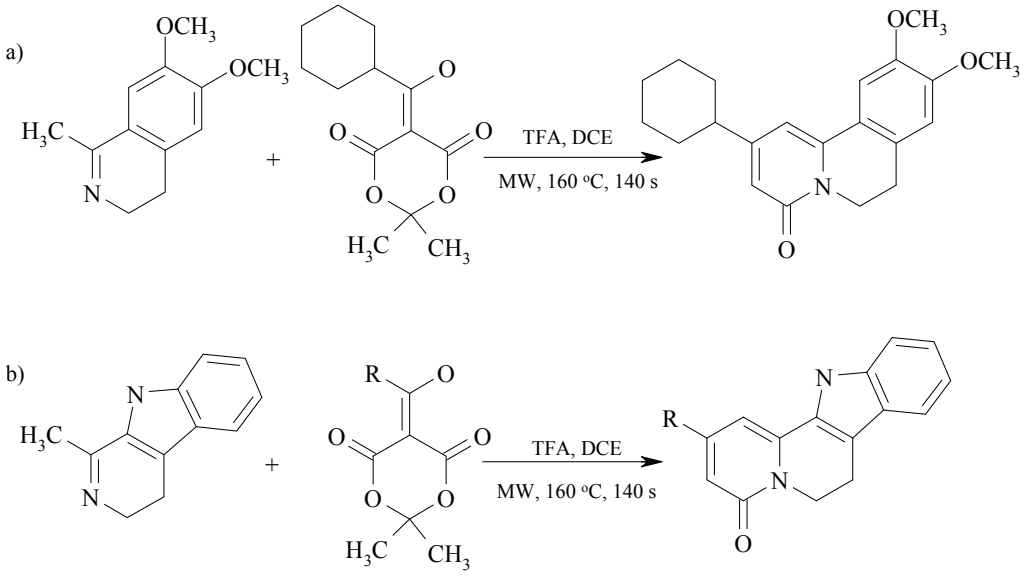

Figure 20. 2-Pyridone synthesis from the reaction of acyl-ketenes and imines.

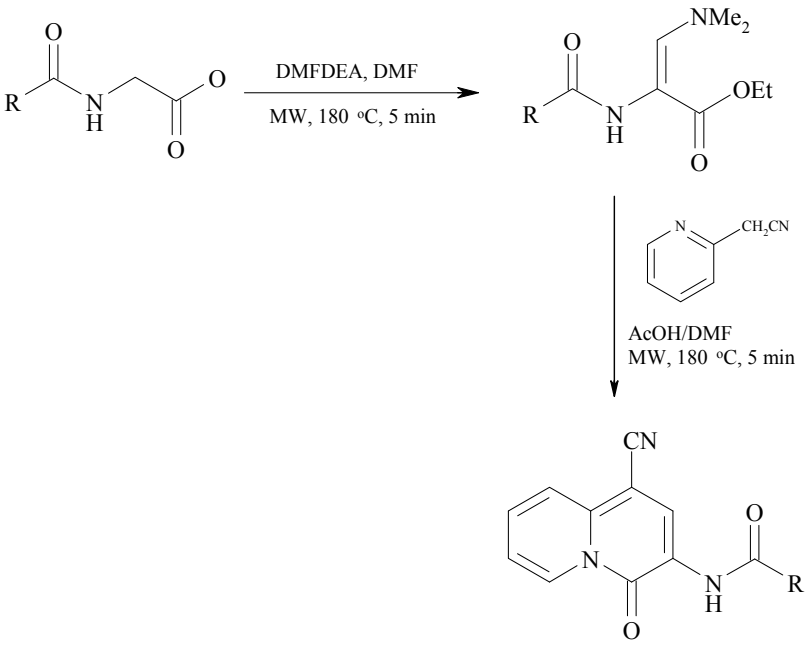

Figure 21. Synthesis of ring fused 2-pyridones via aminopropenoates.

yields and shorter reaction time. Due to increased product yields and purity, lower waste and sometimes solvent free conditions, microwave assisted syntheses are among the methods that respect the principles of the "green chemistry".

Acknowledgement

The authors would like to thank the Ministry of Education, Science and Technological Development of the Republic of Serbia for the financial support (project 172013).

REFERENCES

[1] N.Y. Gorobets, B.H. Yousefi, F. Belaj, C.O. Kappe, Rapid microwave-assisted solution phase synthesis of substituted 2-pyridone libraries, Tetrahedron **60** (2004) 8633––8644.

[2] Q. Li, L.A. Mitscher, L.L. Shen, The 2-pyridone antibacterial agents: bacterial topoisomerase inhibitors, Med. Res. Rev. **20** (2000) 231–293.

[3] Y. Fujita, H. Oguri, H. Oikawa, Biosynthetic studies on the antibiotics PF1140: a novel pathway for a 2-pyridone framework, Tetrahedron Lett. **46** (2005) 5885–5888.

[4] A. Fassihi, D. Abedi, L. Saghaie, R. Sabet, H. Fazeli, G. Bostaki, O. Deilami, H. Sadinpou, Synthesis, antimicrobial evaluation and QSAR study of some 3-hydroxypyridine-4-one and 3-hydroxypyran-4-one derivatives, Eur. J. Med. Chem. **44** (2009) 2145–2157.

[5] G. Semple, B.M. Andersson, V. Chhajlani, J. Georgsson, M.J. Johansson, Å. Rosenquist, L. Swanson, Synthesis and Biological activity of kappa opioid receptor agonists. Part 2: Preparation of 3-aryl-2-pyridone analogues generated by solution- and solid-phase parallel synthesis methods, Bioorg. Med. Chem. Lett. **13** (2003) 1141––1145.

[6] R.L.T. Parreira, O. Abrahão Jr., S.E. Galembeck, Conformational preferences of non-nucleoside HIV-1 reverse transcriptase inhibitors, Tetrahedron **57** (2001) 3243–3253.

[7] P.S. Dragovich, T.J. Prins, R. Zhou, E.L. Brown, F.C. Maldonado, S.A. Fuhrman, L.S. Zalman, T. Tuntland, C.A. Lee, A.K. Patick, D.A. Matthews, T.F. Hendrickson, M.B. Kosa, B. Liu, M.R. Batugo, J.P.R. Gleeson, S.K. Sakata, L. Chen, M.C. Guzman, J.W. Meador, R.A. Ferre, S.T. Worland, Structure-Based Design, Synthesis, and Biological Evaluation of Irreversible Human Rhinovirus 3C Protease Inhibitors. 6. Structure−Activity Studies of Orally Bioavailable, 2-Pyridone-Containing Peptidomimetics, J. Med. Chem. **45** (2002) 1607–1623.

[8] L.A. Hasvold, W. Wang, S.L. Gwaltney, T.W. Rockway, L.T.J. Nelson, R.A. Mantei, S.A. Fakhoury, G.M. Sullivan, Q. Li, N.H. Lin, L. Wang, H. Zhang, J. Cohen, W.Z. Gu, K. Marsh, J. Bauch, S. Rosenberg, H.L. Sham, Pyridone-containing farnesyltransferase inhibitors: synthesis and biological evaluation, Bioorg. Med. Chem. Lett. **13** (2003) 4001–4005.

[9] J.J. Parlow, R.G. Kurumbail, R.A. Stegeman, A.M. Stevens, W.C. Stallings, M.S. South, Design, Synthesis, and Crystal Structure of Selective 2-Pyridone Tissue Factor VIIa Inhibitors, J. Med. Chem. **46** (2003) 4696–4701.

[10] J.J. Parlow, M.S. South, Synthesis of 2-pyridones as tissue factor VIIa inhibitors, Tetrahedron **59** (2003) 7695––7701.

[11] D.Ž. Mijin, G.S. Ušćumlić, N.V. Valentić, A.D. Marinković, Sinteza arilazo piridonskih boja, Hem. Ind. **65** (2011) 517–532.

[12] V.P. Litvinov, S.G. Krivokolysko, V.D. Dyachenko, Synthesis and properties of 3-cyanopyridine-2(1H)-chalcogenones. Review, Chem. Heterocyclic Comp. **35** (1999) 509–540.

[13] N. Pemberton, E. Chorell, F. Almqvist, Microwave-Assisted Synthesis and Functionalization of 2-Pyridones, 2-Quinolones and Other Ring-Fused 2-Pyridones, Top. Heterocycl. Chem. **1** (2006) 1–30.

[14] G. Pastelin, R. Mendez, E. Kabela, A. Farah, The search for a digitalis substitute II milrinone (Win 47203) its action on the heart-lung preparation of the dog, Life Sci. **33** (1983) 1787–1796.

[15] J.M. Mirković, D.Ž. Mijin, S.D. Petrović, Milrinon-svojstva i sinteza, Hem. ind. **67** (2012) 17–25

[16] V. Åberg, F. Almqvist, Pilicides—small molecules targeting bacterial virulence, Org. Biomol. Chem. **5** (2007) 1827–1834.

[17] L. Cegelski, J.S. Pinkner, N.D. Hammer, C.K. Cusumano, C.S. Hung, E. Chorell, V. Åberg, J.N. Walker, P.C. Seed, F. Almqvist, M.R. Chapman, S.J. Hultgren, Small-molecule inhibitors target Escherichia coli amyloid biogenesis and biofilm formation, Nat. Chem. Biol. **5** (2009) 913–919.

[18] K. Eggert, D. Squillacote, P. Barone, R. Dodel, R. Katzenschlager, M. Emre, A. J. Lees, O. Rascol, W. Poewe, E. Tolosa, C. Trenkwalder, M. Onofrj, F. Stocchi, G. Nappi, V. Kostic, J. Potic, E. Ruzicka, W. Oertel, Safety and efficacy of perampanel in advanced Parkinson's disease: A randomized, placebo-controlled study, Movement Disord. **25** (2010) 896–905.

[19] D.J. Dyer, V.Y. Lee, R.J. Twieg, The forgotten liquid crystals of Daniel Vorlander: A new look at mesogenic 4-pyridones, Liquid Cryst. **23** (1997) 551–560.

[20] V. Štětinová, V. Grossmann, Effects of known and potential antioxidants on animal models of pathological processes (diabetes, gastric lesions, allergic bronchospasm), Exp. Toxicol. Pathol. **52** (2000) 473–479.

[21] F. You, R.J. Twieg, Aromatic nucleophilic substitution with 4-hydroxypyridine, Tetrahedron Lett. **40** (1999) 8759–8762.

[22] D. Gibson, D. Clarke, Ch. Winscom, Photographic elements containing a de-aggregating compound and dye-forming coupler, (Eastman Kodak Co. US) US 6841344 (2005).

[23] G. Jones, Pyridines and their benzo derivatives: synthesis. In: A. McKillop (Ed.), Comprehensive heterocyclic chemistry II, Pergamon Press, Oxford, 1996, p. 167.

[24] G. Jones, Pyridines and their benzo derivatives: synthesis. In: Boulton A, A. McKillop (Ed.), Comprehensive heterocyclic chemistry, Pergamon Press, Oxford, 1984, p. 395.

[25] I. Guareschi, Oxypiridine aus β-diketonen, Chem. Zentr. **1** (1899) 289–290.

[26] A.O. Fitton, R.K. Smalley, Practical Heterocyclic Chemistry, Academic Press, London, 1968, p. 71.

[27] D.Ž. Mijin, G.S. Ušćumlić, N.V. Valentić, Synthesis and investigation of solvent effects on the ultraviolet absorption spectra of 5-substituted-4-methyl-3-cyano-6--hydroxy-2-pyridones, J. Serb. Chem. Soc. **66** (2001) 507–516.

[28] D. Mijin, A. Marinković, Synthesis of N-Substituted 4,6-Dimethyl-3-cyano-2-pyridones Under Microwave Irradiation, Synthetic Commun. **36** (2006) 193–198.

[29] M. Mišić-Vuković, D. Mijin, M. Radojković-Veličković, N.Valentić, V. Krstić, Condensation of 1,3-diketones with cyanoacetamide: 4,6-disubstituted-3-cyano-2-pyridones, J. Serb. Chem. Soc. **63** (1998) 585–599.

[30] M. Berson, J.P. Calmon, Effect of substituents on the keto-enol equilibriums of aromatic β-diketones in aqueous solution, C.R. Chim. **273** (1971) 181–184.

[31] R.M. Silverstain, G.C. Bassler, T.C. Morill, Spectrophotometric Indentification of Organic Compounds, Wiley, New York, 1981, pp. 195, 316.

[32] J. Dostanić, N. Valentić, G. Uščumlić, D. Mijin, Synthesis of 5-(substituted phenylazo)-6-hydroxy-4-methyl-3--cyano-2-pyridones from ethyl 3-oxo-2-(substituted phenylazo)butanoates, J. Serb. Chem. Soc. **76** (2011) 499––504.

[33] A.S. Alimmari, A.D. Marinković, D.Ž. Mijin, N.V. Valentić, N. Todorović, G.S. Uščumlić, Synthesis, structure and solvatochromic properties of 3-cyano-4,6-diphenyl-5-(3- and 4-substituted phenylazo)-2-pyridones, J. Serb. Chem. Soc. **75** (2010) 1019–1032.

[34] N.V. Valentić, Ž.J. Vitnik, D.Ž. Mijin, G.S. Uščumlić, N. Todorović, I.O. Juranić, Linear Free Energy Relationships of the ^{13}C NMR chemical shifts in 5-(3- and 4-substituted arylazo)-4,6-dimethyl-3-cyano-2-pyridones, ARKIVOC (2009) 227–240.

[35] D. Mijin, G. Uščumlić, N. Perišić-Janjić, I. Trkulja, M. Radetić, P. Jovančić, Synthesis, properties and colour assessment of some new 5-(3- and 4-substituted phenylazo)-4,6-dimethyl-3-cyano-2-pyridones, J. Serb. Chem. Soc. **71** (2006) 435–444.

[36] D.Ž. Mijin, G.S. Uščumlić, N.U. Perišić-Janjić, N.V. Valentić, Substituent and solvent effects on the UV/Vis absorption spectra of 5-(3- and 4-substituted arylazo)--4,6-dimethyl-3-cyano-2-pyridones, Chem. Phys. Lett. **418** (2006) 223–229.

[37] G.S. Uščumlić, D.Ž. Mijin, N.V. Valentić, V.V. Vajs, B.M. Sušić, Substituent and solvent effects on the UV/Vis absorption spectra of 5-(4-substituted arylazo)-6-hydroxy-4-methyl-3-cyano-2-pyridones, Chem. Phys. Lett. **397** (2004) 148–153.

[38] N.Ž. Prlainović, D.I. Bezbradica, Z.D. Knežević-Jugović, R.T. Kozlowska, D.Ž. Mijin, A Kinetic study of *Candida rugosa* lipase-catalyzed synthesis of 4,6-dimethyl-3-cyano-2-pyridone, J. Braz. Chem. Soc. **21** (2010) 2285––2293.

[39] D.Ž. Mijin, B.D. Milić, M.M. Mišić-Vuković, Synthesis of substituted 3-cyano-2-pyridones: Part IV Influence of 3-alkyl-2,4-pentanedione and *N*-alkyl cyanoacetamide structure on the enzyme catalyzed synthesis of substituted 3-cyano-2-pyridones, Indian J. Chem., B **45** (2006) 993–1003.

[40] C.O. Kappe, Controlled microwave heating in modern organic synthesis, Angew. Chem. Int. Ed. **43** (2004) 6250–6284.

[41] C.O. Kappe, D. Dallinger, The impact of microwave synthesis on drug discovery, Nat. Rev. Drug Discov. **5** (2006) 51–63.

[42] D. Stuerga, M. Delmotte, in: A. Loupy (Ed.), Microwaves in Organic Synthesis, Wiley-VCH, Weinheim, 2002.

[43] C.O. Kappe, D. Dallinger, S.S. Murphree, Practical Microwave Synthesis for Organic Chemists - Strategies, Instruments, and Protocols, Wiley-VCH, Weinheim, 2009.

[44] D.Ž. Mijin, S.D. Petrović, Primena mikrotalasne tehnike u organskoj hemiji i organskoj hemijskoj tehnologiji, Hem. Ind. **59** (2005) 224–229.

[45] B. Wathey, J. Tirney, P. Lindstrom, J. Westman, The impact of microwave-assisted organic chemistry on drug discovery, Drug Discov. Today **7** (2002) 373–380.

[46] Y. Fernández, A. Arenillas, J. Ángel Menéndez, in: S. Grundas (Ed.), Advances in Induction and Microwave Heating of Mineral and Organic Materials, InTech, Rijeka, 2011, pp. 723–752.

[47] P.J. Walter, S. Chalk, H.M. Kingston, in: H.M. Kingston, S.J. Haswell (Eds.), Microwave-Enchanced Chemistry, Fundamentals, Sample Preparations and Applications, American Chemical Society, Washington DC, 1997, pp. 55–222.

[48] L. Jassie, R. Savesz, T. Kierstead, E. H. Asty, S. Matz in: H.M. Kingston, S.J. Haswell (Eds.), Microwave-Enhanced Chemistry, Fundamentals, Sample Preparations and Applications, American Chemical Society, Washington DC, 1997, pp. 569–611.

[49] W. G. Engelhart, in: H.M. Kingston, S.J. Haswell (Eds.), Microwave-Enchanced Chemistry, Fundamentals, Sample Preparations and Applications, American Chemical Society, Washington DC, 1997, pp. 613–638.

[50] S. Ravichandran, E.Karthikeyan, Microwave Synthesis - A Potential Tool for Green Chemistry, Int. J. ChemTech. Res. **3** (2011) 466–470.

[51] E. Klingsberg, Pyridine and its Derivitives, Part I, Interescience, New York, 1960, pp. 272–273, 362–364.

[52] H. Schmid, Process for the preparation of pyridone compounds, (Sandoz AG), DE 4314430 (1994).

[53] J.M. Bobbit, D.A. Scola, Synthesis of Isoquinoline Alkaloids. II. The Synthesis and Reactions of 4-Methyl-3-pyridinecarboxaldehyde and Other 4-Methyl-3-Substituted Pyridines, J. Org. Chem. **25** (1960) 560–564.

[54] J.M. Dostanić, D.R. Lončarević, P.T. Banković, O.G. Cvetković, D.M. Jovanović, D.Ž. Mijin, Influence of process parameters on the photodegradation of synthesized azo pyridone dye in TiO_2 water suspension under simulated sunligh**,** J. Environ. Sci. Health, A **46** (2011) 70–79.

[55] C. Dave, G. Chaitanya, D.A. Shah, Y.K. Agrawal, A simple and convient synthesis of 4,6-disubstituted 3-cyanopyridin-2(1H)-ones under solvent-free microwave conditions, Indian J. Chem., B **43** (2004) 885–887.

[56] D.Z. Mijin, M. Baghbanzadeh, C. Reidlinger, C.O. Kappe, The microwave-assisted synthesis of 5-arylazo-4,6--disubstituted-3-cyano-2-pyridone dyes, Dyes Pigm. **85** (2010) 73–78.

[57] S.S. Al-Neyadi, A.H. Hassan, I.M. Abdou, Microwave-assisted synthesis of 2(1*H*)-pyridones and their glucosides as cell proliferation inhibitors, Nucleos. Nucleot. Nucl. **30** (2011) 120–134.

[58] A. Abadi, O. Al-Deeb, A. Al-Afify, H. El-Kashef, Synthesis of 4-alkyl (aryl)-6-aryl-3-cyano-2(1*H*)-pyridinones and their 2-imino isosteres as nonsteroidal cardiotonic agents, Farmaco **54** (1999) 195–201.

[59] R. Jia, S. Tu, Y. Zhang, B. Jiang, J. Zhang, C. Yao, F. Shi, An efficient and greener approach to the synthesis of 3,5-dicyanopyridin-2(1H)-one derivatives in aqueous media under microwave irradiation conditions, J. Heterocyclic Chem. **44** (2007) 1177–1180.

[60] H. Rodriguez, M. Suarez, R. Perez, A. Petit,; A. Loupy, Solvent-free synthesis of 4-aryl substituted 5-alkoxycar-

bonyl-6-methyl-3,4-dihydropyridones under microwave irradiation, Tetrahedron Lett. **44** (2003) 3709–3712.

[61] Y. Xiang, W.-J. Zhu, One-pot synthesis of pyridones and related compounds under microwave irradiation in water, Jiamusi Daxue Xuebao (Ziran Kexueban) **28** (2010) 753–755. [C.A. 154\2010 109398].

[62] S.-J. Tu, X. Deng, D.-Q. Shi, Y. Gao, J.-C. Feng, Microwave assisted synthesis of pyridone derivatives, Chin. J. Chem. **19** (2001) 714–715. [C.A. 135\2001 303753].

[63] S. Tu, C. Miao, F. Fang, Y. Feng, T.Li, Q. Zhuang, X. Zhang, S. Zhu, D. Shi, New potential calcium channel modulators: design and synthesis of compounds containing two pyridine, pyrimidine, pyridone, quinoline and acridine units under microwave irradiation, Bioorg. Med. Chem. Lett. **14** (2004) 1533–1536.

[64] J.H.M. Lange, P.C. Verveer, S.J.M. Osnabrug, G.M. Visser, Rapid microwave-enhanced synthesis of 4-hydroxyquinolinones under solvent-free conditions, Tetrahedron Lett. **42** (2001) 1367–1369.

[65] T.N. Glasnov, W. Stadlbauer, C.O. Kappe, Microwave-Assisted Multistep Synthesis of Functionalized 4-Arylquinolin-2(1*H*)-ones Using Palladium-Catalyzed Cross-Coupling Chemistry, J. Org. Chem. **70** (2005) 3864–3870.

[66] T. Kappe, A.S. Karem, W. Stadlbauer, Synthesis of benzohalogenated 4-hydroxy-2(1*H*)-quinolones, J. Heterocycl. Chem. **25** (1988) 857–862.

[67] N. Vetrivel, S.T. Selvi, R. Sasi, Microwave-assisted synthesis of quinoline alkaloids: 4-methoxy-1-methyl-2-quinolinone and its analogs, ARKIVOC **10** (2006) 82–89.

[68] K. Arya, M. Agarwal, Microwave prompted multigram synthesis, structural determination, and photo-antiproliferative activity of fluorinated 4-hydroxyquinolinones, Bioorg. Med. Chem. Lett. **17** (2007) 86–93.

[69] H.K. Lee, H. Cao, T.M. Rana, Design, Microwave-Assisted Synthesis, and Photophysical Properties of Small Molecule Organic Antennas for Luminescence Resonance Energy Transfer, J. Comb. Chem. **7** (2005) 279–284.

[70] C-S. Jia, Y-W. Dong, S-J. Tu, G-W. Wang, Microwave-assisted solvent-free synthesis of substituted 2-quinolones, Tetrahedron **63** (2007) 892–897.

[71] P.W. Anzalone, A.R. Baru, E.M. Danielson, P.D. Hayes, M.P. Nguyen, A.F. Panico, R.C. Smith, R.S. Mohan, Bismuth Compounds in Organic Synthesis. A One-Pot Synthesis of Homoallyl Ethers and Homoallyl Acetates from Aldehydes Catalyzed by Bismuth Triflate, J. Org. Chem. **70** (2005) 2091–2096.

[72] M. Larhed, A. Hallberg, Microwave-Promoted Palladium-Catalyzed Coupling Reactions, J. Org. Chem. **61** (1996) 9582–9584.

[73] J. Li, A.W.H. Mau, C.R. Strauss, The use of palladium on porous glass for catalytic coupling reactions, Chem. Commun. **1997** (1997) 1275–1276.

[74] N. Garg, M. Larhed, A. Hallberg, Heck Arylation of 1,2-Cyclohexanedione and 2-Ethoxy-2-cyclohexenone, J. Org. Chem. **63** (1998) 4158–4162.

[75] K. Olofsson, M. Larhed, A. Hallberg, Highly Regioselective Palladium-Catalyzed Internal Arylation of Allyltrimethylsilane with Aryl Triflates, J. Org. Chem. **63** (1998) 5076–5079.

[76] A. Stadler, S. Pichler, G. Horeis, C.O. Kappe, Microwave-enhanced reactions under open and closed vessel conditions. A case study, Tetrahedron **58** (2002) 3177–3183.

[77] P.M. Fresneda, P. Molina, S. Delgado, A novel approach to the indoloquinoline alkaloids cryptotackieine and cryptosanguinolentine by application of cyclization of o-vinylsubstituted arylheterocumulenes, Tetrahedron **57** (2001) 6197–6202.

[78] B.V. Suma, A.K. Rochani, C.H.S. Venkataramana, J. Jays, V. Madhavan, Synthesis, Characterization, invitro Antibacterial, Anti-inflammatory Evaluations of Novel 4-Quinolone containing Pyrazolidinedione derivatives, Int. J. ChemTech. Res. **2** (2010) 2156–2162.

[79] H. Emtenäs, C. Taflin, F. Almqvist, Efficient microwave assisted synthesis of optically active bicyclic 2-pyridinones *via* Δ^2-thiazolines, Mol. Div. **7** (2003) 165–169.

[80] E. Chorell, S. Edvinsson, F. Almqvist, Improved procedure for the enantioselective synthesis of dihydrooxazolo and dihydrothiazolo ring-fused 2-pyridones, Tetrahedron Letters **51** (2010) 2461–2463.

[81] H. Emtenäs, L. Alderin, F. Almqvist, An Enantioselective Ketene−Imine Cycloaddition Method for Synthesis of Substituted Ring-Fused 2-Pyridinones, J. Org. Chem. **66** (2011) 6756–6761.

[82] H. Emtenäs, K. Åhlin, J. S. Pinkner, S. J. Hultgren, F. Almqvist, Design and Parallel Solid-Phase Synthesis of Ring-Fused 2-Pyridinones That Target Pilus Biogenesis in Pathogenic Bacteria, J. Comb. Chem. **4** (2002) 630–639.

[83] N. Pemberton, L. Jakobsson, F. Almqvist, Synthesis of Multi Ring-Fused 2-Pyridones via an Acyl-Ketene Imine Cyclocondensation, Org. Lett. **8** (2006) 935–938.

[84] J. Westman, R. Lundin, J. Stalberg, M. Ostbye, A. Franzen, A. Hurynowicz, Alkylaminopropenones and Alkylamino-Propenoates as Efficient and Versatile Synthons in Microwave-Assisted Combinatorial Synthesis, Comb. Chem. High T. Scr. **5** (2002) 565–571.

[85] N. Pemberton, E. Chorell, F. Almqvist, Microwave-assisted synthesis and functionalization of 2-pyridones, 2-quinolones and other ring-fused 2- pyridones, Top. Heterocycl. Chem. **1** (2006) 1–30.

IZVOD

MIKROTALASNA TEHNIKA U SINTEZI 2-PIRIDONA I JEDINJENJA NA BAZI 2-PIRIDONA

Dušan Ž. Mijin, Jelena M. Marković, Danijela V. Brković, Aleksandar D. Marinković

Tehnološko–metalurški fakultet Univerziteta u Beogradu, Karnegijeva 4, p.pr. 3503, 11120 Beograd, Srbija

(Pregledni rad)

Aromatična heterociklična jedinjenja predstavljaju veoma značajnu grupu jedinjenja zbog svoje biološke i medicinske primene. Šestočlana heterociklična jedinjenja koja sadrže azot (npr. piridini, piridoni, pirimidini, piperidini, piperazini) se puno koriste u medicini jer poseduju određena farmakološka svojstva, a poseban značaj imaju 2-piridoni i 4-piridoni. Derivati 2-piridona su posebno interesantni jer je 2-piridonska struktura prisutna u mnogim jedinjenjima prirodnog porekla od kojih mnoga poseduju biološku aktivnost. Zbog široke primene jedinjenja koja u sebi sadrže piridonsku strukturu razvijen je veliki broj postupaka za njihovu sintezu. Konvencionalni način izvođenja organskih sinteza podrazumeva zagrevanje spoljašnjim izvorima toplote pri čemu se toplota prenosi kondukcijom, što predstavlja spor i neefikasan metod prenosa energije, jer zavisi od toplotne provodljivosti materijala, pa je temperatura reaktora veća od temperature reakcione smeše. Nasuprot tome, mikrotalasno zračenje je efikasan izvor zagrevanja koji direktno prenosi energiju kroz interakciju sa polarnim molekulima prisutnim u reakcionoj smeši. Mikrotalasne sinteze se ubrajaju među metode koje poštuju principe takozvane „zelene hemije" što predstavlja razlog više za ovakvo izvodjenje sinteza. U okviru rada dat je pregled sinteza 2-piridona i jedinjenja koja sadrže 2-piridonsko jezgro primenom mikrotalasne tehnike. Pregled obuhvata sinteze koje su izvršene kako u savremenim laboratorijskim mikrotalasnim reaktorima tako i one koje su izvršene u komercijalnim mikrotalasnim pećnicama za domaćinstvo. Takođe je ukazano na prednosti mikrotalasne sinteze u odnosu na konvencionalni način zagrevanja.

Ključne reči: Heterociklična jedinjenja • Medicinska hemija • Mikrotalasna organska hemija • 2-Hinolon • Kondenzovani *N*-supstituisani 2-piridoni

Analogija prenosa količine kretanja, toplote i mase pri vertikalnom hidrauličkom transportu inertnih čestica

Darko R. Jaćimovski[1], Radmila V. Garić-Grulović[1], Željko B. Grbavčić[2], Mihal M. Đuriš[1], Nevenka M. Bošković-Vragolović[2]

[1]*IHTM, Centar za katalizu i hemijsko inženjerstvo, Univerzitet u Beogradu, Njegoševa 12, Beograd, Srbija*
[2]*Tehnološko–metalurški fakultet, Univerzitet u Beogradu, Karnegijeva 4, Beograd, Srbija*

Izvod

U ovom radu prikazani su rezultati eksperimentalnih ispitivanja prenosa količine kretanja, toplote i mase zid–fluid u vertikalnom hidrauličkom transportu inertnih čestica i pri strujanju fluida u cevi istog prečnika. Eksperimentalna ispitivanja vršena su istovremenim merenjem potrebnih parametara za definisanje navedenih prenosa. Cilj ovih ispitivanja bio je određivanje koeficijenata prenosa pri vertikalnom hidrauličkom transportu inertnih čestica i uspostavljanje analogije tri prenosa. Eksperimentalni sistem predstavljala je vertikalna transportna cev prečnika 25,4 mm snabdevena omotačem za zagrevanje parom, kao i segmentom transportne cevi prepariranim rastopom benzoeve kiseline. Kao fluid korišćena je voda, a vršen je transport staklenih sfernih čestica prečnika 1,94 mm. U rezultatima su prikazani dobijeni koeficijenti trenja, prelaza toplote i prelaza mase. Korišćenjem koncepta pseudofluida, pokazano je postojanje analogije prenosa količine kretanja, toplote i mase u transportnoj cevi za paralelni režim strujanja.

Ključne reči: vertikalni dvofazni tok fluid-čestice, prenos količine kretanja, prenos toplote, prenos mase, analogija..

Dostupno na Internetu sa adrese časopisa: http://www.ache.org.rs/HI/

NAUČNI RAD

UDK 544.4:66.011

Hem. Ind. **68** (1) 15–25 (2014)

doi: 10.2298/HEMIND130207025J

Potpuno definisanje vertikalnog dvofaznog toka fluid–čestice podrazumeva poznavanje fluido-dinamike i prenosnih karakteristika ovih sistema. Vertikalni dvofazni tok ne predstavlja samo transport čvrstog materijala već sve više predstavlja sastavni deo različitih kontaktora fluid–čestice kao što su modifikovani fontanski i fontansko–fluidizovani slojevi sa cevnim umetkom ili cirkulacioni fluidizovani slojevi [1–4].

Gradijent pritiska pri vertikalnom transportu fluida i čestica, sastoji se od gradijenta pritiska usled efektivne težine čestica, F_e, i gradijenta pritiska usled trenja smeše fluida i čestica o zid transportne cevi, F_w [5–7]:

$$-\frac{\mathrm{d}p}{\mathrm{d}z} = F_e + F_w = \left(\rho_p - \rho_f\right)g\left(1-\varepsilon\right) + F_w \tag{1}$$

Za gradijent pritiska usled trenja smeše fluid–čestice (koja se kreće), o zidove transportne cevi (jedn. (1)), pretpostavlja se aditivni karakter, tj. da se može razdvojiti na gradijent pritiska usled trenja fluid-zid i gradijent pritiska usled trenja čestice-zid transportne cevi [8–10]:

$$F_w = F_f + F_p \tag{2}$$

Gradijenti pritiska usled trenja fluid–zid, F_f, i čestice zid, F_p, definišu se jednačinama Fanningovog tipa [5]:

$$F_f = 2 f_f \rho_f \frac{U^2}{D_t} \tag{3}$$

$$F_p = 2 f_p \rho_p \frac{\left(1-\varepsilon\right)v^2}{D_t} \tag{4}$$

u kojima je f_f koeficijent trenja fluid–zid, a f_p koeficijent trenja čestice–zid.

Koeficijent trenja fluid–zid transportne cevi određuje se iz korelacija za strujanje fluida bez prisustva čestica za glatku cev [11]:

$$f_f = \frac{0{,}0791}{\mathrm{Re}^{0.25}} \tag{5}$$

Koeficijent trenja čestice–zid većina autora korelisala je u funkciji brzine čestica [8,12,13], ali postoje i kompleksne korelacije koje uključuju i poroznost i relativnu brzinu između fluida i čestica [9]. Korelacija za koeficijent trenja čestice-zid transportne cevi, koja se najčešće koristi u transportnim sistemima tečnost–čestice je [5]:

$$f_p = 7{,}33\times10^{-3}v^{-2} \tag{6}$$

gde je v u $\mathrm{m\cdot s^{-1}}$.

U vertikalnom dvofaznom toku, čestice koje se transportuju svojim prisustvom utiču na karakteristike

Prepiska: R.V. Garić-Grulović, Institut za hemiju, tehnologiju i metalurgiju – Centar za katalizu i hemijsko inženjerstvo, Njegoševa 12, Beograd Srbija.
E-pošta: garic@tmf.bg.ac.rs
Rad primljen: 7. februar, 2013
Rad prihvaćen: 25. mart, 2013

ovih sistema. U ovom transportnom toku, pri svim brzinama fluida, koncentracija čestica po zapremini cevi je ravnomerna. U zavisnosti od brzine fluida i osobina samih čestica izgled vertikalnog toka je različit, tako da su, kao i u ranijim ispitivanjima, uočena dva režima transporta [5,6]:

– Turbulentni tok, koji karakteriše kretanje čestica po krivolinijskim putanjama, tj. radijalno se menja pravac kretanja čestica. Ovaj režim je tipičan za manje brzine fluida, manje poroznosti vertikalnog toka i može se okarakterisati i kao „gusti" tok čestica. Vizuelno podseća na stešnjeno taloženje suspenzije čestica, samo u suprotnom smeru.

– Paralelan tok, koji karakteriše kretanje čestica uglavnom po pravolinijskim putanjama. Ovaj režim se javlja pri većim brzinama fluida i predstavlja „redak" tok čestica u transportnoj cevi.

Jedan od najboljih kriterijuma za procenu režima strujanja u vertikalnom toku tečnost–čestice je, po modelu Daya sa sar., parametar γ[14]:

$$\gamma = \rho_p v^2 - \rho_f u^2 \tag{7}$$

gde je granična vrednost promene režima za $\gamma = 0$.

Na osnovu datog kriterijuma definisan je normalizovani parametar γ^* [5]:

$$\gamma^* = \frac{\rho_p v^2 - \rho_f U^2}{\rho_f U_t^2} \tag{8}$$

Za $\gamma^*<0$ vertikalni tok se nalazi u režimu turbulentnog toka, a ako je $\gamma^*>0$ u paralelnom režimu transporta čestica.

U literaturi su malobrojni podaci o prenosu toplote u vertikalnom toku tečnost-čvrste relativno teške čestice. Većina objavljenih radova bavi se prenosom toplote u vertikalnom toku tečnih suspenzija sitnih čestica ili krupnih čestica voća i povrća u prehrambenoj industriji [6,15–17]. Jedna od objavljenih eksperimentalnih korelacija za sisteme sa teškim česticama je [6]:

$$j_H = \frac{6565}{\mathrm{Re}_m^{1,5}} \text{ za } 2800 < \mathrm{Re}_m < 15000 \tag{9}$$

$$j_H = \frac{0,0395}{\mathrm{Re}_m^{0,25}} \text{ za } 15000 < \mathrm{Re}_m < 32000 \tag{10}$$

gde je Re_m Reynoldsov broj za smešu fluid–čestice.

Kao i u slučaju prenosa toplote i za prenos mase u vertikalnom toku tečnost–krupne čestice u literaturi ima vrlo malo podataka. Korelacija koja važi za transportni sistem krupne čestice–tečnost je [18]:

$$j_D = \frac{0,0395}{\mathrm{Re}_m^{0,25}} \text{ za } 15000 < \mathrm{Re}_m < 32000 \tag{11}$$

koja je takođe data za Reynoldsov broj za smešu fluid––čestice.

Kod jednofaznih tokova, posebno pri turbulentnom režimu strujanja, postoji nekoliko analogija, od kojih su najpoznatije: Reynoldsova, Chilton–Colburnova, Von Karmanova i Prantlova [19]. U vertikalnom toku fluida i čestica, prisustvo druge faze posebno utiče na prenos količine kretanja odnosno ukupni koeficijent trenja, pa samim tim i na uspostavljanje analogije [13,18,20]. Jedna od definisanih analogija, koja je koncipirana u formi Chilton–Colburnove analogije [21], data je za f_w, koeficijent trenja smeše „fluid–čestice"–zid transportne cevi u paralelnom režimu dvofaznog toka kao [6,18]:

$$j_H = j_D = \frac{f_w}{2} \tag{12}$$

U ovom radu biće dati rezultati eksperimentalnih merenja prenosa količine kretanja, toplote i mase. Prvi put u ovom radu, svi potrebni parametari za definisanje navedenih prenosa, mereni su istovremeno u cilju uspostavljanja analogije prenosa pri vertikalnom hidrauličkom transportu.

EKSPERIMENTALNA ISPITIVANJA

Osnovni deo eksperimentalnog sistema bila je transportna bakarna cev (c) prečnika 25,4 mm i dužine 1320 mm (Slika 1). Oko cevi se nalazio omotač (d_1) sa spoljnom termičkom izolacijom, dužine 700 mm. Kroz omotač je strujala zasićena vodena para iz generatora pare (m) na atmosferskom pritisku. Na dnu i vrhu transportne cevi ugrađena su po dva termopara koja su merila temperaturu zida cevi i unutrašnjeg radnog fluida.

Za merenje pritiska na vrhu i dnu transportne cevi ugrađene su piezometarske cevi (i). Na vrhu transportne cevi nalazio se ugradni prsten (d_2) sa unutrašnjim žljebom visine 18,5 mm. Unutar prstena u žljeb nanošena je benzeova kiselina tako da je unutrašnji prečnik prstena bio jednak unutrašnjem prečniku kolone, da se ne bi ometala hidrodinamika. Benzeova kiselina je slabo rastvorna supstanca tako da u vremenu trajanja eksperimenta nije bilo bitne promene geometrije sistema. Masa prstena sa benzeovom kiselinom merena je na početku i kraju eksperimenta posle sušenja prstena.

Smeša fluida i čestica prelivala se na vrhu u sistem za razdvajanje faza. Čestice su se spuštale naniže kroz dozer čvrstih čestica (h) opet ka ulazu u transportnu cev (c), gde su dolazile u kontakt sa fluidom na dnu kolone. Na taj način formiran je vertikalni dvofazni tok suspenzije voda–čestice. Na mestu odvajanja faza nalazio se merač protoka čestica i vode (g).

Karakteristike čestica korišćenih u eksperimentima date su u tabeli 1.

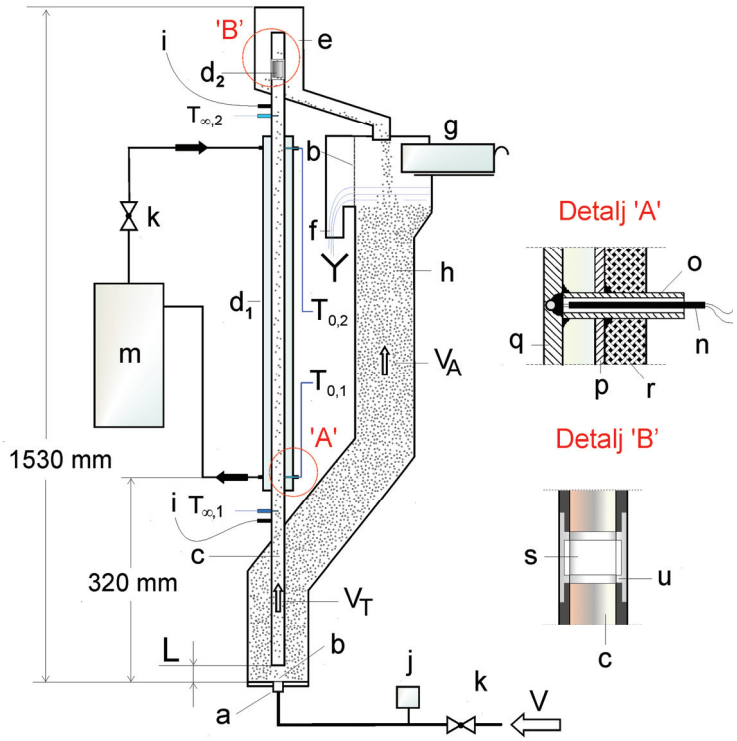

Slika 1. Eksperimentalna aparatura za ispitivanje prenosa količine kretanja, toplote i mase: a- mlaznica, b - raspodeljivač (mreža), c - transportna cev, d_1 - omotač za paru (grejanje), d_2 - prsten ispunjen benzoevom kiselinom, e- preliv čestica i vode, f - preliv vode, g - kutija za merenje protoka čestica, h - dozer čvrstih čestica, i - piezometri, j - merači protoka, k - ventili, L - rastojanje transportne cevi od mlaznice, m - generator pare 30 kW, n - termopar (termoparovi $T_{0,1}$, $T_{0,2}$), o - bakarna cev 8/6 mm, p - omotač oko transportne cevi, q - zid transportne cevi, r - izolacija, s - rastop benzoeve kiseline, u - prsten.
Figure. 1. Schematic diagram of experimental systems: a - inlet nozzle, b - distributor (screen), c - transport tube, d_1 - heating section, d_2 - segment prepared with benzoic acid, e - overflow, f - water overflow, g - box for water and particle flowrate measurements, h - particle dozer, i - piezometers, j - flowmeters, k - valves, L - transport tube to nozzle distance, m - steam generator, 30 kW, n - thermocouples ($T_{0,1}$, $T_{0,2}$), o - copper tube 8/6 mm, p - jacket wall, q - transport tube wall, r - thermoisolation, s - melt of benzoic acid, u - tube segment.

U eksperimentima, kao transportni medijum korišćena je voda, čija se temperatura menjala u opsegu od 18–47 °C. Fizički parametri vode određivani su na srednjoj temperaturi fluida [22].

Tabela 1. Karakteristike čestica [5]

d_p / mm	ρ_p / kg m^{-3}	U_t / m s^{-1}
1,94	2507	0,2878

Na osnovu izmerenih parametara izračunate su vrednosti:

– Koeficijenta prelaza toplote [11,19]:

$$\alpha = \frac{(G_f c_{pf} + G_p c_{pp})(T_{\infty,2} - T_{\infty,1})}{D_t \pi L_H \Delta T_{\ln}} \quad (13)$$

gde je srednja logaritamska razlika temperatura:

$$\Delta T_{\ln} = \frac{(T_{0,2} - T_{\infty,2}) - (T_{0,1} - T_{\infty,1})}{\ln \frac{(T_{0,2} - T_{\infty,2})}{(T_{0,1} - T_{\infty,1})}} \quad (14)$$

– Koeficijenta prelaza mase:

$$k = \frac{\Delta m}{t\, S\, \Delta c} = \frac{\Delta m}{t\, D_t \pi L_D\, \Delta c} \quad (15)$$

korišćenjem metode rastvaranja benzoeve kiseline u struji vode. Pogonska sila za prenos mase je razlika koncentracija benzoeve kiseline na površini (ravnotežna koncentracija) i u fluidu:

$$\Delta c = c^* - c_f \quad (16)$$

S obzirom na to da je benzoeva kiselina slabo rastvorna supstanca, da je eksperiment vršen stalno sa svežom strujom vode i da je površina sa koje se vršio prenos mala, pokazalo se praktično da je $c_f \approx 0$, tj. da je pogonska sila jednaka ravnotežnoj koncentraciji benzoeve kiseline. Korelacije za određivanje ravnotežne koncentracije benzoeve kiseline i koeficijenta difuzije benzoeve kiseline u vodi preuzete su iz literature [23].

REZULTATI I DISKUSIJA

Režimi strujanja pri vertikalnom dvofaznom toku

Na slici 2 prikazana je zavisnost normalizovanog parametra γ^* od poroznosti, ε. Parametar γ^* iztačunat je iz eksperimentalno izmerenih vrednosti brzina čestica i fluida po jednačini (8). Poroznost vertikalnog dvofaznog toka određivana je iz eksperimentalnih vrednosti za pad pritiska i brzinu fluida u vertikalnom toku fluida i čestica, kao i parametara sistema, a na osnovu jednačina (1)–(6), na sledeći način:

$$\varepsilon = 1 - \frac{\left(-\frac{\mathrm{d}p}{\mathrm{d}z}\right) - F_f - F_p}{(\rho_p - \rho_f)g} \tag{17}$$

Poređenja radi, na slici 2 je prikazana i zavisnost γ^*–ε, gde je poroznost direktno eksperimentalno određivana u transportnoj cevi prečnika, D_t = 24 mm [5]. Očigledno je da su dobijene iste zavisnosti, bez obzira na način eksperimentalnog određivanja poroznosti transportnog toka, a mala razlika u prečniku transportne cevi nije uticala na dobro slaganje rezultata.

Na slici 2 se uočava promena nagiba zavisnosti $\gamma^* = f(\varepsilon)$ oko vrednosti poroznosti 0,85. Posle ove vrednosti poroznosti, vertikalni tok ulazi u oblast paralelnog režima, jer je posle te vrednosti i $\gamma^*>0$. Interesantno je pomenuti da se vrednost poroznosti od 0,85 pojavljuje kao karakteristična vrednost u partikulativnoj fluidizaciji, pri kojoj dolazi do promene u ekspanziji fluidizovanog sloja, što je okarakterisano kao promena u mehanizmu prenosa količine kretanja [5,14,24,25]. S obzirom na pojavu vrednosti poroznosti od 0,85 i u hidrauličkom transportu, može se smatrati da pri toj vrednosti dolazi do promene u mehanizmu prenosa količine kretanja što za rezultat ima promenu režima transporta.

Prenos količine kretanja

Ukupni gradijent pritiska u vertikalnom toku smeše tečnost–čvrste čestice, sastoji se od tri komponente: gradijenta pritiska usled efektivne težine čestica, F_e, gradijenta pritiska usled trenja fluid–zid transportne cevi, F_f, i gradijenta pritiska usled trenja čestice–zid transportne cevi, F_p, tj. na osnovu jednačina (1) i (2):

$$-\frac{\mathrm{d}p}{\mathrm{d}z} = F_e + F_f + F_p \tag{18}$$

Na osnovu eksperimentalnih podataka za ukupni gradijent pritiska (–dp/dz) i poroznost (ε), kao i izračunatih vrednosti za gradijent pritiska usled trenja fluid–zid (jedn. (3) i (5)), određen je gradijent pritiska usled trenja čestice–zid:

$$F_p = -\frac{\mathrm{d}p}{\mathrm{d}z} - F_e - F_f \tag{19}$$

Na slici 3 su prikazani udeli gradijenata pritisaka, efektivne težine čestica, trenja fluid–zid cevi i čestice––zid cevi u ukupnom gradijentu pritiska u zavisnosti od brzine fluida. Pri malim brzinama fluida, kada je koncentracija čestica visoka, dominantni udeo u ukupnom gradijentu pritiska ima efektivna težina čestica. Sa po-

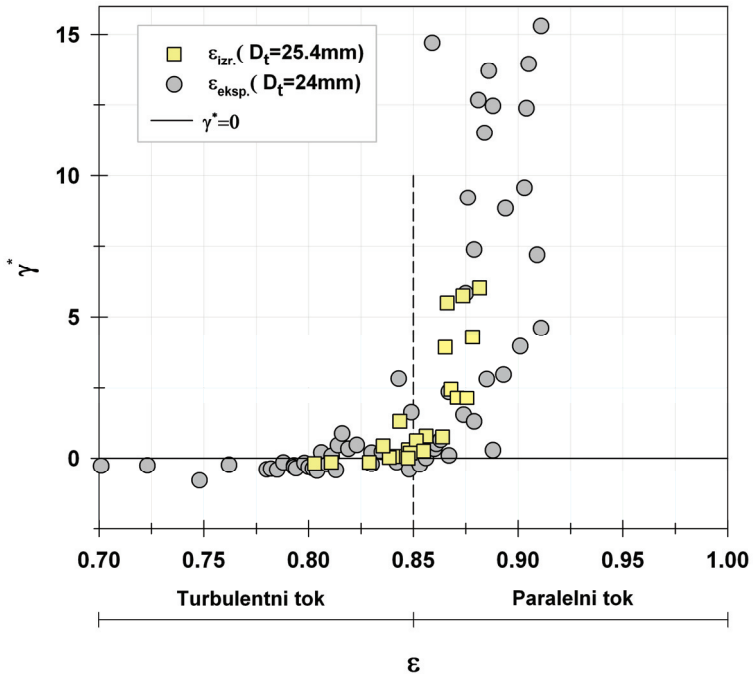

Slika 2. Zavisnost parametra γ^* od poroznosti vertikalnog dvofaznog toka (d_p = 1,94 mm).
Figure 2. Relationship of γ^* vs. ε for vertical two-phase liquid-solids flow (d_p = 1.94 mm).

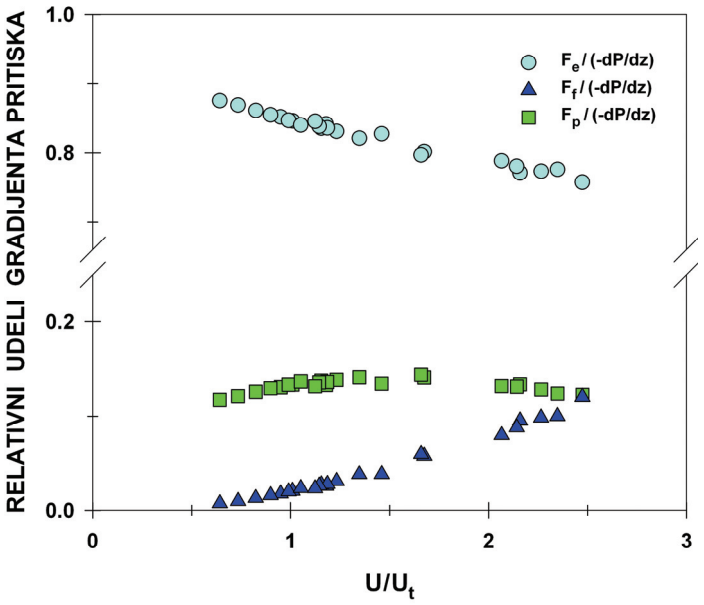

Slika 3. Relativni udeli gradijenta pritiska u zavisnosti od brzine fluida u vertikalnom toku smeše tečnost-čestice (d_p = 1,94 mm).
Figure 3. Variation of pressure drop ratios with superficial fluid velocity (d_p = 1.94 mm).

rastom brzine tečnosti raste i trenje fluid–zid kao i njegov udeo u ukupnom gubitku pritiska, sve do vrednosti oko 12%, pri brzini fluida $U/U_t \approx 2{,}5$.

Pri manjim brzinama fluida (do $U/U_t \approx 1{,}5$) gradijent pritiska usled trenja čestice–zid je veći od gradijenta pritiska usled trenja fluid–zid. Takođe, interesantno je napomenuti da je udeo trenja čestice–zid u ukupnom padu pritiska približno 14%, u celom opsegu ispitivanih brzina fluida ($0{,}6<U/U_t<2{,}5$). Takođe, na osnovu iznetog, može se zaključiti da se trenje čestice-zid transportne cevi u vertikalnom dvofaznom toku tečnost-čestice ne može zanemariti, što je u literaturi česta pretpostavka [26].

Koncept pseudofluida

S obzirom na to da pri transportu fluida kroz cev „struji“ smeša čestica i fluida, vertikalni tok čestica i fluida može se tretirati kao jednofazni tok fluida [27,28], okarakterisan svojom prividnom gustinom:

$$\rho_m = \varepsilon\rho_f + (1-\varepsilon)\,\rho_p \tag{20}$$

i viskoznošću [29]:

$$\mu_m = \mu \exp\left(\frac{5(1-\varepsilon)}{3\varepsilon}\right) \tag{21}$$

Po analogiji sa jednačinom (3) definiše se gradijent pritiska usled trenja smeše (pseudofluida) na zid transportne cevi:

$$F_w = 2\, f_w\, \rho_f \frac{U_m^2}{D_t} \tag{22}$$

gde je f_w koeficijent trenja pseudofluid-zid transportne cevi, odnosno:

$$f_w = \frac{F_w D_t}{2\rho_m U_m^2} \tag{23}$$

Srednja površinska brzina pseudofluida, U_m, predstavlja ukupni zapreminski protok čestica i fluida po jedinici površine transportne cevi [28]:

$$U_m = \frac{G_f}{\rho_f A_t} + \frac{G_p}{\rho_p A_t} \tag{24}$$

Modifikovani Reynoldsov broj za smešu fluid–čestice (pseudofluid) je:

$$\mathrm{Re}_m = \frac{D_t \rho_m U_m}{\mu_m} \tag{25}$$

U našim prethodnim ispitivanjima [28], za oblast paralelnog strujanja pseudofluida, koeficijent trenja pseudofluid–zid transportne cevi (f_w), u zavisnosti od modifikovanog Reynoldsovog broja za pseudofluid (Re_m), korelisan je jednačinom:

$$\frac{f_w}{2} = \frac{0{,}0395}{Re_m^{0{,}25}}, \quad 15000 < Re_m < 32000 \tag{26}$$

Na slici 4 je prikazana zavisnost eksperimentano dobijenih vrednosti koeficijenta trenja pseudofluid–zid transportne cevi (f_w), od Reynoldsovog broja pseudofluida (Re_m), kao i vrednosti koeficijenta trenja fluid–zid pri jednofaznom strujanju fluida (f_f).

Razlika u vrednostima koeficijenata trenja fluida i pseudofluida, posledica je prisustva čestica u toku

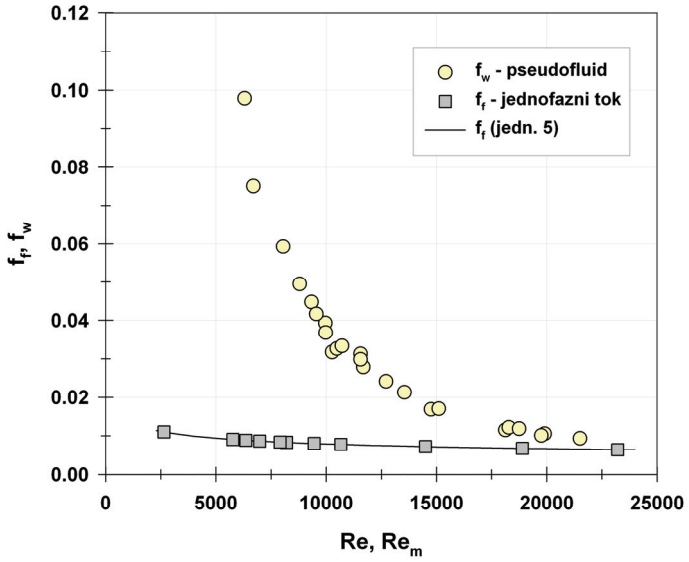

Slika 4. Zavisnost koeficijenata trenja fluida i pseudofluida o zid transportne cevi od Reynoldsovog broja fluida i pseudofluida.
Figure 4. Variation of f_f and f_w with Re number for the fluid and pseudofluid.

pseudofluida, koje svojim kretanjem, naročito u turbulentnom režimu transportnog toka, remete uniformnost pseudofluida.

Prenos toplote

Eksperimentalni podaci za koeficijent prelaza toplote u vertikalnom toku fluida i čestica u zavisnosti od površinske brzine fluida, prikazani na slici 5, pokazuju da vrednosti koeficijenta prelaza toplote rastu sa porastom brzine transporta. U opsegu Reynoldsovog broja 6000–15000 koeficijent prelaza toplote ima vrednosti oko 5 kW/m^{2}K. Ova vrednost koeficijenta prelaza toplote pripada turbulentnom režimu vertikalnog toka za koji je karakteristično nepravilno kretanje čestica čime one u izvesnoj meri mešaju fluid i stvaraju slične uslove prenosa toplote sa zida cevi. U ovoj oblasti je očigledno da presudan uticaj na prenos imaju prisutne čestice a ne brzina fluida. Na slici 5 su prikazani i eksperimentalni podaci za koeficijent prelaza toplote dobijeni u jednofaznom toku fluida. Primetno je intenziviranje prenosa toplote u režimu turbulentnog transportnog toka upravo zbog prisustva čestica koje se kreću i radijalno čime značajno smanjuju debljinu termičkog graničnog sloja i intenziviraju prenos.

Pri vrednostima Re>15000 dolazi do porasta koeficijenta prelaza toplote sa porastom brzine fluida. Ovo

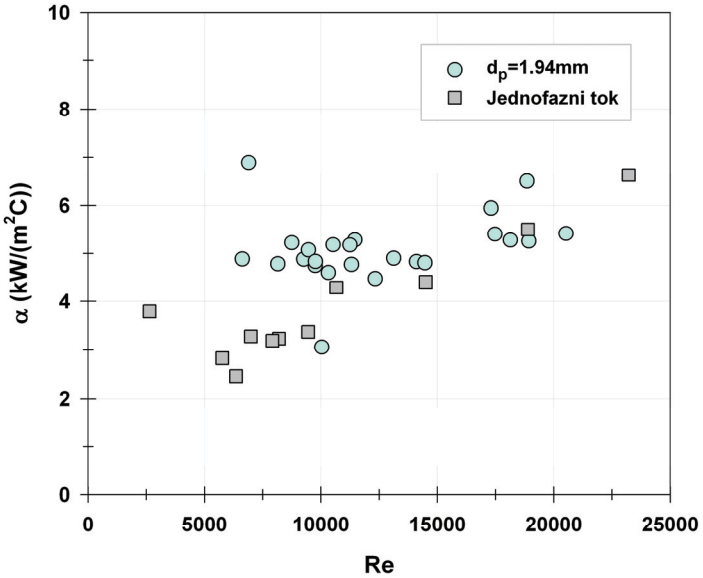

Slika 5. Zavisnost koeficijenta prelaza toplote od Reynoldsovog broja.
Figure 5. Relationship of α vs. Re.

predstavlja oblast paralelnog režima vertikalnog toka [6], gde čestice zbog pravolinijskog kretanja ne utiču značajno na prenos toplote već je od presudnog značaja brzina fluida. U ovom režimu i koncentracija čestica je značajno smanjena tako da se pri velikim brzinama približava jednofaznom toku.

Prenos mase

Na osnovu dosadašnjih ispitivanja o uticaju brzine strujanja na koeficijent prelaza mase u vertikalnom toku fluida i čestica, generalni zaključak je da koeficijent prelaza mase neznatno zavisi od promene brzine fluida [18].

Zavisnost koeficijenta prelaza mase od Reynoldsovog broja prikazana je na slici 6. Koeficijent prelaza mase u ispitivanom opsegu Reynoldsovih brojeva, približno je konstantan. Eksperimentani podaci pokazuju, da režimi strujanja vertikalnog toka čestica i fluida, ne utiču značajnije na prenos mase.

Na slici 6, takođe su prikazani podaci za prenos mase u jednofaznom toku. Poređenjem rezultata dobijenih u jednofaznom toku fluida i pri transportu čvrstih čestica očigledno je intenziviranje prenosa u turbulentnom režimu transportnog toka čestica. Ulaskom sistema u režim paralelnog toka, kao i kod prenosa toplote, postaje zanemarljivo prisustvo čestica na intenzitet prenosa.

Analogija prenosa

Dobijeni rezultati eksperimentalnih ispitivanja uporedjeni su u cilju uspostavlajnja analogije prenosa. S obzirom da se radi o sistemu sa prisutnim česticama, prvo je napravljeno poredjenje prenosa mase i toplote. Dobijeni podaci za prenos preračunati su na veličine: prenosa toplote (j_H) i prenosa mase ($j_{D,\text{eksp.}}$) – slika 7. Primetna je razlika u dobijenom rezultatu za prenos mase, tj. primetno su veće vrednosti faktora prenosa mase od vrednosti faktora prenosa toplote.

Eksperimentalna merenja prenosa toplote i mase vršena su na bitno različitim dužinama transportne cevi (L_H/D_t = 27,56, L_D/D_t = 0,73), tj. pri ovim merenjima termički granični sloj je bio formiran, dok su merenja prenosa mase vršena u zoni formiranja difuzionog graničnog sloja. Kao rezultat navedenih eksperimentalnih uslova dobijeni su veći koeficijenti prenosa mase.

Koristeći literaturnu korelaciju, za strujanje fluida u kratkim cevima [18]:

$$j_D = \frac{j_{D,\text{eksp.}}}{1+0{,}144\,\text{Re}^{0{,}25}(D_t / L_D)} \text{ za } L_D / D_t \le 10 \qquad (27)$$

korigovane vrednosti eksperimentalno dobijenog faktora prenosa mase, pokazuju bolje slaganje sa eksperimentalnim vrednostima faktora prenosa toplote (slika 7).

Na slici 7 je primećeno i da postoje različite vrednosti Reynoldsovog broja (ΔRe), za isti eksperiment, što je posledica pozicija zona merenja toplote i mase (slika 1), odnosno vrednosti srednjih temperatura u zonama merenja prenosa toplote ($T_{sr,f}$) i prenosa mase ($T_{\infty,2}$). Uticaj fizičkih parametara fluida na različitim temperaturama doveo je do različite vrednosti Re broja. Da bi se uporedili, dobijeni eksperimentalni rezultati su svedeni na iste uslove [22,30], korišćenjem zavisnosti (11):

$$(j_D)_{T_{sr,f}} = (j_D)_{T_{\infty,2}} \frac{(\text{Re}_m^{0,25})_{T_{\infty,2}}}{(\text{Re}_m^{0,25})_{T_{sr,f}}} \qquad (28)$$

Uvođenjem koncepta pseudofluida, čime se vertikalni tok tretira kao jednofazni, izvršeno je poređenje

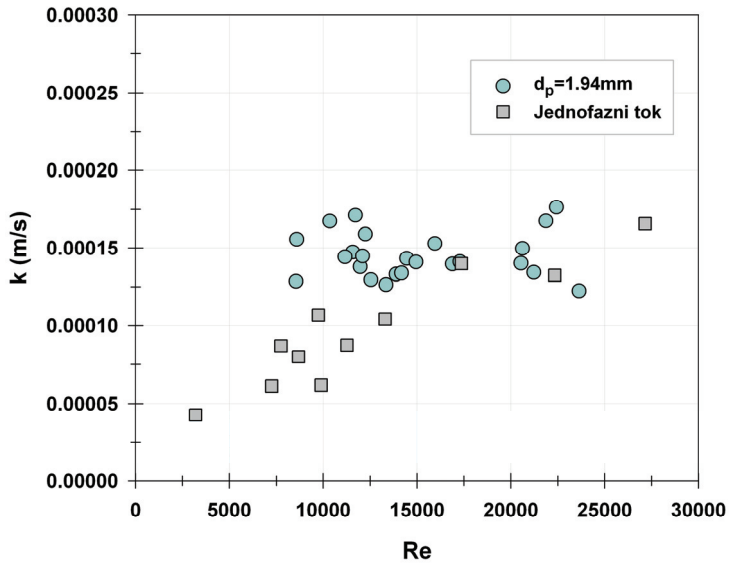

Slika 6. Zavisnost koeficijenta prenosa mase od Reynoldsovog broja.
Figure 6. Relationship of k vs. Re.

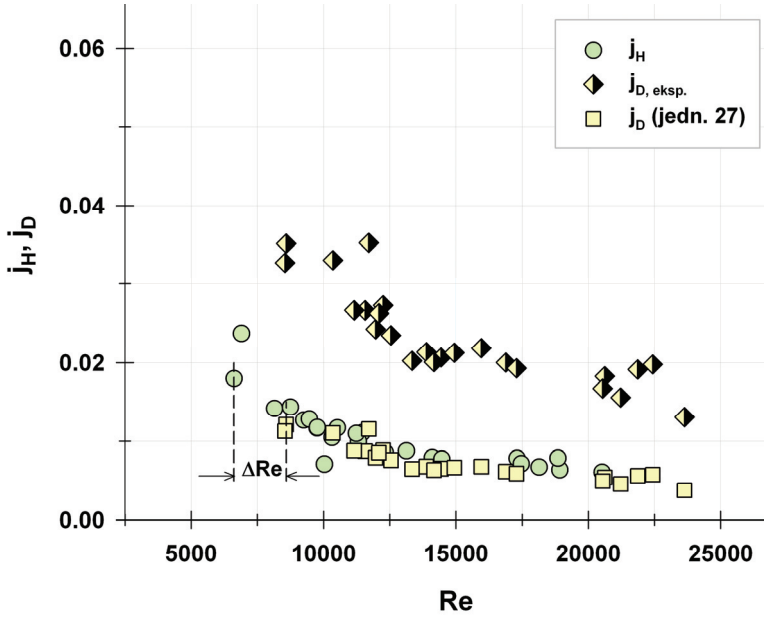

Slika 7. Prenos toplote i prenos mase, u vertikalnom dvofaznom toku fluid–čestice.
Figure 7. Heat and mass transfer in vertical two-phase fluid–particle flow.

parametara prenosa količine kretanja, toplote i mase, u formi Cilton-Colburnove analogije. Na slici 8 su prikazane zavisnosti koeficijenta trenja pseudofluida o zid transportne cevi, faktora prenosa toplote i faktora prenosa mase od Reynoldsovog broja pseudofluida.

Analogije prenosa količine kretanja, toplote i mase, postoji pri većim vrednostima Reynoldsovog broja pseudofluida, odnosno u oblasti paralelnog režima strujanja pseudofluida (Re_m>15000). Analogija prenosa toplote i mase postoji u celom opsegu ispitivanja.

Srednje apsolutno odstupanje podataka za prenos toplote ($j_{H,m}$) od podataka za koeficijent trenja pseudofluida o zid transportne cevi (f_w/2), je 12,74%, dok je srednje apsolutno odstupanje podataka za prenos mase ($j_{D,m}$) od trenja pseudofluida (f_w/2), 25,38% (Re_m> >15000).

ZAKLJUČAK

Izvršena su eksperimentalna ispitivanja istovremenim merenjem potrebnih parametara za definisanje

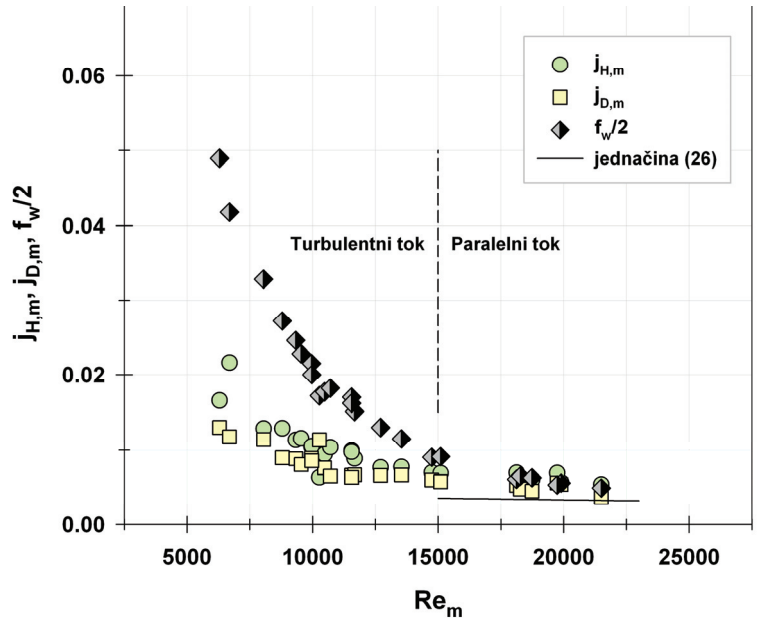

Slika 8. Analogija prenosa količine kretanja, toplote i mase u vertikalnom toku pseudofluida.
Figure 8. Analogy among momentum, heat and mass transfer, in vertical flow of pseudofluid.

prenosa količine kretanja, toplote i mase u vertikalnom transportnom sistemu tečnost–čestice.

Pri vertikalnom dvofaznom toku utvrđena su dva režima strujanja, turbulentni režim pri manjim brzinama i paralelni režim pri većim brzinama čestica i fluida. Promena režima strujanja definisana je parametrom γ^*. Karakteristična vrednost poroznosti za $\gamma^* = 0$ je $\varepsilon \cong 0{,}85$.

Rezultati ispitivanja prenosa toplote i mase su pokazali intenziviranje prenosa u režimu turbulentnog transportnog toka, u kome je evidentan uticaj čestica na termički i difuzioni granični sloj. U režimu paralelnog toka, čestice zbog manje koncentracije i pravolinijskog kretanja, ne utiču značajno na prenos toplote i mase, tako da se vrednosti koeficijenata prelaza približavaju vrednostima za jednofazni tok fluida.

U analizi rezultata korišćen je koncept pseudofluida, u cilju uspostavljanja analogije prenosa, u kome je vertikalni transportni tok tretiran kao jednofazni tok pseudofluida.

Eksperimentalno je dokazano da postoji analogija prenosa toplote i mase u celom opsegu ispitivanja, dok je analogija prenosa količine kretanja, tolote i mase utvrđena samo u paralelnom režimu transportnog toka.

Lista simbola

A_t površina poprečnog preseka transportne cevi, m^2
c_{pf} specifični toplotni kapacitet fluida, J/kg°C
c_{pp} specifični toplotni kapacitet čestica, J/kg°C
c^* rastvorljivost benzeove kiseline na granici faza, kg/m^3
c_f masena koncentracija benzeove kiseline u fluidu, kg/m^3
d_p prečnik čestica, m
D_t prečnik transportne cevi, m
D_{AB} koeficijent difuzije, m^2/s
f_f koeficijent trenja fluid-zid transportne cevi
f_p koeficijent trenja čestice–zid transportne cevi
f_w koeficijent trenja smeše "fluid–čestice"–zid transportne cevi
F_e gradijent pritiska usled efektivne težine čestica, Pa/m
F_f gradijent pritiska usled trenja fluid–zid transportne cevi, Pa/m
F_p gradijent pritiska usled trenja čestice–zid transportne cevi, Pa/m
F_w gradijent pritiska usled trenja smeše "fluid–čestice"–zid transportne cevi, Pa/m
g ubrzanje zemljine teže, m/s^2
G_f maseni protok fluida kroz transportnu cev, kg/s
G_p maseni protok čestica kroz transportnu cev, kg/s
j_D faktor prenosa mase, $\mathrm{Sh}/\mathrm{ReSc}^{1/3}$
$j_{D,m}$ faktor prenosa mase zid–pseudofluid, $\mathrm{Sh}/(\mathrm{Re_m Sc_m}^{1/3})$
j_H faktor prenosa toplote, $\mathrm{Nu}/\mathrm{RePr}^{1/3}$
$j_{H,m}$ faktor prenosa toplote zid-pseudofluid, $\mathrm{Nu}/(\mathrm{Re_m Sh_m}^{1/3})$
k koeficijent prelaza mase, m/s
L_H dužina zone zagrevanja, m
L_D dužina zone prenosa mase, m
m masa benzeove kiseline, kg
Nu Nuselt-ov broj ($= \alpha D_t / \lambda_f$)
P dinamički pritisak fluida u transportnoj cevi, Pa
Pr Prandtl-ov broj, ($= \mu c_{pf} / \lambda_f$)
$\mathrm{Pr_m}$ Prandtl-ov broj pseudofluida ($= \mu_m c_{pf}/\lambda_f$)
Re Reynoldsov broj ($= D_t \rho_f U / \mu$)
$\mathrm{Re_m}$ modifikovani Reynoldsov broj smeše fluid–čestice ($= D_t \rho_m U_m / \mu_m$)
S unutrašnja površina zida kolone sa koje se vrši prenos mase, m^2
Sc Schmidt-ov broj ($= \mu / \rho_f D_{AB}$)
$\mathrm{Sc_m}$ Schmidt-ov broj pseudofluida ($= \mu_m/\rho_m D_{AB}$)
Sh Sherwood-ov broj ($= k D_t / D_{AB}$)
t vreme, s
T temperatura, °C
T_0 temperatura površine, °C
T_∞ temperatura fluida, °C
$T_{\infty,1}$ temperature fluida u ulaznoj zoni zagrevanja, °C
$T_{\infty,2}$ temperature fluida u izlaznoj zoni zagrevanja, °C
$T_{0,1}$ temperatura zida transportne cevi na ulazu pare u omotač, °C
$T_{0,2}$ temperatura zida transportne cevi na izlazu pare iz omotača, °C
$T_{sr,f}$ srednja temperatura fluida ($= (T_{\infty,1} + T_{\infty,2})/2$), °C
U površinska brzina fluida u transportnoj cevi, m/s
U_m površinska brzina smeše fluid–čestice, m/s
U_t brzina slobodnog taloženja, odnosno odnošenja usamljene čestice, m/s
v brzina čestica u transportnoj cevi, m/s
V protok vode kroz mlaznicu (sl. 1)
V_A protok vode kroz dozer čvrstih čestica (sl. 1)
V_T protok vode kroz transportnu cev (sl. 1)
z vertikalna koordinata, m

Grčka slova

α koeficijent prelaza toplote, W/m^2 °C
Δ promena neke veličine
ε poroznost u transportnoj cevi
γ parametar režima strujanja smeše fluid–čestice, definisan jedn.(7)
γ^* bezdimenzioni parametar režima strujanja smeše fluid–čestice, definisan jedn.(8)
λ_f koeficijent toplotne provodljivosti fluida, W/m°C
μ dinamička viskoznost fluida, Pa·s
μ_m dinamička viskoznost smeše fluid-čestice, Pa·s
ρ_f gustina fluida, kg/m^3
ρ_p gustina čestica, kg/m^3
ρ_m gustina smeše "fluid–čestice" ($= \varepsilon\rho_f + (1-\varepsilon)\rho_p$), kg/m^3
δ_{sr} srednje apsolutno odstupanje:

$$= 100\frac{1}{n}\sum_{1}^{n}\frac{\left|j_{H,m}-\left(f_w/2\right)\right|}{j_{H,m}},$$

$$= 100\frac{1}{n}\sum_{1}^{n}\frac{\left|j_{D,m}-\left(f_w/2\right)\right|}{j_{D,m}}), \%$$

Zahvalnica

Ovaj rad je urađen uz finasijsku pomoć Ministarstva prosvete i nauke Republike Srbije (projekat br.172022).

LITERATURA

[1] J. Yerushalmi, A. Avidan, High-Velocity Fluidization, in Fluidization, Academic Press, London, 1985, pp. 225––291.

[2] J.R. Grace, High-Velocity Fluidized Bed Reactors, Chem. Eng. Sci. **45** (1990) 1953–1966.

[3] Y. Zheng, J.X. Zhu, J. Wen, S.A. Martin, A.S. Bassi, A. Margaritis, The Axial Hydrodynamic Behavior in Liquid-Solid Circulating Fluidized Bed, Can. J. Chem. Eng. **77** (1999) 284–290.

[4] A. Cecen-Erbil, Annulus leakage and distribution of the fluid flow in a liquid spout–fluid bed with a draft tube. Chem. Eng. Sci. **58** (2003) 4739–4745.

[5] Ž.B. Grbavčić, R.V. Garić, D.V. Vuković, Dž.E. Hadžismajlović, H. Littman, M.H. Morgan III., S.Đ. Jovanović, Hydrodynamic Modeling of Vertical Liquid-Solids Flow, Powder Technol. **72** (1992) 183–191.

[6] R.V. Garić-Grulović, Ž.B. Grbavčić, Z.Lj. Arsenijević, Heat Transfer and Flow Pattern in Vertical Liquid-Solids Flow, Powder Technol. **145** (2004) 163–171.

[7] K. Nakamura, C.E. Capes, Vertical Pneumatic Conveying: A Theoretical Study of Uniform and Annular Flow Models, Can. J. Chem. Eng. **51** (1973) 39–46.

[8] C.E. Capes, K. Nakamura, Vertical Pneumatic Conveying: An Experimental Study with Particles in the Intermediate and Turbulent Flow Regimes, Can. J. Chem. Eng. **51** (1973) 31–38.

[9] W.C. Yang, A Correlation for Solids Friction Factor in Vertical Pneumatic Conveying Lines, AIChE J. **24** (1978) 548–552.

[10] L.S. Leung, The Ups and Down of Gas-Solids Flow – A Review, in Fluidization, 3rd Eng. Found. Conf., Proc., N.H. Henniker, J. Matsen, J.H. Grace, Eds., Plenum Press, New York, 1980, pp. 25–68.

[11] R.B. Bird, W.E. Stewart, E.N. Lightfoot, Transport Phenomena, Wiley, New York, 1960.

[12] H. Konno, S.J. Saito, Pneumatic Conveying of Solids Through Straight Pipes, J. Chem. Eng. Japan **2** (1969) 211–217.

[13] R. Garić, Ž. Grbavčić, Lj. Rožić, Indirect determination of the particle-wall friction coefficient in the vertical pneumatic and hydraulic conveying of coarse particles, J. Serb. Chem. Soc. **61** (1996) 391–400.

[14] J.Y. Day, H. Littman, M. H. Morgan III, A New Choking Velocity Correlation for Vertical Pneumatic Conveying, Chem. Eng. Sci. **45** (1990) 355–360.

[15] N.J. Heppel, Measurement of the liquid-solid heat transfer coefficient during continuous sterilization of liquids containing particles, in Proceedings of 4th Int. Cong. on engineering and food, Edmonton, Alberta, Canada, 1985.

[16] S. Mankad, K.M. Nixon, P.J. Fryer, Measurements of particle-liquid heat transfer in systems of varied solids fraction, J. Food Eng. **31** (1997) 9–33.

[17] M. Barigou, S. Mankad, P.J. Fryer, Heat transfer in two-phase solid-liquid food flows: a review, Food Bioprod. Process. **76** (1998) 3–29.

[18] R.V. Garić-Grulović, Ž.B. Grbavčić, N.M. Bošković-Vragolović, Z. Lj. Arsenijević, Mass transfer in vertical liquid–solids flow of coarse particles, Powder Technol. **189** (2009) 130–136.

[19] J. Welty, C.E. Wicks, G.L. Rorrer, R.E. Wilson, Fundamentals of Momentum, Heat and Mass transfer, 5th ed., John Wiley and Sons, New York, 2008.

[20] M. Kuriyama, E. Harada, H. Konno, Analogy between heat and momentum transfer for the flow of solid-liquid suspension in a cylindrical pipe, Int. Chem. Eng. **30** (1990) 703–711.

[21] T.H. Chilton, A.P. Colburn, Mass transfer (absorption) coefficients: Prediction from Data on Heat Transfer and Fluid Friction, Ind. Eng. Chem. **26** (1934) 1183–1187.

[22] H.J. Perry, Chemical Engineer's Handbook, 6th ed., McGraw-Hill, New York, 1987.

[23] S. Kumar, S.N. Upadhyay, V.K. Mathur, On the Solubility of Benzoic Acid in Aqueous Carboxymethylcellulose Solutions, J.Chem. Eng. Data **23** (1978) 139–141.

[24] J.P. Couderc, in J. F. Davidson, R. Clift, D. Harrison (Eds.), Fluidization, Academic Press, London, 2nd ed., (1985), Ch. l. p. 1.

[25] Ž.B. Grbavčić, R.V. Garić, Dž.E. Hadžismajlović, S.Dj. Jovanović, D. V. Vuković, H. Littman, H. M. Morgan III, Variational Model for Prediction of the Fluid-Particle Interphase Drag Coefficient and Particulate Expansion of Fluidized and Sedimenting Beds, Powder Technol. **68** (1991) 199–211.

[26] P.A. Shamlou, Hydraulic Transport of Particulate Solids, Chem. Eng. Comm. **62** (1987) 233–249.

[27] R. Di Felice, P.U. Foscolo, L.G. Gibilaro, S. Rapagna, The interaction of particles with a fluid-particle pseudo-fluid, Chem. Eng. Sci. Short Commun. **46** (1991) 1873–1877.

[28] R.V. Garić-Grulović, Ž.B. Grbavčić, Z.Lj. Arsenijević, A pseudo-fluid representation of vertical liquid-coarse solids flow, J. Serb. Chem. Soc. **70** (2005) 775–784.

[29] E. Barnea, J. Mizrahi, A generalized approach to the fluid dynamics of particulate systems: Part 1. General correlation for fluidization and sedimentation in solid multiparticle systems, Chem. Eng. J. **5** (1973)171–189.

[30] A.P. Duduković, Proučavanje uticaja koaksijalno postavljenih objekata na prenos mase po zidovima cilindričniih cevi i na otpore strujanju adsorpcionom metodom, magistarski rad, TMF, Beograd, 1977.

SUMMARY

MOMENTUM, HEAT, AND MASS TRANSFER ANALOGY FOR VERTICAL HYDRAULIC TRANSPORT OF INERT PARTICLES

Darko R. Jaćimovski[1], Radmila V. Garić-Grulović[1], Željko B. Grbavčić[2], Mihal M. Đuriš[1], Nevenka M. Bošković-Vragolović[2]

[1]*IChTM - Department for Catalysis and Chemical Engineering, Njegoseva 12, Belgrade, Republic of Serbia*
[2]*Faculty of Technology and Metallurgy, Karnegijeva 4, Belgrade, Republic of Serbia*

(Scientific paper)

Wall-to-bed momentum, heat and mass transfer in the vertical liquid-solids flow, as well as in the single phase flow, were studied. The aim of this investigation was to establish the analogy among those phenomena. Also, effect of particle concentration on momentum, heat and mass transfer was studied. The experiments in hydraulic transport were performed in 25.4 mm I.D. cooper tube equipped with a steam jacket, using spherical glass particles of 1.94 mm in diameter and water as a transport fluid. The segment of the transport tube used for mass transfer measurements had internal coating made of benzoic acid. In the hydraulic transport two characteristic flow regimes were observed: turbulent and parallel particle flow regime. The transition between two characteristic regimes ($\gamma^* = 0$), occurs at a critical voidage $\varepsilon \approx 0.85$. The vertical two-phase flow was considered as the pseudofluid, and modified mixture-wall friction coefficient (f_w) and modified mixture Reynolds number (Re_m) were introduced for system characterization. Experimental data show that the wall-to-bed momentum, heat and mass transfer coefficients, in vertical flow of pseudofluid, for the turbulent regime are significantly higher than in parallel regime. Wall-to-bed, mass and heat transfer coefficients in hydraulic transport of particles were much higher than in single-phase flow for lower Reynolds numbers (Re < 15000), while for high Reynolds numbers (Re > 15000), there was not significant difference. The experimental data for wall-to-bed momentum, heat and mass transfer in vertical flow of pseudofluid in parallel particle flow regime, verify analogy among these three phenomena.

Keywords: Vertical flow liquid-particles • Flow regime • Momentum transfer • Heat transfer • Mass transfer • Analogy

Lipid oxidative changes in tradititional dry fermented sausage *Petrovská klobása* during storage

Branislav V. Šojić[1], Ljiljana S. Petrović[1], Anamarija I. Mandić[2], Ivana J. Sedej[2], Natalija R. Džinić[1], Vladimir M. Tomović[1], Marija R. Jokanović[1], Tatjana A. Tasić[2], Snežana B. Škaljac[1], Predrag M. Ikonić[2]

[1]*Faculty of Technology, University of Novi Sad, Novi Sad, Serbia*
[2]*Institute for Food Technology, University of Novi Sad, Novi Sad, Serbia*

Abstract

The influence of drying and ripeninig conditions (traditional and industrial) in the production of dry fermented sausage *Petrovská klobása*, on fatty-acid composition and oxidative changes in lipids, during 7 months of storage, was investigated. During the storage period, the sum of unsaturated fatty acids and the content of free fatty acids were significantly higher ($p < 0.05$), while the content of malondialdehyde was significantly lower in the sausage subjected to traditional conditions of drying and ripening. At the end of the storage period, contents of pentanal and hexanal in the sausage subjected to traditional conditions of drying and ripening (4.03 and 1.67 μg/g, respectively) were significantly lower ($p < 0.05$) in comparison with these contents in the sausage subjected to industrial conditions of drying and ripening. Traditional conditions of drying and ripening at lower temperatures have led to lower oxidative changes in lipids in traditional dry fermented sausage *Petrovská klobása* during storage period.

Keywords: *Petrovská klobása*, lipid oxidation, storage time.

Available online at the Journal website: http://www.ache.org.rs/HI/

SCIENTIFIC PAPER

UDC 637.523/.524.033

Hem. Ind. **68** (1) 27–34 (2014)

doi: 10.2298/HEMIND130118024S

In many European countries, demand for traditional food is constantly increasing. Traditional fermented sausages are products mainly produced in small family communities across Europe [1]. *Petrovská klobása* is a traditional dry fermented sausage produced in Bački Petrovac (the province of Vojvodina, Serbia) exclusively from pork meat and fat with the addition of red hot paprika powder, salt, garlic, caraway and sugar. Red hot paprika has a dominant role in the formation of aroma of the *Petrovská klobása*. This product is also characterized by a dark-red colour and firm consistency [2]. Fermented sausages are products that contain a high percentage of fat. Fat is responsible for numerous properties of the fermented sausages. From a physiological aspect, fat is an important source of energy as well as of essential fatty acids and liposoluble vitamins [3]. Products formed during lipolysis and lipid oxidation have an important role in the formation of odour, taste and texture of the final product. However, fermented sausages also show some negative properties as a consequence of high content of animal fat [4]. Lipolysis is the first step in the process of autooxidation of free fatty acids [5]. Moreover, the oxidative degradation of lipids of meat and meat products involves the oxidation of unsaturated fatty acids, especially polyunsaturated fatty acids and cholesterol [6]. Polyunsaturated fatty acids having three or more double bonds are primarily tied to phospholipids and are important for the development of the characteristic flavor state of food. The free radicals formed in lipid oxidation ($R^{\bullet}$) react with oxygen producing peroxy radicals ($ROO^{\bullet}$). In this initial process $ROO^{\bullet}$ react with several RH resulting in lipid hydroperoxides (ROOH), which are the main primary products of oxidation [7––9]. Moreover, during secondary oxidation changes in free fatty acids, compounds such as aldehydes, ketones, carboxylic acids are being created. Aldehydes are the main products formed during the lipid oxidation. In addition to the important role in the formation of aroma, aldehydes have also toxic properties. Even in small amounts aldehydes disturb the favorable sensory properties of food [10, 11, 12]. These compounds are very reactive in redox transformation and are intermediates in many biochemical reactions. Also, many aldehydes formed during the smoking process or from lipid peroxides are carcinogenic and can cause diseases of the digestive tract [13]. Propanal and hexanal are the most commonly used indicators of lipid oxidation in food due to their higher oxidative stability in detection compared to unsaturated aldehydes [14,15]. Propanal is a typical product of the n-3 oxidation and hexanal is a product of oxidative degradation of n-6 polyunsaturated fatty acids [16], while octanal is most probably a product of secondary oxidation of oleic acid [13]. Ansorena *et al*. [11], Misharina *et al*. [17] and Valencia *et al*. [9] studied the changes in the content of alde-

Correspondence: B.V. Šojić, Faculty of Technology, University of Novi Sad, Bul. Cara Lazara 1, 21000 Novi Sad, Serbia.
E-mail: bsojic@gmail.com
Paper received: 18 January, 2013
Paper accepted: 29 March, 2013

hydes as indicators of lipid oxidation in the fermented sausages during the storage period.

Vaštag *et al.* [18], Tasić *et al*. [2] and Ikonić *et al.* [19] studied the changes in proteins at different stages of ripening to the final degradation products (biogenic amines) during drying and ripening of *Petrovská klobása*, while Danilović *et al*. [20] dealt with identification of functional microflora in traditional dry fermented sausage *Petrovská klobása*.

However, it is little known about lipid oxidative changes in traditional dry fermented sausage *Petrovská klobása* during processes of drying, ripening and storage. The aim of this study was to comparatively examine the effect of drying and ripening methods (in the traditional and industrial conditions) and storage time on fatty-acid composition and oxidative changes in lipids of the traditional dry fermented sausage *Petrovská klobása*.

EXPERIMENTAL

Material

Sausages were produced in the winter period by using traditional manufacturing technology. Stuffing for the experimental sausages was made from chilled lean pork and fat in relation 85:15. Pork and firm fat tissue were grounded to pieces the size of 10 mm, and then the following ingredients were added: 2.50% red hot paprika powder, 1.80% salt, 0.20% raw garlic paste, 0.20% caraway and 0.15% crystal sugar. Starter cultures were not added so the sausages were subjected to spontaneous fermentation. Stuffing was hand-mixed, using a specific technique of tipping over and squashing for 10 min. The made stuffing was then filled into collagen casings (diameter of 55 mm). The sausages were subjected to straining during 24h. Subsequently sausages were smoked in chamber in the traditional way for 12 days with breaks. The atmospheric conditions during smoking were: 5–10 °C and *RH* 75–85%. After the smoking process, sausages were divided into 2 groups (T and I). Sausages of the T group were subjected to uncontrolled drying and ripening in traditional conditions *(t* = 0–10 °C, *RH* 95–80%) until achieving the moisture content of 35% (90 days). Sausages of I group were subjected to controlled drying conditions *(*8–10 °C, *RH* 90–75%) until achieving the moisture content of 35% (60 days). After the drying process, both groups of sausages were stored, *t* = 10 °C, *RH* = 75%, for 7 months.

Methods

Fatty acid profile determination

The method of Folch *et al.* [21] was used for the extraction of lipids from sausages. The fatty acid composition was determined by gas chromatography. For the preparation of fatty acid methyl esters, KOH/ /methanol was used. A Perkin–Elmer Varian, series 1400 gas chromatograph fitted with a packed column (3 m×3.0 mm, a stationary phase GP 10% SPTM-2330 on inert carrier 100/120 Chromosorb WAW) and flame ionization detection was used (Perkin-Elmer, Waltham, Massachusetts, USA). The temperature of both the injection port and the detector was 250°C. The carrier gas was N_2, with flow rate of 20 mL/min. The sample volume was 2.0 μL. The identification of the fatty acid methyl esters was by comparison of the retention times of peaks in the sample with those of standard pure compounds (Sigma-Aldrich Chemical, St. Louis, MO, USA). Fatty acids methyl esters were quantified as percentage of total methyl esters.

Determination of total fat

Total fat content of sausages was determined by application of ISO standard method [22].

Determination of free fatty acids

Free fatty acids content determined using the ISO standard method [23] and calculated as mg KOH/g lipid.

TBARS determination

TBARS (2-thiobarbituric acid reactive substances) test was performed using to the method of Bostoglou *et al*. [24], with modifications. Total volume of TCA was added to the sample and extraction was performed in ultrasonic bath XUB 12 (Grant Instruments, Cambridge, UK) [8]. Spectrophotometer Jenway 6300 (Jenway, Felsted, United Kingdom) was used. TBARS values were expressed as milligrams of malondialdehyde per kilogram of sample.

Aldehydes determination

Static headspace gas chromatographic (SHS–GC) analyses were performed on Agilent 7890A GC System (Agilent Technologies, Santa Clara, CA, USA) equipped with a capillary split/split less inlet, total electronic pneumatic control of gas flow, headspace auto sampler and FID. Static headspace (SHS) sampling was performed with the headspace sampler, CombiPAL System (CTC Analytics, Zwingen, Switzerland). A 2.5 mL HS syringe for CombiPAL was used, for the injection of 2.0 mL of vapor phase from the 10 mL headspace vials. Chromatographic conditions and aldehydes standard preparation is performed according to Mandić *et al*. [25]. Homogenized sample was accurately weighed (2.00 g) into 10 mL scruecapped headspace vial.

Statistical analysis

Statistical analysis was carried out using STATISTICA 8.0 (StatSoft, Inc., Tulsa, OK, USA). All data were presented as mean value with their standard deviation indicated (mean ± *SD*). Variance analysis (ANOVA) was

performed, with a confidence interval of 95% ($p < 0.05$). Means were compared by t-test and Duncan's multiple range test.

RESULTS AND DISCUSSION

Fatty-acid composition of sausages subjected to traditional (sausage T) and industrial conditions (sausage I) of drying and ripening at the end of the drying process as well as after 2 and 7 months of storage are shown in Table 1.

At the end of the drying process sums of saturated fatty acids in sausages T and I groups amounted to 33.28 and 33.74%, respectively. These values were not significantly different ($p > 0.05$). However, during the entire period of storage the amount of saturated fatty acids was significantly lower ($p < 0.05$) in sausages produced in traditional conditions (sausage T), compared to those in sausages produced in industrial conditions (sausage I) of drying and ripening. Content of oleic acid (C18:1) in sausages of T and I groups was 45.69 and 45.22%, respectively. These values did not change significantly ($p > 0.05$) during storage period. Similar results were also achieved by Ansorena *et al*. [11]. There was no significant difference ($p > 0.05$) in the content of oleic acid between the investigated sausages neither at the end of the drying process nor during storage period. Linoleic and linolenic acids contents did not differ significantly ($p > 0.05$) during storage period in sausages of T and I groups. Obtained results are likely caused by good oxidative stability of sausages during the storage period [9]. Except for differences in the content of linolenic acid after 2 months of storage, there were no significant differences ($p > 0.05$) in the content of polyunsaturated fatty acids (C18: 2 and C18: 3), nor in the sum of polyunsaturated fatty acids

Table 1. The fatty acid composition in traditional dry fermented sausage Petrovská klobása *during storage; xy – the values of the same column significantly differ with 95% probability (p < 0.05); abc – the values of the same row significantly differ with 95% probability (p < 0.05)*

Fatty acid	Sausage	End of drying	2 months	7 months
C14:0	T	1.14±0.00yb	1.19±0.00ya	0.96±0.03yc
	I	1.20±0.01x	1.25±0.04x	1.35±0.24x
C16:0	T	20.38±0.33	20.58± 0.32	19.98± 0.37y
	I	20.15±0.39b	21.14±0.29a	20.73±0.17xab
C17:0	T	0.15±0.01yc	0.34±0.02yb	0.45±0.00xa
	I	0.36±0.03xb	0.52±0.01xa	0.18±0.01yc
C18:0	T	11.61± 0.09yb	12.51± 0.09a	11.65±0.06b
	I	12.02±0.08xb	12.43±0.08a	11.78±0.20b
C16:1	T	2.48±0.06	2.52±0.11x	2.51±0.03x
	I	2.30±0.45a	1.97±0.02yb	1.83±0.02yb
C17:1	T	0.23±0.02yb	0.34±0.02xa	0.34±0.05xa
	I	0.35±0.06xa	0.24±0.01yb	0.24±0.02yb
C18:1	T	45.69±0.32	44.96±0.31	45.33±0.31
	I	45.22±0.22	44.94±0.23	45.18±0.34
C20:1	T	1.31±0.02yb	1.25±0.04yb	1.43±0.04ya
	I	1.38±0.04xb	1.38±0.03xb	1.63±0.27xa
C18:2	T	15.98±0.16a	15.22±0.14b	16.28±0.34a
	I	15.99±0.14a	14.95±0.33b	16.01±0.11a
C18:3	T	1.00±0.02	1.05±0.01x	1.08±0.11
	I	0.97±0.04	0.86±0.01y	1.05±0.27
ΣSFA	T	33.28±0.42b	34.62±0.22ya	33.01±0.34yb
	I	33.74±0.35c	35.35±0.32xa	34.05±0.27xb
ΣUFA	T	66 .69±0.33a	65.33±0.11xb	66.96±0.43xa
	I	66.20±0.03a	64.34±0.12yc	65.93±0.14yb
ΣPUFA	T	16.98± 0.15b	16.26±0.14c	17.36±0.23a
	I	16.96±0.11a	15.81±0.32b	17.06±0.16a
ΣUFA/ΣSFA	T	2.00±0.03a	1.89±0.01xb	2.03±0.01xa
	I	1.96±0.02a	1.82±0.02yb	1.94±0.01ya
ΣPUFA/ΣSFA	T	0.51±0.01b	0.47±0.00xc	0.53±0.00xa
	I	0.50±0.00a	0.45±0.01yb	0.50±0.01ya

between T and I sausage groups. Moreover, after 2 and 7 months of storage, the sum of unsaturated fatty acids, relation U/S and P/S, were significantly higher (p < 0.05) in sausages produced in traditional conditions of drying and ripening. Thus, lower temperatures during the drying process have led to lower oxidation changes in unsaturated fatty acids in the sausage produced in traditional conditions of drying and ripening. On the other hand Summo *et al*. [26] and Rubio *et al*. [27] found that during prolonged storage there is no significant change in fatty acid composition in fermented sausages.

Total fat content at the end of the drying process, and then until the end of storage period ranged in an interval of 31.23–41.08% in sausage T and from 32.67 to 44.93% in sausage I (Table 2).

Obtained values for total fat content are in accordance with data from literature for similar products in the type of fermented sausages [28]. During storage period, the total fat content was significantly lower (p < 0.05) in sausage produced in traditional conditions of drying and ripening (sausage T) in relation to this content in the sausage produced in industrial conditions of drying and ripening (sausage I). Obtained distinctions are likely a consequence of fast drying of the sausages subjected to industrial conditions of drying and ripening. Free fatty acid content at the end of the drying process were within the range of 7.11 mg KOH/g of lipids for the sausage I and 14.62 mg KOH/g of lipids for the sausage T (Table 2). The obtained results are in agreement with the results of Vukovic *et al*. [28] and Muguerza *et al.* [29], for similar products in the type of fermented sausages. In both sausages during the entire storage period, free fatty acid content was significantly increasing (p < 0.05). The increase in free fatty acids content is probably the result of endogenous enzymes activity as well as the activity of enzymes of microorganisms [5]. Moreover, lipolitic changes are followed by oxidative changes that compounds such as unsaturated fatty acids and cholesterol are easily subjected to [29]. Malondialdehyde is a typical degradation product formed during lipid oxidation of polyunsaturated fatty acids [30]. At the end of the drying process in sausages produced in traditional and industrial conditions of drying and ripening, the content of malondialdehyde was 0.79 and 1.25 μg/g, respectively (Table 3).

These results are in agreement with literature data [9,31] but in contrast with the results of other authors [27,32]. Unlike the sausage I, in the sausage T, malondialdehyde content was reduced after 2 months of storage period. Malondialdehyde values after 7 months of storage period were 0.16 μg/g for sausage T and 0.93 μg/g for sausage I, and were significantly lower (p < < 0.05) compared to the determined value of malon-

Table 2. Total fat content and free fatty acid content in traditional dry fermented sausage Petrovská klobása *during storage; xy – the values of the same column significantly differ with 95% probability (p < 0.05); abc – the values of the same row significantly differ with 95% probability (p < 0.05)*

Parameter	Sausage	End of drying	2 months	7 months
Total fat, %	T	31.23±0.46yc	35.24±0.25yb	41.08±0.33ya
	I	32.67± 0.29xc	39.66±0.23xb	44.93±0.27xa
Free fatty acid content, mg KOH/g lipid	T	14.62±0.01xc	26.02±0.01xb	35.09±0.01xa
	I	7.11±0.01yc	13.93±0.01yb	28.15±0.01ya

Table 3. Lipid oxidation parameters in traditional dry fermented sausage Petrovská klobása *during storage; xy – the values of the same column significantly differ with 95% probability (p < 0.05); abc – the values of the same row significantly differ with 95% probability (p < 0.05)*

Lipid oxidation parameter	Sausage	End of drying	2 months	7 months
TBARS, mg malondialdyde/kg	T	0.79±0.02ya	0.36±0.01yb	0.16±0.02yc
	I	1.25±0.00xb	1.63±0.02xa	0.93±0.00xc
Aldehydes content, μg/g				
Propanal	T	1.86±0.53b	0.94±0.01yb	32.59±1.57a
	I	2.68±0.26b	4.80±0.10xb	44.32±10.67a
Pentanal	T	1.16±0.38c	2.75±0.12xb	4.03±0.25ya
	I	1.61±0.08b	0.89±0.06yb	9.52±2.40xa
Hexanal	T	0.12±0.08b	0.05±0.00yb	1.67±0.07ya
	I	0.05±0.00b	0.22±0.01xb	4.94±1.29xa
Heptanal	T	0.24±0.07c	1.65±0.09xa	0.52±0.02b
	I	0.30±0.12c	1.40±0.05ya	0.86±0.21b
Octanal	T	3.24±1.26xa	0.22±0.03yb	0.35±0.01b
	I	0.87±0.11ya	0.50±0.03xb	0.61±0.17b

dialdehyde in sausages of T and I groups after 2 months of storage. Reduction of malondialdehyde values during storage was probably the result of interaction of malondialdehyde with compounds such as sugars, nitrites, amino acids [33]. Furthermore, malondialdehyde values at the end of the drying process as well as during the entire period of storage in the tested sausages were significantly lower ($p < 0.05$) in sausage subjected to traditional conditions of drying and ripening. The content of malondialdehyde is negatively correlated with the free fatty acid content in both sausages at the end of the drying process as well as during the entire period of storage. Berger *et al*. [34] suggest that lower values of free fatty acids content may be a result of intense oxidative changes. Obtained results show that oxidation of free fatty acids in the traditional dry fermented sausage *Petrovská klobása* during prolonged storage period (7 months) is slower when sausages are processed under conditions of drying and ripening at lower temperatures.

Table 3 shows aldehyde content at the end of the drying process and during 2 and 7 months of storage. Aldehydes are bearers of a wide range of fragrances and flavors in food [10]. Propanal was the most dominant aldehyde at the end of the drying process as well as during storage period in both groups of sausages. It is in agreement with literature data [15]. At the end of the drying process, the content of octanal was significantly higher ($p < 0.05$) in the sausage produced in traditional conditions of drying and ripening, while the content of propanal, pentanal, hexanal and heptanal in this sausage was not significantly different ($p > 0.05$) in relation to the sausage produced in industrial conditions of drying and ripening. After 2 months of storage, the content of propanal ranged in an interval of 0.94 μg/g in the sausage T to 4.80 μg/g in the sausage I. After that, the content of propanal was significantly increased ($p < 0.05$) in both groups of sausages. The content of hexanal in the tested sausages of T and I groups, after 2 months of storage was 0.05 and 0.22 μg/g, respectively. The obtained results of hexanal content are very similar to values that were found in fermented sausages by Josquin *et al*. [15] and Misharina *et al*. [17]. Following two months of storage, content of propanal, hexanal and octanal was significantly lower ($p < 0.05$) in the sausage produced in traditional conditions of drying and ripening, while the content and pentanal and octanal was significantly higher ($p < 0.05$) in this sausage in relation to the content of aldehydes in the sausage produced in industrial conditions of drying and ripening (Table 3). Moreover, after 7 months of storage, the content of propanal, pentanal and hexanal in both groups of sauseges was significantly increased ($p < 0.05$). Significant increase in the content of aldehydes during storage period in fermented sausages was determined by Valencia *et al*. [9], Ansorena *et al*. [11] and Misharina *et al*. [17]. However, the content of heptanal was significantly ($p < 0.05$) decreased after 2 months of storage while octanal showed a tendency to decrease at the completion of the drying process. Heptanal and octanal decreasing trend was present in both sausages, which is probably a consequence of an interaction of aldehydes with amino and -SH groups of proteins. These reactions lead to lower evaporability of aldehydes in detection [35]. Additionally, longer storage period, especially at higher temperatures, can lead to degradation of malondialdehyde and other aldehydes, leading to the formation of volatile compounds of lower molecular weight [36]. After 7 months of storage, propanal content ranged in an interval of 32.59 μg/g in the traditional, to 44.32 μg/g in the sausage produced under industrial conditions of drying and ripening. There was no significant difference ($p > 0.05$) between the obtained values of propanal content. Obtained results of propanal content in *Petrovská klobása* were much higher than the values found in fermented sausages by Josquin *et al*. [15]. On the other hand, the content of pentanal and hexanal was significantly lower ($p < 0.05$) in the traditional than in sausage produced in industrial drying conditions. Moreover, after 7 months of storage, values of heptanal in sausages of T and I groups amounted to 0.52 and 0.86 μg/g, respectively. The obtained values were similar to values determined in sausages from the Mediterranean by Ansorena *et al*. [11] and Demeyer *et al*. [37]. After 7 months of storage numerical values of the contents of heptanal and octanal in sausages produced in the traditional drying and ripening conditions were less than those values in sausages produced under industrial conditions of drying and ripening. However, the obtained values were not significantly different ($p > 0.05$). Lower values of the content of aldehyde after 7 months of storage in sausage T indicate better oxidative stability of the sausage produced in conditions of slower drying and ripening at lower temperatures.

CONCLUSION

During storage period, the sum of unsaturated fatty acids and the content of free fatty acids in the sausage produced in traditional conditions were significantly higher ($p < 0.05$) compared to the sausage produced in industrial conditions of drying and ripening while the sums of polyunsaturated fatty acids between the investigated sausages were not significantly different ($p > 0.05$). At the end of the storage period content of malondialdehyde and saturated aliphatic aldehydes was lower in the sausage produced in the traditional conditions of drying and ripening.

Obtained results indicate that conditions of slower drying and ripening at lower temperatures result in less lipid oxidative changes in traditional dry fermented sausage *Petrovská klobása* during prolonged storage period (7 months).

Acknowledgement

Research was financially supported by the Ministry of Education, Science and Technological Development, Republic of Serbia, project TR31032. These results are also part of the project No 114-451-3464/2013, which is financially supported by the Provincial Secretariat for Science and Technological Development, Autonomous Province of Vojvodina, Republic of Serbia.

REFERENCES

[1] R. Talon, I. Lebert, A. Lebert, S. Leroy, M. Garriga, T. Aymerich, E.H. Drosinos, E. Zanardi, A. lanieri, M.J. Fraqueza, L. Patarata, A. Lauková, Traditional dry fermented sausages produced in small –scale processing units in Mediterranean countries and Slovakia. 1. Microbial ecosystems of processing environments, Meat Sci. **77** (2007) 570–579.

[2] T. Tasić, P. Ikonić, A. Mandić, M. Jokanović, V. Tomović, S. Savatić, Lj. Petrović, Biogenic amines content in traditional dry fermented sausage Petrovská klobása as possible indicator of good manufacturing practice, Food Cont. **23** (2012) 107–112.

[3] A. Olivares, J. Navarro, M. Flores, Establishment of the contribution of volatile compounds to the aroma of fermented sausages at different stages of processing and storage, Food Cont. **115** (2009) 1464–1472.

[4] W. Visessanguan, S. Benjakul, S. Riebroy, N. Mongkol Yarchai, W. Tapingkae, Changes in lipid composition and fatty acid profile of Nham, a Thai fermented pork sausage, during fermentation, Food Chem. **94** (2006) 580–588.

[5] L. Zhao, Y. Jin, C. Ma, H. Song, H. Li, Z. Wang, S. Xiao, Physico-chemical characteristics and free fatty acid composition of dry fermented mutton sausages as affected by the use of various combinations of starter culturesand spices, Meat Sci. **88** (2011) 761–766.

[6] E. Hansen, D. Juncher, P. Henckel, A. Karlsson, G. Bertelsen, L.H. Skibsted, Oxidative stability of chilled pork chops following long term freeze storage, Meat Sci. **68** (2004) 185–191.

[7] G. Gandemer, Lipids in muscles and adipose tissues, changes during processing and sensory properties of meat products, Meat Sci. **62** (2002) 309–321.

[8] A. Mandić, Antioxidant activities of grape seed extracts from white grape varieties, Ph. D. Thesis, University of Novi Sad, Novi Sad, Serbia, 2007.

[9] I. Valencia, D. Ansorena, I. Astiasarán, Stability of linseed and antioxidants containing dry fermented sausages: A study of the lipid fraction during different storage conditions, Meat Sci. **73** (2006) 269–277.

[10] J.M. Bruna, E.M. Hierro, L. de la Hoz, D.S Mottram, M. Fernàndez, J.A. Juan Ordóñez, The contribution of *Penicillium aurantiogriseum* to the volatile composition and sensory quality of dry fermented sausages, Meat Sci. **59** (2001) 97–107.

[11] D. Ansorena, I. Astisaran, Effect of storage and packaging on fatty acids composition and oxidation in dry fermented sausages made with added olive oil and antioxidants, Meat Sci. **67** (2004) 237–244.

[12] W. Sun, Q. Zhao, H. Zhao, M. Zhao, B. Yang, Volatile compounds of Cantonese sausage released at different stages of processing and storage, Food Chem. **121** (2010) 319–325.

[13] V. Varlet, C. Prost, T. Serot, Volatile aldehydes in smoked fish: Analysis methods, occurrence and mechanism of formation, Food Chem. **105** (2007) 1536–1556.

[14] M. García-Iñiguezde Ciriano, C. García-Herreros, E. Larequi, I. Valencia, D. Ansorena, I. Astiasarán, Use of natural antioxidants from lyophilized water extracts of *Borago officinalis* in dry fermented sausages enriched in ω-3 PUFA, Meat Sci. **83** (2009) 271–277.

[15] N. Josquin, J. Linssen, J. Houben, Quality characteristics of Dutch-style fermented sausages manufactured with partial replacement of pork back-fat with pure, pre-emulsified or encapsulated fish oil, Meat Sci. **90** (2012) 81–86.

[16] M.A. Augustin, L. Sanguansri, O. Bode, Maillard reaction products asencapsulants for fish oil powders, J. Food Sci. **71** (2006) 25–32.

[17] C.F. Ross, D.M. Smith, Use of volatiles as indicators of lipid oxidation in muscle foods, Compr. Rev. Food Sci. Food Saf. **5** (2006) 18–25.

[18] T.A. Misharina, V.A. Andreenkov, E.A Vashchuk, Changes in the Composition of Volatile Compounds during Aging of Dry-cured Sausages, Appl. Biochem. Microbiol. **37** (2001) 413–418.

[19] Ž. Vaštag, Lj. Popović, S. Popović, Lj. Petrović, D. Peričin, Antioxidant and angiotensin-I converting enzyme inhibitory activity in the water-soluble protein extract from Petrovac Sausage (Petrovská Kolbása), Food Cont. **21** (2010) 1298–1302.

[20] P. Ikonić, Lj. Petrović, T. Tasić, S. Škaljac, M. Jokanović, M. Mandić, B. Ikonić, Proteolysis and biogenic amines formation during the ripening of Petrovská klobása, traditional dry-fermented sausage from Northern Serbia, Food Cont. **30** (2013) 69–75.

[21] B. Danilović, N. Joković, Lj. Petrović, K. Veljović, M. Tolinački, D. Savić, The characterisation of lactic acid bacteria during the fermentation of an artisan Serbian sausage (Petrovská Klobása), Meat Sci. **88** (2011) 668––674.

[22] J. Folch, M. Lees, G.H.S. A.Stanley, A simple method for the isolation and purification of total lipids from animal tissues, J. Biol. Chem. **226** (1957) 497–509.

[23] ISO 1443: Determination of total fat content, International Standards. Meat and Meat Products. International Organization for Standardization, Geneve, 1973.

[24] ISO 660: Determination of the acid value of the fat (Reference method). In:International Standards Animal

and Vegetable Oils and Fats. International Organization for Standardization, Geneve, 1996.

[25] N.A. Botsoglou, D.J. Fletouris, G.E. Papageorgiou, V.N. Vassilopoulos, A.J. Mantis, A.G. Trakatellis, Rapid, sensitive and specific thiobarbituric acid method for measurement of lipid peroxidation in animal tissue, food and feedstuff samples, J. Agric. Food Chem. **42** (1994) 1931––1937.

[26] A. Mandić, I. Sedej, M. Sakač, A. Mišan, Static Headspace Gas Chromatographic Method for Aldehydes Determination in Crackers, Food Analyt. Meth., 2012, DOI: 10.1007/s12161-012-9415-5.

[27] C. Summo, F. Caponio, A. Pasqualone, Effect of vacuum-packaging on the quality level of ripened sausages, Meat Sci. **74** (2006) 249–254.

[28] B. Rubio, B. Martínez, M. García-Cachán, J. Rovira, I. Jaime, Effect of the packaging method and the storage time on lipid oxidation and color stability on dry fermented sausage salchichón manufactured with raw material with a high level of mono and polyunsaturated fatty acids, Meat Sci. **80** (2008) 1182–1187.

[29] E. Muguerza, G. Fista, D. Ansorena, I. Astiasarán, J.G. Bloukas, Effect of fat level and partial replacement of pork backfat with olive oil on processing and quality characteristics of fermented sausages, Meat Sci. **61** (2002) 397–404.

[30] H. Ercoşkun, S.G., Özkal, Kinetics of traditional Turkish sausage quality aspects during fermentation, Food Cont. **22** (2011) 165–172.

[31] L. Hoz, M. D'Arrigo, I. Cambero, J. Ordóñez, Development of an n-3 fatty acid and α-tocopherol enriched dry fermented sausage, Meat Sci. **67** (2004) 485–495.

[32] S. Ruiz-Moyano, A. Martín, M. José Benito, A. Hernández, R. Casquete, M. de Guia Córdoba, Application of *Lactobacillus fermentum* HL57 and *Pediococcus acidi lactici* SP979 as potential probiotics in the manufacture of traditional Iberian dry-fermented sausages, Food Microbiol. **28** (2011) 839–847.

[33] D.R. Janero, Malondialdehyde and thiobarbituric acid reactivity as diagnostic indices of lipid peroxidation and peroxidative tissue injury, Free Radic. Biol. Med. **9** (1990) 515–540.

[34] R.G. Berger, C. Macku, J.B. German, T. Shibamoto, Isolation and identification of dry salami volatiles, J. Food Sci. **55** (1990) 1239–1242.

[35] G. Pignoli, R. Bou, M.T. Rodriguez-Estrada, E.A. Decker, Suitability of saturated aldehydes as lipid oxidation markers in washed turkey meat, Meat Sci. **83** (2009) 412–416.

[36] A. Andrés, R. Cava, J. Ventanas, E. Muriel, J. Ruiz, Lipid oxidative changes throughout the ripening of dry-cured Iberian hams with different salt contents and processing conditions, Food Chem. **84** (2004) 375–381.

[37] D. Demeyer, M. Raemaekers, A. Rizzo, A. Holck, A. De Smedt, B. ten Brink, B. Hagen, C. Montel, E. Zanardi, E. Murbrekk, F. Leroy, F. Vandendriessche, K. Lorentsen, K. Venema, L. Sunesen, L. Stahnke, L. De Vuyst, R. Talon, R. Chizzolini, S. Eorola, Control of bioflavour and safety in fermented sausages: First results of a European project, Food Res. Int. **33** (2000) 171–180.

IZVOD

OKSIDATIVNE PROMENE NA LIPIDIMA TRADICIONALNE SUVE FERMENTISANE KOBASICE *PETROVSKÁ KLOBÁSA* TOKOM SKLADIŠTENJA

Branislav V. Šojić[1], Ljiljana S. Petrović[1], Anamarija I. Mandić[2], Ivana J. Sedej[2], Natalija R. Džinić[1], Vladimir M. Tomović[1], Marija R. Jokanović[1], Tatjana A. Tasić[2], Snežana B. Škaljac[1], Predrag M. Ikonić[2]

[1]*Tehnološki fakultet, Univerzitet u Novom Sadu*
[2]*Institut za prehrambene tehnologije, Univerzitet u Novom Sadu*

(Naučni rad)

U radu je ispitan uticaj načina sušenje i zrenja (u tradicionalnim i industrijskim uslovima) tradicionalno proizvedene fermentisane kobasice (*Petrovská klobása*) tokom 7 meseci skladištenja na masno-kiselinski sastav i oksidativne promene na lipidima. Oksidativne promene na lipidima utvrđene su preko vrednosti malondialdehida i sadržaja zasićenih alifatičnih aldehida. Tokom skladištenja suma nezasićenih masnih kiselina i sadržaj slobodnih masnih kiselina izražen preko vrednosti kiselinskog broja bili su statistički značajno veći ($p < 0,05$) u kobasici podvrgnutoj tradicionalnim uslovima sušenja i zrenja. Sadržaj malondialdehida u kobasici proizvedenoj u tradicionalnim uslovima kretao se u intervalu od 1,27 mg/kg na kraju procesa sušenja do 0,16 mg/kg na kraju vremena skladištenja i bio je statistički značajno manji ($p < 0.05$) u odnosu na taj sadržaj u kobasici podvrgnutoj industrijskim uslovima sušenja i zrenja. Na kraju vremena skladištenja sadržaj pentanala i heksanala u kobasici podvrgnutoj tradicionalnim uslovima (4,03 i 1,67 μg/g, redom) bio je statistički značajno manji ($p < 0,05$) u poređenju sa tim sadržajem u kobasici podvrgnutoj industrijskim uslovima sušenja i zrenja (9,52 i 4,94 μg/g, redom). Tradicionalni uslovi sušenja i zrenja pri nižim temperaturama doveli su do manjih oksidativnih promena na lipidima Petrovačke kobasice.

Ključne reči: *Petrovská klobása* • Oksidacija lipida • Vreme skladištenja

Experimental design of fuse link with ceramic alloy: Cracking problem

Murat Şanyılmaz[1], Sermin Elevli[2]

[1]*Dumlupinar University, Institute of Natural and Applied Science, Kutahya, Turkey*
[2]*Ondokuz Mayis University, Industrial Engineering Department, Samsun, Turkey*

Abstract

Low-voltage (LV) fuse systems, which open a circuit by cutting the current when it exceeds a given value for an adequate period, are used in nonresidential, commercial and industrial buildings. LV-fuse systems consist of a fuse base, fuse link, and a detachable operating handle. The fuse link is made of a ceramic alloy. In this study, a full-factorial experimental design with two levels was used to solve the fracture problem of fuse links. In this scope, performance criteria (compressive strength), factors affecting the performance criteria (moisture ratio, shaping duration, drying duration and firing duration) and factor levels were determined in the initial stage. Main effects and interactions among factors were investigated, and factor-level combinations that maximize the compressive strength were determined according to the analysis results. Finally, the relationship between compressive strength and experimental factors was presented in the form of $f = y(x)$ for prediction purposes.

Keywords: analysis of variance; ceramic alloy; experimental design; fuse system; process improvement.

Available online at the Journal website: http://www.ache.org.rs/HI/

SCIENTIFIC PAPER

UDC 621.316.923:666.3

Hem. Ind. **68** (1) 35–41 (2014)

doi: 10.2298/HEMIND130118023S

Experiments are carried out under controlled conditions in order to discover an unknown effect, test or establish a hypothesis or illustrate a known effect. Traditional experiments, in which one factor is changed and other is kept constant, have some negative aspects in terms of workload, time and costs. In addition, it is not possible to determine potential interactions that occur between two or more factors. The term "designed experiment" or "experimental design" refers to conducting trials upon subject input factors of a system or process to certain purposeful modifications in an effort to determine the effects caused by those modifications on the output [1].

Central composite full factorial experimental designs investigate the effects of two or more factors or input parameters on the output response of a process. All levels of each factor in the experiment are made to match with each level of other factors in the experiment, thus ensuring that all potential combinations of the factors in determined levels are analyzed [2]. The general notation for a central composite full factorial experimental design run at b levels is b^k = # runs, where k is the number of factors. A 2^k full-factorial design is a special type of central composite full factorial experimental design that allows simultaneous operation of the impacts of two-level factors [3,4].

Problem-solving and process-improvement studies related to various fields of activity utilizing experimental design (ED) have increased, particularly in recent years. Studies by Savaşkan *et al.* [5], Williams [6], Moreb and Savsar [7], Temiz and Erol [8], Chan and Calleja [9], Esme *et al.* [10], Pınar *et al.* [11], Raksiri and Chatchaikulsiri [12], Rangabathan *et al.* [13] and Yan and Chyan [14] are good examples. Central composite factorial experimental designs; the Taguchi Method; and response-surface techniques were used in these studies. The studies mainly addressed manufacturing industry. In the present study, a 2^4 full-factorial design was used to solve the cracking problem of fuse link with ceramic alloy produced in the electrotechnical industry. Although there is already a considerable amount of research done in those areas, as far as the authors know there is no work reported utilizing an experimental design on fuse systems.

MATERIALS AND METHODS

Problem definition

A low-voltage (LV) fuse system is a fuse system that opens a circuit by cutting the current when it exceeds a given value for an adequate period of time. These systems are used in nonresidential, commercial and industrial buildings. LV-fuse systems consist of a fuse base, fuse link and a detachable operating handle [15].

This study focused on solving the cracking problem of low-voltage fuse systems, recurring problem in a company that manufactures electrical material with porcelain isolation. The company experienced the cracking problem in manufacturing fuse links after starting to use a new ceramic alloy from a local producer. Since cracks in the fuse system could cause an

Correspondence: S. Elevli, Ondokuz Mayis University, Industrial Engineering Department, Samsun, Turkey.
E-mail: sermin.elevli@omu.edu.tr
Paper received: 18 January, 2013
Paper accepted: 29 March, 2013

explosion or fire by disabling it in the case of a short circuit, they are very risky in terms of safety. For that reason, the "cracking problem" was one that should be solved.

Selection of response variable

The main cause for cracking was the temperature of the copper wire conducting current through the fuse system. Heat, which formed inside the fuse-link body from the copper wire, expanded water and air inside the sand placed in the body to keep temperature and compression low, creating compression inside the fuse-link body and causing it to crack. In order to overcome this problem, the following solution methods were considered:

1. Expansion of the fuse-link interior volume. (Increasing the volume of the sand placed inside the fuse-link body decreases the effect of temperature and compression).

2. Reducing the number of fuse wires from two to one. (The distance from the heat source to the body will increase and the body will be less heated. Furthermore, since each single wire has less volume than a double wire, it would be possible to increase the volume of the sand inside the body).

3. Improving the resistance to compression ratio by making certain modifications in the manufacturing of the fuse-link body.

To apply the first solution, the interior volume of the fuse-link body should be expanded. However, since no modification can be made to exterior dimensions due to standards, expansion of the interior volume will result in decreased body thickness, which might lead to problems such as reduced resistance to impacts. In the second method, the number of wires would be reduced to one in order to increase the interior volume of the fuse-link body. However, it would be necessary to increase the thickness of the wire to handle the current properly. Since this solution will require other high-cost modifications in terms of wire breakage and circuit opening at high voltage – the operation principle of the fuse system — it does not seem applicable at this stage.

For these reasons, it was decided that improving the resistance to compression in the fuse-link body by making modifications in the manufacturing parameters of the fuse link is the most feasible alternative. Thus, the response variable (performance criterion), which is the output of the experimental process under various settings within the data range, was determined to be "compressive strength of LV-fuse links."

Determination of factors and factor levels

The factors thought to have an effect on compressive strength of the LV fuse link are listed below [16,17]:

- humidity ratio of raw material,
- shaping time,
- drying time,
- drying temperature,
- firing time and
- firing temperature.

Since all of the products manufactured in the factory are fired in a common furnace and dried in a common drying furnace, it is not possible to change firing time and drying temperature. These two factors, which can also affect other products, are included in the uncontrollable-factors group. In this case, controllable factors, which affect performance criteria, were found to be humidity ratio, shaping time, drying time and firing temperature.

The humidity ratio for raw material used by the manufacturer is 5%. Since the humidity ratio recommended for ceramic materials is generally 4%, as an alternative to the existing situation a humidity ratio of 4% is appropriate.

Raw materials in the factory are shaped by a press. Since a short pressing time causes expansion and void formation inside the material immediately after the pressing process, shortening the material's resistance, applied pressure time should be extended as much as possible. On the other hand, pressing periods longer than five seconds will mean failure to achieve production targets. Finally, five seconds was chosen as an alternative to the currently used pressing time of three seconds.

When the material is kept in drying room for a prolonged time, the humidity ratio decreases which might cause burning of the material or formation of cracks during firing. For this reason, instead of currently used twelve-hour drying period, a nine-hour drying time was selected.

The firing temperature currently used is 1290 °C. However, increased firing temperatures are desirable for ceramic materials. Therefore, as an alternative, the furnace temperature should be increased to 1310 °C, the highest possible value.

The controllable experimental factors and their levels are presented in Table 1. In the next stages of the paper, the symbols of the factors will be used.

Table 1. Experimental factors and their levels

Factor	Symbol	Low Level (-1)	High Level (+1)
Humidity ratio, %	*A*	4	5
Shaping time, s	*B*	3	5
Drying ime, h	*C*	9	12
Firing temperature, °C	*D*	1290	1310

RESULTS AND DISCUSSION

Conducting experiments

In 2^k full factorial design, since experiments are conducted in all probable combinations of all factor levels, a total of 16 (2^4) different combinations were tested in this study. Experiments were executed in random order to correctly evaluate experimental errors. Five measurements were made for each combination of factors. After manufacturing under the conditions presented in Table 2, the fuse links were tested under internal pressure. During the tests, no horizontal or longitudinal external loads were placed on the bodies. One side of each body was sealed by a bolted-on lid, the other side by a fixed lid. Hydraulic oil was used in inlet of the bolted-on lid. Internal pressure was generated by a hand-operated hydraulic-compression testing device and displayed on the manometer. The internal pressure was increased until cracks appeared on the surface of the body, which led to substantial oil leakage. The maximum pressure value at which the body began to leak was recorded for every sample in the Table 2 as the performance criteria.

Data analysis

Minitab 16 statistical software was used for data analysis. In the first stage, a null hypothesis assuming that the main effects and interactions were equal to zero was tested using *F* test. In Table 3, *p* values smaller than 0.05 indicate that all effects and interactions are not equal to zero at a 5% significance level. In other words, compressive strength basically depends on the main effects of *A*, *B, C* and *D*, and the interaction of *B*C*.

At the second stage, the terms that seemed statistically insignificant compared to other effects were neglected and the related statistics were then calculated with the remaining variables. Table 3 also shows the estimated effects and coefficients of the model. The *t*-tests revealed that the main effects of *A*, *B*, *C*, and *D* are significant at the level 1%, and the interaction of *B*C* is significant at the 5% level.

The absolute value of the factor effects given in Table 3 corresponds to the relative effect of the related experimental factor on the response variable. Since the effect of *A* has the highest absolute value, this factor is the most effective independent variable on compressive strength. The order of factors according to their effects on compressive strength is *A*, *D*, *B*, *C* and *B*C,* starting with the highest value to the lowest.

The positive coefficient means that compressive strength increases as the factor is changed from the low to high levels given in Table 1. On the other hand, if the coefficient is negative, a reduction in the compressive strength occurs as the factor is changed from the low to high levels. That is, the sign of the factor effect shows which level of the factor will give a higher response value. For example, the fact that the raw-material ratio (*A*) is negative means that a low level of this factor will increase compressive strength more than a higher level of the same factor.

In any designed experiment, examining a model for predicted response is important. Coefficients in such a model show the impact of any effect on the response

Table 2. Design matrix [18]

Run No.	Experimental factor								Compressive strength MPa (mean±*SD*)
	Uncoded				Coded				
	A	*B*	*C*	*D*	*A*	*B*	*C*	*D*	
1	4	3	9	1290	–1	–1	–1	–1	4.16±0.16
2	5	3	9	1290	+1	–1	–1	–1	3.42±0.24
3	4	5	9	1290	–1	+1	–1	–1	4.40±0.14
4	5	5	9	1290	+1	+1	–1	–1	3.46±0.22
5	4	3	12	1290	–1	–1	+1	–1	4.25±0.08
6	5	3	12	1290	+1	–1	+1	–1	3.54±0.11
7	4	5	12	1290	–1	+1	+1	–1	4.60±0.22
8	5	5	12	1290	+1	+1	+1	–1	3.81±0.30
9	4	3	9	1310	–1	–1	–1	+1	4.53±0.17
10	5	3	9	1310	+1	–1	–1	+1	3.80±0.25
11	4	5	9	1310	–1	+1	–1	+1	4.67±0.19
12	5	5	9	1310	+1	+1	–1	+1	3.94±0.18
13	4	3	12	1310	–1	–1	+1	+1	4.51±0.16
14	5	3	12	1310	+1	–1	+1	+1	3.88±0.14
15	4	5	12	1310	–1	+1	+1	+1	5.03±0.19
16	5	5	12	1310	+1	+1	+1	+1	4.15±0.15

Table 3. Anova results and estimated coefficients of the model; S = 1.82774, R^2 = 86.93%, R^2 (pred.) = 84.72% and R^2 (adj.) = 86.04%

Source	D.F.	Sum of squares	Adj. mean squares	F	P
Main Effects	4	1621.01	405.25	113.91	0.000
A	1	1181.95	1181.95	332.21	0.000
B	1	121.28	121.28	34.09	0.000
C	1	60.38	60.38	16.97	0.000
D	1	257.40	257.40	72.35	0.000
2-Way interactions	6	34.69	5.78	1.63	0.155
*A*B*	1	8.78	8.78	2.47	0.121
*A*C*	1	0.53	0.53	0.15	0.701
*A*D*	1	1.38	1.38	0.39	0.536
*B*C*	1	22.58	22.58	6.35	0.014
*B*D*	1	0.90	0.90	0.25	0.616
*C*D*	1	0.53	0.53	0.15	0.701
3-Way interactions	4	3.11	0.78	0.22	0.927
*A*B*C*	1	0.53	0.53	0.15	0.701
*A*B*D*	1	0.03	0.03	0.01	0.929
*A*C*D*	1	1.65	1.65	0.46	0.498
*B*C*D*	1	0.90	0.90	0.25	0.616
4-Way interactions	1	4.28	4.28	1.20	0.277
*A*B*C*D*	1	4.28	4.28	1.20	0.277
Residual error	64	227.70	3.56	–	–
Total	79	1890.80	–	–	–
Term	Effect	Coefficient	Std. error of coef.	*T*	*P*
Constant		41.344	0.2043	202.32	0.000
A	–7.688	–3.844	0.2043	–18.81	0.000
B	2.462	1.231	0.2043	6.03	0.000
C	1.737	0.869	0.2043	4.25	0.000
D	3.587	1.794	0.2043	8.78	0.000
*B*C*	1.062	0.531	0.2043	2.60	0.011

for each increase of one unit. Coefficients given in Table 4 were used to create Eq. (1), which indicates the relationship between the compressive strength and experimental factors:

$$Y = 41.344 - 3.844 \times A + 1.231 \times B + \\ + 0.869 \times C + 1.794 \times D + 0.531 \times BC \quad (1)$$

To calculate compressive strength based on Eq. (1), coded values of independent variables presented in Table 1 should be used. In case of real values, Eq. (2) should be used:

$$Y = -153.3810 - 7.6875 \times A - 2.4875 \times B - \\ - 0.8375 \times C + 0.1794 \times D + 0.3542 \times BC \quad (2)$$

R^2 values show which part of the response variable is explained by model terms. These values are calculated using the sums of squares in analysis of the variance table. According to the analysis results, approximately 86% of variability in compressive strength is explained by the factors included in experimental design.

In order to make pair-wise comparisons among the levels of the experimental factors, the Tukey HSD Test was used. According to Table 4, means that do not share the same grouping letter are significantly different. Confidence intervals, including nonzero values, also indicate that significant difference between the factor levels exists.

The main-effect graphics of the factors are presented in Figure 1. The main effect of a factor is the difference between average response variables, which were calculated when the factor was at high and low levels. According to the main-effect graph, the more difference factor-level changes create on response variable, the more vertical the line combining the levels is. The factor *A* appears to have a greater effect on the response, as indicated by a steep slope.

"Interaction" refers to effect of a factor on performance criteria is being dependent on another factor. In the presented analyses, *B*C* interaction, which was found to be significant, was analyzed in a multivari chart in Figure 2. It can be clearly observed that the

Table 4. Grouping Information and 95.0% confidence Intervals

Experimental factor	Level	Mean	Grouping	Confidence Interval		
				Lower	Center	Upper
Humidity ratio-*A*	4	45.19	*A*	-8.532	-7.688	-6.843
	5	37.50	*B*			
Shaping time-*B*	5	42.57	*A*	1.618	2.462	3.307
	3	40.11	*B*			
Drying time-*C*	12	42.21	*A*	0.8927	1.737	2.582
	9	40.48	*B*			
Firing temperature-*D*	1310	43.14	*A*	2.743	3.587	4.432
	1290	39.55	*B*			

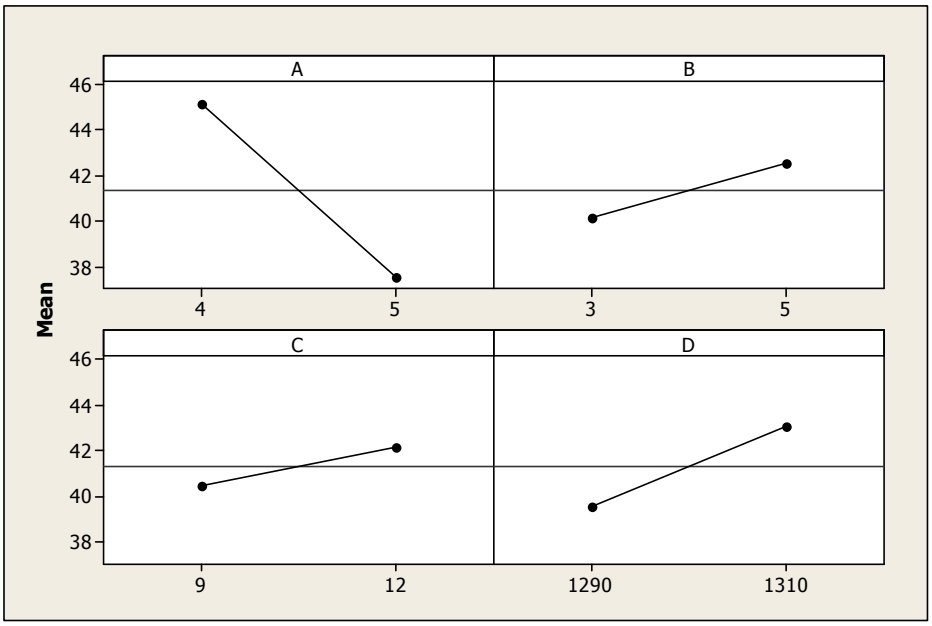

Figure 1. Main effects plot.

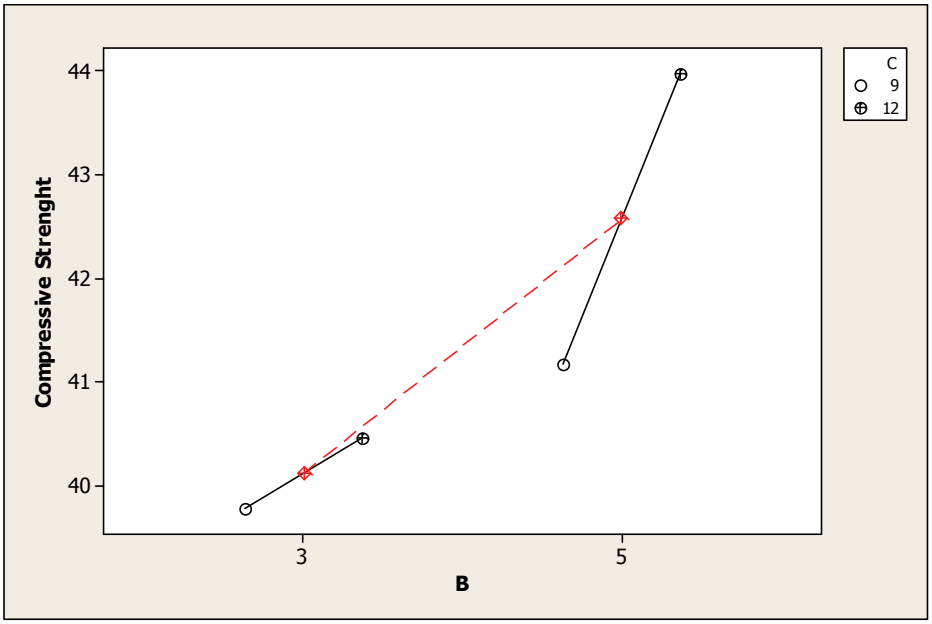

Figure 2. Multi-vari chart.

effect of the increase in drying time (*C*) on compressive strength was significantly different when shaping time (*B*) was at a high level (5 s).

A residual is the difference between an observation and its predicted value, according to the statistical model being studied. Experimental design is based on the assumption that residuals are normally and independently distributed. The residual graphs presented in Figure 3 were used to check the validity of this assumption. Since the residuals lie approximately along a straight line and a pattern — such as sequences of positive and negative residuals — is not observed, it was concluded that the residuals are normally and independently distributed.

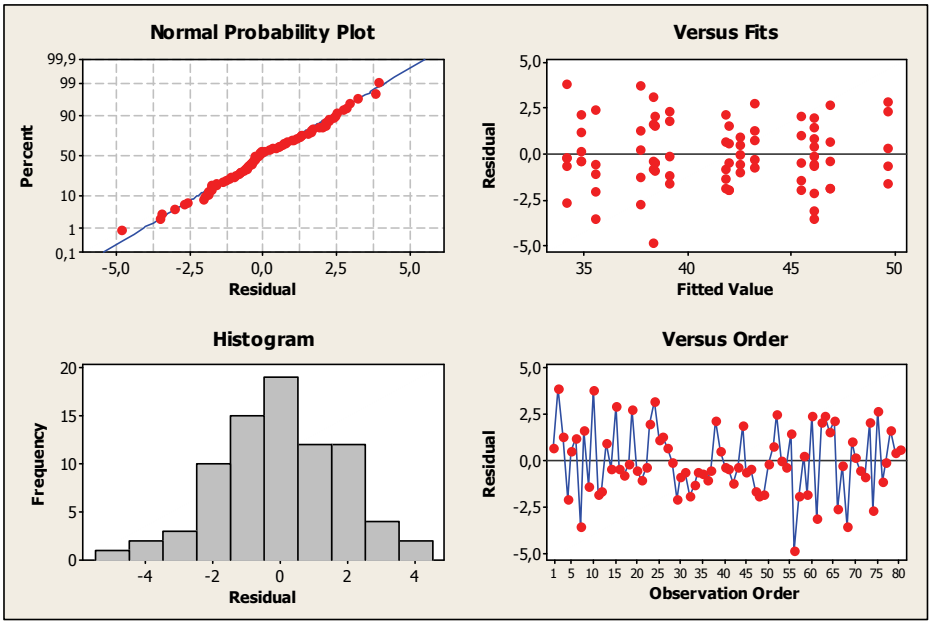

Figure 3. Residual plots.

CONCLUSIONS

Experimental design can be used at the point of greatest leverage to reduce design costs by speeding up the design process, reducing late engineering design changes and reducing product material and labor complexity. Designed experiments are also powerful tools to achieve manufacturing cost savings by minimizing process variation and reducing reworking, scrap and the need for inspection.

In the present study, a 2^4 full-factorial experimental design was used to overcome the problem of cracking in LV-fuse link bodies manufactured in the factory operating in electrotechnical industry. The ultimate goal is to improve the process of making the LV-fuse links. It was found that there was an interaction between shaping time and drying time; that the most important factor affecting the process was raw-material humidity ratio. The factor-level combination that maximizes the compressive strength were: humidity ratio of 4%, shaping time 5 s, drying time 12 h and firing temperature of 1310 °C. Achieved compressive strength with this combination was over 5 MPa, which eliminated the cracking problem. It would be suitable to use a new ceramic alloy in the manufacturing of fuse-link bodies as long as the manufacturing process has been modified based on the determined factor-level combinations.

REFERENCES

[1] N. Çömlekçi, Deney Tasarımı İlke ve Teknikleri, Alfa yayınları, Istanbul, 2003 (in Turkish).

[2] M.L. George, D. Rowlands, M. Price, J. Maxey, Lean Six Sigma Pocket Toolbook, McGraw-Hill, New York, 2005.

[3] W. Navidi, Statistics for Engineers and Scientist, McGraw-Hill Companies, Inc., NewYork, 2008.

[4] D.C. Montgomery, G.C. Runger, N.F. Hubele, Engineering Statistics, John Wiley &Sons, Inc., New York, 2001.

[5] M. Savaşkan, Y. Taptık, M. Ürgen, Deney tasarımı yöntemi ile matkap uçlarında performans optimizasyonu, İTÜ Dergisi/Mühendislik **3** (2004) 117–128 (in Turkish).

[6] P.H. Williams, Designing Experiments for the Modern Micro Industries, www.cepmagazine.org, pp. 58–63 (accessed February, 2006).

[7] A.A. Moreb, M. Savsar, Minimizing defects in tufting process using full factorial design, WSEAS Transact. Business Economics **4** (2007) 54–57.

[8] İ. Temiz, S. Erol, Bulanık akiş tipi çizelgeleme problemi için çok amaçli genetik algoritma, J. Fac. Eng. Arch. Gazi Univ. **22** (2007) 855–862 (in Turkish).

[9] F. Chan, H. Calleja, Design strategy to optimize the reliability of grid-connected pv systems, IEEE Transactions on Industrial Electronics, 56 (2009) 4465-4472.

[10] U. Esme, A. Sagbas, F. Kahraman, Prediction of surface roughness in wire electrical discharge machining using design of experiments and neural networks, Iran. J. Sci. Technol., B **33** (2009) 231–240.

[11] A.M. Pınar, A. Güllü, L. Paralı, A.F. Pınar, Hidrolik tahrikli eğrisel hareketlerin pozisyonlama doğruluğunun modellenmesi, 5. Uluslararası İleri Teknolojiler Sempozyumu (IATS'09), Karabük, 2009 (in Turkish).

[12] C. Raksiri, P. Chatchaikulsiri, CNC wire-cut parameter optimized determination of the stair shape workpiece, World Acad. Sci. Eng. Technol. **70** (2010) 101–106.

[13] S. Ranganathan, T. Senthilvelan, G. Sriram, Mathematical modeling of process parameters on hard turning of AISI 316 SS by WC Insert, J. Sci. Ind. Res. **68** (2009) 592––596.

[14] S.Z. Yan, L.S. Chyan, Performance enhancement of BOTDR fiber optic sensor for oil and gas pipeline monitoring, Opt. Fiber Technol. **16** (2010)100–109.

[15] Elektrik Elektronik Teknolojileri, http://elektroteknoloji.com/blog/bicakli-nh-sigortalar-nedir-parca-ve-gorevleri/ (accessed 05.07.2011).

[16] M.N. Rahaman, Ceramic Processing and Sintering, Marcel Dekker, Inc., New York, 2003.

[17] R.M. German, Sintering Theory and Practice, John Wiley & Sons, New York, 1996.

[18] M. Şanyılmaz, Deney tasarimi ve kalite geliştirme faaliyetlerinde taguchi yöntemi ile bir uygulama, Yüksek Lisans Tezi, Dumlupınar Üniversitesi, Fen Bilimleri Enstitüsü, 2006 (in Turkish).

IZVOD

EKSPERIMENTALNI DIZAJN ZA ISPITIVANJE PATRONA OSIGURAČA OD KERAMIČKE LEGURE: PROBLEM PUCANJA

Murat Şanyılmaz[1], Sermin Elevli[2]

[1]*Dumlupinar University, Institute of Natural and Applied Science, Kutahya, Turkey*
[2]*Ondokuz Mayis University, Industrial Engineering Department, Samsun, Turkey*

(Naučni rad)

Osigurači za niskonaponske sisteme (NN), koji prekidaju strujno kolo kada jačina struje prekorači maksimalnu dozvoljenu vrednost za izvestan period vremena, koriste se u nestambenim, industrijskim i komercijalnim objektima. NN sistemi se sastoje od baze osigurača, kontakta osigurača i odvojive radne ručice. Kontakt osigurača je izrađen od keramičke legure. U ovom radu je korišćen potpuni faktorijelni eksperimentalni plan, sa dva nivoa, da bi se rešio problem pucanja kontakta. Određivana je pritisna čvrstoća kao pokazatelj kriterijuma kvaliteta, a faktori od uticaja na pokazatelj kriterijuma kvaliteta bili su odnos vlage i trajanje oblikovanja, sušenja i pečenja, s tim da su faktori nivoa određivani u početnoj fazi. Ispitivani su glavni efekti i intereakcije između faktora, a kombinacije faktor–nivo koje maksimiziraju pritisnu čvrstoću bili su određeni u odnosu na rezultate analiza. Na kraju, odnos između pritisne čvrstoće i eksperimentalnih faktora predstavljen je u obliku $f = y(x)$ u svrhu predviđanja pritisne čvrstoće.

Ključne reči: Analiza varijanse • Keramička legura • Eksperimentalni dizajn • Sistem osigurača • Poboljšanje procesa

Antioxidant activity of ethanolic extract of *Penicillium chrysogenum* and *Penicillium fumiculosum*

Violeta D. Jakovljević[1], Jasmina M. Milićević[1], Jelica D. Stojanović[1], Slavica R. Solujić[2], Miroslav M. Vrvić[3]

[1]*University of Kragujevac, Faculty of Science, Institute of Biology and Ecology, Kragujevac, Serbia*
[2]*University of Kragujevac, Faculty of Science, Institute of Chemistry, Kragujevac, Serbia*
[3]*University of Belgrade, Faculty of Chemistry, Belgrade, Serbia*

Abstract

The aim of this study was to investigate the biological and chemical activity of the two fungi species, genus *Penicillium*, isolated from wastewater. For the selected species of fungi, different antioxidant activity assays were used: DPPH free-radical scavenging activity, total antioxidant activity, Fe^{2+}-chelating ability and Fe^{3+}-reducing power. Total phenolic content was also determined for ethanolic extract of mycelia. *Penicillium chrysogenum* ethanolic extract contained higher total phenolic content and better total antioxidant capacity as well as ferrous ion chelating ability. *Penicillium fumiculosum* ethanolic extract showed higher DPPH free-radical scavenging activity, as well as reducing power. Based on the obtained results it can be concluded that two types of fungi are potential new sources of natural antioxidants.

Keywords: DPPH free-radical scavenging, ferrous ion chelating ability, reducing power, total antioxidant activity, total phenols, *Penicillium*.

Available online at the Journal website: http://www.ache.org.rs/HI/

SCIENTIFIC PAPER

UDC 628:582.282.123.2:66.06:547.262

Hem. Ind. **68** (1) 43–49 (2014)

doi: 10.2298/HEMIND121102027J

Numerous pharmaceutical properties of medicinal mushrooms that have been used in the traditional oriental medicine are known, including anticancer, antimicrobial, anti-inflammatory and anti-atherosclerotic. In western civilization, the research on medicinal properties of fungi and yeast are relatively new as well as their use for therapeutic purposes. These fungi are a significant source of natural antioxidants due to their production of secondary metabolites. These are compounds such as polysaccharides, triterpenes, and triterpenoids, various acids (*e.g.*, ganodermic acid), β-glucan, vitamins and alkaloids. Phenolics or polyphenols, including flavonoids are the main secondary metabolites of medicinal plants, mushrooms and fungi, responsible for their antioxidant, antimutagenic and antitumor activity [1,2]. Screening of biological activity of endophytic fungi showed that they represent a significant source of new bioactive agents with potential use in medicine, agriculture and industry area. Biologically active ingredients are synthesized in the apex tissue of the hyphal strand of fungi and their extractions are carried out by solvents with different polarity. The biological activity of these substances depends on their chemical structure so that different extraction solvents resulted in various biologically active substances, with different levels of bioactivity. Ethyl acetate extract of endophytic fungi *Xylariaceae sp., Tolypocladium sp., Chaetomium glotosum, Chaetomium sp., Creosphaeria sp.*, contain an extraordinary antioxidant activity [3]. The aqueous extract of mycelium *Tolypocladium sp*. Ts-1 isolated from the fruiting body of a wild *Cordyceps sinensis,* has strong antioxidant activity and is a potential source of natural antioxidants [4]. The methanolic extracts of the fungi *Fusarium, Aspergillus, Penicillium* and *Mucor* species isolated from *L. nicotianifolia* showed significant antioxidant potential and the antioxidant nature of the extracts depended on the concentration [5]. Many species of fungi isolated from the soil, such as *Aspergillus fumigatus*, represent a potential source of natural antioxidants [6]. As active participants in the degradation of organic materials, primarily wood waste, fungi are exposed to large amounts of free radicals in nature. In order to survive and perform their task as scavengers in nature, fungi have developed specific defense mechanisms against a variety of toxins and free radicals.

The fungi species of genus *Penicillium* are very attractive organisms for production of useful protein and biologically active secondary metabolites. It was found that fungi produce pigments that inhibit the cholesterol biosynthesis by binding to the catalytic site of HMG-CoA reductase, a key enzyme in cholesterol biosynthesis [7] and scavenged DPPH radicals [8–10]. Penicillenols secreted by *Penicillium* sp showed biological activity against HL-60 cell lines [11]. Atrovenetin was isolated as a potential antioxidant in some species of *Penicillium* [12]. Different active substances were

Correspondence: Violeta D. Jakovljević, University of Kragujevac, Faculty of Science, Institute of Biology and Ecology, Kragujevac, Serbia.
E-mail: jakovljevicvioleta@gmail.com
Paper received: 2 November, 2012
Paper accepted: 9 April, 2013

isolated from *P. chrysogenum,* like alkaloids, carbohydrates, tannins and terpenoids by using different solvents.

The potential antioxidant activity of two fungal species: *Penicillium chrysogenum* and *Penicillium fumiculosum* was investigated in this study. The fungi were isolated from wastewater of the river basin of Lepenica and Western Morava, Serbia. Total phenolic content was determined by using Folin–Ciocalteu method. The antioxidant activity of alcoholic extract of fermentation broth was carried out by four assays: DPPH free - radical scavenging activity, total antioxidant activity, Fe^{2+}-chelating ability and Fe^{3+}-reducing power.

EXPERIMENTAL

Cultivation and extraction of tested fungal mycelia

The fungal species used in our study were isolated from the wastewaters originating from households, that were flowed directly into the riverbed of the Lepenica and Western Morava River (Serbia). The identification of fungi was carried out at the Institute of Biology and Ecology of Kragujevac, and later became part of our laboratory collection. Fungi were grown on potato dextrose agar at room temperature (28±1 °C) for 7 days. The 250 mL erlenmeyer flask, containing 100 mL of liquid PDB medium was sterilized for 15 min at 121 °C. The media was inoculated with 1 mL of spore suspension to yield specific density and incubated at room temperature for 5 days, with occasional stirring. After the completion of incubation, mycelia were separated from the liquid medium by filtration and drying at 50 °C. Dried mycelium was pulverized and extracted with ethanol (1:1, v/v) three times. The supernatant was separated by centrifugation at 5000 rpm for 10 min, fractions were pooled and ethanolic extract was concentrated under reduced pressure conditions to yield the final extract. Alcoholic extracts of all tested fungal species were stored in dark at 4 °C before being used for the bioactivity test.

DPPH radical scavenging assay

1,1-Diphenyl-2-picrylhydracyl (DPPH) radical scavenging activity was done according to the method by Takao *et al.,* with slight modification [13]. Working solution of extracts was made by diluting stock solution (1 mg/mL). DPPH was dissolved in methanol to obtain the concentration of 8 μg/mL. To 1 mL of DPPH solution, 1 mL of various concentrations of the extracts or the standard (ascorbic acid) solution were added separately. The reaction mixtures were incubated at 37 °C for 30 min, followed by measuring absorbance at 517 nm using pure methanol as blank reference. The DPPH scavenging activity (%) of the standard and extracts was determined using following equation:

$$\text{Inhibition} = [(Ac–As)/Ac]\times 100 \quad (1)$$

where: *Ac* is absorbance of the control sample and As is the absorbance of the tested sample.

Total antioxidant activity

The total antioxidant activity was determined by phosphomolybdenum method according to Prieto *et. al.,* [14]. To 1 mL of samples or standard 2 mL of reagent solution (ammonium molybdate, 4 mM, sodium phosphate ,28 mM and sulphuric acid, 0.6 M) was added and mixed vigorously. All the reaction tubes were incubated at 95 °C for 90 min. The absorbance was measured at 695 nm against blank (methanol) after cooling to room temperature. Ascorbic acid was used as standard. Reducing capacity of the extract has been expressed as the ascorbic acid equivalents.

Total phenolic contents

The total phenolic contents in the extract were determined according to the Folin–Ciocalteu method of Singleton and Rossi with some modifications [15,16]. To 1 mL of ethanolic extracts, 2 mL of 7.5% (w/v) sodium carbonate solution was added and vortexed vigorously. After 5 min, 1 mL of 1:10 diluted Folin––Ciocalteu's phenolic reagent was added and vortexed again. Same procedure was followed for the standard solution of gallic acid. All the tubes were incubated at room temperature for 30 min and the absorbance was measured at 765 nm. The total phenolic content of the extracts was expressed as gallic acid equivalent in mg/g (GAE mg/g extract).

Measurement of ferrous ion chelating ability

The ferrous ion chelating activity of the extracts was measured by the decrease in absorbance at 562 nm of the iron (II)–ferrozine complex according to Carter *et al.* [17] and Yan *et al.* [18]. To 1 mL sample (with different dilution), 1 mL of 0.125 mM $FeSO_4$ solution was added, followed by 1 mL of 0.3125 mM ferrozine. The test tubes were allowed to equilibrate at room temperature for 10 min. The absorbance was measured at 562 nm against blank. EDTA was used as positive control. The ability of the extract to chelate ferrous ion was calculated using the expression on the right of Eq. (1).

Reducing power assay

The reducing power assay was conducted as described by Oyaizu [19]. To 1 mL sample extract at different concentration, 2.5 mL of 0.2 M phosphate buffer, pH 6.6 and 2.5 mL of 1 % potassium ferricyanide were added and mixed vigorously. After incubation at 50 °C for 20 min, 2.5 mL of 10 % trichloroacetic acid was added to the mixture, followed by centrifugation at 3000 rpm for 10 min. Subsequently, 2.5 mL of upper layer of mixture was added to 2.5 mL of distilled water and 0.5 mL of 0.1 % ferric chloride, and the absorbance

of resulting solution was read at 700 nm against blank. Ascorbic acid was used as positive control.

RESULTS

The results of DPPH scavenger activity investigations of ethanolic extracts of tested fungi, showed that the maximum decolorization has *Penicillium fumiculosum* (51.34 %), followed by *P. chrysogenum* (37.42%) at the maximum concentration of 1000 μg/mL. The IC_{50} value against DPPH radical was found to be 974 μg/mL for *P. fumiculosum* and 1336 μg/mL for *P. chrysogenum* (Figure 1). These results indicate that ethanolic extract of tested fungi may serve as effective radical scavenging with DPPH free radical, converting them to stabile products.

The results of examinations of the total antioxidant activity of ethanolic extract of tested fungi are shown in Figure 2. By increasing the concentrations of ethanolic extract from 0.0156 to 1 mg/mL, the total antioxidant activity of the tested fungi also increased. The total antioxidant activity of *P. chrysogenum* (3.874 μg AA/g) was slightly higher in comparison to fungus *P. fumiculosum* (3.171 μg AA/g).

The results of ferrous ion chelating activity of alcoholic extract are shown in Figure 3. Ethanolic extract of *P. chrysogenum* showed better chelating activity than *P. fumiculosum* at concentrations ranging from 0.0125 to 0.500 mg/mL. By increasing the concentration of the extract from 0.5 to 1 mg/mL, the absorbance increased too, but the absorbance values were much higher compared to the blank absorbance. Therefore, this method cannot be successfully applied for higher concentrations of fungi extract, since the results of chelating capacity may not be valid. However, ethanolic extract of fungus *P. chrysogenum* showed a better chelating ability compared to standard EDTA solutions at concentrations from 0.0125 to 0.625 mg/mL.

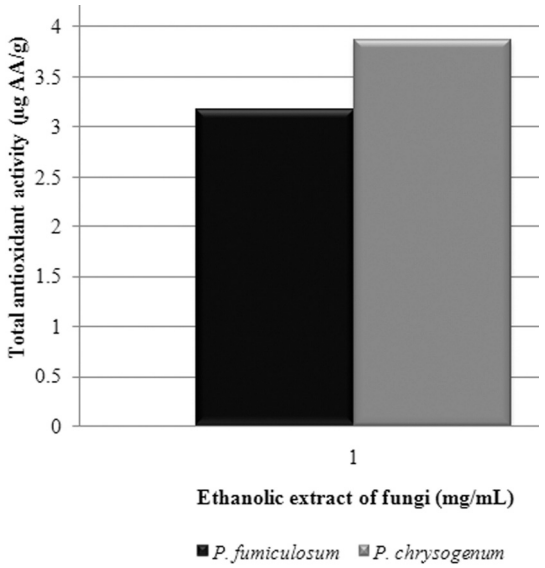

Figure 2. Total antioxidative activity of the ethanolic extract of mycelia.

The results of the total phenolic content in ethanolic extract of *P. chrysogenum* and *P. fumiculosum* are presented in Figure 4. The total phenolic content in the extract of mycelia is slightly different, but fungus *P. chrysogenum* (2.859 mg GAE/g) showed better yield compared to *P. fumiculosum* (2.109 mg GAE/g).

The reducing power of the ethanolic extract of mycelia for tested fungi is shown in Figure 5. The

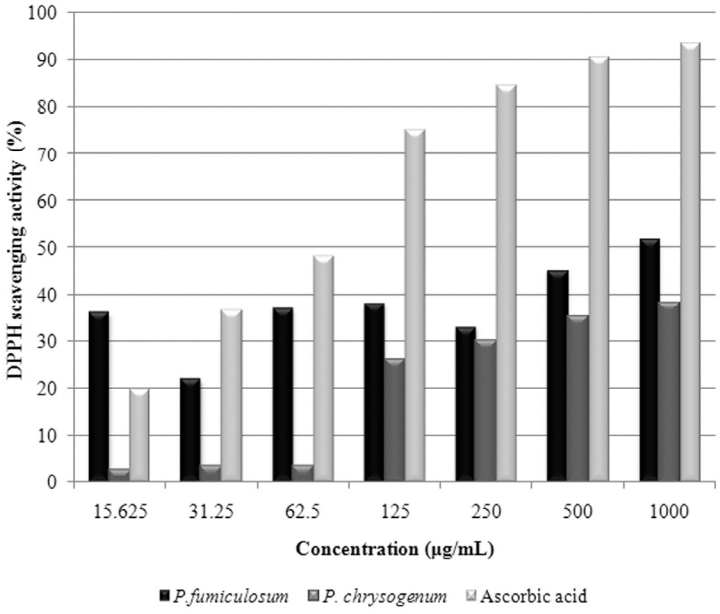

Figure1. DPPH scavenging activity of the ethanolic extract of mycelia against ascorbic acid.

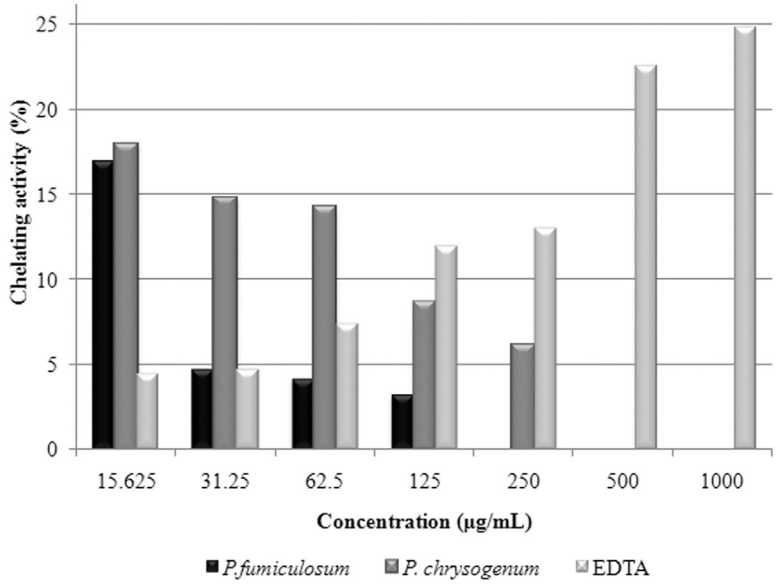

Figure 3. Chelating inhibition of the ethanolic extract of mycelia against EDTA.

reduction potential of the extracts exhibited a dose--dependent activity within a concentration range of 0.015625 to 1 mg/mL. Slightly better reducing ability has fungus *P. fumiculosum* than *P. chrysogenum* for all concentrations of the extract, but it is far less compared to synthetic antioxidant (ascorbic acid).

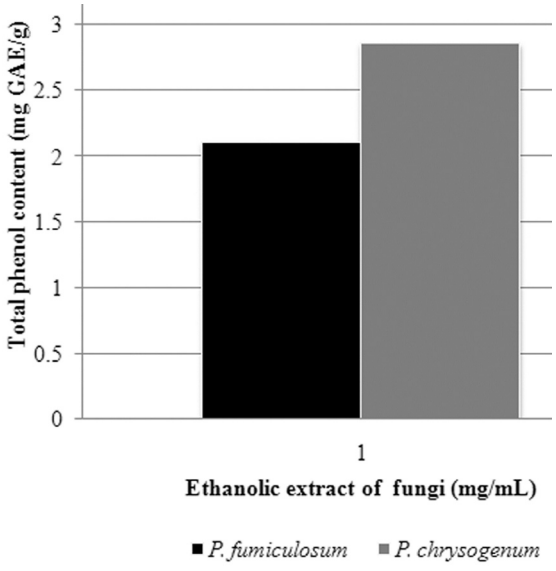

Figure 4. Total phenol content of the ethanolic extract of tested fungi.

DISCUSSION

The need for discovery and development of effective and safe antioxidants from natural sources has prompted scientists to search for sources of these bioactive resources among filamentous fungi. Antioxidant activity, which was examined using four different assays, was confirmed for both tested species of *Penicillium*.

Although DPPH scavenger activity of mycelia extract for tested fungi was lower in comparison to commercial antioxidant (ascorbic acid), activity of 1 mg/mL concentration extracts was between 37.42 and 51.34%. IC_{50} values for these two extracts were still higher than those of tested fungi from genus *Penicillium*. It was found that the percentage inhibition of DPPH free radical ranges from 72 to 88% for *Penicillium sp*. NIOMI-02 [20] to 91.1% in *P. citrinum* [21]. These differences may be attributed to various conditions in which the fungi are grown.

The results suggest that the extract from *P. fumiculosum* mycelium is a promising resource of natural antioxidants.

Alcoholic extract of *P. chrysogenum* showed higher total antioxidant capacity than *P. fumiculosum* at the concentration of 1 mg/mL.

Phenolic compounds have been associated with antioxidative action in biological systems, mainly due to their redox properties, which can play an important role in absorbing and neutralizing free radicals, quenching singlet and triplet oxygen or decomposing peroxides [22]. Extract of *P. chrysogenum* mycelium had higher content of total phenol (2.859 mg GAE/g) than extract of *P. fumiculosum* (2.109 mg GAE/g). However, total phenol content found in some fungi of genus *Penicillium* was much higher than in these two species. It was found that total phenolic content of *P. granulatum* was 7.01 mg GAE/g [23], while in endophytic *Penicillium* species was only 1 mg GAE /g [24].

The obtained results indicate that the total phenolic content correlated with the total antioxidant activity.

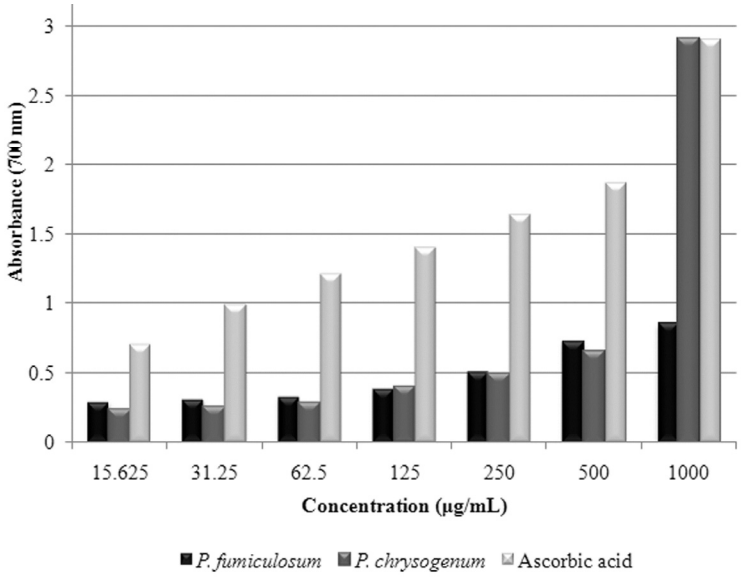

Figure 5. Reducing power (absorbance at 700 nm) of the ethanolic extract of mycelia.

Ferrous ions are most effective pro-oxidants and since they are commonly found in food, they can initiate lipid peroxidation and start a chain reaction that leads to food deterioration [25]. Their interaction with hydrogen peroxide in biological systems leads to formation of highly reactive hydroxyl radicals [26].

The mycelia extracts of tested fungi showed better chelating capacity compared to standard EDTA at concentrations of 0.00156 to 0.0625 mg/mL. Among two tested fungi, the extract of *P. chrysogenum* showed better ferrous ion chelating capacity. There was positive correlation between chelating activity and total phenol content. The results suggest that *P. chrysogenum* contains phenolic compounds/ligands that are the most effective in sequestering ferrous ions by intercepting all coordination sites of metal ions.

The presence of reductants (antioxidants) causes the reduction of the Fe^{3+}/ferricyanide complex to the ferrous form [27]. The extract of *P. fumiculosum* mycelium has better reduction potential than *P. chrysogenum*, as confirmed by reducing power assay. In this case, there is no correlation between total phenolic content and reducing power. These results indicate that the presence of some other compounds in extract, instead of phenol, act as reduktones and inhibit lipid peroxidation by donating a hydrogen atom, thereby terminating the free radical chain reaction [28]. These results are consistent with the results of the antioxidant activity obtained for other fungi, such as *Aspergillus candidus*, *A. fumigates*, *Cladosporium sp*, *Chaetomium sp*, and many mushrooms [29,30], lichens and medicinal plants [31–33].

CONCLUSION

The aim of this study was preliminary examination of whether the selected fungi species could be considered as source of potential natural antioxidants. The results show antioxidative activity of two species of fungi. The highest DPPH free-radical scavenging activity as well as reducing power was shown by *Penicillium fumiculosum.* On the other hand, ethanolic extract of *Penicillium chrysogenum* showed higher total antioxidant capacity, as well as chelating activity and total phenolic content. These results represent a good basis for further analysis of bioactive substances synthesized in fungi that exhibit different effects on antioxidant activity, which would be beneficial for their selective application in biotechnological processes in the future.

Acknowledgments

This research was financially supported by Ministry of Education, Science and Technological Development of the Republic of Serbia (Grant number III 43004).

REFERENCES

[1] E.M. Heider, J.K. Harper, D.M. Grant, A. Hoffman, F. Dugan, D.P. Tomer, K.L. O´Neill, Exploring unusual antioxidant activity in a benzoic acid derivative: a proposed mechanism for citrinin, Tetrahedron **62** (2006) 1199––1208.

[2] R. Yawadio Nsimba, H. Kikuzaki, Y. Konishi, Antioxidant activity of various extracts and fractions of *Chenopodium quinoa* and *Amaranthus spp*. seeds, Food Chem. **106** (2008) 760–766.

[3] P.Y. Zeng, J.G. Wu, L.M. Liao, T.Q. Chen, J.Z. Wu, K.H. Wong, *In vitro* antioxidant activities of endophytic fungi isolated from the liverwort *Scapania verrucosa*, GMR **10** (2011) 3169–3179.

[4] L.P. Zheng, L.W. Gao, J.Q. Zhou, Y.H. Sima, J.W. Wang, Antioxidant activity of aqueous extract of *Tolypocladium sp*. fungus isolated from wild *Cordyceps sinensis,* Afr. J. Biotechnol. **7** (2008) 3004–3010.

[5] N.K. Murthy, K.C. Poshpalatha, C.G. Joshi, Antioxidant activity of endophytic fungus *Phillosticta sp*. isolated from *Guazuma tomentosa*, J. Chem. Res. **3** (2011) 218––225.

[6] D.S. Arora, P. Chandra, Antioxidant activity of *Aspergillus fumigates,* ISRN Pharmacol. **2011** (2011), Article ID 619395, doi:10.5402/2011/619395.

[7] A.W. Albert, Lovastatin and Simvastatin-inhibitors of HMG-CoA reductase and cholesterol biosynthesis, Cardiology **77** (1990) 14–21.

[8] Y. Aniya, T. Yokomakura, M. Yonamine, K. Shimada, T. Nagamine, M. Shimabukuro, H. Gibo, Screening of antioxidant action of various molds and protection of *Monascus anka* against experimentally induced liver injuries of rats, Gen. Pharmacol. **32** (1999) 225–231.

[9] M.A. Dhale, S. Divakar, S. Umesh-Kumar, G. Vijayalakshmi, Isolation and characterization of dihydromonacolin-MV from *Monascus purpureus* for antioxidant properties, Appl. Microbiol. Biotechnol. **73** (2007a) 1197––1202.

[10] M.A. Dhale, S. Divakar, S. Umesh-Kumar, G. Vijayalakshmi, Characterization of dehydromonacolin-MV2 from *Monascus purpureus* mutant, J. Appl. Microbiol. **103** (2007) 2168–2173.

[11] Z.J. Lin, Z.Y. Lu, T.J. Zhu, Y.C. Fang, Q.Q. Gu, W.M. Zhu, Penicillenols from *Penicillium sp*. GQ-7, an endophytic fungus associated with *Aegiceras orniculatum*, Chem. Pharmaceut. Bull. **56** (2008) 217–222.

[12] Y. Ishikawa, K. Mortimoto, S. Iseki, Atrovenetin as a potent antioxidant compound from *Penicillium* species, JAOCS **68** (1991) 666–668.

[13] T. Takao, N. Watanabe, I. Yagi, K. Sakata, A simple screening method for antioxidants and isolation of several antioxidants produced by marine bacteria from fish and shellfish, Biosci. Biotechnol. Biochem. **58** (1994) 1780–1783.

[14] P. Prieto, M. Pineda, M. Aguilar, Spectrophotometric quantitation of antioxidant capacity through the formation of a phosphomolybdenum complex: specific application on the determination of vitamin E1, Anal. Biochem. **269** (1999) 337–341.

[15] V.L. Singleton, R. Orthofer, M. Lamuela-Raventos, Analysis of total phenols and other oxidation substrates and antioxidants by means of Folin-Ciocalteu reagent oxidants and antioxidants, Method Enzymol. **299** (1999) 152–178.

[16] V.L. Singleton, J.A. Rossi, Colorimetry of total phenolics with phosphomolybdic-phosphotungstic acid reagents, Am. J. Enol. Vitic. **16** (1965) 144–158.

[17] P. Carter, Spectrophotometric determination of serum iron at the submicrogram level with a new reagent – ferrozine, Anal. Biochem. **40** (1971) 450–458.

[18] L.Y. Yan, L.T. Teng, T.J. Jhi, Antioxidant properties of Guava fruits: comparison with some local fruits, SAJ **3** (2006) 9–20.

[19] M. Oyaizu, Studies on product of browning reaction prepared for glucose amine, Jap. J. Nut. **44** (1986) 307––315.

[20] M.A. Dhale, A.S. Vijay-Raj, Pigment and amylase production in *Penicillium sp* NIOM-02 and its radical scavenging activity, Int. J. Food Sci. Technol. **44** (2009) 2424–2430.

[21] D.S. Arora, P. Chandra, *In vitro* antioxidant potential of some soil fungi: screening of functional compounds and their purification from *Penicillium citrinum*. Appl. Biochem. Biotechnol. **165** (2011) 639–651.

[22] D. Huang, B. Ou, R.L. Prior, The chemistry behind antioxidant capacity assays, J. Agric. Food Chem. **53** (2005) 1841–1856.

[23] P. Chandra, D.S. Arora, Optimization of antioxidant potential of *Penicillium granulatum* Bainier by statistical approaches, ISRN Microbiol. **2012** (2012), Article ID 452024, doi: 10.5402/2012/452024.

[24] N.K. Murthy, K.C. Pushpalatha, C.G. Joshi, Antioxidant activity and phytochemical analysis of endophytic fungi isolated from *Lobelia nicotianifolia*, J. Chem. Pharm. Res. **3** (2011) 218–225.

[25] C.H. Lin, Y.T. Wei, C.C. Chou, Enhanced antioxidative activity of soybean koji prepared with various filamentous fungi, Food Microbiol. **23** (2006) 628–633.

[26] J.M.C. Gutteridge, B. Halliwell, The deoxyribose assay: an assay both for free hydroxyl radical and for site specific hydroxyl radical production, BJ Letters. **253** (1988) 932–933.

[27] I. Hinneburg, H.J.D. Dorman, R. Hiltunen, Antioxidant activities of extracts from selected culinary herbs and species, Food Chem. **97** (2006) 122–129.

[28] R. Xing, H. Yu, S. Lui, W. Zhang, Q. Zhang, Z. Li, P. Li, Antioxidant activity of differently regioselective chitosan sulfates *in vitro*, Bioorg. Med. Chem. **13** (2005) 1387––1392.

[29] M. Kozarski, A. Klaus, M. Nikšić, M. M. Vrvić, N. Todorović, D. Jakovljević, L.J.L.D. Van Griensven, Antioxidative activities and chemical characterization of polysaccharide extracts from the widely used mushrooms *Ganoderma applanatum*, *Ganoderma lucidum*, *Lentinus edodes* and *Trametes versicolor*, J. Food Comp. Anal. **26** (2012) 144–153

[30] A. Klaus, M. Kozarski, M. Niksic, D. Jakovljevic, N. Todorovic, L.J.L.D. Van Griensven, Antioxidative activities and chemical characterization of polysaccharides extracted from the basidiomycete *Schizophyllum commune,* LWT - Food Sci. Technol. **44** (2011) 2005–2011

[31] M.F Rios, C.M.G. Pajan, R. H. Galan, A.J.M. Sanchez, I.G. Gallado, Synthesis and free radical scavenging activity of a novel metabolite from the fungus *Colletotrichium gloeosporioides*, Bioorg. Med. Chem. Lett. **16** (2006) 5836––5839.

[32] L.M. Cheung, P.C.K. Cheung, Mushroom extracts with antioxidant activity against lipid peroxidation, Food Chem. **89** (2005) 403–409.

[33] S.S. Ali, N. Kasoju, A. Luthra, A. Singh, H. Sharanabasava, A. Sahu, U. Bora, Indian medicinal herbs as sources of antioxidants, Food Res. Int. **41** (2008) 1–15.

IZVOD

ANTIOKSIDATIVNA AKTIVNOST ETANOLNOG EKSTRAKTA *Penicillium chrysogenum* I *Penicillium fumiculosum*

Violeta D. Jakovljević[1], Jasmina M. Milićević[1], Jelica D. Stojanović[1], Slavica R. Solujić[2], Miroslav M. Vrvić[3]

[1]*Univerzitet u Kragujevcu, Prirodno–matematički fakultet, Institut za biologiju i ekologiju, Kragujevac, Srbija*
[2]*Univerzitet u Kragujevcu, Prirodno–matematički fakultet, Institut za hemiju, Kragujevac, Srbija*
[3]*Univerzitet u Beogradu, Hemijski fakultet, Beograd, Srbija*

(Naučni rad)

Cilj našeg rada bio je ispitivanje biološke i hemijske aktivnosti dve vrste gljiva iz roda *Penicillium* koje su izolovane iz otpadnih voda. Na odabranim vrstama gljiva *Penicillium chrysogenum* i *Penicillium fumiculosum* ispitivana je potencijalna antioksidativna aktivnost. Na etanolnom ekstraktu micelije testiranih gljiva, primenjene su četiri različite antioksidativne metode: sposobnost hvatanja DPPH slobodnih radikala, ukupni antioksidativni kapacitet, Fe^{2+}-helataciona aktivnost i Fe^{3+}-redukujući kapacitet. Ukupan sadržaj fenolnih jedinjenja u etanolnom ekstraktu micelija određen je metodom po Folin–Ciocalteu. Veća količina ukupnih fenola izmerena je u etanolnom ekstraktu micelije *P. chrysogenum* koji je ispoljio i veću ukupnu antioksidativnu i fero-helatacionu aktivnost. Sa druge strane, etanolni ekstrakt micelije *P. fumiculosum* imao je znatno veći procenat inhibicije DPPH slobodnih radikala i neznatno veći redukcioni kapacitet. Na osnovu dobijenih rezultata može se zaključiti da testirane vrste gljiva sintetišu različite sekundarne metabolite koji se mogu primeniti kao prirodni antioksidanti u prehrambenoj i farmaceutskoj industriji.

Ključne reči: Aktivnost hvatanja DPPH slobodnih radikala • Helataciona aktivnost • Redukujući kapacitet • Ukupan antioksidativni kapacitet • Ukupna količina fenola • *Penicillium*

Industrijske emergentne hemikalije u životnom okruženju

Mirjana B. Vojinović Miloradov[1], Maja M. Turk Sekulić[1], Jelena R. Radonić[1], Nataša B. Milić[2], Nevena N. Grujić Letić[2], Ivana J. Mihajlović[1], Maja Lj. Milanović[2]

[1]Univerzitet u Novom Sadu, Fakultet tehničkih nauka, Trg Dositeja Obradovića 6, 21000 Novi Sad, Srbija
[2]Univerzitet u Novom Sadu, Medicinski fakultet, Hajduk Veljkova 3, 21000 Novi Sad, Srbija

Izvod

Industrijske emergentne zagađujuće hemikalije, IEmH, su grupa supstanci koje se dominantno generišu industrijskom i antropogenom aktivnošću i putem otpadnih voda unose u sve sfere životne sredine. IEmH nisu uključene u rutinske monitoring programe, a sudbina, ponašanje i (eko)toksikološki efekti su još uvek nepoznati. IEmH se koriste u svakodnevnom životu, ali i doprinose stalnoj kontaminaciji vode, vazduha, biosistema i čoveka. Razvoj naprednih osetljivih analitičkih metoda i integralnih pasivnih uzorkivača omogućio je kvantifikovanje rezidua industrijskih emergentnih supstanci vrlo niskih koncentracija, reda veličine ppb, ppt i niže, u biotskim i abiotskim matriksima. Granične vrednosti i rutinski monitoring IEmH nije definisan zakonskom regulativom na nivou Evropske Unije. U okviru projekta NATO, *Science for Peace and Security*, 984087, sproveden je preliminarni skrining površinske vode Dunava u okolini Novog Sada i registrovano preko 140 različitih organskih emergentnih hemikalija.

Ključne reči: industrijske emergentne supstance, industrijska otpadna voda, Dunav, Novi Sad.

Dostupno na Internetu sa adrese časopisa: http://www.ache.org.rs/HI/

STRUČNI RAD

UDK 504.5(497.113Dunav):628:54

Hem. Ind. **68** (1) 51–62 (2014)

doi: 10.2298/HEMIND121110028V

Industrijske emergentne hemikalije, IEmH, su specifična grupa jedinjenja prepoznatih kao zagađujuće materije, koje se dominantno generišu sintezom u okviru različitih industrijskih grana kao što su hemijska, petrohemijska, metalna i farmaceutska industrija [1]. Maksimalno dozvoljene koncentracije i rutinski monitoring IEmH nije definisan postojećim zakonskim regulativama na nivou Evropske Unije, dok su sudbina, transport i ekotoksičnost IEmH za sada nepoznate i u fazi su istraživanja. Iako primarno detektovane u površinskim vodama velikih rečnih slivova, rezidue IEmH su kasnije kvalitativno registrovane i u zemljištu, vazduhu, sedimentu, rečnom mulju i drugim abiotskim, ali i biotskim matriksima [2,3]. Kao aktivne supstance brojnih industrijskih i komercijalnih proizvoda (različiti farmaceutici, dezinfekciona sredstva, proizvodi za ličnu i kućnu higijenu, deterdženti, usporivači gorenja, nanomaterijali, pesticidi, plastifikatori, antikorozivi i drugi), IEmH su prisutne u svakodnevnom životu [4]. Početkom 21. veka prepoznate su i detektovane kao potencijalno hazardne i vrlo toksične komponente sa mogućim kancerogenim, mutagenim i teratogenim efektima [5]. IEmH se detektuju u vrlo niskim koncentracijama reda veličine ppb, ppt i nižim, u površinskim i podzemnim vodama. Već dugi niz godina IEmH su prisutne u prirodnim recipijentima koji prihvataju industrijske i komunalne otpadne vode i različitim fizičko–hemijskim fenomenima difuzije i raspodele se transportuju i akumuliraju u biotskim i abiotskim matriksima. Veliki broj hemikalija, dominantno organskog i, u manjoj meri, neorganskog porekla, pripada grupi industrijskih emergentnih supstanci koje „poboljšavaju“ kvalitet svakodnevnog života, ali i doprinose konstantnoj kontaminaciji vode, vazduha, biosistema i čoveka. Prisustvo u površinskim vodama i migracija u podzemne vode, kao i mogućnost dospevanja u izvorišta pijaće vode, mogući su načini unosa IEmH i u organizam čoveka. Rad predstavlja prvi pregled i opis specifičnih fizičko–hemijskih svojstava emergentne grupe hemikalija na srpskom jeziku.

OSNOVNE FIZIČKO–HEMIJSKE KARAKTERISTIKE INDUSTRIJSKIH EMERGENTNIH HEMIKALIJA

Jedna od novoprepoznatih fizičko–hemijskih karakteristika IEmH u životnoj sredini je pseudoperzistencija. Permanentno ispuštanje otpadnih voda iz industrijskih postrojenja za prečišćavanje i direktan unos u akvatične sisteme bez tretmana, izazivaju pojavu nove karakteristike – pseudoperzistencije. I pored relativno kratkog vremena polu-života ($t_{1/2}$) pojedinih industrijskih emergentnih hemikalija, karakteristika konstantnog prisustva IEmH i delovanje na akvatične organizme kategorizuje ih u pseudoperzistentne polutante. U medijumima životne sredine, pseudoperzistencija emergentnih supstanci javlja se kao rezultat znatno veće brzine unosa od brzine razgradnje IEmH jedinjenja [6]. Degradacija IEmH fizičko-hemijskim procesima, kao što su hidroliza, fotoliza, oksido–redukcija, kao i biološkim procesima, od kojih je primarna mikrobiološka degra-

Prepiska: M.Lj. Milanović, Medicinski fakultet, Hajduk Veljkova 3, 21000 Novi Sad, Srbija.
E-pošta: majam021@yahoo.com
Rad primljen: 10. novembar, 2012
Rad prihvaćen: 29. mart, 2013

dacija, u sprezi je sa njihovom stalnom emisijom i unosom u akvatične medijume. Prisustvo IEmH u ekstremno niskim i vremenski konstantnim koncentracijama izdvaja ih od konvencionalnih polutanata. Nano i niže koncentracije emergentnih supstanci permanentno su prisutne u vodi i time se IEmH klasifikuju i u grupu „*trace*" polutanata. Biodostupnost emergentnih supstanci od posebnog je značaja za akvatične organizme, jer se biotski matriks akvatičnih ekosistema nalazi pod direktnim pritiskom permanentnog dejstva IEmH. Savremenim istraživanjima je potvrđeno da dugotrajna upotreba i ekspozicija niskim dozama IEmH ima različite negativne efekte na biosistem, kao i na čoveka. Procena i predviđanje sinergetskih i inhibitornih efekata koje IEmH imaju na zdravlje čoveka vrlo je zahtevan i kompleksan istraživački zadatak. Poseban problem u vezi sa pseudoperzistentnim industrijskim polutantima jeste nedostatak relevantnih toksikoloških studija koje bi pružile neophodne podatke o mehanizmima delovanja IEmH na živi svet, u dužem vremenskom periodu [5]. Postojeće studije, naročito u našem okruženju, ograničene su na konvencionalne polutante koji, prisustvom u površinskim vodama i njihovom intenzivnom eksploatacijom, negativno utiču na ukupan kvalitet svih biosistema [7].

Koncentracija industrijskih emergentnih hemikalija u akvatičnom medijumu može se predvideti na osnovu emisije supstance u otpadnu vodu, dostupnih podataka o transformaciji supstance u životnoj sredini i količini otpadne vode po stanovniku. Procenjena koncentracija u okolini (eng. predicted environmental concentration, PEC) izračunava se na sledeći način [8]:

$$PEC = \frac{\text{Elokal} \times F}{OVS \times \text{Kapacitet} \times \text{Faktor} \times R} \quad (1)$$

gde je *OVS* dnevna količina otpadne vode po stanovniku, *Kapacitet* – kapacitet postrojenja za tretman otpadne vode, *F* udeo emisije posmatrane supstance u površinsku vodu, *Faktor* – faktor koji uzima u obzir adsorpciju supstance na suspendovane čestice, *R* faktor razblaženja, a *Elokal* lokalna emisija supstance u otpadnu vodu.

Procena rizika po životnu sredinu može se izračunati poređenjem procenjene koncentracije supstance u okolini, PEC sa koncentracijom za koju je procenjeno da nema biološke efekte (eng. *predicted no-effect concentration*, *PNEC*). Odnos *PEC* i *PNEC* vrednosti treba da bude manji od jedinice, u suprotnom, rizik po životnu sredinu postoji i odgovarajuće mere moraju se preduzeti kako bi se rizik smanjio [8]:

$$\xleftarrow{\text{Rizik}} 1 < \frac{PEC}{PNEC} < 1 \xrightarrow{\text{Nema rizika}} \quad (2)$$

S obzirom na to da grupa IEmH pripada širokom opsegu različitih vrsta jedinjenja, generalizacija njihovih fizičko–hemijskih karakteristika nije jednostavna. IEmH su dominantno lipofilne supstance, bioakumulativne i biomagnifikativne, čije log K_{ow} vrednosti leže u opsegu od –4,36 do 10,76. Mogu biti i polarne i nepolarne, sa rastvorljivošću u vodi od najniže 10^{-56} do 2,4 g/l [9]. Takođe mogu imati kisela, bazna ili neutralna svojstva i nalaziti se u vidu jona ili zviterjona. Fizičko–hemijska svojstva industrijskih emergentnih polutanata, kao što su rastvorljivost, isparljivost, sposobnost adsorpcije i apsorpcije, biorazgradljivost, stabilnost, perzistencija, polarnost i druga značajno se razlikuju i zavise od molekulske strukture i broja asimetričnih ugljenikovih atoma. Korelacijom na osnovu molekulske strukture utvrđeno je da estri, aromatični alkoholi i nitril grupa povećavaju sposobnost biodegradacije dok aromatični amini, jodidi, nitro i azo grupa povećavaju perzistenciju jedinjenja. IEmH pokazuju akutnu i više hroničnu toksičnost, kao i ekotoksičnost, sa specifičnošću dejstva ekstremno niskih koncentracija. Fenomen niskih koncentracija u poslednje vreme izaziva posebnu pažnju, naročito kod emergentnih hemijskih supstanci koje ometaju rad endokrinog sistema živih organizama (eng. *Endocrine Disrupting Substances*, EDS) i predstavljaju rizik za ljudsko zdravlje i životnu sredinu. Poremećaj rada endokrinih žlezda posledica je stalnog prisustva IEmH, kao mono-molekula, u niskim koncentracionim nivoima. Piko i nano koncentracije IEmH odgovaraju biološkim koncentracijama hormona u organizmu, jer se broj molekula kreće u opsegu $6{,}023 \times 10^{11}$ do $6{,}023 \times 10^{14}$. Nano koncentracioni nivoi i nano dimenzije mono-molekula odlikuju supstance koje pripadaju IEmH. Karakteristične osobine određene grupe emergentnih jedinjenja su i veoma raznovrsna i razgranata, dendrimerna struktura molekula, što je uzrok niže viskoznosti rastvora jedinjenja u odnosu na rastvore linearnih molekula sličnog hemijskog sastava i molarne mase. Veliki broj krajnjih polarnih funkcionalnih grupa omogućavaju dobru rastvorljivost jedinjenja i mogućnost različitih hemijskih reakcija i transformacija.

Polarna i/ili nepolarna priroda čitavog ili jednog dela molekula pojedinih IEmH često sprečava/otežava difuziju jedinjenja kroz graničnu površinu dve faze heterogenog sistema, a time i disperziju molekula iz vode u druge medijume životne sredine. Difuzione karakteristike IEmH su u skladu sa vrednostima koeficijenata difuzije karakterističnim za gasovitu, tečnu i čvrstu agregaciju [10,11].

Biološko i fiziološko dejstvo većine emergentnih supstanci zavisi od niskih doza. Utvrđeno je da odnos dejstva i doze nije obavezno linearan, odnosno nemonotona funkcija povezuje biološke efekte i koncentraciju. Za neke hemikalije, u koje spada i određen broj industrijskih emergentnih supstanci, u novije vreme otkriveno je da je toksična aktivnost više izražena pri niskim dozama. Efekat niskih doza karakterističan je za

mnoge supstance sa hormonskom aktivnošću (hormonske otrove, supstance koje ometaju rad endokrinog sistema), sintetske estrogene (kontraceptivne pilule), dioksine, pesticide, plastične aditive (bisfenol A, ftalate), konzervanse (parabene, triklosan), surfaktante, deterdžente i sastojke kozmetičkih proizvoda (benzofenone). Efekti niskih ili vrlo niskih doza do sada nisu dovoljno izučavani, jer je niske koncentracione nivoe bilo teško kvantifikovati. Pod pritiskom javnosti i sve većeg broja naučnih istraživanja koja ukazuju na paradoks niskih doza, evropska agencija EFSA (eng. *European Food Safety Authority*) je odobrila reevaluaciju toksičnosti niskih doza hemikalija, dominantno emergentnih supstanci, sa primarnim fokusom na bisfenol A i druge supstance koje ometaju rad endokrinog sistema.

Razvoj industrijskih procesa, upotreba različitih sintetskih emergentnih hemikalija, fenomen konstantnog prisustva i procena štetnih efekata nano koncentracija IEmH, zahtevaju pomeraje tradicionalnih pristupa i formiraju potpuno nov koncept analize i zaštite životne sredine [1,5,6].

KLASIFIKACIJA EMERGENTNIH SUPSTANCI

Danas CAS (eng. *Chemical Abstract Service*) registruje više od 32 miliona različitih organskih supstanci, pri čemu je od toga 15 miliona komercijalno dostupnih jedinjenja. Nažalost, neophodna kontrola i regulativni propisi postoje samo za 250000 CAS supstanci, što iznosi 1,6% od komercijalno korišćenih emergentnih supstanci (EmS). Većina EmS nisu registrovane, nemaju katastarske liste i definisane MDK (maksimalno dozvoljena koncentracija) i EQT (eng. *Environmental Quality Target*).

U okviru Projekta NORMAN (od eng. *Network of reference laboratories for monitoring of emerging environmental pollutants*) [12] definisana je dinamično otvorena lista najfrekventnije registrovanih i kvantifikovanih emergentnih supstanci. Prema NORMAN, EmS su definisane kao „supstance detektovane u životnoj sredini koje nisu uključene u rutinske monitoring programe u EU i čija sudbina, ponašanje i (eko)toksikološki efekti još uvek nisu potpuno poznati“. Najnoviju NORMAN listu čini 27 kategorija (klasa) sa više od 750 registrovanih emergentnih supstanci, a spisak EmS se proširuje i dopunjuje novo-prepoznatim supstancama sa emergentnim karakteristikama i delovanjem. EmS se najčešće klasifikuju na osnovu namene i primene, specifičnih efekata koje izazivaju, izvora emisije i tipa ekspozicije.

Prema navedenim kriterijumima, jedinjenja koja spadaju u grupu EmS mogu biti industrijske hemikalije, sredstva za ličnu i kućnu higijenu, dezinfekciona sredstva i nusproizvodi, kozmetički proizvodi, deterdženti, aditivi i agensi, farmaceutici, antioksidansi, usporivači gorenja, aditivi u proizvodnji nafte i naftnih derivata, biološki metaboliti i toksini, steroidi, ksenoestrogeni i druge supstance koje ometaju rad endokrinog sistema, površinski aktivne materije, nanočestice, pesticidi i proizvodi njihove degradacije, različiti plastifikatori, teški metali, antikorozivi, boje, lakovi i druga.

Procena ekspozicije akvatičnih sistema bazira se primarno na detektovanju koncentracionih nivoa emergentnih hemijskih komponenata u uzorcima vode i sedimenta [13]. Za industrijske emergentne supstance neophodna je kvantifikacija i definisanje kompleksnih procesa kojima IEmH podležu u životnoj sredini kao što su sorpcija, desorpcija i particija između čvrste i tečne faze, formiranje kompleksa u rastvorima, abiotske i biološke transformacije, oksido-redukcioni i fotolitički procesi i dr. U domenu pomenutih prioriteta, adekvatno i efikasno uzorkovanje, kao i odgovarajuće instrumentalne analitičke metode od ključnog su značaja za dobijanje relevantnih podataka o koncentracijama i sudbini industrijskih emergentnih supstanci u akvatičnim ekosistemima.

UZORKOVANJE INDUSTRIJSKIH EMERGENTNIH HEMIKALIJA U VODENIM EKOSISTEMIMA

Usavršavanje savremenih analitičkih metoda, prvenstveno izuzetno osetljive i visoko selektivne masene spektrofotometrije, doprinelo je razvoju detektovanja rezidua emergentnih supstanci ekstremno niskih koncentracija u svim tipovima akvatičnih sistema [14]. Ranija istraživanja su bila uglavnom fokusirana na nepolarna i slabo polarna jedinjenja, kao što su PCBs (polihlorovani bifenili), PAHs (policiklični aromatični ugljovodonici), hlorovani rastvarači ili hlorovani pesticidi, kao što su DDT i derivati ili lindan i drugi. U poslednje vreme više pažnje se posvećuje savremenim polifunkcionalnim i često polarnim pesticidima, biocidima, lekovima, proizvodima za ličnu i kućnu higijenu i industrijskim hemikalijama [12].

Dok je u poslednje vreme fokus istraživanja bio usmeren ka razvoju novih, senzitivnijih analitičkih instrumenata i metoda, manja pažnja se posvećivala razvoju odgovarajućih tehnika uzorkovanja. Procedura za uzorkovanje i kvantifikaciju rezidualnih količina emergentnih supstanci u vodenoj sredini u većini slučajeva bazirana je bila na metodologiji preuzetoj iz rutinskog monitoringa prioritetnih organskih supstanci, i uglavnom se sastojala od periodičnog uzorkovanja. Ovakav tip uzorkovanja daje diskretne vrednosti koncentracija polutanata. U odsustvu vremenski integrisanih merenja, teško je registrovati određene vremenske oscilacije stepena kontaminacije sredine, kao i ekstremne epizodne emisione događaje. Problem se posebno odnosi na polarne emergentne supstance [12]. Vreme zadržavanja hidrofilnih komponenata u vodenoj sredini je kraće od vremena zadržavanja hidrofobnih organskih jedinjenja. Prisustvo dominantno hidrofilnih jedinjenja

u određenim akvatičnim sistemima (otpadne, površinske vode) može biti rezultat epizodnih akcidentnih događaja, koji mogu biti kratkotrajni i rezultirati visokim koncentracionim skokovima. Pojavila se potreba za razvojem odgovarajuće metodologije uzorkovanja i analitičke procedure, prilagođene detekciji i kvantifikaciji polutanata integrisanim modelom radi dobijanja adekvatne procene ekotoksikološkog rizika [12].

Jedno od rešenja problematike periodičnog uzorkovanja jeste povećanje frekvencije uzorkovanja ili instaliranje automatskih sistema uzorkovanja koji kolektuju veći broj uzoraka u određenom vremenskom periodu. Spajanje uzoraka prikupljenih na svakih sat vremena u jedan kompozitni dvadesetčetvoročasovni uzorak ili kontinualna on-line merenja specifičnih setova parametara, neka su od rešenja koja bi obezbedila reprezentativnost rezultata monitoringa emergentnih supstanci. Oba rešenja su skupa i u mnogim slučajevima nepraktična, s obzirom na to da zahtevaju reprezentativne lokalitete uzorkovanja i dodatnu infrastrukturu ili personal radi obezbeđenja, rukovanja i održavanja mehanički automatizovane opreme. Poslednjih decenija istraživanja su se fokusirala na iznalaženje alternativnih metoda uzorkovanja, kako bi se postojeći nedostaci prevazišli. Alternativa tradicionalnim metodama jeste primena pasivnih uzorkivača koji se postavljaju u dužem vremenskom periodu (od nekoliko dana do nekoliko nedelja), kako bi obezbedili dobijanje srednjih vrednosti koncentracija za određeni kontinualni vremenski interval (eng. *time-weighted average concentrations*, TWA) [15,16].

Pasivno uzorkovanje predstavlja savremenu tehniku za vremenski integrisana merenja koncentracionih nivoa zagađujućih materija prisutnih u različitim medijumima životne sredine, vazduhu, vodi i sedimentu, izuzetno pogodnu za različite tipove monitoringa. Poslednjih decenija, različiti tipovi pasivnih uzorkivača predmet su fundamentalnih, razvojnih i primenjenih istraživanja u okviru velikog broja interdisciplinarnih studija. Rezultatima fundamentalnih istraživanja postižu se nova i proširuju postojeća znanja o fenomenima transporta polutanata između medijuma pasivnog uzorkivača i okolnog fluida. Razvojnim procesima usavršava se tehnika uzorkovanja i unapređuju konstruktivne performanse samih uređaja, dok monitoring programi širom Evrope uvode pasivnu metodologiju u oblasti u kojima do sada nije bila praktično primenjena [17].

Metodologija pasivnog uzorkovanja koristi se za monitoring životne sredine od sedamdesetih godina prošlog veka, razvojem i primenom prvih uzorkivača za procenu kvaliteta vazduha i izloženosti radnog prostora potencijalno opasnim zagađujućim materijama u vazduhu [17]. Nasuprot tome, pasivni uzorkivači prilagođeni praćenju kvaliteta vode, vazduha, zemljišta i sedimenta su u fazi razvoja i uvođenja.

Razvojem pasivnih uzorkivača sa semi-permeabilnim membranama (eng. *Semipermeable Membrane Device*, SPMD), počinje široka primena u monitoringu perzistentnih organskih polutanata i drugih nepolarnih organskih jedinjenja u vodenim sredinama [18]. Deset godina kasnije, uvođenjem POCIS uzorkivača (eng. *Polar Organic Chemical Integrative Sampler*) [19,20] i *Chemcatcher* koncepta [21–23], pogodnih za uzorkovanje hidrofilnih organskih jedinjenja, uključujući industrijske hemikalije, prvenstveno nove grupe pesticida, farmaceutike i proizvode za ličnu negu, naglo raste broj publikacija o razvoju, optimizaciji rada i primeni pasivnih uzorkivača za industrijske emergentne supstance prisutne u akvatičnim sistemima. U skorije vreme objavljen je veliki broj članaka koji opisuju dizajn, postupak kalibracije, procene kvaliteta i primenu različitih tipova uređaja za monitoring vode [15,24–27], kao i nekoliko revijalnih članaka o mogućoj primeni pasivnih uzorkivača u praćenju prisustva industrijskih emergentnih supstanci u vodenim sredinama [28,29].

Pasivno uzorkovanje predstavlja metodu koja svojim osnovnim karakteristikama pruža niz prednosti, kako u analitičkim, tako i u praktičnim okvirima istraživačkog rada. Osnovne karakteristike metode uzorkovanja su jednostavna konstrukcija uređaja (sadrže uglavnom pojedinačne polimerne sorpcione medijume), niska cena, tehnička jednostavnost u radu, mogućnost kontinualnog rada tokom dužeg vremenskog perioda, kao i činjenica da pasivnim uzorkivačima za rad nije potrebna električna energija. Danas, ovi uređaji predstavljaju deo razvojne strategije monitoringa velikog broja prioritetnih i industrijskih emergentnih hemikalija u akvatičnim medijumima.

U okviru eksperimentalnog istraživačkog rada, metodologija pasivnog uzorkovanja primenjuje se istovremeno kao komparativna i alternativna metoda standardnoj metodologiji. Dobijeni podaci pružaju informacije o dugotrajnoj kontaminaciji vodenih ekosistema određenim industrijskim emergentnim i prioritetnim supstancama, verifikaciju rezultata dobijenih klasičnim metodama uzorkovanja i komparaciju visine koncentracionih nivoa na velikom broju prostorno udaljenih tačaka. Koncentracioni nivoi detektovani u vodi i sedimentu, na istom lokalitetu u različitim vremenskim periodima, omogućuju analizu raspodele industrijskih emergentnih supstanci između dva medijuma (tečnost/čvrsta faza) i praćenje trenda prostornih i sezonskih varijacija.

Razvijeni za *„in-situ“* ili laboratorijska merenja, pasivni ili „difuzni“ uzorkivači (eng. *passive sampler*, PAS) pogodni su za prikupljanje zagađujućih materija prisutnih u vodi i sedimentu, dinamikom koju kontrolišu parametri prirodnih fenomena prenosa mase – fluks i koeficijent spontane multikomponentne difuzije.

Analiti se akumuliraju u odgovarajućem sorpcionom materijalu unutar pasivnog uzorkivača. Sorpciona faza može biti rastvarač, hemijski reagens, apsorpcioni polimer ili porozni adsorpcioni materijal. S obzirom na to da je najveći broj uzorkivača za hidrofobna jedinjenja baziran na difuziji i apsorpciji u neporoznim polimerima, većina uzorkivača polarnih organskih jedinjenja (na primer, industrijska emergentna jedinjenja) i metala zasniva se na difuziji kroz porozne membrane i sorpciji na selektivnim adsorpcionim materijalima. U novije vreme predstavljen je novi pasivni uzorkivač za polarna organska jedinjenja koji se zasniva na dostizanju stanja ravnotežnog zasićenja sorpcionog medijuma [30]. Osnovu uzorkivača čini polimerni materijal (eng. *poly-(ethylene-co-vinyl acetate-co-carbon monoxide*), PEVAC) koji je pokazao intenzivniju sorpciju za nekoliko vrsta polarnih pesticida i farmaceutika, u odnosu na silikonske materijale. Izbor pogodnih materijala kao polimernih apsorbenata sa velikim kapacitetom zadržavanja, predstavlja optimalan pristup u budućem razvoju tehnologija pasivnog uzorkovanja vode i može zameniti trenutno korišćene složene uzorkivače bazirane na adsorpciji. Akumulacija jedinjenja u medijumu uzorkivača odvija se u periodu od nekoliko dana do nekoliko nedelja.

Pasivni uzorkivači doprinose porastu osetljivosti analitičkih metoda, s obzirom na to da se unutar polimernog sorpcionog medijuma odvija pre-koncentrovanje i čuvanje analita. Za razliku od mnogih klasičnih metoda, opisan tip uzorkovanja omogućuje povećanje osetljivosti za širok opseg komponenata i poboljšanje stabilnosti analita unutar uzorka, bez dodatnih tretmana (podešavanja pH vrednosti i drugo). U nekim slučajevima, primena pasivnih uzorkivača omogućuje smanjenje, ili čak potpunu eliminaciju upotrebe velikih količina ekstrakcionih rastvarača. Nakon uzorkovanja, zagađujuće supstance akumulirane u medijumu uzorkivača se ekstrahuju i određenim analitičkim postupkom kvantifikuju. Dobijeni rezultati daju podatke o prosečnim nivoima koncentracija polutanta u vodi (slika 1) u integrisanom vremenskom periodu.

ANALIZA PRISUSTVA INDUSTRIJSKIH EMERGENTNIH HEMIKALIJA U VODENOJ SREDINI

Registrovanje rezidua industrijskih emergentnih supstanci zahteva savremene analitičke metode niskih granica detekcije, kao što su gasna hromatografija/masena spektrometrija – GC/MS, gasna hromatografija/tandem masena spektrometrija – GC–MS/MS, tečna hromatografija/masena spektrometrija – LC/MS ili tečna hromatografija/tandem masena spektrometrija – LC–MS/MS [31–37]. Jedan od specifikuma analize emergentnih supstanci jeste i složenost uzoraka (kao što su otpadne vode ili kanalizacioni mulj), kao i problem analize većeg broja jedinjenja iz jedinstvenog uzorka.

Priprema uzoraka

Selektivna i visoko efikasna ekstrakcija čvrstom fazom (SPE) kod koje se, kao sorbent, koristi kopolimer divinilbenzena i vinilpirolidana (npr. Oasis HLB) jedna je od najčešće korišćenih metoda za koncentrovanje emergentnih analita [38,39]. Pre ekstrakcije, uzorcima se dodaje izotopski obeležen interni standard [38] i uzorci se najčešće eluiraju pomoću metanola [38], smeše dihlormetana i acetonitrila [40] ili smeše acetona i metanola [41–43]. Osim metode SPE [44–46], koristi se i mikroekstrakcija na čvrstoj fazi (SPME), koja se bazira na polidimetilsiloksanu (PDMS) kao materijalu za izdvajanje analita iz uzorka vode, ali se takođe koriste i alternativni sorpcioni materijali kao što su poliakrilati, kopolimeri PDMS sa divinilbenzenom, kao i kopolimeri polietilenglikola sa divinilbenzenom. Tradicionalna metoda tečno-tečne (LL) ekstrakcije se ređe koristi.

Metode analize uzoraka

Nakon prekoncentracije uzoraka nekom od pomenutih tehnika (SPE, SPME ili LL), uzorci se analiziraju

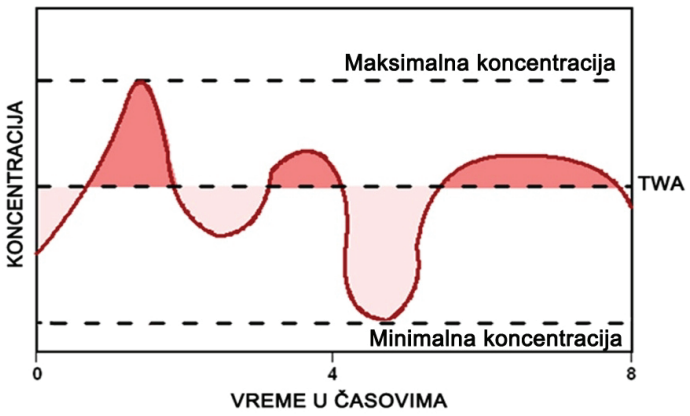

Slika 1. Prosečne vrednosti koncentracije zagađujuće materije u integrisanom vremenskom periodu.
Figure 1. Average concentrations of pollutants over integrated time period.

kombinovanim metodama kao što su LC/MS ili GC/MS, kao i kombinacijom LC–MS/MS [31–34,47–52]. Prikaz najčešće korišćenih metoda za pripremu i analizu uzoraka vode i detekciju određenih industrijskih emergentnih hemikalija dat je u tabeli 1.

Najčešće detektovane industrijske emergentne hemikalije u slivu Dunava

S obzirom na to da je velika teritorija aluvijalne ravni Dunava, hemijski ekostatus sliva reke od izuzetnog je značaja za stanovništvo država kroz koje protiče: Nemačke, Austrije, Slovačke, Mađarske, Hrvatske, Srbije, Bugarske, Rumunije, Moldavije, Ukrajine i drugih u okviru sliva. Pored standardnih ekotoksikoloških ispitivanja, detekcija i kvantifikacija industrijskih emergentnih hemikalija prepoznata je kao neophodan segment za utvrđivanje hemijskog ekostatusa Dunava i njegovih pritoka.

U okviru različitih istraživačkih ekspedicija i projekata u Dunavu i pritokama detektovan je značajan broj industrijskih emergentnih i određen broj prioritetnih supstanci [60–64]. Istraživanja su bila fokusirana na sledeće grupe jedinjenja: farmaceutike i njihove metabolite (kofein, karbamazepin, 4-formilaminoantipirin (4-FAA), 4-acetilaminoantipirin (4-AAA), ciprofloksacin, eritromicin, azitromicin, ibuprofen, diklofenak, sulfametoksazol, trimetoprim, gemfibrozil, bezafibrat, ketoprofen, naproksen, lorazepam, sotalol), pesticide i njihove degradacione produkte (karbendazim, bentazon, 2,4-dihlorofenoksi sirćetna kiselina (2,4-D), mekoprop, antrazin, terbutilazin, diuron, izoproturon, simazin, propazin), sredstva za ličnu higijenu (metiljasmonat, ciklo-heksasiloksan), usporivače gorenja (trifenilfosfat), perfluorne kiseline (PFOS, PFOA, PFHpA, PFNA), supstance koje ometaju rad endokrinog sistema (nonilfenol (NP), 4-nonilfenoksi sirćetna kiselina (NPE_1C), oksifenol (OP), nonilfenol etoksilati (NPEOs), bisfenol A, estron), aromatične komponente (metiljononi), benzotriazoli i druge IEmH.

Istraživanja su pokazala da se određene EmS češće registruju u samom Dunavu nego u njegovim pritokama [38]. Karakteristično je da se kofein, gemfibrozil, nitrofenoli, PFHpA, PFOA, PFOS, karbamazepin, sulfametoksazol, terbutilazin, NPE_1C i benzotriazoli detektuju skoro u svakom uzorku vode Dunava. U pritokama frekventnije se registruju simazin, bisfenol A i nonilfenol [60,64]. Uočena pojava objašnjava se specifičnim emisionim izvorima, degradacionim procesima i razblaženjem nakon ulivanja u Dunav. Maksimalne koncentracije u uzorcima Dunava detektovane su za sulfametoksazol (11600 ng/l), ciprofloksacin (2610 ng/l), gemfibrozil (1700 ng/l), kofein (1467 ng/l), eritromicin (420 ng/l), benzotriazol (380 ng/l), 4-AAA (354 ng/l), NPE_1C (307 ng/l), nonilfenol (240 ng/l), trimetoprim (223 ng/l), 4-FAA (213 ng/l), toliltriazol (130 ng/l), bisfenol A (68 ng/l), karbamazepin (66 ng/l) i terbutilazin (63 ng/l), a u pritokama reke Dunav za kofein (6798 ng/l), NPE_1C (3352 ng/l), nonilfenol (1400 ng/l), karbamazepin (945 ng/l), ibuprofen (718 ng/l), bisfenol A (490 ng/l) [38,61,64]. Samo u malom broju uzoraka površinske vode Dunava, nonilfenol i bisfenol A su detektovani u vrlo visokim koncentracijama. Registrovana pojava ukazuje na specifične koncentrisane primarne izvore emisije supstanci, degradacione procese u vodenoj sredini i turbulentan režim strujanja.

U R. Srbiji relativno visoki koncentracioni nivoi PFNA detektovani su u Tisi, čije su prosečne vrednosti iznosile 108 ng/l. U istim uzorcima površinskih slojeva Tise, detektovani su i PFUnA, PFOA i PFOS sa maksimalnim koncentracijama i do 10, 3 i 3 ng/l, redom [38]. Perfluoro rezidue u slivu Dunava ukazuju na to da se u tok reke Tise ispuštaju industrijske otpadne vode specifič-

Tabela 1. Metode za pripremu uzoraka i detekciju pojedinih predstavnika industrijskih emergentnih hemikalija
Table 1. Methods for sample preparation and detection of individual representatives of industrial emerging chemicals

Analiti	Priprema uzorka	Detekcija	Literatura
DBP, DEHP - ftalati, BPA - plastifikator	SPE	GC/MS	Baugros i sar [53]
Perfluorne kiseline (PFOS, PFOA)	SPE	LC/MS	So i sar. [54]
Benzotriazol	SPE	GC/MS	Kiss i Fries [55]
Bisfenol A	SBSE (eng. *stir bar sorptive extraction*)	GC/MS	Kawaguchi i sar. [56]
Sedativi, hipnotici – butalbital, pentobarbital, heksobarbital, antikonvulzivi – fenobarbital	Filtracija / SPE	GC/MS	Peschka i sar. [32]
Antidepresivi	SPE	Kapilarna elektroforeza–MS (TOF)	Himmelsbach i sar. [57]
Antidepresivi – fluoksetin, citalopram, fluvoksamin, sertralin	SPE i LL ekstrakcija	HPLC (ESI)–MS/MS	Vasskog i sar. [31]
Antibiotik – oksitetraciklin	–	Imunoeseji	Himmelsbach i Buchberger [58]
Farmaceutici, proizvodi za ličnu higijenu	SPE (Oasis HLB)	LC–MS/MS	Loos i sar. [38]
Farmaceutici, regulatori lipida	SPE ili LL ekstrakcija	Kapilarna elektroforeza–MS	Ahrer i sar. [59]
Proizvodi za ličnu higijenu	LL ekstrakcija	GC	Teijon i sar. [39]

nog proizvodnog procesa u okviru koga se umesto PFOA, koristi PFNA.

Aktivne supstance farmaceutskih proizvoda se otpadnim vodama unose u Dunav, prilično podjednako duž čitavog toka [60,61,63]. Istraživanjima je utvrđen specifično visok nivo koncentracija karbamazepina (5*H*-dibenzo[*b,f*]azepin-5-karboksiamid, $C_{15}H_{12}N_2O$) na svim mernim mestima, što se objašnjava neočekivano velikom upotrebom i nekontrolisanim odlaganjem ovog antiepileptika. Registrovana je direktno proporcionalna korelacija između naseljenosti područja kroz koje protiče reka i prisustva farmaceutika u površinskim slojevima rečnih tokova do dubine od 1m. Specifičan porast rezidualnih nivoa sulfametoksazola (4-amino-N-(5-metilizoksazol-3-il)-benzensulfonamid, $C_{10}H_{11}N_3O_3S$) izmeren je na lokalitetima donjeg toka Dunava. Kako bi se stekao uvid u poreklo rezidua antibakterijskog sulfonamida, sprovedena su detaljnija istraživanja u pritokama donjeg toka reke, kojima je utvrđeno da se uočen porast koncentracionih nivoa sulfametoksazola javlja kao posledica visokih koncentracija ovog farmaceutika u pritokama Velika Morava (85 ng/l), Timok (62 ng/l), Iskar (77 ng/l), Rusenski Lom (69 ng/l) i Arges (204 ng/l). Nizvodno od Beograda, nakon ulivanja Velike Morave u Dunav (1110 km od ušća Dunava), detektovane su koncentracije ibuprofena (nesteroidni antiupalni lek, (*RS*)-2-[4-(2-metilpropil)fenil]propanska kiselina, $C_{13}H_{18}O_2$) u opsegu od 9 do 27 ng/l. Smatra se da su nivoi posledica povećane koncentracije ibuprofena u Velikoj Moravi, gde su registrovane vrednosti od 34 ng/l. Na ušću Dunava, ibuprofen je detektovan u koncentraciji od 5 ng/l [60].

Prisustvo pesticida u površinskim vodama Dunava i pritoka, u velikoj meri zavisi od perioda godine u kome se uzorkovanje realizuje. Značajne sezonske oscilacije u nivoima koncentracija mogu se uočiti, zavisno od dinamike poljoprivredne proizvodnje i tretiranja obradivog zemljišta u blizini reke. Najviše koncentracije za 2,4-D, jednog od najčešće primenjivanih herbicida, izmerene su nizvodno od Budimpešte i neposredno uz severnu granicu Vojvodine (oko 50 ng/l). Koncentracioni nivoi bentazona ujednačeni su duž čitavog toka Dunava i iznose od 5 do 10 ng/l. Nezavisno od regiona, detektovane koncentracije izoproturona i diurona bile su oko 5 ng/l i manje [38,64].

Zbog načina analitičkog postupka kvantifikacije nonilfenola (NP), u literaturi se objavljuju koncentracije isključivo >50 ng/l. Samo u malom broju analiziranih uzoraka vode Dunava detektovano je prisustvo NP (kod Gornjeg Milanovca (240 ng/l) i Vilkova (180 ng/l)) [38]. Prekoračenje standarda kvaliteta (eng. *Environmental Quality Standard*, EQS) definisanog direktivom Evropske unije (eng. *Water Framework Directive*, WFD) od 0,3 μg NP/l uočeno je u dve pritoke Dunava, Argesu (1300 ng/l) i Timoku (500 ng/l). Smatra se da je osnovni uzrok izmerenih visokih koncentracija nonilfenola direktno izlivanje netretirane otpadne vode [60]. Najviši nivoi koncentracija alkilfenolnih komponenata (NP iznad 2,83 mg/kg) u sedimentu detektovani su u okolini Pančeva [65]. Bisfenol A, supstanca koja ometa rad endokrinog sistema i u proceduri je priključivanja listi prioritetnih supstanci definisanoj EU direktivama, detektovan je u reci Savi, u koncentracijama većim od 246 ng/l. U Dunavu, bisfenol A izmeren je u pojedinim uzorcima vode, u relativno niskim koncentracijama (frekvencija detektovanja 29%) na sledećim lokalitetima: kod Bratislave, nakon ulivanja Morave, (116 ng/l), nizvodno od Budimpešte (12 ng/l), nizvodno od ulivanja Drave (27 ng/l) i na ušću Save (15 ng/l) [60,61].

Analizom vode Dunava duž čitavog toka, u svakom analiziranom uzorku kvantifikovani su značajni koncentracioni nivoi antikorozivne industrijske emergentne hemikalije benzotriazola [60,66]. Najviše prosečne vrednosti izmerene za 1H-benzotriazol (oko 213 ng/l) i toliltriazol (81 ng/l) [38] niže su u poređenju sa monitoring podacima drugih rečnih slivova Evrope (Rajne, Elbe i reke Po) [67–69].

U okviru međunarodnog NATO projekta [63,66,70,71] izvršen je preliminarni skrining najfrekventnije detektovanih industrijskih emergentnih hemikalija na odabranim lokalitetima aluvijalne ravni Dunava u okolini grada Novog Sada. Tačke uzorkovanja (slika 2) odabrane su sa ciljem utvrđivanja uticaja industrijskih i komunalnih otpadnih voda grada Novog Sada na kvalitet vode Dunava. Ovakav tip istraživanja po prvi put se sprovodi u okolini grada Novog Sada, Vojvodini i Srbiji.

Primarnim skriningom uzoraka površinske vode Dunava u okolini grada Novog Sada detektovano je više od 150 organskih polutanata iz grupe industrijskih emergentnih i prioritetnih supstanci. Preliminarna kvalitativna analiza ukazuje na prisustvo kofeina, metiljasmonata, cikloheksasiloksana, trifenilfosfata, terc-butiloksaspirodeka-dien-diona, metiljonona i benzotriazola [66]. Kvantitativna analiza potvrdila je prisustvo rezidua kofeina i njegovih metabolita teobromina i teofilina i antikoroziva, benzotriazola, u svim analiziranim uzorcima vode Dunava. U okviru proširenog obima kvantitativnih određivanja, u deset uzoraka površinske vode aluvijalne ravni Dunava (u regionu Vojvodine) detektovano je (frekvencija detektovanja 97%) prisustvo rezidua metomila (*S*-metil-*N*-(metilkarbamoiloksi)-tioacetimidat), karbamatnog polarnog pesticida koji se nalazi na otvorenoj NORMAN listi trenutno najfrekventnije registrovanih i kvantifikovanih emergentnih supstanci. Detektovani koncentracioni nivoi ukazuju na permanentno prisustvo IEmH u površinskim slojevima Dunava kod Novog Sada, kao i na potrebu sistematskog praćenja određenog broja pseudoperzistentnih jedinjenja u akviferu aluvijalne ravni Dunava u dužem vre-

Slika 2. Tačke preliminarnog skrininga odabranih emergentnih supstanci u okolini grada Novog Sada.
Figure 2. The points selected for preliminary screening of emerging substances in the vicinity of Novi Sad.

menskom periodu. Potrebno je obezbediti analizu uzoraka u više prostornih i vremenskih koordinata i povećati broj analiziranih jedinjenja, kako bi se stekao potpuniji uvid u hemijski ekostatus Dunava, prvenstveno na mestima ispuštanja industrijske otpadne vode i komunalne vode onečišćene industrijskim hemikalijama koje se svakodnevno koriste.

OPTEREĆENOST VODOTOKOVA HEMIJSKOM EMISIJOM INDUSTRIJSKIH EMERGENTNIH HEMIKALIJA

Za praćenje opterećenosti vodotokova koriste se maseni fluks i masa opterećenja vode. Maseni fluks je specifična veličina za određeno područje i izražava se kao masa industrijskog polutanta koji prolazi kroz određenu oblast u jedinici vremena (masa/vreme/površina). Masa opterećenja vode (W) predstavlja zbir svih masenih flukseva i izražava se kao masa/vreme (kg/s ili t/godina):

$$W = C \times Q = C \times K \times i \times A \quad (3)$$

gde je: C – koncentracija polutanta, ng/l, Q – protok vode, m^3/s, K – Darsijev koeficijent filtracije, i – hidraulički gradijent, m/m, a A – poprečni presek upravan na pravac tečenja, m^2 [72].

Koncentracije industrijskih emergentnih hemikalija na mestu izlivanja u površinske recipijente mogu biti relativno konstantne s obzirom na permanentnu emisiju iz industrijskih postrojenja i domaćinstava. Opterećenost vodotokova određenim industrijskim emergentnim hemikalijama, odnosno koncentracija polutanta koja se u jedinici vremena ispušta u vodotok, može se jednostavno izračunati poznavanjem koncentracije IEmH i protoka vode. Velike reke imaju relativno konstantan ukupan protok. Protok Dunava iznosi približno, u m^3/s: 1180 u Austriji, 1400 u Mađarskoj, 2460 u Srbiji nizvodno od Tise, 3200 nizvodno od Velike Morave, 4830 nizvodno od Timoka i 6420 nizvodno od Argesa [38]. Poznavanje vrednosti masenog fluksa i ukupnog opterećenja vodotokova određenim IEmH je neophodno jer omogućuje upravljanje rizikom, izbor adekvatnog tretmana za prečišćavanje vode i uštedu troškova, prioritizaciju polutanata i selekciju lokaliteta, razvoj modela rane predikcije, donošenje odluka odgovarajućih regulatornih tela i optimalno integralno upravljanje zaštitom životne sredine.

ZAKLJUČAK

U radu je po prvi put na srpskom jeziku dat pregled nalaženja i karakterističnih fizičko-hemijskih svojstava industrijskih emergentnih hemikalija u životnoj sredini. Za industrijske emergentne supstance, ne postoji zakonska regulativa i odgovarajući pravilnici, obavezan monitoring kao i definisane maksimalno dozvoljene koncentracije u različitim medijumima životne sredine.

Industrijske emergentne hemikalije su novoprepoznata grupa supstanci, koje nisu uključene u rutinske monitoring programe i čija sudbina, ponašanje i (eko)-toksikološki efekti veoma niskih koncentracija, reda veličine ppb, ppt i niže u biotskim i abiotskim matriksima još uvek nisu potpuno poznati.

Pasivno uzorkovanje je prepoznato kao jedna od najprihvatljivijih tehnika za vremenski integrisana merenja koncentracionih nivoa industrijskih emergentnih supstanci prisutnih u različitim medijumima životne sredine, posebno u vodi i sedimentu.

Na osnovu prvih skrining analiza površinske vode Dunava u okolini Novog Sada registrovano je više od 140 organskih jedinjenja među kojima su i industrijske emergentne hemikalije.

S obzirom na to da relevantna procena rizika za većinu IEmH ne može biti realizovana sa dovoljnom sigurnošću, potrebne su inovirane osetljive instrumentalne metode analize i detekcije, uz modele predviđanja i sistem ranog upozorenja u cilju preventivnih aktivnosti, što predstavlja nov koncept kontrolnog monitoringa zaštite životne sredine.

Zahvalnica

Rezultati prikazani u radu deo su istraživanja realizovanih u okviru programa NATO Science for Peace and Security (ESP.EAP.SFPP 984087), projekta br. 680-00--140/2012-09/13 i projekta III46009 finansiranog od strane Ministarstva prosvete, nauke i tehnološkog razvoja Republike Srbije.

LITERATURA

[1] M. Vojinović Miloradov, M. Dimkić, M. Stupavski, S. Jokanović, B. Beronja, B. Tot, M. Stošić, Emerging substances of concern and their occurrence in surface water and groundwater, TOP 2011, Časta, Papirnička, Slovak Republic, 2011, Proceedings, pp. 277–288.

[2] I. Mihajlovic, M. Vojinovic-Miloradov, E. Fries, Application of Twisselmann extraction, SPME, and GC-MS to assess input sources for organophosphate esters into soil, Environ. Sci. Technol. **45** (2011) 2264–2269.

[3] I. Mihajlovic, E. Fries, Atmospheric deposition of chlorinated organophosphate flame retardants (OFR) onto soils, Atmos. Environ. **56** (2012) 177–183.

[4] E. Fries, I. Mihajlovic, Pollution of soils with organophosphorus flame retardants and plasticizers, J. Environ. Monit. **13** (2011) 2692–2694.

[5] M. Vojinović-Miloradov, M. Turk Sekulić, J. Radonić, I. Mihajlović, M. Stošić, Emerging substances of concern – a shift in traditional thinking, XV International Eco-Conference on environmental protection of urban and suburban settlements, Novi Sad, Serbia, 2011, Proceedings, pp. 265–271.

[6] M. Vojinović Miloradov, M. Turk Sekulić, J. Radonić, J. Kiurski, D. Milovanović, I. Spanik, I. Mihajlović, Pseudo-persistent pollutant in the environment: emerging substances, XVII International Symposium on Analytical and Environmental Problems, Szeged, Hungary, 2011, Proceedings, pp. 180–184.

[7] M. Dalmacija, B. Dalmacija, D. Krčmar, M. Prica, Lj. Rajić, S. Rončević, O. Gavrilović, Solidifikacija/stabilizacija sedimenta vodotoka Krivaja zagađenog metalima, Hem. Ind. **66** (2012) 469–478.

[8] J.O. Straub, Environmental risk assessment for new human pharmaceuticals in the European Union according to the draft guideline/discussion paper of January 2001, Toxicol Lett. **131** (2002) 137–143.

[9] K.H. Wedepohl, C.W. Correns, D.M. Shaw, Behavior during weathering and rock Alteration, in: Handbook of geochemistry, Vol II Part 4, Elements Kr(36) to Ba(56), Springer-Verlag, New York, 1978.

[10] J. Radonić, M. Vojinović-Miloradov, M. Turk-Sekulić, J. Kiurski, M. Đogo, D. Milovanović, The octanol-air partition coefficient KOA as a predictor of gas-particle partitioning of polycyclic aromatic hydrocarbons and polychlorinated biphenyls at industrial and urban sites, J. Serb. Chem. Soc. **76** (2011) 447–458.

[11] J. Radonić, D. Ćulibrk, M. Vojinović-Miloradov, B. Kukić, M. Turk-Sekulić, Prediction of gas-particle partitioning of PAHs based on M5' model trees, Thermal Science **15** (2011) 105–114.

[12] NORMAN (Network of Reference Laboratories for Monitoring of Emerging Environmental Pollutants). The Norman Database on Emerging Substances, http:// //www.norman-network.net (pristupljeno 2.03.2012.).

[13] R.P. Schwarzenbach, B.I. Escher, K. Fenner, T.B. Hofstetter, C.A. Johnson, U. von Gunten, B. Wehrli, The challenge of micropollutants in aquatic systems, Science **313** (2006) 1072–1077.

[14] C. Zwiener, F.H. Frimmel, LC-MS analysis in the aquatic environment and in water treatment – A critical review. Part II: Applications for emerging contaminants and related pollutants, microorganisms and humic acids, Anal. Bioanal. Chem. **378** (2004) 862–874.

[15] B. Vrana, I.J. Allan, R. Greenwood, G.A. Mills, E. Dominiak, K. Svensson, J. Knutsson, G. Morrison, Passive sampling techniques for monitoring pollutants in water, TrAC Trends Anal. Chem. **24** (2005) 845–868.

[16] K. Booij, B. Vrana, J.N. Huckins, in: R. Greenwood, G. Mills, B. Vrana (Eds.), Theory, modelling and calibration of passive samplers used in water monitoring, Comprehensive Analytical Chemistry Series 48, Elsevier, Amsterdam, 2007, pp. 141–169.

[17] M. Turk, J. Jakšić, M. Vojinović Miloradov, J. Klanova, Post-war levels of persistent organic pollutants (POPs) in

air from Serbia determined by active and passive sampling methods, Environ. Chem. Lett. J. **5** (2007) 109–113.

[18] J.N. Huckins, G.K. Manuweera, J.D. Petty, D. Mackay, and J.A. Lebo, Lipid-containing semipermeable membrane devices for monitoring organic contaminants in water, Environ. Sci. Technol. **27** (1993) 2489–2496.

[19] A. Alvarez, Development of an integrative sampling device for hydrophilic organic contaminants in aquatic environments, PhD Thesis, University of Missouri-Columbia, 1999.

[20] J.D. Petty, J.N. Huckins, D.A. Alvarez, Device for sequestration and concentration of polar organic chemicals from water, US Patent 6,478,961 (2002).

[21] J.K. Kingston, R. Greenwood, G.A. Mills, G.M. Morrison, B.L. Persson, Development of a novel passive sampling system for the time-averaged measurement of a range of organic pollutants in aquatic environments, J. Environ. Monitor. **2** (2000) 487–495.

[22] B. Vrana, G.A. Mills , E. Dominiak, R. Greenwood, Calibration of the Chemcatcher passive sampler for the monitoring of priority organic pollutants in water, Environ. Pollut. **142** (2006) 333–343.

[23] B. Vrana, G.A. Mills , M. Kotterman , P. Leonards , K. Booij, R. Greenwood, Modelling and field application of the Chemcatcher passive sampler calibration data for the monitoring of hydrophobic organic pollutants in water, Environ. Pollut. **145** (2007) 895–904.

[24] A. Kot-Wasik, B. Zabiegała, M. Urbanowicz, E. Dominiak, A. Wasik, J. Namieśnik, Advances in passive sampling in environmental studies, Anal. Chim. Acta **602** (2007) 141–163.

[25] S.L. MacLeod, E.L. McClure, C.S. Wong, Laboratory calibration and field deployment of the polar organic chemical integrative sampler for pharmaceuticals and personal care products in wastewater and surface water, Environ. Toxicol. Chem. **26** (2007) 2517–2529.

[26] G. Ouyang, J. Pawliszyn, Configurations and calibration methods for passive sampling techniques, J. Chromatogr., A **1168** (2007) 226–235.

[27] F. Stuer-Lauridsen, Review of passive accumulation devices for monitoring organic micropollutants in the aquatic environment, Environ. Pollut. **136** (2005) 503––524.

[28] G.A. Mills, B. Vrana, I. Allan, D.A. Alvarez, J.N. Huckins, R. Greenwood, Trends in monitoring pharmaceuticals and personal-care products in the aquatic environment by use of passive sampling devices, Anal. Bioanal. Chem. **387** (2007) 1153–1157.

[29] H. Söderström, R.H. Lindberg, J. Fick, Strategies for monitoring the emerging polar organic contaminants in water with emphasis on integrative passive sampling: Tools for the REACH Programme – analytical methods for the evaluation of industrial contaminants, J. Chromatogr., A **1216** (2009) 623–630.

[30] J.A. Magnér, T.E. Alsberg, D. Broman, Evaluation of poly(ethyleneco- vinyl acetate-co-carbon monoxide) and polydimethylsiloxane for equilibrium sampling of polar organic contaminants in water, Environ. Toxicol. Chem. **28** (2009) 1874–1880.

[31] T. Vasskog, U. Berger, P. Samuelsen, R. Kallenborn, E. Jensen, Selective serotonin reuptake inhibitors in sewage influents and effluents from Tromso, Norway, J. Chromatogr., A **1115** (2006) 187–195.

[32] M. Peschka, J.P. Eubeler, T.P. Knepper, Occurrence and fate of barbiturates in the aquatic environment, Environ. Sci. Technol. **40** (2006) 7200–7206.

[33] M. Gros, M. Petrovic, D. Barcelo, Development of a multi-residue analytical methodology based on liquid chromatography-tandem mass spectrometry (LC–MS/ /MS) for screening and trace level determination of pharmaceuticals in surface and wastewaters, Talanta **70** (2006) 678–690.

[34] T.A. Ternes, R. Hirsch, J. Mueller, K. Haberer, Methods for the determination of neutral drugs as well as beta-blockers and b2- sympathomimetics in aqueous matrices using GC/MS and LC/MS/MS, Fresen. J. Anal. Chem. **362** (1998) 329–340.

[35] W. Buchberger, Current approaches to trace analysis of pharmaceuticals and personal care products in the environment, J. Chromatogr., A **1218** (2011) 603–618.

[36] I. Rodríguez, J.B. Quintana, J. Carpinteiro, A.M. Carro, R.A. Lorenzo, R. Cela, Determination of acidic drugs in sewage water by gas chromatography mass spectrometry as tert-butyldimethysilyl derivatives, J. Chromatogr., A **985** (2003) 265–274.

[37] M. Zapadlo, J. Krupčík, T. Kovalczuk, P. Májek, I. Špánik, D.W. Armstrong, P. Sandra, Enhanced comprehensive two-dimensional gas chromatographic resolution of polychlorinated biphenyls on a non-polar polysiloxane and an ionic liquid column series, J. Chromatogr., A **1218** (2011) 746–751.

[38] R. Loos, G. Locoro, S. Contini, Occurrence of polar organic contaminants in the dissolved water phase of the Danube River and its major tributaries using SPE-LC-MS2 analysis, Water Res. **44** (2010) 2325–2335.

[39] G. Teijon, L. Candela, K. Tamoh, A. Molina-Díaz, A.R. Fernández-Alba, Occurrence of emerging contaminants, priority substances (2008/105/CE) and heavy metals in treated wastewater and groundwater at Depurbaix facility (Barcelona, Spain), Sci. Total Environ. **408** (2010) 3584–3595.

[40] Z. Sun, W. Schussler, M. Sengl, R. Niessner, D. Knopp, Selective trace analysis of diclofenac in surface and wastewater samples using solid-phase extraction with a new molecularly imprinted polymer, Anal. Chim. Acta **620** (2008) 73–81.

[41] M. Gros, T.M. Pizzolato, M. Petrovic, M. Jose Lopez de Alda, D. Barcelo, Trace level determination of beta-blockers in waste waters by highly selective molecularly imprinted polymers extraction followed by liquid chromatography-quadrupole-linear ion trap mass spectrometry, J. Chromatogr., A **1189** (2008) 374–384.

[42] E. Beltran, E. Caro, R.M. Marce, P.A.G. Cormack, D.C. Sherrington, F. Borrull, Synthesis and application of a carbamazepine-imprinted polymer for solid-phase extraction from urine and wastewater, Anal. Chim. Acta **597** (2007) 6–11.

[43] K. Demeestere, M. Petrovic, M. Gros, J. Dewulf, H. Van Langenhove, D. Barcelo, Trace analysis of antidepressants in environmental waters by molecularly imprinted polymer-based solid-phase extraction followed by ultra-performance liquid chromatography coupled to triple quadrupole mass spectrometry, Anal. Bioanal. Chem. **396** (2010) 825–837.

[44] S.M.R. Wille, K.E. Maudens, C.H. Van Peteghem, W.E. Lambert, Development of a solid phase extraction for 13 "new" generation antidepressants and their active metabolites for gas chromatographic–mass spectrometric analysis, J. Chromatogr., A **1098** (2005) 19–29.

[45] B. Srđenović, V. Đorđević-Milić, N. Grujić, R. Injac, Ž. Lepojević, Simultaneous HPLC determination of caffeine, theobromine, and theophylline in food, drinks, and herbalproducts, J. Chromatogr. Sci. **46** (2008) 144––149.

[46] N. Milić, M. Milanović, N. Grujić Letić, M. Turk Sekulić, J. Radonić, I. Mihajlović, M. Vojinović Miloradov, Occurrence of antibiotics as emerging contaminant substances in aquatic environment, Int. J. Environ. Health Res. **23** (2013) 296–310.

[47] A. Togola, H. Budzinski, Multi-residue analysis of pharmaceutical compounds in aqueous samples, J. Chromatogr., A **1177** (2008) 150–158.

[48] J. Debska, A. Kot-Wasik, J. Namiesnik, Fate and analysis of pharmaceutical residues in the aquatic environment, Crit. Rev. Anal. Chem. **34** (2004) 51–67.

[49] A.C. Hogenboom, W.M.A. Niessen, D. Little, U.A.Th. Brinkman, Accurate mass determinations for the confirmation and identification of organic microcontaminants in surface water using on-line solid-phase extraction liquid chromatography electrospray orthogonal-acceleration time-of-flight mass spectrometry, Rapid Commun. Mass Spectrom. **13** (1999) 125–133.

[50] T. Storm, C. Hartig, T. Reemtsma, M. Jekel, Exact mass measurements on-line with high-performance liquid chromatography on a quadrupole mass spectrometer, Anal. Chem. **73** (2001) 589–595.

[51] A. Marcia, F. Borrull, M. Calull, C. Aguilar, Determination of some acidic drugs in surface and sewage treatment plant waters by capillary electrophoresis-electrospray ionization-mass spectrometry, Electrophoresis **25** (2004) 3441–3449.

[52] T.A. Ternes, Analytical methods for the determination of pharmaceuticals in aqueous environmental samples, TrAC Trends Anal. Chem. **20** (2001) 419–434.

[53] J.B. Baugros, B. Giroud, G. Dessalces, M.F. Grenier-Loustalot, C. Cren-Olive, Multiresidue analytical methods for the ultra-trace quantification of 33 priority substances present in the list of REACH in real water samples, Anal. Chim. Acta **607** (2008) 191–203.

[54] M.K. So, S. Taniyasu, N. Yamashita, J.P. Giesy, J. Zheng, Z. Fang, S.H. Im, P.K.S. Lam, Perfluorinated compounds in coastal waters of Hong Kong, South China, and Korea, Environ. Sci. Technol. **38** (2004) 4056–4063.

[55] A. Kiss, E. Fries, Occurrence of Benzotriazoles in the Rivers Main, Hengstbach and Hegbach (Germany), Environmental Science and Pollution Research, Special Series: Chemical and Biological Environmental Monitoring **16** (2009) 702–710.

[56] M. Kawaguchi, K. Inoue, M. Yoshimura, N. Sakuri, N. Okanouchi, R. Ito, Y. Yoshimura, H. Nakazawa, Trace analysis of phenolic xenoestrogens in water samples by stir bar sorptive extraction with in situ derivatization and thermal desorption–gas chromatography–mass spectrometry, J. Chromatogr., A **1041** (2004) 19–26.

[57] M. Himmelsbach, W. Buchberger, C. Klampfl, Development of an analytical method for the determination of antidepressants in water samples by capillary electrophoresis with electrospray ionization mass spectrometric detection, Electrophoresis **27** (2006) 1220–1226.

[58] M. Himmelsbach, W. Buchberger, Residue analysis of oxytetracycline in water and sediment samples by high-performance liquid chromatography and immunochemical techniques, Microchim. Acta **151** (2005) 67–72.

[59] W. Ahrer, E. Scherwenk, W. Buchberger, Determination of drug residues in water by the combination of liquid chromatography or capillary electrophoresis with electrospray mass spectrometry, J. Chromatogr., A **910** (2001) 69–78.

[60] I. Liska, F. Wagner, J. Slobodnik (Eds.), Joint Danube Survey 2, Final Scientific Report, ICPDR- International Commission for the Protection of the Danube River, Vienna, 2008, http://www.icpdr.org/jds (pristupljeno 20.06.2012).

[61] Reduction of environmental risks, posed by Emerging Contaminants, through advanced treatment of municipal and industrial wastes, EMCO, Project no. CT 2004-509188, 2004-2007, http://www.cid.csic.es/emco/ /home.htm (pristupljeno 25.01.2012).

[62] The NATO Science for Peace and Security Programme: Drinking Water Quality Risk Assessment and Prevention in Novi Sad municipality, Serbia, ESP.EAP.SFP 984087, http://www.izzs.uns.ac.rs/nato/ (pristupljeno 16.07.2012).

[63] N. Grujić, N. Milić, M. Turk Sekulić, J. Radonić, M. Milanović, I. Mihajlović, M. Vojinović Miloradov, Quantification of emerging organic contaminants in the Danube River samples by HPLC, Chemické Listy **106** (2012) 264––266.

[64] M.A. Dimkić, D. Đurić, M. Milovanović, M. Laušević, G. Jevtić, A. Petković, Natural attenuation of emerging pharmaceuticals by bank filtration in addressing regional groundwater management issues, Water Research and Management **1** (2011) 29–45.

[65] V. Micić, T. Hofmann, Occurrence and behaviour of selected hydrophobic alkylphenolic compounds in the Danube River, Environ. Pollut. **157** (2009) 2759–2768.

[66] M. Vojinović Miloradov, I. Špánik, J. Radonić, M. Turk Sekulić, D. Milovanović, M. Đogo, O. Vyviurska, The monitoring of emerging substances of municipal and industrial waste water from Novi Sad area discharged in to the Danube River, Chemické Listy **106** (2011) 244––245.

[67] T. Reemtsma, S. Weiss, J. Mueller, M. Petrovic, S. Gonzalez, D. Barcelo, F. Ventura, T.P. Knepper, Polar pollutants entry into the water cycle by municipal waste-

water: a European perspective, Environ. Sci. Technol. **40** (2006) 5451–5458.

[68] W. Giger, C. Schaffner, H.-P.E. Kohler, Benzotriazole and tolyltriazole as aquatic contaminants. 1. Input and occurrence in rivers and lakes, Environ. Sci. Technol. **40** (2006) 7186–7192.

[69] T. Reemtsma, Liquid chromatography-mass spectrometry and strategies for trace-level analysis of polar organic pollutants, J. Chromatogr., A **1000** (2003) 477––501.

[70] N. Grujic, N. Milic, M. Turk Sekulic, M. Vojinovic Miloradov, M. Milanovic, J. Radonic, Determination of emerging substance as human waste indicator in the Danube River samples, 6th SETAC World Congress/SETAC Europe 22nd Annual Meeting, Berlin, Germany, 2012, Book of Abstracts, TU 096.

[71] N. Grujic, M. Vojinovic Miloradov, N. Milic, M. Turk Sekulic, I. Mihajlovic, D. Adamovic, Determination of methylxanthines in the Danube River samples by high performance liquid chromatography, European Conference on Analytical Chemistry – EUROanalysis16, Belgrade, Serbia, 2011, Book of Abstracts, EN31.

[72] M. Kübert, M. Finkel, Contaminat mass disharge estimation in groundwater based on multi-level point measurements: A numerical evaluation of expected errors, J. Contam. Hydrol. **84** (2006) 55–80.

SUMMARY

INDUSTRIAL EMERGING CHEMICALS IN THE ENVIRONMENT

Mirjana B. Vojinović Miloradov[1], Maja M. Turk Sekulić[1], Jelena R. Radonić[1], Nataša B. Milić[2], Nevena N. Grujić Letić[2], Ivana J. Mihajlović[1], Maja Lj. Milanović[2]

[1]*University of Novi Sad, Faculty of Technical Sciences, Trg Dositeja Obradovića 6, 21000 Novi Sad, Serbia*
[2]*University of Novi Sad, Faculty of Medicine, Hajduk Veljkova 3, 21000 Novi Sad, Serbia*

(Professional paper)

Recently, considerable interest has grown concerning the presence of the emerging industrial chemicals, EmIC. They are contaminants that are dominantly released by industrial and anthropogenic activities, but enter environment. EmIC are widely used as industrial chemicals (new and recently recognized), global organic contaminants (flame retardant chemicals), pharmaceuticals (for both human and animal use), endocrine-modulating compounds, biological metabolites, personal care products, household chemicals, nanomaterials (energy storage products, lubricants), anticorrosive and agricultural chemicals and others that are applied to a variety of everyday items such as clothing, upholstery, electronics and automobile interiors. NORMAN (Network of reference laboratories for monitoring of emerging environmental pollutants) has established an open, dynamic list of emerging substances and pollutants. EmIC have been recently detected in the environment due to their long-term presence, pseudo-persistence and increased use. Improvements in sophisticated analytical methods and time integrative passive sampling have enabled the identification and quantification of EmIC, in very low concentrations (ppb, ppt and lower), which likely have been present in all environmental mediums for decades. Passive technology is an innovative technique for the time-integrated measurement of emerging contaminants in water, sediment, soil and air. Passive samplers are simple handling, cost-effective tool that could be used in environmental monitoring programs. These devices are now being considered as a part of an emerging strategy for monitoring various industrial chemicals and priority pollutants in the aquatic environment. EmIC are substances that are not included in the routine monitoring programes and whose fate, behavior and (eco)toxicological effects are still not well understood. Emerging pollutants have no regulatory standards based on peer-reviewed science. EmIC might jeopardize aquatic environment. The first screening analyses of emerging industrial and priority organic contaminants in the Danube surface water, in the vicinity of Novi Sad, have been done and approximately more than 140 compounds have been registered. The new sampling campaign, screening and target analyses are in progress.

Keywords: Industrial emerging contaminants • Industrial wastewater • Danube • Novi Sad

Physicochemical and geochemical characterization of geothermal waters sedimentation tendency at Sijarinska spa and Vranjska Spa (Serbia)

Nebojša Č. Mitić, Dragan T. Stojiljković, Bratislav Ž. Todorović, Ljubiša S. Nikolić, Staniša T. Stojiljković, Suzana Cakić

Faculty of Technology, University of Niš, Leskovac, Serbia

Abstract

A comprehensive analysis of physicochemical parameters in geothermal waters from the sites in Sijarinska spa (drill hole B-4) and Vranjska spa (drill hole VG-2) in order to investigate their tendency to form deposits in the pipe installation is presented. Both drill holes, B-4 and VG-2 possess utilization capacity of 30/27 L s^{-1} with water temperatures 75–90 °C. VG-2 water does not show any tendency of (or shows very little) sedimentation compared to the B-4 water. The behavior of the geothermal water from the B-4 hole was examined in real conditions of water flow through the pipe installation in Sijarinska spa. The results of geochemical analysis of B-4 water show that aragonite is the predominant mineral in the sediment (98%) with small amount of calcite, vaterite and anhydrite.

Keywords: geothermal water, LSI, RSI, sediment, aragonite.

Available online at the Journal website: http://www.ache.org.rs/HI/

PROFESSIONAL PAPER

UDC 551.23(497.11):549.742.21:53/54

Hem. Ind. **68** (1) 63–67 (2014)

doi: 10.2298/HEMIND121002026M

Geothermal waters have significant energy potential and therefore represent a potential future source of energy. Considering overall savings in energy, large supplies and less harmfulness to the environment, the use of geothermal energy has an even more significant role and a great advantage compared to the energy sources based on fossil, non-renewable fuels, in which the release of CO_2 (and other gases that affect global warming) is much greater.

What sedimentary mineral will occur in the water from a hydrothermal source during cooling process depends on the mineralogical composition of parent rock, the nature and composition of the solution and its subsequent genesis. Flowing through pipe installation water creates sediments, which is a massive problem for using geothermal energy since sediments reduce the flow; decrease the inner diameter of the pipe and therefore the transfer of heat energy to the pipe wall [1–3]. As a measure of water's tendency to create sediments (precipitation of $CaCO_3$), Langelier's Saturation Index (LSI) and Ryznar's Stability Index (RSI), are used. A positive LSI value indicates that the examined water does not dissolve the protective carbonate layer of (mostly $CaCO_3$) and has no tendency to corrode [4–6]. An RSI value below 7, indicates that the examined water has a strong preference for carbonate deposition. These parameters were used for comparison with the actual behavior of the geothermal water during flow through the pipe installation in the experimental conditions and in the pipe installations itself.

Sijarinska spa and Vranjska spa are located in Southern Serbia and are rich in geothermal water wells. Despite the large number of geothermal wells (15 in Sijarinska spa and 4 in Vranjska spa), only some of them, after pouring and cooling to ambient temperature, showed sedimentation. The reasons for examining the sediments content in these waters are mainly related to energy and economical costs. In regards to this, the object of this analysis is the sedimentation of waters from drill hole B-4 (Sijarinska spa, depth 1232 m) and drill hole VG-2 (Vranjska spa, depth 867 m). Although these locations are relatively close by, geographic characteristics and chemical composition of these waters are different and they have different physicochemical parameters [7-11].

EXPERIMENTAL

Experimental procedure

Water analyses were performed at a flow of geothermal water in installations in Sijarinska spa and Vranjska spa. Laboratory analyses were performed for the flow through a glass tube of "snake" form, 230 cm in length and 10 mm diameter tube, for 6 h, keeping water temperatures identical to the temperatures in drilling holes B-4 and VG-2 (75/90 °C). The flow of geothermal water was achieved by using peristaltic pump Tesa S. A. (Renens). Rotations per minute of the peristaltic pump were regulated by a potentiometer Symmetry SK 313, power 400 W, voltage 230 V and frequency 50 Hz (Figure 1). Thermoregulation was performed by temperature controller device Symmetry SK 302. The flow of water through this pipe was 10 times

Correspondence: D.T. Stojiljković, Faculty of Tehnology, Bulevar Oslobođenja 124, 16 000 Leskovac, Serbia.
E-mail: draganstо24@yahoo.com
Paper received: 2 October, 2012
Paper accepted: 9 April, 2013

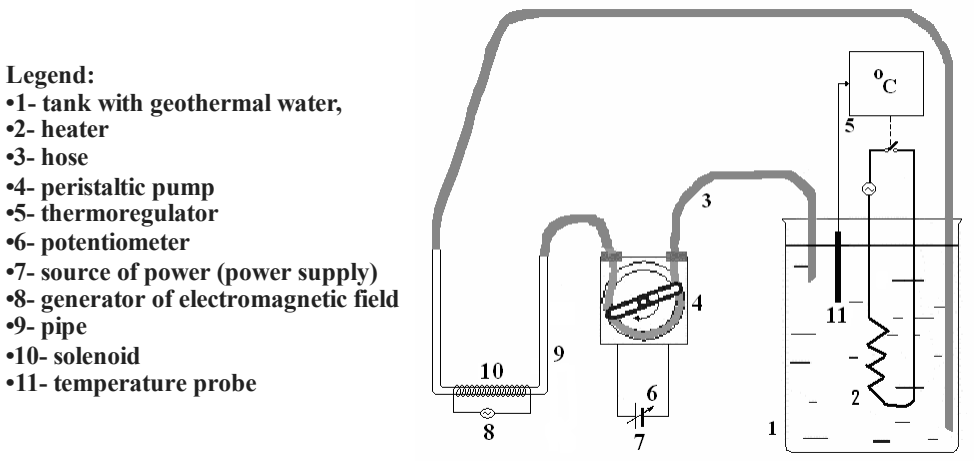

Figure 1. Apparatus for sedimentation in the laboratory conditions.

lower than the flow in pipe installations (0.015 compared to 0.15 L s^{-1}). These parameters were used for comparison with the actual behavior of the geothermal water during flow through the pipe installation in the experimental conditions and in the pipe installations itself. Installations on the tube B-4 in Sijarinska spa included setting a new 1 m-long pipe, diameter 3/4'' (for this study), for determining the sedimentation of geothermal water in the real conditions.

Concentrations of HCO_3^-, Cl^-, SO_4^{2-} and NH_4^+ and turbidity were calculated in accordance with SRPS ISO/IEC 17025:2006 standard.

Analysis of sediment

Powdered rock was treated (12 h) with acetate buffer (acetic acid (1 M)/sodium acetate (1 M) solution at pH 5.0) [11,12] to remove most of the carbonates. This method ensures that carbonate fraction is solubilized. It appears that the treatment of sediments with the acetic acid/sodium acetate is the most efficient and simple method for removing carbonates with a minimal damage to other minerals present [13]. The analysis was performed in order to determine quantitative content of carbonates in comparison to total sediment content.

Analytical methods

Scanning electron microscopy (SEM)/Energy dispersive spectrometry (EDS). All SEM/EDS work was carried out using a Jeol JSM-35 electron microscope equipped with Tracor TN2000 energy dispersive X-ray spectrometer. Operating conditions for energy-dispersive analyses were 25 keV accelerating voltage, 0.1 μA beam current and a beam spot diameter of approximately 3 μm.

X-Ray diffraction (XRD). XRD analysis of the Sijarinska spa sediments was performed by Philips diffractometer (PW 1050/25) equipped with proportional counter and discriminator, using N-filtered Cu radiation at 40 kV and 20 mA.

Inductively coupled plasma-optical emision spectrometry. Major ions in the water and in the whole-rock sample and its carbonate fraction were analyzed by ICP-OES. A Spectroflame ICP-OES instrument was employed and Ar was used as the plasma gas. Total uncertainty (including accuracy error) of the analysis is in the range 5–20%.

RESULTS AND DISCUSION

The results of the analysis of examined major ions and physicochemical parameters of the geothermal waters B-4/VG-2 are given in Tables 1 and 2. Table 1 shows the individual concentrations of ions present in the B-4 and VG-2 waters. Based on the results it can be concluded that the B-4 water has high ion content.

Table 1. Concentration (mg L^{-1}) of major ions in B-4 and VG-2 waters

Component	Sample	
	B-4	VG-2
Na^+	1050	880
Ca^{2+}	45	20
Sr^{2+}	1	1
Mg^{2+}	15	<5
Fe^{3+}/Fe^{2+}	<1	<1
HCO_3^-	2800	400
Cl^-	85	40
SO_4^{2-}	90	60
NH_4^+	<1	<1

The high content (>90%, specification of major carbon species depending on pH) of HCO_3^- compared to H_2CO_3 and CO_3^{2-} is due to pH value of the environment (7.5/7.3) which explains its high concentration (Table 1) and total hardness of water (Table 2). The high content of major ions (Table 1) affects the physico-

chemical characteristics and leads to increased electrical conductivity (Table 2).

Table 2. Physicochemical parameters of B-4 and VG-2 waters

Parameter	Sample	
	B-4	VG-2
pH	7.5	7.3
Temperature, °C	75	90
Total hardness, °dH	9.2	3.4
Permanent hardness, °dH	1.0	0.6
m-Alkality, mL 0.1 M HCl L^{-1}	460	67
Electrical conductivity, μS cm^{-1}	4370	1240
Turbidity, NTU	3	1.3
Solids, mg L^{-1}	2980	1050
pHs	6.05	6.86
LSI	1.45	0.44
RSI	4.60	6.42

Geothermal waters B-4/VG-2 show moderately basic chemical reaction and based on the temperature values (Table 2), these waters qualify as hyperthermal geothermal waters. Judging by the values of electrical conductivity and total dry residue mass, they fit into mineral waters with high mineral content (Table 2) category. According to the values of total hardness (Table 2) these waters fall into the moderately hard waters. Among cations, the most abundant is Na^+ and of anions HCO_3^- (Table 1). The difference in the total hardness can be explained by the difference in HCO_3^-, Ca^{2+} and Mg^{2+} content (Table 1). The difference in m--alkality (Table 2) is also an indicator of different behavior of geothermal waters B-4/VG-2.

Based on the obtained pHs value, LSI and RSI were determined. The value of pHs, which is in line with the saturation pH was determined using a nomogram [4,5,7], and according to Eq. (1):

$$pHs = f[t] - f[Ca^{2+}] - f[A] + f[R] \quad (1)$$

where: $f[t]$ – the dependence on the temperature of the geothermal water, °C, $f[Ca^{2+}]$ – the dependence on the concentration of Ca^{2+}, mg L^{-1}, $f[A]$ – the dependence of m-alkalinity, cm^3 0.1 M HCl L^{-1} and $f[R]$ – the dependence of the total content of dissolved substances, mg L^{-1}.

Determined LSI and RSI values, according to the Eqs. (2) and (3):

$$LSI = pH - pHs \quad (2)$$

$$RSI = 2pHs - pH \quad (3)$$

A positive LSI value (Table 2) indicates that B-4/VG-2 examined waters show no tendency to corrosion. RSI value (Table 2) indicates that B-4 water has a strong preference for deposition of carbonates, in contrast to VG-2, whose tendency to sedimentation is very low. Unlike carbonates, other minerals present in these waters do not show a marked tendency to deposition on the pipe walls. These results were confirmed experimentally by the actual behavior of the geothermal water during the flow through the pipe installation that is in use in Sijarinska spa and Vranjska spa, as well as in laboratory conditions. In laboratory conditions, during the flow of geothermal water B-4, the development of sediment took place, while in the case of VG-2 water no sedimentation occurred. During the flow of water B-4 through the pipe installation, set on the spring place in real time in Sijarinska spa, for a period of 10 days in 1 m long tube (setup of a new tube done in order to be studied for this paper), was established that total sediment content of 157 g, corresponded to difference in tube mass before and after sedimentation.

In the B-4 hole itself the measured CO_2 concentration in geothermal fluid was high (7.9 g L^{-1} [7]. Therefore, it causes a negative temperature coefficient of solubility of $CaCO_3$ so that a decrease in temperature increases the solubility [14]. By cooling the water from the B-4 hole to 20 °C, and by subsequent filtering and drying, 3.6×10^{-2} g L^{-1} of sediment was obtained. On the basis of measured sediment in the pipe (which is 157 g) during 10 days and the flow of geothermal water of 0,15 L s^{-1}, the calculated value is 1.2×10^{-3} g L^{-1}. By comparing the content of sediments in the B-4 water at 20 °C (3.6×10^{-2} g L^{-1}) and the amount that was settled in the pipe installations (1.2×10^{-3} g L^{-1}) 3.3% of deposit is formed on the walls of the tubes (Figure 2). These results are the total amount of sediment that was settled by the B-4 water cooling as opposed to the results received when the water did not flow through pipe installations.

The mineralogy of the B-4 sediment (SEM/EDS/X--ray) in pipe installation and laboratory conditions is the same and relatively simple. $CaCO_3$ is the principal components (>99%) along with minor amount of $CaSO_4$ (anhydrite, <0.5%, Figure 3). $CaCO_3$ mineralogy studies have indicated that aragonite is the predominant mineral in the B-4 sediment (98%) with lesser amount of calcite and vaterite (>1%, Figure 3). The presence of Sr cations (Table 1; Figure 2) causes formation of aragonite and explains its dominance in the sediment. Due topresence of Sr^{2+} in aqueous solution, the surface energy term in nucleation is modified, leading to possible metastable nucleation of aragonite [15].

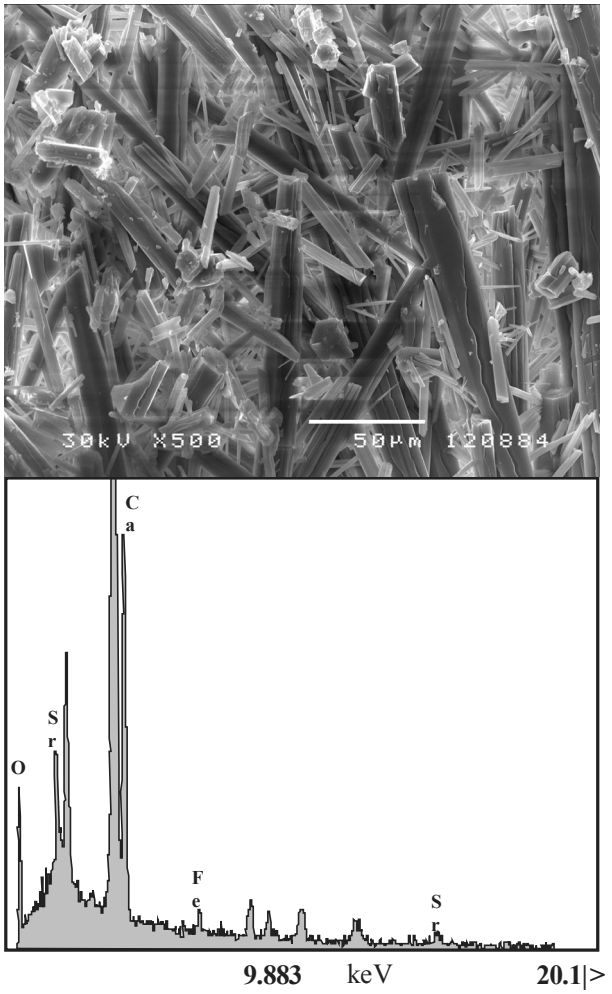

Figure 2. SEM and EDS of sediment formed by deposition of B-4 water in pipe instalations.

CONCLUSION

In this paper, the chemical composition and physicochemical characteristics of geothermal waters B-4 and VG-2 are investigated in order to determine their tendency towards formation of deposits in the pipe installation. Geochemical analysis revealed the concentration of major ions in the samples whose presence causes sedimentation and certain physicochemical properties. LSI 1.45/0.44 and RSI 4.60/6.42 values for B-4/VG-2 explain geochemical behaviour of these geothermal waters. During the flow of geothermal water B-4 the deposits were created, which coincides with the behavior of the same water in real conditions in the installation. In experimental conditions of flow through the pipe installation of geothermal water from the VG-2, the formation of deposits did not take place. Obtained LSI and RSI values indicate that the geothermal water of Vranjska spa (VG-2) is more favorable for use in piping installations because it exhibits less tendency to form deposits. Indeed, the results of mineralogical and geochemical analyses of B-4 water and sediment show the presence of Sr^{2+} (1 g L^{-1}) in the B-4 and VG-2 waters, which in the case of B-4 causes the formation of aragonite (98% of the total sediment). Also, results show 3.3% of deposits on the pipe walls from the total mass of sediment that would be settled by B-4 water cooling as opposed to the results received when the water did not flow through pipe installations.

Acknowledgment

Authors gratefully acknowledge the support by the Ministry of Education, Science and Technological Development of the Republic of Serbia, Project TR 33034.

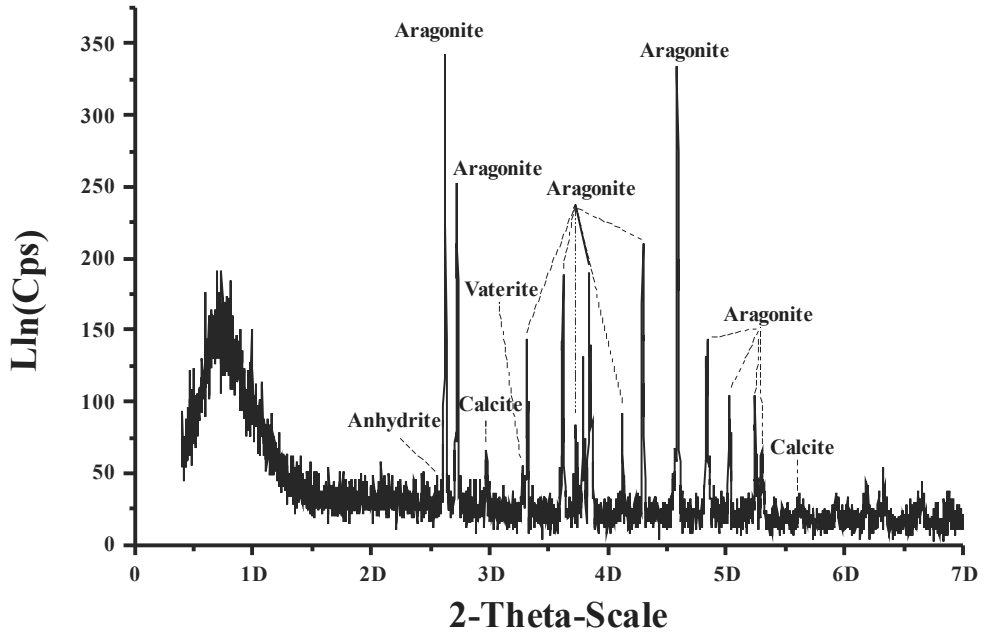

Figure 3. XRD of sediment formed by deposition of B-4 water in the laboratory conditions.

REFERENCES

[1] A. Fathi, T. Mohamed, G. Claude, G. Maurin, B.A. Mohamed, Water Res. **40** (2006) 1941–1950.

[2] F. Alimi, M. Tlili, M.B. Amor, C. Gabrielli, G. Maurin, Desalination **206** (2007) 163–168.

[3] J.K. Kronenberg, IEEE Trans. Magn. **21** (1985) 2059––2061.

[4] P. Milanović, Monograph, IHTM, Belgrade, 2002.

[5] M.A. Кулийски, Наукова Думка, Kiev 1980.

[6] L.C. Lipus, D. Dobersek, Chem. Eng. Sci. **62** (2007) 2089––2095.

[7] D.T Stojiljković, S.T. Stojiljković, N.Č. Mitić, M.D. Pejić, M. Đurović-Petrović, Thermal Science **10** (2006) 195––203.

[8] D.T. Stojiljković, N.Č. Mitić, A.A. Šmelcerović, B.M. Kaličanin, M.Ž. Tasić-Kostov, M.D. Đurović-Petrović, Thermal Science **15** (2011) 643–648.

[9] M. Milivojević, M. Martinović, in Proceedings of World Geothermal Congress, Antalya, Turkey, 2005, p. 24.

[10] P.B. Dokmanović, O.Ž. Krunić, M.K. Martinović, S.M. Magazinović, Thermal Science **16** (2012) 21–30.

[11] M. Lyle, R.G. Heath, J.M. Robins, Geochim. Cosmochim. Acta **48** (1984)1705–1715.

[12] P.I. Premović, N.Z. Pavlović, M.S. Pavlović, N.D. Nikolić, Geochim. Cosmochim. Acta **57** (1993) 1433–1446.

[13] R.J. Cook, Clay Miner. **27** (1991) 73–80.

[14] S. Arnórsson, Geothermics **18** (1989) 183–190.

[15] I. Sunagawa, Y. Takahashi, H. Imai, J. Miner. Petrol. Sci. **102** (2007) 174–181.

IZVOD

FIZIČKOHEMIJSKA I GEOHEMIJSKA KARAKTERIZACIJA SKLONOSTI KA SEDIMENTACIJI GEOTERMALNIH VODA SA LOKALITETA SIJARINSKA BANJA I VRANJSKA BANJA (SRBIJA)

Nebojša Č. Mitić, Dragan T. Stojiljković*, Bratislav Ž. Todorović, Ljubiša S. Nikolić, Staniša T. Stojiljković, Suzana Cakić

Tehnološki fakultet u Leskovcu, Univerzitet u Nišu, Srbija

(Stručni rad)

Predstavljena je sveobuhvatna analiza fizičkohemijskih parametara u geotermalnim vodama sa lokaliteta u Sijarinskoj Banji (bušotina B-4) i Vranjskoj Banji (bušotina VG-2) u cilju ispitivanja njihovih sklonosti ka stvaranju naslaga u cevnim instalacijama. Bušotine B-4/VG-2 imaju kapacitet iskorišćenja 30/27 L s^{-1} sa temperaturama vode 75/90 °C. S tim u vezi, određene su pHs vrednosti a onda su izračunate LSI i RSI vrednosti, kao mere sklonosti ka stvaranju naslaga. Rezultati analize pokazuju da bušotine B-4/VG-2 imaju LSI 1.45/0.44 i RSI 4.6/6.4, što znači da VG-2 voda ne pokazuje (ili pokazuje vrlo malu) sedimentaciju u odnosu na B-4 vodu tako da je povoljnija za korišćenje u cevnim instalacijama. Ispitivano je i ponašanje geotermalne vode B-4 u realnim uslovima u Sijarinskoj Banji, protokom kroz cevnu instalaciju. Ovi rezultati su provereni i potvrđeni geohemijskom analizom. Rezultati geohemijske analize B-4 vode pokazuju da je aragonit dominantni mineral u sedimentu (98%) sa manjim količinama kalcita, vaterita i anhidrita. Dominantnost ovog minerala u odnosu na druge oblike $CaCO_3$ uslovljena je prisustvom katjona Sr^{2+} u B-4 vodi. Takođe, rezultati ovih analiza pokazuju količinu od 3,3% sedimenta na cevnim instalacijama u odnosu na sediment koji bi nastao hlađenjem B-4 vode bez njene energetske iskoristivosti.

Ključne reči: Geotermalne vode • LSI • RSI • Sediment • Aragonit

Uticaj pakovanja u modifikovanoj atmosferi i vakuumu na odabrane hemijske parametre svežine kalifornijske pastrmke (*Oncorhynchus mykiss*) i odrezaka šarana (*Cyprinus carpio*)

Jelena A. Babić[1], Mirjana R. Dimitrijević[2], Milan P. Milijašević[1], Vesna Ž. Đorđević[1], Radivoj B. Petronijević[1], Slaven M. Grbić[3], Aurelija T. Spirić[1]

[1]*Institut za higijenu i tehnologiju mesa, Beograd, Srbija*
[2]*Univerzitet u Beogradu, Fakultet veterinarske medicine, Beograd, Srbija*
[3]*Slaven d.o.o., Banja Luka, Bosna i Hercegovina*

Izvod

Cilj ovih istraživanja bio je da se ispita uticaj pakovanja u modifikovanoj atmosferi i vakuumu na promene vrednosti ukupno isparljivog azota (TVB-N) i pH mesa kalifornijske pastrmke (*Oncorhynchus mykiss*) i šarana (*Cyprinus carpio*), kao odabranih hemijskih parametara svežine mesa ribe i da se ustanove najpodesnije smeše gasova za pakovanje ove dve slatkovodne vrste riba. Za potrebe ovog istraživanja formirane su po tri grupe uzoraka očišćene pastrmke i odrezaka šarana. Prve dve grupe su upakovane u modifikovanu atmosferu sa različitim odnosom gasova: 60% CO_2 + 40% N_2 (I grupa) i 40% CO_2 + 60% N_2 (II grupa), dok je III, kontrolna, grupa upakovana u vakuum. Svi uzorci su čuvani pri istovetnim uslovima na temperaturi od +3 °C, a zatim su prvog, sedmog i četrnaestog dana čuvanja obavljena ispitivanja. Dobijeni rezultati ukazuju da je na vrednost TVB-N u uzorcima pastrmke i odrezaka šarana bitno uticao sastav upotrebljene gasne smeše. Tokom četrnaest dana čuvanja vrednosti za TVB-N u uzorcima sve tri grupe pastrmke i odrezaka šarana statistički su značajno porasle ($p < 0,001$). Najmanji rast vrednosti za TVB-N ustanovljen je u I grupi uzoraka pastrmke i odrezaka šarana, dok je porast vrednosti za TVB-N bio najveći u uzorcima III grupe. Najniža pH vrednost ustanovljena je u uzorcima pastrmke i odrezaka šarana koji su upakovani u modifikovanu atmosferu sa 60% CO_2 + 40% N_2 (I grupa). Rast pH vrednosti u uzorcima pastrmke upakovane u vakuum ustanovljen je tokom celog perioda ispitivanja, dok je u uzorcima odrezaka šarana upakovanim u vakuum rast pH vrednosti ustanovljen samo do sedmog dana ispitivanja. Smeša gasova sa 60% CO_2 + 40% N_2 pokazala se kao najpodesnija za pakovanje sveže pastrmke i odrezaka šarana.

Ključne reči: modifikovana atmosfera, pastrmka, šaran, svežina, ukupan isparljivi azot, pH.

Dostupno na Internetu sa adrese časopisa: http://www.ache.org.rs/HI/

NAUČNI RAD

UDK 664.8.033:597:66

Hem. Ind. **68** (1) 69–76 (2014)

doi: 10.2298/HEMIND130304030B

Činjenica da sveža riba predstavlja veoma kvarljivu namirnicu (pH > 6,0; a_w > 0,98) uticala je da fokus proizvođača bude usmeren ka iznalaženju optimalne metode konzervisanja ribe. Međutim, poslednjih godina u svetu, potrošači sve izraženije zahtevaju da u svakom trenutku u ponudi imaju svežu ribu, s obzirom na to da, kao takva, ima najprihvatljivije senzorne karakteristike. Ovaj trend je uslovio razvoj efikasnog koncepta pakovanja u modifikovanu atmosferu (MAP), koji ribi obezbeđuje duži rok održivosti i očuvanje osnovnih parametara svežine [1]. MAP se, danas, koristi u proizvodnji sveže i ohlađene hrane, uključujući sirovo i termički obrađeno meso, živinu, ribu, paste, voće i povrće i, u novije vreme, kafu, čaj i pekarske proizvode. U cilju dobijanja što kvalitetnijih proizvoda u odnosu na senzorna svojstva, u industrijskoj preradi se poljoprivredni proizvodi podvrgavaju brojnim procesima i operacijama [2]. Međutim, u današnje vreme postoji zahtev tržišta za namirnicama koje su minimalno prerađene i bez dodatih konzervanasa i aditiva [3], tako da je hrana upakovana u modifikovanu atmosferu sve više prisutna u maloprodaji. Pakovanje u modifikovanoj atmosferi se može definisati kao uklanjanje vazduha iz pakovanja i njegova zamena određenim gasom ili smešom gasova. Svrha ove tehnologije je da se produži održivost hrane sprečavanjem ili usporavanjem biohemijskih procesa (oksidacija masti, formiranje metmioglobina) i rasta bakterija kvara [4]. Gasovi koji se najviše koriste u tehnologiji pakovanja u modifikovanu atmosferu su ugljen-dioksid (CO_2), kiseonik (O_2) i azot (N_2) [5]. Ovi gasovi se koriste u različitim kombinacijama, a njihove uloge u modifikovanoj atmosferi su veoma različite. Dok je N_2 inertan gas kome je zadatak da spreči kolaps pakovanja, CO_2 može inhibirati rast nekoliko vrsta mikroorganizama, posebno onih koji izazivaju nastanak kvara i neprijatnih mirisa kod namirnica koje se čuvaju na temperaturi frižidera. Prednost ugljen-dioksida je i

Prepiska: J.A. Babić, Institut za higijenu i tehnologiju mesa, Kaćanskog 13, 11000 Beograd, Srbija.
E-pošta: babicdzela@yahoo.com.au
Rad primljen: 4. mart, 2013
Rad prihvaćen: 10. april, 2013

što nije toksičan za ljude [6]. Kiseonik ima značajnu ulogu u MAP-u, pogotovo u pakovanju svežeg mesa [5]. Prisustvo kiseonika održava pigment mioglobin u mesu u oksigenisanoj formi, oksimioglobinu, i, na taj način, daje mesu svetlocrvenu boju, prihvatljivu za potrošača. Međutim, smanjenjem koncentracije kiseonika u pakovanju može da se spreči oksidacija masti i nastajanje užeglosti masne komponente u mesu, ribi i pekarskim proizvodima. Oksidacija masti bi dovela do nastanka neprijatnog mirisa i ukusa ili do promene boje proizvoda.

Iako su i drugi gasovi, kao što su azot-oksid, sumpor-dioksid, etilen, hlor, ozon i propilen-oksid eksperimentalno korišćeni, oni se ne primenjuju u MAP tehnologiji zbog bezbednosti proizvoda, propisa koji ograničavaju njihovu upotrebu i cene pakovanja [7]. Mešavine gasova sa visokom koncentracijama CO_2 i N_2 su privukle najveću pažnju istraživača koji su se tokom protekle decenije bavili problematikom pakovanja ribe. Međutim, uticaj pakovanja u modifikovanu atmosferu na održivost sveže ribe i najpodesnija smeša gasova zavise od vrste ribe koja se pakuje, sadržaja masti, inicijalne mikrobiološke kontaminacije, manipulacije ribom posle izlova, zapreminskog odnosa gasa i proizvoda u pakovanju i, što je najvažnije, metode pakovanja i uslova skladištenja [6,8]. U nekim slučajevima, MAP može da utiče na sniženje kvaliteta upakovane ribe zbog rastvaranja CO_2 u mesu ribe, usled čega nastaje ugljena kiselina, a pri manjim vrednostima pH smanjuje se i kapacitet mesa ribe da vezuje vodu usled čega dolazi do izdvajanja mesnog soka u pakovanju koji je idealna podloga za razvoj mikroorganizama kvara [6,9]. Iz tih razloga je neophodno da se odredi optimalni odnos gasova u smeši u zavisnosti od karakteristika proizvoda koji se pakuje i sistema za pakovanje.

Kao hemijski indikator svežine ribe smatra se vrednost ukupno isparljivog azota (*total volatile basic nitrogen* – TVB-N). Ukupno isparljivi azot čine jedinjenja koja su odgovorna za nastanak neprijatnog mirisa i ukusa mesa ribe, a tu spadaju amonijak, dimetilamin (DMA), trimetilamin (TMA), amini koji nastaju dekarboksilacijom amino-kiselina, kao i druga azotna jedinjenja koja u alkalnom obliku postaju isparljiva [10,11]. Amonijak nastaje bakterijskom dezaminacijom proteina, peptida i amino-kiselina kao i autolitičkom razgradnjom adenozin monofosfata (AMP). Dimetilamin i trimetilamin nastaju degradacijom trimetilamin-oksida (TMAO), jedinjenja koje ima značajnu ulogu u osmoregulaciji i čije je prisustvo dokazano kod svih morskih i velikog broja slatkovodnih riba. Aktivnošću endogenih enzima riba dolazi do razgradnje TMAO i nastanka DMA i formaldehida [12]. Pod anaerobnim uslovima, bakterije uzročnici kvara mesa, koristeći TMAO kao krajnji akceptor elektrona u anaerobnoj respiraciji, dovode do formiranja TMA, koji predstavlja jedinjenje odgovorno za pojavu karakterističnog mirisa kod kvara ribe [13].

Cilj ovih istraživanja bio je da se ispita uticaj pakovanja u modifikovanoj atmosferi i vakuumu na promene vrednosti ukupnog isparljivog azota (TVB-N) i pH mesa kalifornijske pastrmke (*Oncorhynchus mykiss*) i šarana (*Cyprinus carpio*) i da se ustanove najpodesnije smeše gasova za pakovanje ove dve slatkovodne vrste riba.

MATERIJAL I METODE

Kalifornijska pastrmka (*Oncorhynchus mykiss*), koja je korišćena u eksperimentu, je gajena u identičnim uslovima i potiče iz istog bazena za intenzivni uzgoj. Ribnjak u kome je gajena pastrmka nalazi se na obroncima planine Zlatibor. Za potrebe ispitivanja uzorkovano je 54 jednogodišnjih pastrmki prosečne mase 273 g. Riba je živa transportovana od ribnjaka do pogona za klanje i preradu, gde je smeštena u prihvatni bazen, a zatim omamljena električnom strujom. Klanje i evisceracija ribe je obavljeno na automatskom uređaju, a pranje trupova ručno, pod mlazom vode. Konzumni šaran (*Cyprinus carpio*) je poticao iz ribnjaka koji se nalazi u ravničarskom delu Srbije, u kome je primenjen poluintenzivni način uzgoja ribe. Za eksperiment je korišćeno 9 dvogodišnjih šarana prosečne mase 2,5 kg. Šarani su živi preneti do pogona za klanje i preradu ribe, gde su omamljeni, zaklani, očišćena im je krljušt, a trup je isečen na odreske debljine 2 cm, pri čemu je od jednog trupa dobijeno po 6 odrezaka. Formirane su po tri grupe uzoraka, a svaku grupu je činilo 18 uzoraka očišćene pastrmke, odnosno odrezaka šarana. Prve dve grupe su upakovane u modifikovanu atmosferu sa različitim odnosom gasova: 60% CO_2 + 40% N_2 (I grupa) i 40% CO_2 + 60% N_2 (II grupa), dok je III, kontrolna, grupa upakovana u vakuum. Za pakovanje uzoraka upotrebljena je mašina za pakovanje „Variovac“ (Variovac Primus, Zarrentin, Nemačka). Kao materijal za pakovanje korišćena je folija OPA/EVOH/PE (orijentisani poliamid/ /etilen vinil alkohol/polietilen, Dynopack, Polimoon, Kristiansand, Norveška) sa niskom propustljivošću za gas (stepen propustljivosti za O_2 – 3,2 $cm^3\ m^{-2}\ dan^{-1}$ pri 23 °C; za N_2 – 1 $cm^3\ m^{-2}\ dan^{-1}$ pri 23 °C; za CO_2 – 14 $cm^3\ m^{-2}\ dan^{-1}$ pri 23 °C i za vodenu paru 15 $cm^3\ m^{-2}\ dan^{-1}$ pri 38 °C). Odnos gas/uzorak u pakovanju bio je 2:1. U toku eksperimenata, svi uzorci su čuvani pri istovetnim uslovima, na temperaturi od 3 °C. Za potrebe ispitivanja, iz svake grupe (I, II i III) prvog, sedmog i četrnaestog dana uzeto je po 6 uzoraka. Svi uzorci su ispitani u duplikatu.

Hemijska ispitivanja

Vrednost pH je određena prema standardnoj metodi SRPS ISO 2917/2004 (pH metar-Cyber Scan 510) [14].

Ukupno isparljivi azot (TVBN) je određen prema EU referentnoj metodi koja je data u *Commission Regulation* (EC), No. 2074/2005 [15].

Metode statističke obrade podataka

Za statističku obradu podataka (srednja vrednost, mere varijacije, analiza varijanse i *t*-test) korišćen je softverski paket Microsoft Office Excel 2007.

REZULTATI I DISKUSIJA

Ukupno isparljivi azot

Rezultati ispitivanja prosečnih vrednosti ukupno isparljivog azota za uzorke pastrmki upakovanih u modifikovanu atmosferu i vakuum prikazani su na slici 1.

Na osnovu prikazanih rezultata može da se vidi da se prvog dana prosečan sadržaj TVB-N u sve tri grupe uzoraka pastrmki (9,22±0,32; 8,97±0,46 i 9,10±0,31 mg N/100 g) nije statistički značajno razlikovao ($p > 0,05$). Prosečan sadržaj za TVB-N u uzorcima I (14,15±0,60 mg N/100 g) i II grupe (14,55±0,98 mg N/100 g), nakon sedam dana čuvanja, statistički se značajno razlikovao ($p < 0,001$) u odnosu na prosečni sadržaj za TVB-N u uzorcima III grupe (16,46±1,00 mg N/100 g). Statistički značajna razlika nije ustanovljena ($p > 0,05$) između vrednosti za TVB-N u uzorcima I i II grupe sedmog dana ispitivanja. Četrnaestog dana ispitivanja, između prosečnih vrednosti za TVB-N u uzorcima I (18,17±0,93 mg N/100 g), II (20,90±0,81 mg N/100 g) i III grupe (36,18±2,65 mg N/100 g) ustanovljena je statistički značajna razlika na nivou $p < 0,001$.

Rezultati ispitivanja prosečnih vrednosti ukupno isparljivog azota za uzorke odrezaka šarana upakovanih u modifikovanu atmosferu i vakuum prikazani su na slici 2.

U uzorcima odrezaka šarana, prvog dana ispitivanja, takođe, nije ustanovljena statistički značajna razlika

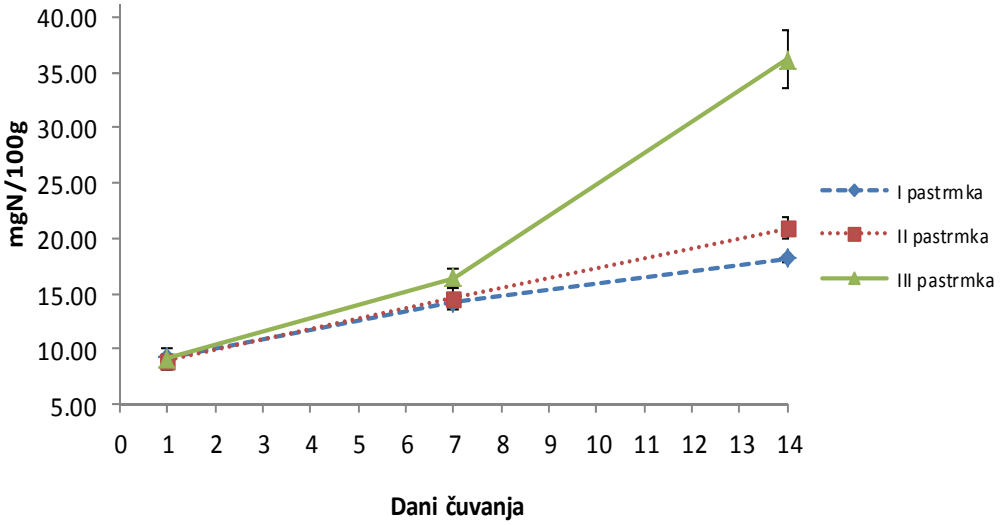

Slika 1. Vrednosti za TVB-N u uzorcima pastrmke upakovanih u modifikovanu atmosferu i vakuumu ($\bar{X}$ ± Sd).
Figure 1. TVB-N values in trout samples packaged in modified atmosphere and vacuum ($\bar{X}$ ±Sd).

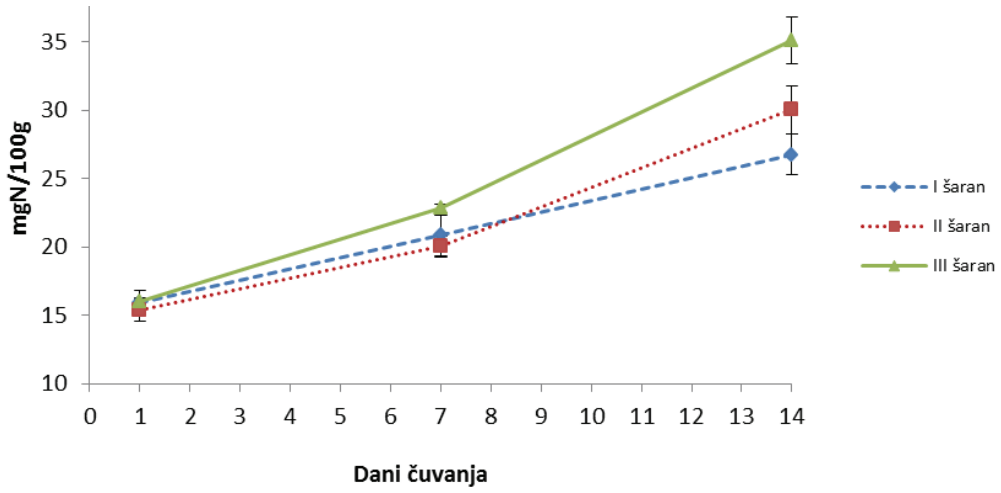

Slika 2. Vrednosti za TVB-N u uzorcima odrezaka šarana upakovanih u modifikovanu atmosferu i vakuumu ($\bar{X}$ ±Sd).
Figure 2. TVB-N values in carp cuts packaged in modified atmosphere and vacuum ($\bar{X}$ ±Sd).

(p > 0,05) između prosečnih vrednosti za TVB-N (15,95± ±0,84; 15,39±0,78 i 16,05±0,27 mg N/100 g). Sedmog dana ispitivanja, prosečna vrednost za TVB-N u uzorcima šarana iz I grupe (20,86±0,78 mg N/100 g) bila je najmanja i statistički značajno se razlikovala (p < 0,05) od prosečne vrednosti za TVB-N u uzorcima III grupe (22,82±1,74 mg N/100 g). Razlika između vrednosti za TVB-N u uzorcima II grupe (20,04±0,75 mg N/100 g) u odnosu na vrednost za TVB-N u uzorcima III grupe bila je na nivou statističke značajnosti od p < 0,001. Između prosečnih vrednosti za TVB-N u uzorcima I i II grupe sedmog dana ispitivanja nije ustanovljena statistički značajna razlika (p > 0,05). Četrnaestog dana ispitivanja, u uzorcima šarana iz I grupe ustanovljena je najmanja prosečna vrednost za TVB-N (26,74±1,48 mg N/100 g), a u uzorcima iz III grupe prosečna vrednost za TVB-N je bila najveća (35,10±1,75 mg N/100 g). Kod uzoraka šarana iz II grupe prosečna vrednost za TVB-N četrnaestog dana ispitivanja iznosila je 30,02±0,31 mg N/100 g. Razlika između prosečnih vrednosti za TVB-N u sve tri grupe odrezaka šarana četrnaestog dana ispitivanja bila je statistički značajna (p < 0,001).

Prosečna vrednost za TVB-N u uzorcima pastrmke (9,10 mg N/100 g) i u uzorcima odrezaka šarana (15,80 mg N/100 g) prvog dana ispitivanja bila je niska, što ukazuje na dobar kvalitet ribe. Arahisar i sar. [16] su u svojim istraživanjima ustanovili da je inicijalna vrednost za TVB-N u filetima pastrmke iznosila 12 mg N/100 g, dok Ježek i Buhtova [17] u filetima šarana na početku ispitivanja pokazuju vrednost za TVB-N od 16,25±0,79 mg N/100 g. Ove razlike u vrednostima za TVB-N, u odnosu na naša ispitivanja, mogu biti posledica različitih vrednosti neproteinskog azota mesa ribe, koje zavise od načina ishrane, vremena izlova, veličine ribe kao i mikrobiološkog kvaliteta mesa ribe [18].

Kao što se može videti sa slika 1 i 2, na vrednosti za TVB-N u uzorcima pastrmke i odrezaka šarana bitno je uticao sastav upotrebljene gasne smeše. Tokom četrnaest dana ispitivanja vrednosti za TVB-N u uzorcima sve tri grupe uzoraka pastrmke i odrezaka šarana statistički su značajno porasle (p < 0,001). Najmanji rast vrednosti TVB-N ustanovljen je u I grupi uzoraka, koji su upakovani u MAP sa 60% CO_2 i 40% N_2, dok je porast vrednosti TVB-N bio najveći u uzorcima pastrmke i odrezaka šarana upakovanim u vakuumu. Ustanovljena razlika za vrednosti TVB-N u ispitanim grupama uzoraka može se objasniti većim procentualnim udelom CO_2 u smeši gasova kod I grupe uzoraka. Naime, osnovna uloga ugljen-dioksida, kao gasa koji se koristi u tehnologiji pakovanja namirnica u MAP, je inhibicija rasta mikroorganizama, posebno bakterija izazivača kvara namirnica koje, svojom metaboličkom aktivnošću, dovode do nastanka azotnih isparljivih jedinjenja. Bakteriostatski efekat CO_2 zavisi od njegove koncentracije i temperature skladištenja uzoraka, a mehanizmi delovanja se zasnivaju na promeni permeabiliteta ćelijske membrane bakterija, inhibiciji enzima, promeni fizičko-hemijskih osobina proteina kao i promeni pH vrednosti bakterijskih ćelija [19]. Sedmog dana ispitivanja nije ustanovljena statistički značajna razlika (p > 0,05) između vrednosti za TVB-N kod I i II grupe uzoraka pastrmke i odrezaka šarana, tj. uzoraka upakovanih u MAP. Ovi rezultati ukazuju da je ukupan broj bakterija u mesu ribe sedmog dana ispitivanja bio nizak, tako da je smeša gasova sa manjim udelom ugljen-dioksida (40% CO_2 + 60% N_2) uspešno ihnibirala rast mikroorganizama, što je imalo za posledicu manju vrednost TVB-N. U toku daljeg skladištenja došlo je do povećanja broja mikroorganizama, tako da je za inhibiciju njihove aktivnosti bila potrebna veća koncentracija ugljen-dioksida, što potvrđuje statistički značajna razlika (p < 0,001) između vrednosti TVB-N u uzorcima pastrmke i odrezaka šarana iz I i II grupe četrnaestog dana ispitivanja.

Ispitivanja koja su sproveli Masnijom i sar. [20], takođe ukazuju na bakteriostatski efekat ugljen-dioksida i, posledično, smanjenje vrednosti TVB-N. Ovi autori su ustanovili sporiji rast vrednosti TVB-N u odrescima brancina koji su bili upakovani u modifikovanu atmosferu koja se sastojala od 80% CO_2 + 20% N_2, i 100% CO_2 u odnosu na kontrolnu grupu, kod koje se u pakovanju umesto modifikovane atmosfere nalazio vazduh. U kontrolnoj grupi, vrednost za TVB-N je devetog dana eksperimenta dostigla 23 mg N/100 g, dok je u uzorcima pakovanim u 100% CO_2 dvadeset prvog dana ispitivanja iznosila 20 mg N/100 g. Gimenez i sar. [1] su, ispitujući uticaj nekoliko različitih smeša gasova (10% O_2 + 50% CO_2 + 40% N_2; 10% O_2 + 50 % CO_2 + 40% Ar; 20% O_2 + 50% CO_2 + 30% N_2; 20% O_2 + 50% CO_2 + 30% Ar; 30% O_2 + 50% CO_2 + 20% N_2; 30% O_2 + 50% CO_2 + + 20% Ar) na parametre održivosti fileta pastrmke skladištenih na +1 °C, ustanovili, između ostalog, da je ovaj vid pakovanja veoma efikasan u sprečavanju stvaranja TVB-N, bez obzira na smešu gasova koja se koristi. U literaturi ne postoji određen limit za vrednost TVB-N u mesu pastrmke, a navedeni autori uzimaju kao kritičnu vrednost 25 mg N/100 g. U našim istraživanjima vrednosti TVB-N u uzorcima pastrmke upakovane u MAP-u (I i II grupa) su bile ispod navedenog limita prihvatljivosti u toku celog perioda čuvanja, dok je u uzorcima pastrmke upakovane u vakuumu (III grupa) četrnaestog dana ispitivanja vrednost TVB-N iznosila 36,18±2,65 mg N/100 g, tj. bila je znatno iznad limita koji ovi autori preporučuju za pastrmku.

Uticaj inhibitornog efekta ugljen-dioksida na sadržaj TVB-N u odrescima šarana ispitali su Milijašević i sar. [21], koji su dokazali najmanju vrednost za TVB-N u odrescima šarana upakovanim u modifikovanu atmosferu koju je sačinjavao 100% CO_2. Ježek i Buhtova [17] su, u svojim istraživanjima, takođe, ustanovili manju vrednost TVB-N u filetima šarana upakovanim u MAP

(69% N_2 + 25% CO_2 + 5% O_2 + 1% CO) u odnosu na grupu uzoraka koja je čuvana u uslovima frižidera na temperaturi od +2 °C. Ovi autori, kao gornji limit prihvatljivosti za TVB-N u mesu šarana preporučuju 20 mg N/100 g. U našim ispitivanjima, vrednost za TVB-N je u odrescima šarana upakovanim u modifikovanu atmosferu (I i II grupa) dostigla limit koji su ovi autori preporučili četrnaestog dana ispitivanja, dok je kod uzoraka upakovanih u vakuumu (III grupa) ta vrednost dostignuta sedmog dana ispitivanja.

pH vrednost

Rezultati ispitivanja prosečnih pH vrednosti u uzorcima pastrmke upakovanih u modifikovanu atmosferu i vakuumu prikazani su na slici 3.

U našim istraživanjima, prvog dana ispitivanja, prosečna pH vrednost u uzorcima pastrmke iz I (6,38±±0,07), II (6,40±0,04) i III grupe (6,39±0,09) se nije statistički značajno razlikovala ($p > 0,05$). Sedmog dana ispitivanja ustanovljena je statistički značajna razlika ($p < 0,001$) između prosečnih pH vrednosti uzoraka iz I (6,27±0,08) i II grupe (6,31±0,04) i prosečne pH vrednosti uzoraka pastrmke iz III grupe (6,48±0,05). Između prosečnih pH vrednosti uzoraka iz I i II grupe statistički značajna razlika je bila na nivou $p < 0,01$. Četrnaestog dana ispitivanja, razlika između prosečnih pH vrednosti uzoraka iz I (6,15±0,09), II (6,29±0,05) i III grupe (6,62±±0,08) bila je na nivou statističke značajnosti od $p < 0,001$. U I grupi uzoraka pastrmke pad pH vrednost je bio statistički značajan ($p < 0,01$) u toku celog eksperimenta. Ustanovljena pH vrednost u II grupi uzoraka je statistički značajno bila manja ($p < 0,001$) sedmog dana ispitivanja u odnosu na pH vrednost prvog dana ispitivanja. Prosečna pH vrednost uzoraka iz II grupe se nije statistički značajno menjala ($p > 0,05$) od sedmog do četrnaestog dana ispitivanja. Porast pH vrednosti u III grupi uzoraka pastrmke bio je statistički značajan ($p < 0,001$) u toku celog eksperimenta.

Rezultati ispitivanja prosečnih pH vrednosti u uzorcima odrezaka šarana upakovanih u modifikovanu atmosferu i vakuum prikazani su na slici 4.

U uzorcima šarana sve tri grupe prosečne pH vrednosti prvog dana ispitivanja nisu se statistički značajno razlikovale (6,50±0,02; 6,51±0,01 i 6,52±0,09), ($p > 0,05$). Sedmog dana ispitivanja pH vrednost uzoraka iz I (6,48±±0,08) i II grupe (6,52±0,04) bila je statistički značajno manja ($p < 0,05$) u odnosu na pH vrednost uzoraka iz III grupe (6,62±0,03). Između prosečnih pH vrednosti uzoraka iz I i II grupe nije ustanovljena statistički značajna razlika ($p > 0,05$). U uzorcima I grupe, četrnaestog dana ispitivanja, prosečna pH vrednost (5,94±1,11) bila je statistički značajno manja ($p < 0,001$) od prosečnih pH vrednosti uzoraka iz II i III grupe (6,24±0,07; 6,49±0,17). Razlika između prosečnih pH vrednosti uzoraka iz II i III grupe bila je na nivou statističke značajnosti od $p < 0,05$.

U I i II grupi uzoraka odrezaka šarana nije došlo do statistički značajnih promena pH vrednosti ($p > 0,05$) do sedmog dana ispitivanja. Međutim, nakon sedmog dana ispitivanja, u uzorcima upakovanim u MAP-u ustanovljen je pad pH vrednosti na nivou statističke značajnosti od $p < 0,001$, za I grupu i od $p < 0,01$, za II grupu. U uzorcima odrezaka šarana upakovanim u vakuum, sedmog dana ispitivanja ustanovljen je rast pH vrednosti ($p < 0,05$). Prosečna pH vrednost uzoraka iz III grupe nije se statistički značajno menjala ($p > 0,05$) od sedmog do četrnaestog dana ispitivanja.

Postmortalna vrednost pH mišićnog tkiva ribe varira između 6,0 i 7,1, u zavisnosti od godišnjeg doba, vrste ribe i drugih faktora [22]. Usled nakupljanja mlečne kiseline nastale u fazi glikolize pod anaerobnim uslovima, postmortalna pH vrednost ribe opada, a stepen njenog smanjenja utiče na kvalitet mesa ribe [23].

Na slikama 3 i 4 može da se uoči da je najniža pH vrednost ustanovljena u uzorcima pastrmke i odrezaka šarana koji su upakovani u modifikovanu atmosferu sa 60% CO_2 + 40% N_2 (I grupa). Ježek i Buhtova [24],

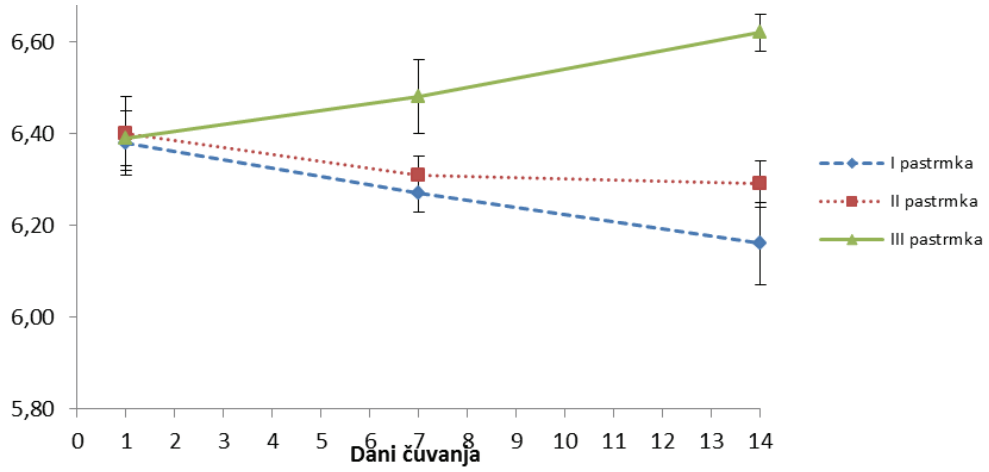

Slika 3. pH vrednosti u uzorcima pastrmke upakovanih u modifikovanu atmosferu i vakuumu ($\bar{X}$ ±Sd).
Figure 3. pH values in trout samples packaged in modified atmosphere and vacuum ($\bar{X}$ ±Sd).

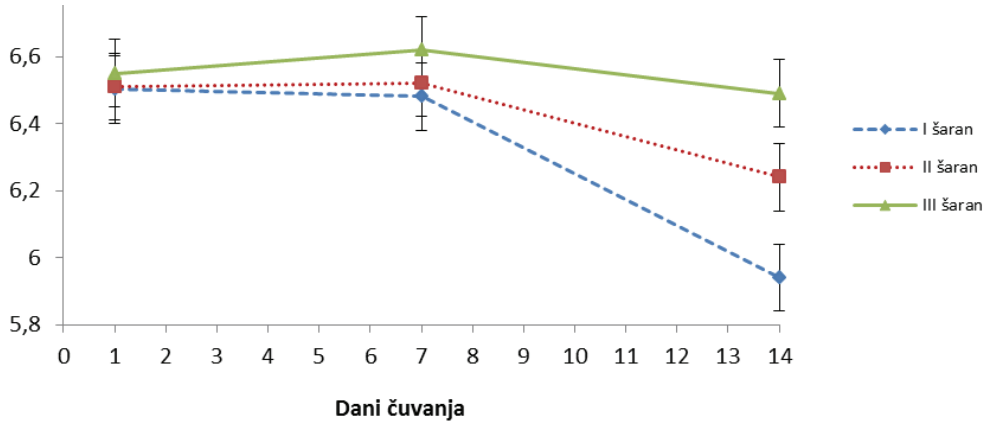

Slika 4. pH vrednosti u uzorcima odrezaka šarana upakovanih u modifikovanu atmosferu i vakuumu ($\bar{X}$ ±Sd).
Figure 4. pH values in carp cuts packaged in modified atmosphere and vacuum ($\bar{X}$ ±Sd).

takođe, konstatuju pad pH vrednosti u filetima šarana upakovanim u smešu gasova koja se sastojala od 80% O_2 i 20% CO_2. Prvog dana ispitivanja, pH vrednost iznosila je 6,46±0,22 da bi nakon petnaestog dana skladištenja na temperaturi od 2 °C iznosila 6,17±0,10. Studija sprovedena na odrescima šarana [21] pokazala je da je pad pH vrednosti bio najizraženiji u grupi uzoraka upakovanih u atmosferu sa 100% CO_2. Znatno nižu pH vrednost u uzorcima ribe upakovane u modifikovanu atmosferu sa većim procentom CO_2 ustanovili su i drugi autori [20,25,26] i objašnjavaju je povećanim rastvaranjem CO_2 u mesu ribe i posledičnim stvaranjem ugljene kiseline. Međutim, Stenstrom [27] je dokazao da na pad pH vrednosti mesa ribe, takođe, mogu uticati i kiseli proizvodi metabolizma različitih vrsta bakterija. Porast pH vrednosti u III grupi uzoraka pastrmke i odrezaka šarana upakovanih u vakuumu u našim ispitivanjima može biti posledica nakupljanja veće količine baznih proizvoda koji nastaju aktivnošću bakterija uzročnika kvara mesa [28].

ZAKLJUČCI

Na osnovu dobijenih rezultata može se zaključiti da se u pogledu odabranih hemijskih parametara kao što su TVB-N i pH kao najpodesnija smeša za pakovanje sveže pastrmke i odrezaka šarana pokazala smeša gasova sa 60% CO_2 i 40% N_2.

Zahvalnica

Ova istraživanja su sprovedena u okviru realizacije projekata TR 31011 i TR 31075 koje, u okviru Programa istraživanja u oblasti tehnološkog razvoja za period 2011-2014. godine, finansira Ministarstvo prosvete, nauke i tehnološkog razvoja Republike Srbije.

LITERATURA

[1] B. Gimenez, P. Roncales, J.A. Beltran, Modified atmosphere packaging of filleted rainbow trout, J. Sci. Food Agric. **82** (2002) 1154–1159.

[2] S. Popov, Biotehnologija-izazov za prehrambenu industriju, Hem. Ind. **61**(5) (2007) 246–250.

[3] S. Kocić-Tanackov, G.Dimić, I.Tanackov, D. Pejin, Lj. Mojović, J.Pejin, Antifungal activity of Oregano (*Origanum vulgare* L.) extract on the growth of *Fusarium* and *Penicilium* species isolated from food, Hem. Ind. **66**(1) (2012) 33–41.

[4] M. Milijašević, B. Velebit, L. Turubatović, J. Jovanović, J. Babić, Uticaj različitih smeša gasova na održivost svežeg junećeg mesa, Tehnologija mesa **49**(5-6) (2008) 161––164.

[5] L. Martinez, D. Djenane, I. Cilla, J.A. Beltran, P. Roncales, Effect of varying oxygen concentrations on the shelf life of fresh pork sausages packaged in modified atmosphere, Food Chem. **94** (2006) 219–225.

[6] M. Sivertsvik, W.K. Jeksrud, J.T. Rosnes, A review of modified atmosphere packaging of fish and fishery products – significance of microbial growth, activities and safety, Int. J. Food Sci. Tech. **37** (2002) 107–127.

[7] A.L. Brody, „Nano, Nano“ Food Packaging Technology, J. Food Technol. **12** (2003) 52–54.

[8] N. Bøknæs, C. Österberg, J. Nielsen, P. Dalgraad, Influence of freshness and frozen storage temperature on quality of thawed cod fillets stored in modified atmosphere packaging, Lebensm. Wiss. Technol. **33** (2000) 244–248.

[9] A.E. Goulas, M.G. Kontominas, Effect of modified atmosphere packaging and vacuum packaging on the shelf-life of refrigerated chub mackerel (*Scomber japonicus*): biochemical and sensory attributes, Eur. Food Res. Technol. **224** (2007) 545–553.

[10] J. Debevere, G. Boskou, Effect of modified atmosphere packaging on the TVB/TMA producing microflora of cod fillets, Int. J. Food Microbiol. **31** (1996) 221–229.

[11] C. Ruiz-Capillas, A. Moral, Sensory and biochemical aspects of quality of whole bigeye tuna (*Thunnus obe-*

sus) during bulk storage in controlled atmospheres, Food Chem. **89**(3) (2005) 347–354.

[12] H.H. Huss, Quality and quality changes in fresh fish. FAO Fisheries Technical Paper 348, FAO, 1995.

[13] L. Gram, H.H. Huss, Microbiological spoilage of fish and fish products, Int. J. Food Microbiol. **33** (1996) 121–137.

[14] SRPS ISO 2917, 2004, Određivanje pH vrednosti.

[15] Commission regulation (EC) 2074/2005 of 5 December 2005 laying down implementing measures for certain products under Regulation (EC) No 853/2004 of the European Parliament and of the Council and for the organisation of official controls under Regulation (EC) No 854/2004 of the European Parliament and of the Council and Regulation (EC) No 882/2004 of the European Parliament and of the Council, derogating from Regulation (EC) No 852/2004 of the European Parliament and of the Council and amending Regulations (EC) No 853/2004 and (EC) No 854/2004.

[16] Ş. Arashisar, O. Hisar, M. Kaya, T. Yanik, Effect of modified atmosphere and vacuum packaging on microbiological and chemical properties of rainbow trout (*Oncorhynchus mykiss*) fillets, Int. J. Food Microbiol. **97** (2004) 209–214.

[17] F. Ježek, H. Buchtová, Shelf-life of cilled muscle of common carp (*Cyprinus carpio* L.) packeged in carbon monoxide enriched modified atmosphere, Acta Vet. Brno **79** (2010) 117–125.

[18] J.J. Connell, Methods of assessing and selecting for quality. In: Connell JJ (ed.) Control of fish quality. Fishing News Books, Oxford, 1990, pp. 122–150.

[19] J.M. Farber, Microbiological aspects of modified-atmosphere packing technology – a review, J. Food Sci. **9** (1991) 58–70.

[20] P. Masniyom, S. Benjakul, W. Visessanguan, Shelf-life extension of refrigerated seabass slices under modified atmisphere packaging, J. Sci. Food Agric. **82** (2002) 873––880.

[21] M. Milijašević, J. Babić, M.Ž. Baltić, A. Spirić, B. Velebit, B. Borović, D. Spirić, Uticaj različitih smeša gasova na promene nekih mikrobioloških i hemijskih parametara u odrescima šarana (*Cyprinus carpio*) upakovanih u modifikovanu atmosferu, Tehnologija mesa **51**(1) (2010) 66––70.

[22] S. Simeonidou, K. Govaris, K. Vareltzis, Quality assessment of seven Mediterranean fish species during storage on ice, Food Res. Int. **30**(7) (1998) 479–484.

[23] I.N.A. Ashie, J.P. Smith, B.K. Simpson, Spoilage and shelf-life extension of fresh fish and shellfish, Crit. Rev. Food Sci. **36**(1&2) (1996) 87–121.

[24] F. Ježek, H. Buchtová, Physical and chemical changes in fresh chilled muscle tissue of common carp (*Cyprinus carpio* L.) packed in a modified atmosphere, Acta Vet. Brno **76** (2007) 83–92.

[25] L. Provincial, M. Gil, E. Guillen, V. Alonso, P. Roncales, J.A. Beltran, Effect of modified atmosphere packaging using different CO_2 and N_2 combinations on physical, chemical, microbiological and sensory changes of fresh sea bass (*Dicentrarchus labrax*) fillets, Int. J. Food Sci. Tech. **45** (2010) 1828–1836.

[26] N. Stamatis, J.S. Arkoudelos, Effect of modified atmosphere and vacuum packaging on microbial, chemical and sensory quality indicators of fresh, filleted *Sardina pilchardus* at 3 °C, J. Sci. Food Agric. **87** (2007) 1164––1171.

[27] I.J. Stenstrom, Microbial flora of cod fillets (*Gadus morhua*) stored at 2 °C in different mixtures of carbon dioxide and nitrogen/oxygen, J. Food Protect. **48** (1985) 585–589

[28] C. Riuz-Capillas and A. Moral, Residual effect of CO_2 on hake (Merluccius merluccius L) stored in modified and controlled atmospheres, Eur. Food Res. Technol. **212** (2001) 413–420.

SUMMARY

EFFECT OF MODIFIED ATMOSPHERIC CONDITIONS AND VACUUM PACKAGING ON SELECTED CHEMICAL PARAMETERS THAT DEFINE FRESHNESS OF RAINBOW TROUT (*Oncorhynchus mykiss*) AND CARP (*Cyprinus carpio*)

Jelena A. Babić[1], Mirjana R. Dimitrijević[2], Milan P. Milijašević[1], Vesna Ž. Đorđević[1], Radivoj B. Petronijević[1], Slaven M. Grbić[3], Aurelija T. Spirić[1]

[1]*Institute of Meat Hygiene and Technology, Belgrade, Serbia*
[2] *University of Belgrade, Faculty of Veterinary Medicine, Belgrade, Serbia*
[3]*Slaven d.o.o., Banja Luka, Bosnia i Herzegovina*

(Scientific paper)

The purpose of food packing in modified atmospheric conditions is to extend its sustainability by preventing both biochemical processes and growth of spoilage bacteria. Gases or their mixtures which are mostly used in the modified atmosphere food packing technology are carbon-dioxide (CO_2), oxygen (O_2) and nitrogen (N_2). The aim of our research was to examine the influence of packaging in modified atmosphere and vacuum on the total volatile basic nitrogen (TVB-N) content and pH in muscle of rainbow trout (*Oncorhynchus mykiss*) and common carp (*Cyprinus carpio*), as well as to determine the most suitable gas mixtures for packing of these freshwater species. Three sample groups of trout and carp cuts were investigated. The first two groups were packaged in modified atmosphere with different gas ratios: 60%CO_2+40%N_2 (I group) and 40%CO_2+60%N_2 (II group), whereas the samples from third, control group, (III group) were vacuum packaged. During trials, samples were stored in refrigerator at +3°C. Determination of TVB-N and pH was performed on 1st, 7th and 14th day of storage. The obtained results indicate that all investigated mixtures of gases as well as vacuum had a significant influence on the values of TVB-N in trout and carp cut samples. The lowest increase in TVB-N was established in trout and carp cut samples from the group I, whereas the highest increase was established in samples from group III. Statistical significant difference (p < 0,001) between the average values of TVB-N for trout (I group: 18.17±0.93; II group: 20.90±0.81 and III group: 36.18±2.65 mg N/100 g) and carp cuts (I group: 26.74±1.48; II group: 30.02±0.31 and III group: 35.10±1.75 mg N/100 g) was established on the 14th day. The lowest pH value was measured in samples packaged in modified atmosphere with 60% CO_2+40% N_2 (I group). On the 14th day of testing obtained value was 6,15 ± 0,09 for trout and 5.94±1.11 for carp samples. Increase in pH value in trout samples packed in vacuum was established during the whole period of investigation (p < 0,001), while in carp cut samples packaged in vacuum the increase in pH value (p < 0,05) was established up to 7th day of testing. Based on the obtained results it can be concluded that gas mixture consisting of 60% CO_2 and 40% N_2 was the most suitable for packaging of fresh trout and carp cuts in terms of selected chemical parameters, such as TVB-N and pH.

Keywords: Modified atmosphere • Trout • Carp • Freshness • Total volatile base nitrogen • pH

Urobilinogenic chlorophyll catabolite behavior in oxygen-containing moiety

Nina M. Djapic

University of Novi Sad, Technical Faculty "Mihajlo Pupin", Zrenjanin, Serbia

Abstract

The urobilinogenic chlorophyll catabolite being exposed to oxygen-containing moiety, after three months, forms the C-8^2-hydroxy urobilinogenic chlorophyll catabolite. The chromatographic and spectroscopic methods have been used to study the hydroxylated urobilinogenic chlorophyll catabolite product formed. Using liquid chromatography–mass spectrometry and nuclear magnetic resonance spectroscopy C-8^2 hydroxylated urobilinogenic chlorophyll catabolite was identified. Analysis of the results obtained enables the propositions of the reaction mechanism.

Keywords: urobilinogenic chlorophyll catabolite, C-8^2 hydroxylation.

Available online at the Journal website: http://www.ache.org.rs/HI/

SCIENTIFIC PAPER

UDC 543.4:581.19:66.094.32

Hem. Ind. **68** (1) 77–82 (2014)

doi: 10.2298/HEMIND130118029D

The oxidation of chlorophylls by molecular triplet oxygen in aqueous methanol solutions happens to all chlorophylls that have an intact β-ketoester structure at the isocyclic ring [1]. The first oxidation product formed is the hydroxylated chlorophylls' derivative. The oxidation process continues further and the reaction was named the allomerization [2]. The allomerization occurs through chemical or enzymatic pathway and a complex mixture of products is formed [3]. An early stage reaction in chlorophyll breakdown, under natural conditions, is the allomerization [4,5]. The reversed--phase (RP) and normal phase (NP) high-performance liquid chromatography (HPLC) was utilized in the separation of chlorophyll allomers [6,7]. The HPLC coupled with mass spectrometry (HPLC–MS) in conjunction with UV–Vis absorption has been used for analysis of chlorophyll allomers [8–10]. The nuclear magnetic resonance (NMR) spectroscopy was used in assignment of several allomers [11–13]. The allomerization is initiated in aqueous methanol solution containing traces of bases, acids and metals. The base catalyzed allomerization mechanism comprises the removal of the acidic α-proton at chlorophylls' C-13^2 position and formation of an enolate. After keto-enol tautomerization of the C-13^1=C-13^2 double bond the allomer is formed. Free radical mechanism was proposed for the allomerization [14]. Further investigations support an idea of alternative allomerization pathway [10]. There is still not enough data to back up proposed acid catalyzed allomerization mechanism of chlorophylls. The urobilinogenic chlorophyll catabolite isolated from the *Parrotia persica* autumnal leaves differs from chlorophylls and chlorophyll catabolites by having one carbon atom less [15]. The *Parrotia persica* urobilinogenic chlorophyll catabolite structure (**1**) refers to urobilinogen and the carbon atom numeration is the same as in urobilinogen. The C-8^2 hydroxylation of *Parrotia persica* urobilinogenic chlorophyll catabolite in deutero methanol containing traces of water and acid is described in this paper. RP LC-MS and ^{1}H-NMR spectra were used in the identification of C-8^2-hydroxy urobilinogenic chlorophyll catabolite (**2**) and the mechanisms that can explain the formation of the C-8^2-hydroxy urobilinogenic chlorophyll catabolite are proposed.

MATERIALS AND METHODS

The urobilinogenic chlorophyll catabolite was isolated from *Parrotia persica* (*Pp*), Hamamelidaceae autumnal leaves according to the methods described previously [15]. The isolated *Pp* urobilinogenic chlorophyll catabolite was left for 3 months in the NMR tube, in the cold and dark place. After 3 months the RP LC––MS analysis was done. The LC chromatogram revealed the presence of two compounds. The final purification was done by RP HPLC using Waters 600 HPLC system coupled with Waters 2996 PDA UV–Vis detector (Waters Corp., Milford, USA) and RP EP 250 mm×16 mm Nucleosil 100-7 C_8 column along with RP EP 30 mm×16 mm Nucleosil 100-7 C_8 precolumn (Macharey--Nagel, Oesingen, Switzerland). The detection wavelength was set at 244 nm, temperature of the column was kept at 22 °C and the injection volume was 2 ml *via* loop injection. The mobile phase consisted of water (0.1% trifluoroacetic acid (TFA)):methanol, 1:1 (v/v) and operating an isocratic flow of 3.2 ml/min. The urobilinogenic chlorophyll catabolite was collected to obtain 1.92 mg and the C-8^2-hydroxy urobilinogenic chlorophyll catabolite was collected to obtain 0.20 mg. All solvents used were HPLC grade (Acros Organics, Geel,

Correspondence: University of Novi Sad, Technical Faculty "Mihajlo Pupin", Djure Djakovica bb, 23000 Zrenjanin, Serbia.
E-mail: djapic@tfzr.uns.ac.rs
Paper received: 18 January, 2013
Paper accepted: 15 April, 2013

Belgium). The recording of the ^{1}H-NMR spectrum was done under the same conditions as described previously [15].

RESULTS AND DISCUSSION

The *Parrotia persica* (*Pp*) urobilinogenic chlorophyll catabolite (**1**) was, after recording of the NMR spectra, left in the cold and dark place for 3 months. After 3 months the RP LC–MS chromatogram was recorded. The chromatogram revealed the presence of two compounds (Figure 1).

Methanol and acidified water eluent can influence the formation of hydrogen bonds in the solution and reduce the interactions between compounds. The stationary phase particle surface can form hydrogen bonds with the compounds being separated. The prolonged retention time of the C-8^2-hydroxy urobilinogenic chlorophyll catabolite (**2**) can be attributed to additional hydroxyl group present that can form hydrogen bond with the silanol sites of the column packing. The ESI-MS showed a molecular ion at *m*/*z* 633, an $[M+H]^+$ for the *Pp* urobilinogenic chlorophyll catabolite (**1**), Figure 2. C-8^2-hydroxy derivative showed a molecular ion at *m*/*z* 651, an $[M+H]^+$ for the C-8^2-hydroxy *Pp* urobilinogenic chlorophyll catabolite (**2**). The sample was subsequently purified by semi-preparative HPLC under the same conditions as described previously [15].

The ^{1}H-NMR spectra were recorded for all purified compounds. The ^{1}H-NMR spectra of the *Pp* urobilinogenic chlorophyll catabolite (**1**) and its C-8^2-hydroxy derivative (**2**) are depicted in Figures 3 and 4, respectively.

The difference between the two ^{1}H-NMR spectra is the absence of the signal for the C-8^2 proton in the C-8^2-hydroxy *Pp* urobilinogenic chlorophyll catabolite (Figure 4). The chemical shifts, multiplicity and coupling constants of the *Pp* urobilinogenic chlorophyll catabolite (**1**) were as published previously [15]. The chemical shifts, multiplicity and coupling constants of the isolated C-8^2-hydroxy *Pp* urobilinogenic chlorophyll catabolite (**2**) are depicted in Table 1.

In chlorophylls, the acidic catalyzed allomerization mechanism is comprised of protonation of the C-13^1 oxo group. This mechanism was not sufficient to explain the formation of the C-13^2-hydroxy and C-13^2--methoxy chlorophylls [10]. The other mechanism proposed for the allomerization of chlorophylls was a free

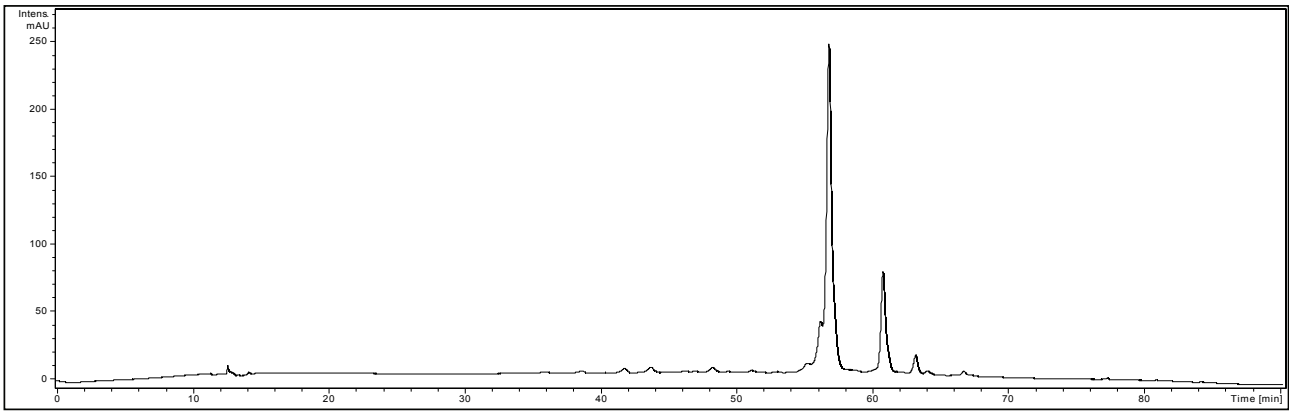

Figure 1. The chromatogram of the Pp urobilinogenic chlorophyll catabolite and its C-8^2-hydroxy derivative separated on the analytical RP C_8 column. Conditions: mobile phase: water (0.1 % TFA): methanol, gradient elution, the proportion of methanol was increased linearly from 10 to 100% in 70 min and in next 20 min elution was continued with methanol. The column temperature was 22 ℃, flow rate 0.2 ml/min, detection. UV 244 nm, injection: 10 µl via autosampler.

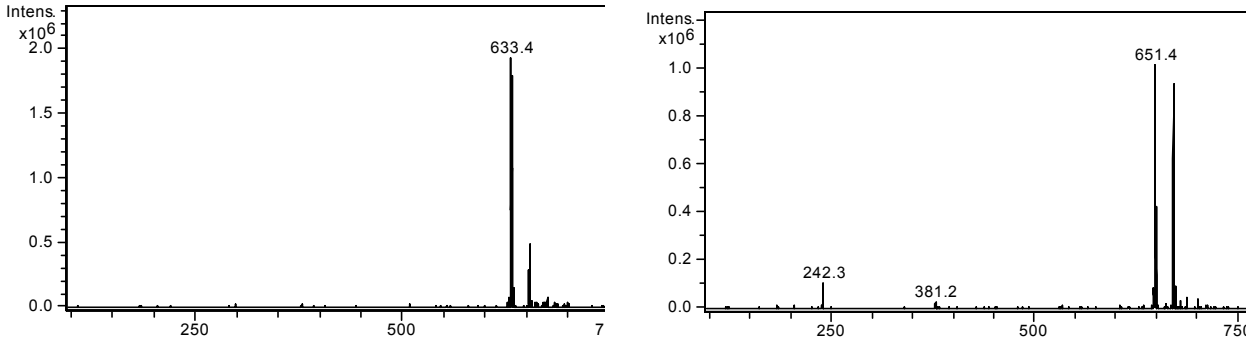

Figure 2. Electro-spray ionization (ESI) MS of Pp *urobilinogenic chlorophyll catabolite and its C-8^2-hydroxy derivative extracted at 57.0 and 60.9 min, respectively.*

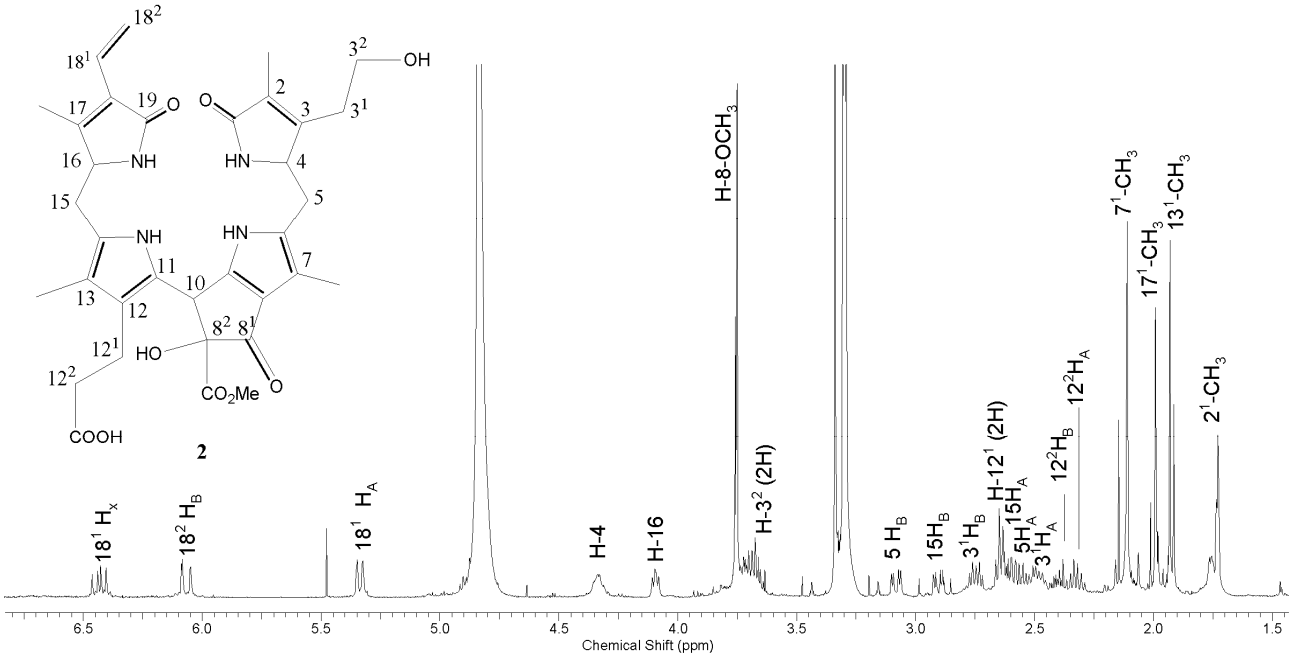

*Figure 3. The ^{1}H-NMR spectrum of Pp urobilinogenic chlorophyll catabolite (**1**).*

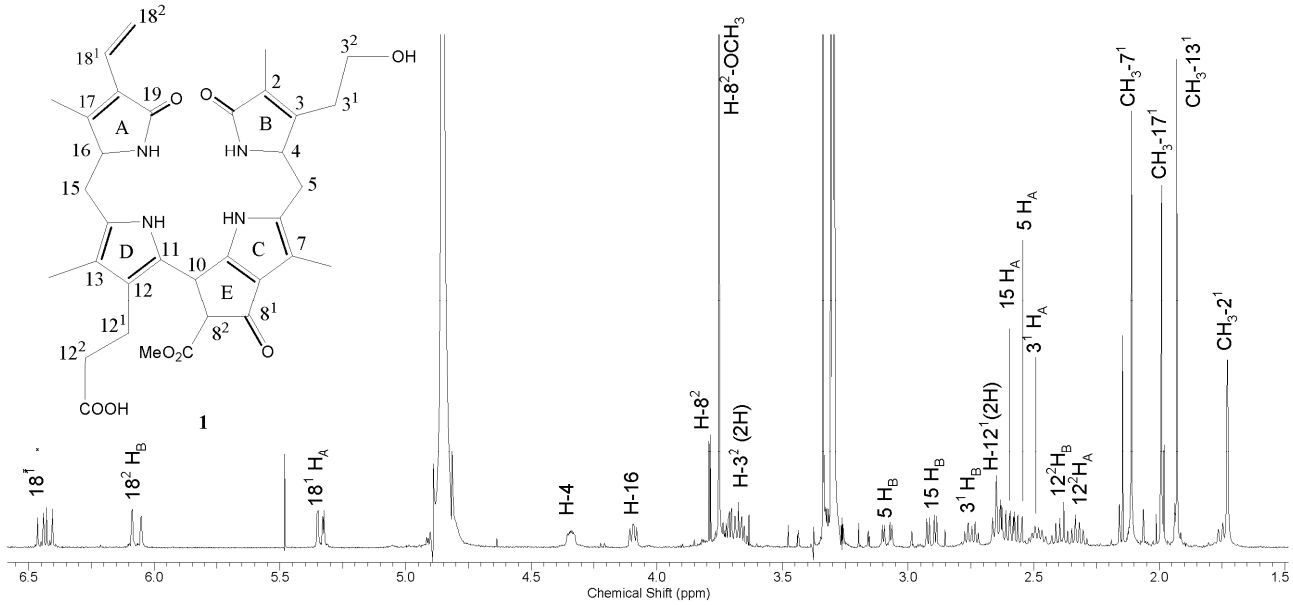

*Figure 4. The ^{1}H-NMR spectrum of the C-8^2-hydroxy Pp urobilinogenic chlorophyll catabolite (**2**).*

Table 1. ^{1}H-NMR (500 MHz) data in CD_3OD of the isolated C-8^2-hydroxy Pp *urobilinogenic chlorophyll catabolite (**2**)*

H/C	δ_H, multiplicity	J / Hz
1	1.73 *s*	
2		
2^1		
3	2.49 *dd* H_A,	6.9; 14.8,
3^1	2.75 *dd* H_B	6.6; 13.8
3^2	3.68 *m* H_A and H_B	
4	4.34 *m*	

Table 1. Continued

H/C	δ_H, multiplicity	*J* / Hz
5	2.57 *dd* H_A,	8.5; 14.9;
	3.08 *dd* H_B	13.8; 5.6
6		
7		
7^1	2.11 *s*	
8		
8^1		
8^2		
8^3		
8^4	3.75 *s*	
9		
10	Signal being located under residual HDO signal	
11		
12		
12^1	2.65 *dd* H_A and H_B	7.4; 15.4
12^2	2.33 *dd* H_A,	6.9; 14.8;
	2.41 *dd* H_B	7.8; 15.6
12^3		
13		
13^1	1.93 *s*	
14		
15	2.60 *dd* H_A,	5.9; 14.5;
	2.91 *ddd* H_B	2.4; 5.2; 14.6
16	4.09 *dt*	5.5; 2.0
17		
17^1	1.99 *s*	
18		
18^1	6.43 *dd*	17.8;12.3
18^2	5.34 *dd* H_A,	13.6; 2.2;
19	6.07 *dd* H_B	17.7; 2.3

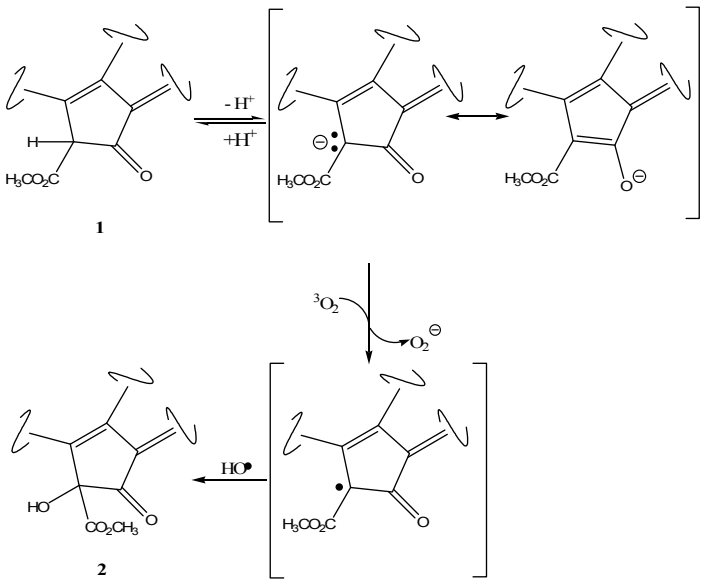

*Figure 5. The mechanism adopted from literature that can be proposed for the formation of the C-8^2-hydroxy Pp urobilinogenic chlorophyll catabolite (**2**) from the Pp urobilinogenic chlorophyll catabolite (**2**), for brevity only ring E is shown [14].*

radical one (Figure 5), which was able to explain the formation of the previously mentioned chlorophyll allomers [14].

CONCLUSIONS

The evidences described, clearly indicated that the *Pp* urobilinogenic chlorophyll catabolite (**1**), under the acidic conditions, in the presence of trifluoroacetic acid (TFA), which was used as a modifier during the chromatographic separation, in aqueous methanol solution upon standing for months induces the formation of the C-8^2-hydroxy *Pp* urobilinogenic chlorophyll catabolite (**2**). The mechanism proposed for the allomerization of chlorophylls can explain the formation of the C-8^2--hydroxy *Pp* urobilinogenic chlorophyll catabolite (**2**). The chromatographic and spectroscopic methods described can facilitate the identification of the C-8^2-hydroxy urobilinogenic chlorophyll catabolite (**2**).

REFERENCES

[1] R. Willstaetter, A. Stoll, Untersuchungen ueber Chlorophyll, Springer, Berlin, 1913, p. 29.

[2] L.G. Johnston, W.F. Watson, The allomerization of chlorophyll, J. Chem. Soc. **1956** (1956) 1203–1212.

[3] F.C. Pennington, H.H. Strain, W.A. Svec, J.J. Katz, Preparation and properties of 10-hydroxychlorophylls a and b, J. Am. Chem. Soc. **89** (1967) 3875–3880.

[4] G.A. Hendry, J.D. Houghton, S.B. Brown, The Degradation of Chlorophyll – a Biological Enigma, New Phytol. **107** (1987) 255–302.

[5] M.N. Merzlyak, V.A. Kovrizhnikh, K.N. Timofeev, Superoxide mediated chlorophyll allomerization in a dimethyl sulphoxide-water mixture, Free Rad. Res. Commun. **15** (1991) 197–201.

[6] P.M. Schaber, J.E. Hunt, R. Fries, J.J. Katz, High-performance liquid-chromatography study of the chlorophyll allomerization reaction, J. Chromatogr. **316** (1984) 25–41.

[7] P. Kuronen, K. Hyvarinen, P. H. Hynninen, I. Kilpelainen, High Performance Liquid Chromatographic Separation and Isolation of the Methanolic Allomerization Products of Chlorophyll a, J. Chromatogr. **654** (1993) 93–104.

[8] R.B. van Breeman, F.L. Canjura, S.J. Schwartz, High-performance liquid chromatography – continuous flow fast atom bombardment mass spectrometry of chlorophyll derivatives, J. Chromatogr. **542** (1991) 373–383.

[9] A. Rahamani, C. B. Eckardt, R. G. Brereton, J. R. Maxwell, The Use of Liquid Chromatography-Mass Spectrometry to Monitor the Allomerization Reactions of Chlorophyll a and Pheophytin a: Identification of the Allomers of Pheophytin a, Photochem. Photobiol. **57** (1993) 1048––1052.

[10] R.G. Brereton, A. Rahamani, Y.Z. Liang, O.M. Kvalheim, Investigation of the allomerization reaction of chlorophyll a: use of diode array HPLC, mass spectrometry and chemometric factor analysis for the detection of early products, Photochem. Photobiol. **59** (1994) 99–110.

[11] I. Kilpelainen, S. Kaltia, P. Kuronen, K. Hyvarinen, P. H. Hynninen, Assignment of the 1H and 13C NMR spectra of 132(R)-methoxychlorophyll a using the two-dimensional HMQC and HMBC techniques, Magn. Reson. Chem. **32** (1994) 29–35.

[12] J. Helaja, K. Hyvarinen, S. Heikkinen, I. Kilpelainen, P.H. Hynninen, Solution Structures of 13(2)-methoxy Chlorophyll a Epimers, J. Mol. Struct. **354** (1995) 71–79.

[13] K. Hyvarinen, J. Helaja, P. H. Hynninen, An Unexpected Allomer of Chlorophyll: 132(S)-Hydroxy-10-Methoxy chlorophyll b, Tetrahedron Lett. **39** (1998) 9813–9814.

[14] P.H. Hynninen, Mechanism of the Allomerization of Chlorophyll: The inhibition of the Allomerization by Carotenoids Pigments, Z. Naturforsch., Teil B **36** (1981) 1010–1016.

[15] N. Djapic, M. Pavlovic, Chlorophyll catabolite from *Parrotia persica* autumnal leaves, Rev. Chim. (Bucuresti) **59** (2008) 878–882.

IZVOD

PONAŠANJE UROBILINOGENSKOG KATABOLITA HLOROFILA U ATMOSFERI KOJA SADRŽI KISEONIK

Nina M. Đapić

Univerzitet u Novom Sadu, Tehnički fakultet „Mihajlo Pupin“, Zrenjanin, Srbija

(Naučni rad)

Urobilinogenski katabolit hlorofila stajanjem u atmosferi koja sadrži kiseonik, nakon tri meseca, formira C-8^2-hidroksi urobilinogenski katabolit hlorofila. Korišćene su hromatografske i spektroskopske metode za proučavanje formiranog hidroksi urobilinogenskog katabolita hlorofila. Upotrebom tečne hromatografije-masene spektrometrije i nuklearne magnetne rezonantne spektroskopije identifikovan je C-8^2-hidroksi urobilinogenski katabolit hlorofila. Dobijeni rezultati ukazuju da urobilinogenski katabolit hlorofila izolovan iz jesenjeg lišća biljke *Parrotia persica* u prisustvu tragova kiseline, koja je korišćena kao modifikator tokom hromatografskog razdvajanja, u vodenom rastvoru metanola i u atmosferi koja sadrži kiseonik nakon nekoliko meseci stajanja uzrokuje stvaranje C-8^2-hidroksi urobilinogenskog katabolita hlorofila. Analiza dobijenih rezultata omogućava predlog reakcionog mehanizma. Mehanizam kiselo katalizovane alomerizacije hlorofila podrazumeva protonovanje C-13^1 okso grupe. Ovaj mehanizam nije mogao da objasni stvaranje C-13^2-hidroksi i C-13^2-metoksi hlorofila. Drugi predložen mehanizam podrazumeva alomerizaciju hlorofila po slobodno radikalskom mehanizmu koji je mogao da objasni stvaranje prethodno navedenih alomera hlorofila.

Ključne reči: Urobilinogenski katabolit hlorofila • C-8^2 hidroksilacija

Temporal concentration changes of beryllium-7 and lead-210 in ground level air in Serbia

Marija M. Janković, Dragana J. Todorović, Jelena D. Nikolić, Milica M. Rajačić, Gordana K. Pantelić, Nataša B. Sarap

University of Belgrade, Vinča Institute of Nuclear Sciences, Radiation and Environmental Protection Department, P.O. Box 522, 11001 Belgrade, Serbia

Abstract

^{7}Be, ^{210}Pb and ^{137}Cs activity concentrations in ground level air at five monitoring stations (MS Vinča, Zeleno Brdo, Zaječar, Vranje and Zlatibor) in Serbia were determined during the period from May 2011 to September 2012, as part of the Serbian monitoring project. Activity of the radionuclides in air was determined on a HPGe detector (Canberra, relative efficiency 20%) by standard gamma spectrometry. Concentrations of cosmogenic ^{7}Be, ranged from 1.5 to 8.8 mBq m^{-3} and exhibited maxima in the spring/summer period. The maximum concentrations for ^{210}Pb were generally observed in the fall for all investigated locations, and concentrations were in the range 3.6×10^{-4}–30×10^{-4} Bq m^{-3}. The activity concentrations of anthropogenic ^{137}Cs in ground level air, during the observed period, were in the range 0.3–8 μBq m^{-3}. The variations in ^{7}Be/^{210}Pb activity ratio for the investigated stations are also presented.

Keywords: Radioactivity, ground level air, ^{7}Be, ^{210}Pb, ^{137}Cs.

Available online at the Journal website: http://www.ache.org.rs/HI/

SCIENTIFIC PAPER

UDC 502.3(497.11):504.5:546.45

Hem. Ind. **68** (1) 83–88 (2014)

doi: 10.2298/HEMIND130320031J

Nuclear weapon tests conducted in the atmosphere and releases of radioactive material from nuclear facilities are the main causes of man-made radioactive contamination in the human environment. Once released in the atmosphere, long-range atmospheric transport processes can cause widespread distribution of radioactive matter or they might, as in the case of Chernobyl accident, originate from a single point. The resulting fallout consisting of short- and long-lived radionuclides, eventually affects humans either directly or indirectly by entering the food chain through plants and animals. In both cases, fallout causes a health hazard to the population, either through direct irradiation or consumption of contaminated food products. Potential danger of radioactive particles inhalation must be determined and controlled based on levels and types of radioactivity. Accurate data on natural radionuclide concentration in air is essential, not only because exposure to natural radionuclides greatly contributes to radiation exposure [1], but also because this information contributes to studies of atmospheric circulation of air masses [2].

Particle reactive radionuclides such as ^{7}Be and ^{210}Pb have been used as atmospheric tracers for studying environmental processes such as cloud scavenging and precipitation [3,4], aerosol transit and residence times in the troposphere [5,6], aerosol deposition velocities [7-10] and the fate of pollutants [11].

^{7}Be is a radioactive element (half-life 53.3 days) produced by cosmic rays in spallation processes with light elements (N, O and C), in the lower stratosphere (~70%) and the upper troposphere (~30%). Following production, ^{7}Be is promptly attached to aerosols with a diameter of 0.3–0.6 mm whose residence time in the atmosphere is around 20 days [12]. In the troposphere, apart from its decay, ^{7}Be is removed by wet deposition (the major mechanism for removal) and dry deposition. In ground level air, the residence time of ^{7}Be is around 10 days [13].

Natural ^{210}Pb (half-life 22.3 years) is an effective tracer of the history of continental surface air masses and could be used to identify soil aerosol sources. As a member of ^{222}Rn decay series, it is a decay product of primordial ^{238}U, but can also be found as a product of coal combustion and nuclear explosions in very small amounts (< 1%). Concentrations of ^{210}Pb in air exhibit maxima during autumn, which may be attributed to an increased emanation of radon [14,15]. Deposition of ^{210}Pb also varies with geographic position and is generally found in higher concentrations at mid-latitudes. Still, emanation of radon and therefore concentrations of ^{210}Pb in surface air are affected by many factors, as atmospheric pressure, temperature inversion, vegetation, snow coverage, etc.

Since ^{7}Be is of cosmogenic origin and its production rate is high in the upper troposphere and decreases with atmospheric depth, its concentrations in air increase with altitude. On the contrary, the concen-

Correspondence: M.M. Janković, University of Belgrade, Vinča Institute of Nuclear Sciences, Radiation and Environmental Protection Department, P.O. Box 522, 11001 Belgrade, Serbia.

E-mail: marijam@vinca.rs

Paper received: 20 March, 2013

Paper accepted: 15 April, 2013

trations of ^{210}Pb in air decrease with elevation from the ground, due to its higher production rate in the lower troposphere.

The fission product ^{137}Cs (half-life 30 years) is a reliable indicator of anthropogenic pollution caused by nuclear weapon atmospheric tests and local nuclear power plant accidents. Concentrations of ^{137}Cs in the ground level air in the 1990s were in the order of μBq m^{-3}. Seasonal variation in the ^{137}Cs content in air is a valid indicator of the STE processes (stratosphere-to-troposphere exchange). The concentration pattern exhibits one or two maxima in late spring/early summer and winter. The summer maximum is due to STE, whereas the winter maximum is attributed to soil dust resuspension in air from the Chernobyl fallout [16,17].

Due to high population density, heavy traffic and industrial plants located in the outskirts, urban areas are exposed to severe air pollution. In the last decade, air radioactivity monitoring in urban areas has become a part of the pollution monitoring program in most of the European countries. This paper presents the results of the comparative study of air radioactivity monitoring at five sites in Serbia from May 2011 to September 2012.

EXPERIMENTAL

Aerosol samples were collected on filter papers (Whatman 41, 15 cm×25 cm in diameter, relative efficiency for deposited dust 82%) by constant flow rate samplers (air flow 40–60 m^3 h^{-1}, average daily volume in the interval 720–1440 m^3). The filter papers were then ashed at temperatures below 400 °C and a monthly composite sample containing 30–31 daily filters was formed (volume in the interval 30×10^3–60×10^3 m^3) [18]. The activity of ^{7}Be, ^{210}Pb and ^{137}Cs was determined on a HPGe detector (Canberra relative efficiency 20%) by standard gamma spectrometry. Detector calibration was performed using secondary reference radioactive material in the geometry of plastic containers, vials, which were obtained from the primary reference radioactive materials, Czech metrological Institute, Praha, OL-9031-116/8, type ERX, with the total activity of 114.9 kBq on 03.03.2008 (^{241}Am, ^{109}Cd, ^{139}Ce, ^{57}Co, ^{60}Co, ^{88}Y, ^{113}Sn, ^{85}Sr ^{137}Cs and ^{210}Pb). The detection threshold of ^{7}Be in air was 5×10^{-6} and 5×10^{-6} Bq m^{-3} for ^{210}Pb and 5×10^{-7} Bq m^{-3}for ^{137}Cs. Counting time intervals were 60000 s. The background spectrum was regularly recorded prior to or after sample counting. The combined measurement uncertainty of the results was calculated at the 95% level of confidence (k = 2).

RESULTS AND DISCUSSION

In the analyzed samples levels of ^{7}Be, ^{210}Pb and ^{137}Cs were detected. Concentrations of these radionuclides in ground level air at different locations in Serbia during the period May 2011–September 2012 are presented in Figures 1–3, respectively.

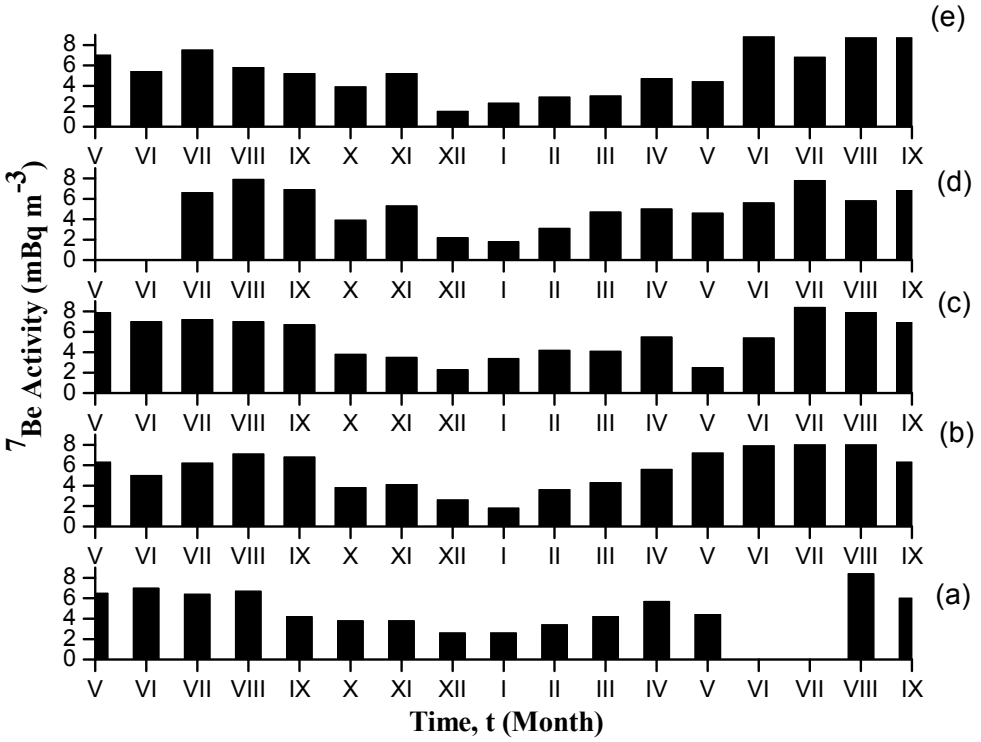

Figure 1. ^{7}Be activity in the ground level air at: a) Vinča, b) Zeleno Brdo, c) Zaječar, d) Vranje and e) Zlatibor.

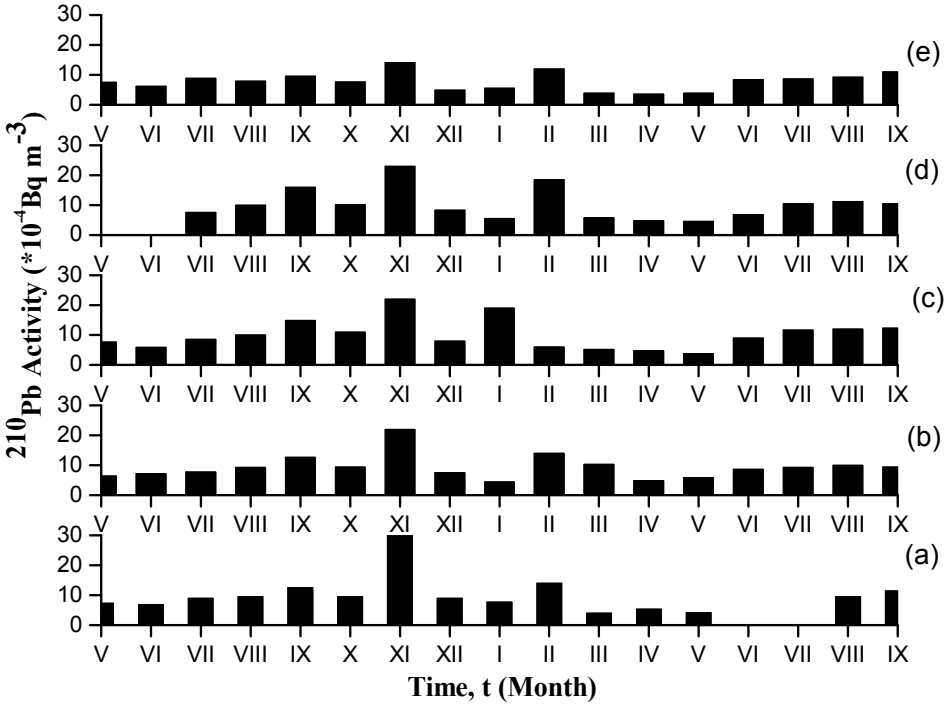

Figure 2. ^{210}Pb activity in the ground level air at: a) Vinča, b) Zeleno Brdo, c) Zaječar, d) Vranje and e) Zlatibor.

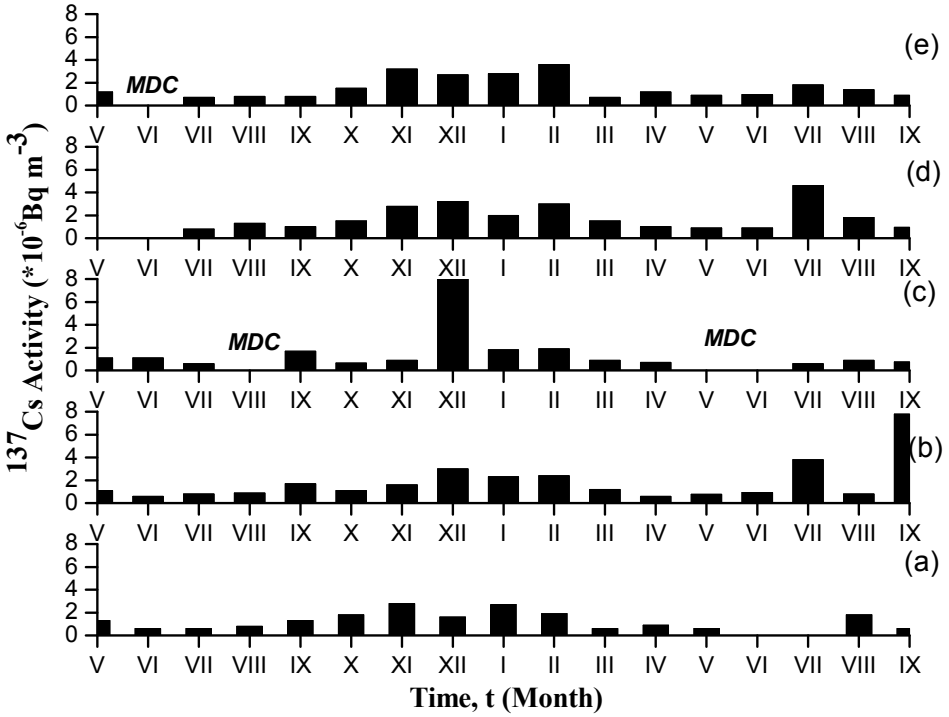

Figure 3. ^{137}Cs activity in the ground level air at: a) Vinča, b) Zeleno Brdo, c) Zaječar, d) Vranje and e) Zlatibor.

Concentrations of ^{7}Be in air were in the range of 1.5 (Zlatibor, XII 2011)–8.8 mBq m^{-3} (Zlatibor, VI 2012), and exhibited maximum in spring/summer and minimum in winter (Figure 1). This variation of ^{7}Be is similar for all investigated locations. The highest ^{7}Be activity concentrations during the warm season in the investigated region were attributed to more efficient vertical transport of air masses during that period. A phenomenon that advocates for the observed high values during summer is the elevation of the tropopause during the warm summer months at midlatitudes [19]. During the winter months, when temperatures are low and atmo-

sphere is more ''stable'', the tropopause height is lower and therefore the concentrations of ^{7}Be in surface air are low.

These results obtained for ^{7}Be at five investigated locations in Serbia are in good agreement with other Belgrade studies [20,21] and with results obtained at other locations in Europe. For example, Durana *et al.* [22] presented 1977–1994 results for the Bratislava atmosphere, showing that the ^{7}Be activity rarely exceeded 6 mBq m^{-3}, and that it reached its maximum in June. Likewise, during period 1993–1997 Azahra *et al.* [23] measured ^{7}Be in Granada, and demonstrated that the highest values were reached in summer. Similar results for ground level ^{7}Be were shown by Irlweck *et al.* [24] as well as other studies [12,25,26].

The average concentration per month of Be-7 in Europe is usually several mBq m^{-3}. For example, in Thessaloniki (Greece) the average monthly concentration of Be-7 is in the range 1–10 mBq m^{-3}. The listed countries are located at similar geographical latitude [5,22]. Feely *et al.* [27] reported for the same latitude in New York City (40°73' N) 4.55 mBq m^{-3} for ^{7}Be averaging for the period 1970–1985, while McNeary and Baskaran [28] at a site in the southwest area of Detroit, Michigan (42°25' N), 175 m above mean sea level and 1m above ground reported 4.83 mBq m^{-3} for ^{7}Be, averaged for the period October 1999–February 2001. It must be noted that the environmental concentration of ^{7}Be in the temperate zones is about 3 mBq m^{-3} in the surface air [29].

Contents of ^{210}Pb vary from 3.6×10^{-4} Bq m^{-3} (Zlatibor, IV 2012) to 30×10^{-4} Bq m^{-3} (Vinča, XI 2011) (Figure 2). The maximal ^{210}Pb values were observed during November at all locations, while the minimum was observed during March–May period. The higher values of ^{210}Pb during November might be attributed to the frequent inversion conditions of the surface air layers, resulting in a build-up of radon and its decay products in ground-level air, while the relative low values during December might be due to the low emanation of radon from the frozen or snow-covered soil. The minimal values of ^{210}Pb concentrations in ground level air during the spring might reflect high washout. The obtained values of ^{210}Pb concentrations during the summer period showed a weak increase, although the higher air mixing within the troposphere during the warm summer months was expected to deplete ^{210}Pb in ground-level air, since its concentrations in the air decreased with elevation from the earth's surface.

The obtained values for ^{210}Pb in the ground level air at different locations presented in this paper are in good agreement with values for ^{210}Pb obtained in Belgrade during 1985–1996 [30], 1996–2001 [21] and 2004–2009 [31].

The activity concentrations of anthropogenic ^{137}Cs in ground level air, during the observed period, were at level < MDC – 8 μBq m^{-3} (Figure 3). The content of ^{137}Cs in ground level air presented in this paper is lower than the values of ^{137}Cs in the Belgrade city area during 1991–1996 [32], with maximum in the spring/summer

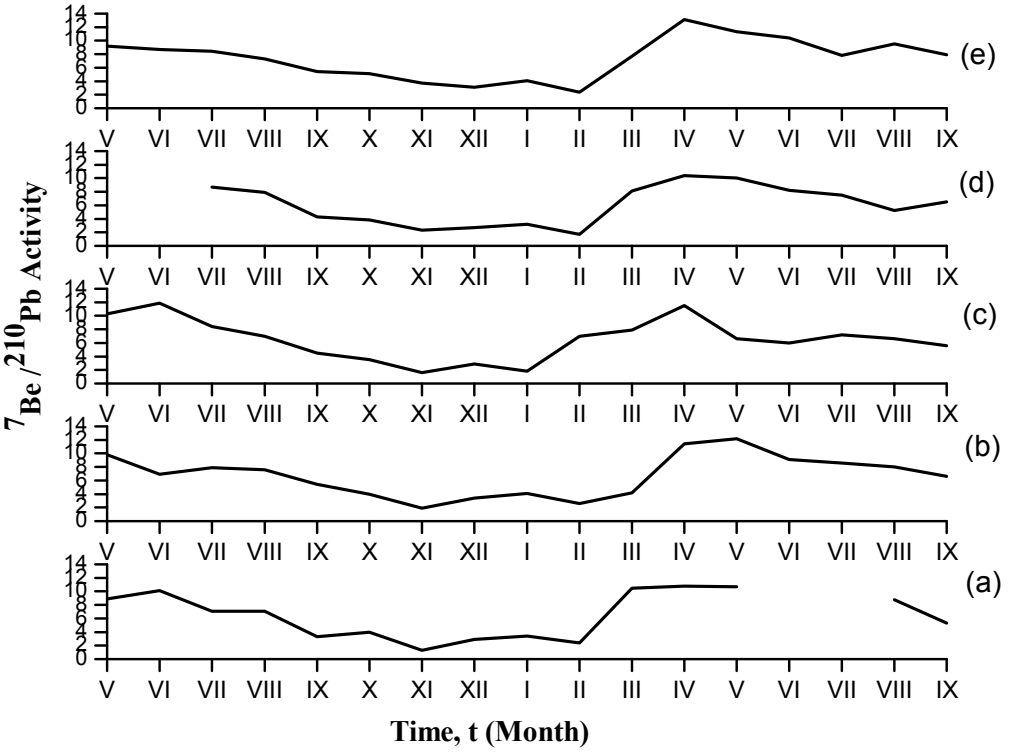

Figure 4. Temporal variation of ^{7}Be/^{210}Pb concentration ratio.

period and another pronounced maximum during winter months (XI–II). The high concentration of ^{137}Cs in the winter is due to agricultural activities in the surrounding fields that induced local surface dust resuspension effect, while high concentration in the summer is due to air exchange weather conditions [32].

The variations in ^{7}Be/^{210}Pb activity ratio for the five investigated locations are presented in Figure 4. The ^{7}Be/^{210}Pb ratios were in the range of 1.3–10.8 (Vinča), 1.9–12.2 (Zeleno Brdo), 1.6–11.9 (Zaječar), 1.7–10.4 (Vranje) and 2.4–13.1 (Zlatibor), with spring maximums and late fall/winter minimums.

CONCLUSIONS

Time dependent activity of ^{7}Be, ^{210}Pb and ^{137}Cs, measured in ground level air at five different locations in Serbia during May 2011 to September 2012 are presented. The typical pattern of seasonal variations was observed for ^{7}Be and ^{210}Pb activity concentrations. The obtained values for ^{7}Be concentrations in ground level air show a fluctuation which has oscillatory characteristics with enhanced activity in spring-summer months. This fluctuation is likely related to the seasonal thinning of tropopause, which facilitates and enhances the stratosphere – troposphere vertical air mass mixing. Inverse trend was obtained for ^{210}Pb with the highest value during November for all locations. The obtained concentrations of ^{137}Cs are in the μBq m^{-3} range. The time dependence behavior of ^{7}Be/^{210}Pb concentration ratio shows that higher intensity of vertical convection of air during warm season results in air – masses transfer from higher altitudes.

Acknowledgment

The investigation was partially supported by the Ministry of Education, Science and Technological Development of the Republic of Serbia under the Project III43009.

REFERENCES

[1] R. L. Kathren, Radioactivity in the environment, sources, distribution and surveillance, University of Washington, Harwood Academic Publishers, Newark, NJ, 1984.

[2] E. Gomez, F. Garcias, M. Casas, V. Cerda, Determination of natural gamma emitters in surfaces air, J. Environ. Anal. Chem. **56** (1994) 327–335.

[3] D.M. Koch, D.J. Jacob, W.C. Graustein, Vertical transport of tropospheric aerosols as indicated by ^{7}Be and ^{210}Pb in a chemical tracer model. J. Geophys. Res. **101** (1996) 18651–18666.

[4] H. Liu, D. Jacob, I. Bey, R. Yantosca, Constraints from ^{210}Pb and ^{7}Be on wet deposition and transport in a global three-dimentional chemical tracer model driven by assimilated meteorological fields. J. Geophys. Res. **106** (2001) 12109–12128.

[5] C. Papastefanou, A. Ioannidou, S. Stoulos, M. Manolopoulou, Atmospheric deposition of cosmogenic ^{7}Be and ^{137}Cs from fallout of the Chernobyl accident, Sci. Total Environ. **170** (1995) 151–156.

[6] R. Winkler, F. Dietl, G. Frank, J. Tschiersch, Temporal variations of ^{7}Be and ^{210}Pb size distributions in ambient aerosol. Atmos. Environ. **32** (1998) 983–991.

[7] J.A. Young, W.B. Silker, Aerosol deposition velocities on the Pacific and Atlantic Oceans calculated from ^{7}Be measurements, Earth. Planet. Sci. Lett. **50** (1980) 92––104.

[8] E.A. Crecelius, Prediction of marine atmospheric deposition rates using ^{7}Be deposition velocities, Atmos. Environ. **15** (1981) 579–582.

[9] K.K. Turekian, L.K. Benninger, E.P. Dioan, ^{7}Be and ^{210}Pb total deposition fluxes at New Haven, Connecticut and at Bermuda, J. Geophys. Res. **88** (1983) 5411–5415.

[10] G. Lujaniene, Study of removal processes of ^{7}Be and ^{137}Cs from the atmosphere. Chechoslovak, J. Phys. **53** (2003) S57–S65.

[11] C. Papastefanou, A. Ioannidou, Influence of air pollutants in the ^{7}Be size distribution of atmospheric aerosols, Aerosol Sci.Technol. **24** (1996) 102–106.

[12] J.S. Gaffney, N.A. Marley, M.M. Cunningham, Natural radionuclides in fine aerosols in the Pittsburgh Area, Atmos. Environ. **38** (2004) 3191–3200.

[13] A. Baeza, L.M. del Río, A. Jiménez, C. Miró, J.M. Paniagua, M. Rufo, Analysis of the temporal evolution of atmospheric ^{7}Be as a vector of the behavior of other radionuclides in the atmosphere, J. Radioanal. Nucl. Chem. **207** (1996) 331–344.

[14] K. Hirose, T. Honda, S. Yagashita, Y. Igaradhi, M. Aoyama, Deposition behaviors of ^{210}Pb, and thorium isotopes observed in Tsukuba and Nagasaki Japan, Atmos. Environ. **38** (2004) 6601–6608.

[15] A. Ioanidou, C. Papastefanou,^{7}Be, ^{22}Na and ^{210}Pb in the atmosphere at mid latitude 40^{o} N, Nucleus **34** (1997) 111–115.

[16] R.J. Larsen, C. Sanderson, J. Kada, EML surface air sampling programme, New York: US Energy Dept., 1995.

[17] G. Manic, S. Petrovic, V. Manic, D. Popovic, D. Todorovic, Radon concentrations in a spa in Serbia, Environ. Int. **32** (2006) 533–537.

[18] D. Popovic, D. Todorovic, V. Spasic Jokic, G. Djuric, Air Radioactivity monitoring in Serbia, in Environmetal Technologies: New Developements, Ed. Burcu Ozkaraova Gungor, Publ. I-Tech Inc, Vienna, 2007, pp. 147––166.

[19] P.F. Gustafson, M.A. Kerrigan, S.S. Brar, Comparison of beryllium-7 and caesium-137 radioactivity in ground level air, Nature **191** (1961) 454–456.

[20] Report on the levels of exposure of general public to environmental ionizing radiation in Rebublic of Serbia, Serbian Radiation Protection and Nuclear Safety Agency, Belgrade, 2011.

[21] D. Todorović, D. Popović, G. Djurić, M. Radenković, ^{7}Be to ^{210}Pb concentration ratio in ground level air in Belgrade area, J. Eniviron. Radioact. **79** (2005) 297–307.

[22] L. Durana, M. Chudy, L. Masarik, Investigation of ^{7}Be in the Bratislava atmosphere, J. Radioanal. Nucl. Ch. **207** (1996) 345–356.

[23] M. Azahra, J. J. López-Peñalver, M. A. Camacho-García, C. Gonzáles-Gómez, T. El Bardouni, H. Boukhal, Atmospheric concentration of ^{7}Be and ^{210}Pb in Granada, Spain, J. Radioanal. Nucl. Chem. **261** (2004) 401–405.

[24] K. Irlweck, K. Hinterdorfer, V. Karg, Beryllium-7 and Ozone correlations in surface atmosphere, Naturwiessenschaften **84** (1997) 353–356.

[25] F. Cannizzaro, G. Greco, M. Raneli, M. C. Spitale, E. Tomarchio, Behaviour of ^{7}Be air concentration observed during a period of 13 years and comparison with sun activity, Nucl. Geophys. **9** (1995) 597–607.

[26] C. Dueñas, M. C. Fernández, E. Liger, J. Carretero, Gross alpha, gross beta activities and ^{7}Be concentrations in surface air, analysis of their variations and prediction model, Atmos. Environ. **33** (1999) 3705–3715.

[27] H.W. Feely, R.J. Larsen, C.G. Sanderson, Factors that cause seasonal variations in Beryllium-7 concentrations in surface air, J. Environ. Radioactivity **9** (1989) 223–249.

[28] D. McNeary, M. Baskaran, Depositional characteristics of ^{7}Be and ^{210}Pb in Southeastern Michigan, J. Geophys. Res. **108** (D7) (2003) 4210.

[29] UNSCEAR, Ionizing Radiation: Sources and Biological Effects, United Nations Scientific Committee on the Effects of Atomic Radiation, United Nations, New York, 1982.

[30] D. Todorović, D. Popović, G. Đurić, M. Radenković, ^{210}Pb in ground-level air in Belgrade city area, Atmos. Environ. **34** (2000) 3245–3248.

[31] D. Todorović, D. Popović, J. Nikolić, J. Ajtić, Radioactivity monitoring in ground level air in Belgrade urban area, Radiat. Prot. Dosim. **142** (2010) 308–313.

[32] D. Todorović, D. Popović, G. Đurić, Concentration measurements of ^{7}Be and ^{137}Cs in ground level air in the Belgrade city area, Environ. Int. **25** (1999) 59–66.

IZVOD

AKTIVNOST BERILIJUMA-7 I OLOVA-210 U PRIZEMNOM SLOJU ATMOSFERE U SRBIJI

Marija M. Janković, Dragana J. Todorović, Jelena D. Nikolić, Milica M. Rajačić, Gordana K. Pantelić, Nataša B. Sarap

Univerzitet u Beogradu, Institut za nuklearne nauke Vinča, Laboratorija za zaštitu od zračenja i zaštitu životne sredine, p. pr. 522, 11001 Beograd, Srbija

(Naučni rad)

Prirodni radionuklidi ^{7}Be i ^{210}Pb često se koriste kao atmosferski traseri u cilju izučavanja fizičkih procesa u atmosferi kao što su formiranje oblaka i padavina, transport i vreme života aerosola u troposferi, brzina depozicije, i evolucija zagađivača u atmosferi. Sa druge strane, fisioni produkt ^{137}Cs je pouzdani indikator antropogenog zagađenja, izazvanog vazdušnim nuklearnim probama i akcidentima u nuklearnim elektranama. Zbog velike gustine naseljenosti, gustog saobraćaja i industrije, urbane oblasti su izložene ozbiljnom zagađenju vazduha. U poslednjoj deceniji, monitoring radioaktivnosti vazduha u urbanim sredinama je postao deo opšteg programa monitoringa životne sredine u većini evropskih zemalja. Ovaj rad predstavlja rezultate komparativne studije radioaktivnosti u vazduhu u pet gradova u Srbiji od maja 2011. do septembra 2012. Koncentracije aktivnosti ^{7}Be, ^{210}Pb i ^{137}Cs u uzorcima prizemnog sloja vazduha na pet meteoroloških stanica (MS Vinča, Zeleno Brdo, Zaječar i Zlatibor) su određene na HPGe detektoru (Canberra, relativna efikasnost 20%) metodom gama spektrometrije. Koncentracije aktivnosti kosmogenog ^{7}Be su se kretale u rasponu od 1.5 do 8.8 mBq m^{-3} uz izražen maksimum u proleće/leto. Maksimalne koncentracije aktivnosti ^{210}Pb su dobijene u jesen na svim ispitivanim lokacijama, a opseg rezultata je bio 3.6×10^{-4}–30×10^{-4} Bq m^{-3}. Oba ova radionuklida ispoljavaju tipične sezonske varijacije. Vremenske varijacije odnosa ^{7}Be/^{210}Pb su takođe ispitivane i pokazuju maksimum u leto i minimum u zimskom periodu. Ovi ekstremumi su posledica jače vertikalne konvekcije vazduha u leto odnosno veće stabilnosti i manjeg vertikalnog mešanja vazdušnih masa u zimu. Koncentracija aktivnosti prizvedenog radionuklida ^{137}Cs u posmatranom periodu je bila 0.3–8 μBq m^{-3}, sa izraženim maksimumima u letnjem i zimskom periodu. Visoka koncentracija ^{137}Cs u zimskom periodu je posledica poljoprivrednih aktivnosti u okolini ispitivanih lokacija, koje dovode do povećane lokalne resuspenzije prašine, dok je letnji maksimum uslovljen razmenom i mešanjem vazdušnih masa, tipičnom za vremenske prilike u ovom godišnjem dobu.

Ključne reči: Radioaktivnost • Prizemni sloj atmosfere • ^{7}Be • ^{210}Pb • ^{137}Cs

Aluminium and calcium ions binding to pectin in sugar beet juice – model of electrical double layer

Tatjana A. Kuljanin[1], Lidija R. Jevrić[1], Biljana Lj. Ćurčić[1], Milica R. Nićetin[1], Vladimir S. Filipović[1], Jasna P. Grbić[2]

[1]*University of Novi Sad, Faculty of Technology, Bulevar cara Lazara 1, 21000 Novi Sad, Serbia*
[2]*University of Novi Sad, Institute for Food Technology, Bulevar cara Lazara 1, 21000 Novi Sad, Serbia*

Abstract

In sugar industry, there is a problem with the presence of undesirable macromolecules such as pectins in sugar beet juice. Removal of these compounds is done mostly by CaO. Calcium may cause undesirable process of alkalization of soil in the proximity of sugar factory. The theoretical basis of new juice purificatin method based on the application of $Al_2(SO_4)_3$, $CaSO_4$ and their mixtures are presented. Two model solutions of pectin (0.1%, w/w) are investigated using method of measuring zeta potential. Pure salts $Al_2(SO_4)_3$ and $CaSO_4$, showed better binding with pectin than mixtures. Amount of all studied pure salts and mixtures of Al^{3+} and Ca^{2+} were significantly less (142–710 mg/g_{pectin}) than the average amount of CaO used in classical process (about 9 g/g_{pectin}). Mechanism of discharge of pectin macromolecules in the presence of mixtures of these ions using a model of double electric layer is suggested.

Keywords: pectin, sugar beet, $Al_2(SO_4)_3$, $CaSO_4$, zeta potential, double electric layer.

Available online at the Journal website: http://www.ache.org.rs/HI/

SCIENTIFIC PAPER

UDC 664.12/.121:633.63:66

Hem. Ind. **68** (1) 89–97 (2014)

doi: 10.2298/HEMIND121214032K

One of the most convenient parameters to determine the sugar beet juice purification efficiency is the lime consumption. The lime consumption varies depending on the quality of sugar beet. CaO consumption of individual factories may vary significantly between 1 and 3% depending on the quality of beets. Due to the large quantity of CaO (about 15 g CaO/100 g dry matter of sugar beet juice), calcium may cause undesirable process of alkalization of the soil in the proximity of sugar factory [1]. It is possible to reduce lime consumption down to 1%, but at the same time it would change color and lime salts content of the purified juices as well as the inferior filterability of the juices [2]. There are different improved methods of the purification of sugar beet juice, such as ion exchange, electrolysis, reverse osmosis, ultrafiltration, nanofiltration, etc., but they are at disadvantage due to the high maintenance cost [3,4].

About 60% nonsugar matter of the beet juice are pectin macromolecules. Pectins are ionic plant polysaccharides consisting almost entirely of D-galacturonic acid and galacturonic acid methyl ester residues, acetylated to some degree [5,6]. Coagulation and precipitation of pectins can be performed by process of chemically induced discharging. Due to the dissociation of carboxylic acid groups of galacturonic acid, pectic substances have the negative charge on the surface. These groups can take a part in the binding of divalent or trivalent cations [7,8]. There is a selectivity order of the binding affinity of various divalent cations by citrus and sugar-beet pectins [9–11]: $Cu^{2+} \approx Pb^{2+} >> Zn^{2+} > Cd^{2+} \approx \approx Ni^{2+} > Ca^{2+} > Mg^{2+}$.

There are many studies of applying ions with greater number of positive charges such as Al^{3+}. Al^{3+} is often used in form of hydrolyzed salt $Al_2(SO_4)_3$ for treatment of fresh and waste water [8,12,13]. Previous study [14] has given a simplified scheme of Al^{3+} hydrolysis. With the increase of pH value and concentration of ions, different products of hydrolysis are being formed including nonhydrolyzed ions, monomeric, dimeric and polymeric.

Ion binding to natural organic matter in water expressed as $H^+/Me^{2+,3+}$ molar exchange ratios varied strongly with metal ion: Al^{3+} (2.1–2.7) and Ca^{2+} (0.2––0.5). The bonding strength of Al ions with humic materials compared with divalent metal ions and the order of preference for ion binding are shown: Al^{3+} > > $Cu^{2+} > Pb^{2+} > Cd^{2+} > Ca^{2+}$ [15]. In accordance with this selectivity order, it is clear that applying of Al^{3+} will be efficient in sugar beet juice purification in relation to classical process that utilizes Ca^{2+} compounds [16]. Published research that studied the deposition of macromolecules from juices and by-products of sugar production (in order to determine their quality), gave priority to Al salts from economical and ecological point of view [17,18]. Studying the influence of Al^{3+} during the chemical processing of molasses, established the optimum amount of $Al_2(SO_4)_3$ (0.2–0.4 mol/l) [19]. In [14], studied was the influence of 100% $Al_2(SO_4)_3$ and $Al_2(SO_4)_3$

Correspondence: T.A. Kuljanin, University of Novi Sad, Faculty of Technology, Bulevar cara Lazara 1, 21000 Novi Sad, Serbia.
E-mail: kuljanin@uns.ac.rs
Paper received: 14 December, 2012
Paper accepted: 8 May, 2013

with different shares of $CuSO_4$ on the efficiency of sugar beet pectine separation. It has been proven that the most effective was pure $Al_2(SO_4)_3$ (142–182 mg/g_{pectin}).

In the research presented, the efficiency of ion binding was determined by elektrokinetical method by measuring zeta potential. Beet juice has a concentration of undesirable colloids as most of the waste and contaminated water (about 1 wt.%). Previous practice in the modern plants for the improved water treatment, showed that zeta potential control enhances the removal of colloids. According to this, zeta potential measurements should be effective for the control of discharging pectin and protein particles.

The very important are cation binding characteristics of pectins themselves since the total capacity of pectins to bind metal cations is directly related to the degree of methyl-esterification, degree of polymerization and galacturonic acid content [11,20]. Also, one of the influencing factors, concerning cation binding by pectins, is the remaining part of the coagulant molecules. Anions with greater charge, such as sulfates, have a high tendency to coordinate with metal ions [8]. Therefore, in this paper, were compared activity of $CaSO_4$ with the activity of CaO (in the form of $Ca(OH)_2$) used in the classical treatment of beet juice purification.

It is known that the adsorption of metal ions also influences the presence of the other ions of the same or different valence [14,21]. Also, an aspect ratio of ion size present in solution must not be neglected. The influence of ion size is greater at higher concentrations of ions whose valence is ≥2 and for systems with large electric charge of the colloidal particles [22].

Herein, the efficiency of binding of Al and Ca ions (from $Al_2(SO_4)_3$ and $CaSO_4$) in their mixtures with pectin was studied. The aim of the mixtures investigation was to determine whether the efficiency of coagulation is proportional to the concentrations of Ca^{2+} and Al^{3+} or discrepancies might occur.

Theoretical part

All electrokinetic phenomena are related to the development of electrical double layer (EDL) at the particle/electrolyte interface. EDL consists of two layers: the adsorbed (Stern) and mobile diffuse layer. The potential at the boundary between the Stern layer and the diffuse layer (where hydrodynamic movement of ions is still possible, Figure 1 – shear plane) can be easily measured and it is known as the electrokinetic or zeta potential (ζ) [23–25].

According to the Gouy-Chapman-Stern-Graham's (GCSG) model of EDL, Figure 1 illustrates the structure of EDL on the surface of macromolecule of pectin in the presence of divalent and trivalent salts ($CaSO_4$ and $Al_2(SO_4)_3$) in the aqueous solution. This model is characterized by the localization of ions (Ca^{2+}; Al^{3+}; H^+; SO_4^{2-}; OH^-) in the fixed (Stern) layer and also in the diffuse layer of the solid-liquid interface.

According to the GCSG model, the fixed layer is assumed to be bound by two planes: the Inner Helmholtz plane (IHP) and Outer Helmholtz plane (OHP), which are characterized by the potentials, ψ_{IHP} and ψ_{OHP}. The surface potential of pectin particles (ψ_0) occurs due to the presence of COO^-. According to the GCSG model, the potential change, ψ, between the IHP and OHP is linear, depending on the number, size and

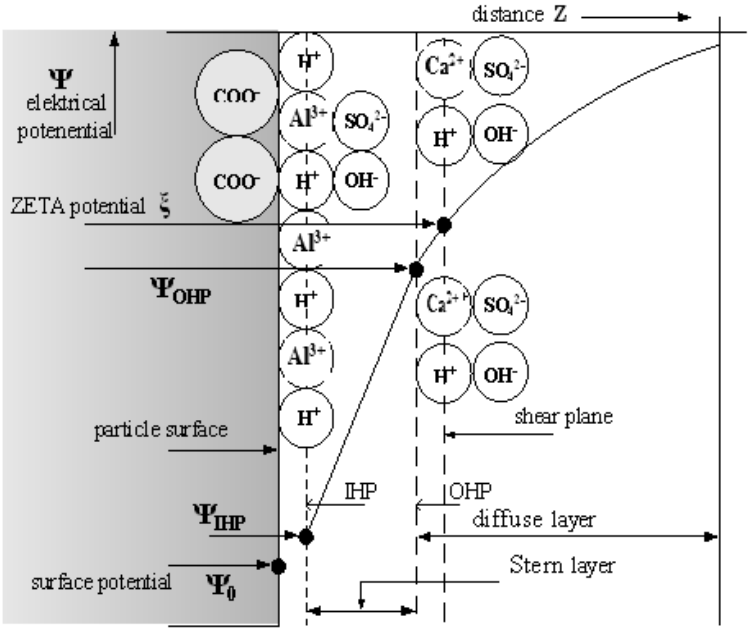

Figure 1. A schematic illustration of the structure of double electric layer (EDL) on surface of macromolecule of pectins according to GCSG model [23].

hydration of Ca^{2+} and Al^{3+}. In the diffuse layer, an exponential potential drop is observed in accordance with the Boltzmann distribution [26].

Adding polyvalent cations leads to release of negative charge on the pectin surface and decrease of zeta potential. By keeping zeta potential close to zero, pectin colloidal particles will discharge and the conditions for effective coagulation and sedimentation of particles will be achieved [25]. Zeta potential measurement method has limitations in theory and technique of work. Because of the wide range of sizes and masses of these colloids, it is impossible to have all zeta potential values of the interval ±5 mV (as attested in the water treatment practice) and total sedimentation cannot be achieved. However, the control of zeta potential based on the average size of the colloid is sufficient to obtain diffuse juice with significantly smaller share of undesirable macromolecules.

EXPERIMENTAL

Material

Pectin preparations were extracted from cossettes (dry matter 72.5%) obtained in the industrial processing of sugar beet (factory Žabalj). Salts, $CaSO_4$ and $Al_2(SO_4)_3$ in crystal hydrate form ($CaSO_4 \times 2H_2O$ and $Al_2(SO_4)_3 \times 18H_2O$), "Zorka Pharma", Šabac (purity of both salts was 99.0%, w/w) were used for preparation of the studied solutions in deionized water. The pH 7 of $Al_2(SO_4)_3$ solutions was regulated before each experiment, using the equivalent amount of Na_2CO_3.

Method of isolation of pectin preparation

Two kinds of pectin preparations were isolated by extraction in acidic conditions in accordance with a standardized laboratory procedure [27]. Extraction conditions were: pH 1.0, 75 °C for 1.0 h, P_1 preparation, while for the P_2 preparation were: pH 3.5, 95 °C and 1.5 h. Extraction of each preparation was repeated three times. Due to differences in the extraction conditions, the resulting pectin preparations had different composition and degree of esterification. High molecular colloidal fraction was isolated from extract by multistep precipitation with 70% ethanol. Extraction procedure has been described in previous work [28].

Determination of molar mass, degree of polymerization and esterification

Basic parameters of the pectin preparation were determined according to standard methods of AOAC [27]. Content of galactouronic acid was calculated using the equation:

$$Gal.A = \frac{m_g 100}{g} \left[\frac{g_{gal.kis.}}{100\ g_{S.M.}} \right] \quad (1)$$

Where the mass of pure galactouronic acid (*Gal.A*) is expressed through equivalents of free (*X*) and esterified carboxy groups (*Y*): $m_g = 176X + 190Y$ (g). In this equation, the values 176 and 190 are the molar masses of dehydrated galactouronic acid and methyl-esterified galactouronic acid (g/mol) [5].

Degree of esterification (DE) was calculated using equation [5,14]:

$$DE = \frac{Y}{X+Y} 100 \quad (2)$$

Average molar mass was determined refractometrically and spectrophotometrically by measuring 5 different concentrations of pectin preparations: 0.0025, 0.005, 0.010, 0.015 and 0.020 g/cm^3 [29]. Degree of polymerization (DP) was calculated by dividing the mean molar mass of the preparation with the molar mass of dehydrated *Gal.A*. The affinity of binding of metal ions depends primarily on the number of binding sites at macromolecule. The number of binding sites (primarily COO^- groups) on the surface of pectin macromolecule was calculated through form [30]:

$$n = DP\left(\frac{Gal.A}{1000}\right)\left(\frac{1-DE}{100}\right) \quad (3)$$

The cation binding capacity of pectin macromolecules, CBC_t, was calculated on the basis of simplified equation [31]:

$$CBC_t = \frac{Gal.A\left(1-\frac{DM}{100}\right)}{176} \left[\frac{\text{mmol}}{g_{SM}}\right] \quad (4)$$

In this paper it is accepted that only free carboxyl group of the galacturonic acid take part in the binding of cations.

In determining the composition of pectin preparation, measurements were repeated twice. If the difference between the two results of the same experiment was more than 5%, measurements were repeated several times.

Plan of the experiment

Experiments were performed in a model-pectin solutions P_1 and P_2 (0.1%, w/w). This concentration corresponds to the mean concentration of pectin in sugar beet juice [24]. Solutions were obtained by dissolving 1 g of pectin preparation in 250 cm^3 of distilled water and leaving it overnight to swell. After that, distilled water was added to 1 dm^3 and for each measurement 50 cm^3 of solution was taken. At each measurement, the pipette was used to add correct volume (in cm^3) of coagulant (pure solutions of $Al_2(SO_4)_3$, $CaSO_4$ or their mixtures) in order to obtain the required concentrations of coagulants (mg/dm^3).

Solutions $Al_2(SO_4)_3$ and $CaSO_4$ were obtained by dissolving 1 g of salt in 200 cm^3 of distilled water. Mixtures of these solutions were prepared in the following proportions of $CaSO_4$ and $Al_2(SO_4)_3$, respectively (calculated according to the pure salt mass): 20:80 (II); 40:60 (III); 60:40 (IV) and 80:20 (V) (%, w/w). From these solutions adequate volume (cm^3), using pipette, was added to 50 cm^3 of 0.1%, w/w, of pectin preparation solutions to obtain the corresponding concentration of coagulants. The range of these concentrations was from 50 to 500 mg/dm^3. Due to incomplete hydrolysis of $Al_2(SO_4)_3$, during preparation of coagulant, the equivalent amount of base must be added to obtain pH 7 solution [19]. In this study, Na_2CO_3 was added in equivalent mass ratio to the pure $Al_2(SO_4)_3$ (1:1.07).

It is known from the literature that the ability of surface complexation of metal ions with polysaccharides increases in the pH range of 3–7 [20]. All measurements were performed at pH 7. At neutral pH value, main cationic form of hydrolysis is Al^{3+} [8]. Also, at pH 7, ions Al^{3+} and Ca^{2+} have limited solubility (minimum solubility of $Al_2(SO_4)_3$ and $CaSO_4$ are 0.36 and 0.24 g/100 ml water at 20 °C). The pH of the solutions was measured using pH Meter MA 5740 at one hour intervals, counting from the moment of their preparation.

After adding the provided amounts of coagulants (I–VI) in the samples of preparations, pH adjusted solutions were stirred for 30 min on a high-speed magnetic stirrer (500 rpm). Then, the solution was stirred for another 5 min at low speed of maximum 20 rpm, to prevent the disaggregation of the already formed floccules. The solution was then allowed to settle down for 5 min. An aliquot taken from the supernatant was used to measure the zeta potential. Measurements were performed at room temperature for 10 different solution concentrations.

Zeta potential measurement

The electrokinetic potential was evaluated by means of electrophoresis using a Zeta Meter ZM-77 [32]. The instrument consists of an electrophoretic cell with platinum electrodes connected to direct current and a stereoscopic microscope equipped with a special ocular micrometer. After adjusting the voltage, an electric recording device was used to measure time needed for a colloidal particle to pass a distance of a standard micrometer division.

From the measured value of 20 particles, an average value was used to derive the zeta potential in the tested solutions using a diagram based on the Helmoltz–Smoluchowski equation for electrophoretic mobility of colloidal particles. Experiments were conducted at 6-fold magnitude on a stereoscopic microscope and voltage adjusted at 150 V. Just before zeta potential measurements, solution temperatures were measured. Zeta potential was read from the diagram and multiplied by a correction factor for a given temperature [32].

RESULTS AND DISCUSSION

In accordance with the described extraction conditions, preparations of different composition and degree of esterification were obtained. These properties depend on the biological origin of raw material, sugar beet ripeness, extraction conditions and experimental procedure. The results are shown in Table 1. Along with results for the average molar masses, the calculated values of the degree of esterification, degree of polymerization, number of binding sites and the cation binding capacity are shown (Table 1).

The content of galacturonic acid in the tested preparations is in accordance with the mean content of pectin found in raw sugar beet juices from diffuser, reported in literature. Degree of esterification of pectin preparations, P_1 and P_2 (72.21 and 39.50, respectively), is inversely proportional to the number of binding sites (124.5 and 217.8). Also, it can be seen from Table 1 that the cation binding capacity (1.045×10^{-3} and 2.480×10^{-3} mmol/g) is proportional to the equivalent of free COOH groups (10.60 and 24.58) which are responsible for the surface charge of pectin particles.

Table 1. Basic physicochemical composition, number of binding sites and the cation binding capacity of pectin preparation

Preparation	P_1	P_2
Solid content, *SC*, g/100 g	82.25	80.35
Equivalent of free COOH groups, $X\times10^5$	10.60	24.58
Equivalent of esterified COOH groups, $Y\times10^5$	27.55	16.05
Content of galacturonic acid, *Gal.A*, %	66.31	72.24
Degree of esterification, *DE*	72.21	39.50
Mean molar mass, M_{Wsr} (g/mol)	87720	119048
Degree of polymerization, *DP*	676	498
Number of binding sites, *n*	124.5	217.8
Cation binding capacity, $CBC_t\times10^3$, mmol/g	1.045	2.480

As coagulants, most efficient are salts that give catonic hydrolysis products of the higher charge, such as $Al_2(SO_4)_3$. At pH below the effective isoelectric point of the metal hydroxide (pHzpc 8), the predominant Al species are positively charged and charge neutralization can be achieved. At pH ~ 7, Al^{3+} can form hydroxyl complexes such as $Al(OH)_2^+$, $Al(OH)^{2+}$ and $Al(OH)_3$. In the vicinity of the isoelectric point, colloidal hydroxy--Al polymers with high charge are also created, that are more efficient in the charge neutralization of the surface of pectin particles [8].

Addition of $Al_2(SO_4)_3$ and $CaSO_4$ reduces steadily the zeta potential of pectin macromolecules. Charge inversion of zeta potential was observed within the whole series of tested coagulant concentrations (Figures 2 and 3). Therefore, in addition to the simple charge neutralization mechanism and ion exchange, a mechanism of specific adsorption occurs. If ions possess a special affinity for the solid surface, but are not chemisorbed, they are known as specifically adsorbed ions. Specifically adsorbed ions adsorb strongly to the surface because of covalent bond forming and solvation effect [23]. Therefore, the specific adsorption of ions will change the surface charge and surface potential of colloidal particles, which may cause the charge inversion. Charge inversion is the occurrence of EDL in which, as measured by electrokinetics, there is more counter charge than charge on the surface. The phenomenon of charge inversion, where changes in the sign of the zeta potential (in our case, "–" to "+"), has not been yet sufficiently clarified from the physical–chemical point of view [33].

According to the GCSG model, specific adsorption takes place in the Inner Helmholtz layer (Figure 1). By analyzing the proposed model in the presence of Ca^{2+}, Al^{3+}, SO_4^{2-} in aqueous solution, the following can be observed:

- The inner Helmholtz plane (IHP) is passing through the centers of Ca^{2+} and Al^{3+} specifically adsorbed (and H^+ adsorbed from the solution) on the negatively charged glycosyl-residues on the pectin macromolecule surface.

- Anions (SO_4^{2-} and OH^-) form a secondary layer due to electrostatic attraction with the ions of Ca^{2+} and Al^{3+} from the Stern layer.

- The outer Helmohltz plane (OHP) is passing through the centers of Ca^{2+}, Al^{3+} and H^+ that are attracted only by the electrostatic forces (Coulombic attraction). Also present are SO_4^{2-} and OH^- from the solution, attracted by the electrostatic forces as oppositely charged ions.

According to the presented model, it is assumed that the increase in Ca^{2+} and Al^{3+}, increases the proportion of specific adsorption of these ions as compared to the proportion of electrostatic Coulombic attractions.

The low amount of Al^{3+} were compared to the amount of Ca^{2+} (from $Al_2(SO_4)_3$ and $CaSO_4$) to achieve the charge inversion on the surface of pectin macro-

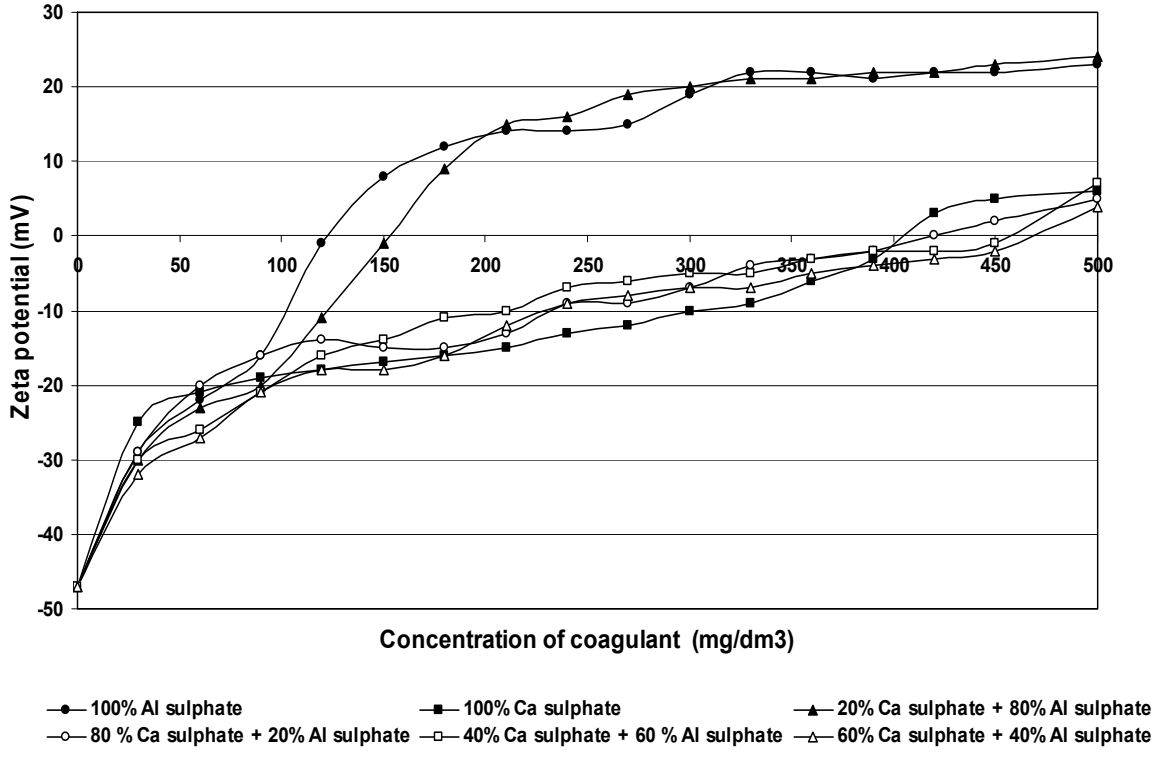

Figure 2. The influence of $Al_2(SO_4)_3$, $CaSO_4$ and their mixtures to the change zeta potential of the pectin preparation P_1.

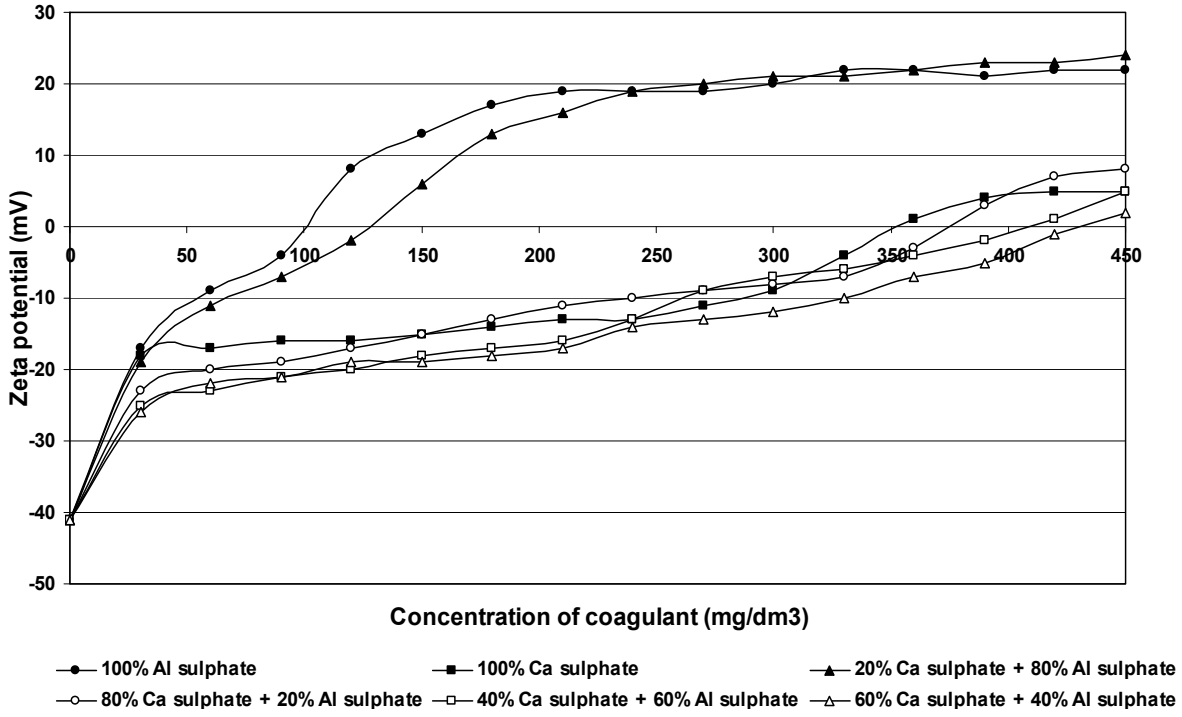

Figure 3. The influence of $Al_2(SO_4)_3$, $CaSO_4$ and their mixtures to the change zeta potential of the pectin preparation P_2.

molecules (Figures 2 and 3). For both tested preparations, about 3.5 times smaller amount of Al^{3+} (120 mg/dm^3 or 182 mg/g$_{pectin}$ for P_1 and 102 mg/dm^3 or 142 mg/g$_{pectin}$ for P_2) are needed compared to Ca^{2+} (405 mg/dm^3 or 610 mg/g $_{pectin}$ for P_1 and 355 mg/dm^3 or 490 mg/g $_{pectin}$ for P_2) for the value of zeta potential to reach zero (Table 2). This can be explained by weaker, electrostatic binding of Ca^{2+} (Coulombic attractions). Since Ca^{2+} are in the last place of the affinity binding scale of divalent ions with biological material [15], specific adsorption of these ions is much smaller compared to the electrostatic binding. In recent literature, the binding of Ca^{2+} with humic materials is explained by gradual formation of humic acid–Ca-OH complex (although the presence of such a complex has not be proven so far) [34,35]. In this way, the mechanism of specific absorption and charge inversion of pectin molecule surfaces in the presence of Ca^{2+} probably occurs *via* the creation of Gal.A–Ca-OH complexes.

It is known that Ca^{2+} have a large dehydration effect of hydrophilic macromolecules such as pectin. The ions with the smaller hydrated radius such as Ca^{2+} will be able to approach the surface closely. The distribution of these ions is faster so they are easily stored, primarily in the diffusion part of EDL. However, in the charge inversion process, valence of counterion is very significant [26]. Al^{3+} have a larger hydrated radius, carry higher charge, reduce zeta potential to zero point at much lower concentrations. This is in accordance with Schulze–Hardy rule and literature [15,36]. From the literature data, Al^{3+} have three times higher binding constant to the cell walls of plant origin (4.36) in relation to the Ca^{2+} (1.44) [34]. Also, due to the high density of Al^{3+} (the density of Al^{3+} is 2.70 g/cm^3, whereas of Ca^{2+} is 1.54 g/cm^3), their electrophoretic mobility is higher, which enables easier location in the Stern layer and neutralization of the negative charge on the surface of pectin macromolecules.

Table 2. Amounts of $Al_2(SO_4)_3$ and $CaSO_4$ (I and VI) and their mixtures (II–V) required for neutralization of the charge of pectin macromolecules

Pure salts and mixtures: $Al_2(SO_4)_3$, $CaSO_4$		Preparation P_1		Preparation P_2	
		mg/dm^3	mg/g$_p$	mg/dm^3	mg/g$_p$
I	100% $Al_2(SO_4)_3$	120	182	100	142
II	20% $CaSO_4$ + 80% $Al_2(SO_4)_3$	155	234	130	180
VI	100% $CaSO_4$	405	610	355	490
V	80% $CaSO_4$ + 20% $Al_2(SO_4)_3$	420	634	370	512
III	40% $CaSO_4$ + 60% $Al_2(SO_4)_3$	460	695	410	568
IV	60% $CaSO_4$+ 40% $Al_2(SO_4)_3$	470	710	435	602

The results show that amount of $Al_2(SO_4)_3$ needed to achieve zero zeta potential of pectin preparations is significantly lower (142–182 mg/g pectin), compared to the removal of humic substances from water [8]. Zeta potential of humic substances in water reached zero value at a concentration about 3 g_{Al} / g_{DM} (pH 7).

Comparing the activity of coagulants with the same cation and different anions, $Al_2(SO_4)_3$ has proved to be significantly more effective than $AlCl_3$ studied in previous work under the same experimental conditions [7]. To achieve a zero value of zeta potential, it was necessary to add 350–390 mg/dm^3 of $AlCl_3$, which is about 3.5 times the amount of $Al_2(SO_4)_3$ (120 mg/dm^3 for P_1 and 102 mg/dm^3 for P_2). However, $CaSO_4$ showed a slight difference compared to the effect of $CaCl_2$ (300–400 mg/dm^3 $CaCl_2$ or 350–420 mg/dm^3 $CaSO_4$ to achieve zero zeta potential) [7]. In the present study, SO_4^{2-} did not have influence on the coagulation effect of Ca^{2+}.

The amount of adsorbed ions in the mixtures depends on the equilibrium between adsorption competition from of the ions, ionic size and stability of bonds between metal ions and surface macromolecules [36]. Using mixtures with different proportions of Al^{3+} and Ca^{2+}, caused a change in adsorption properties and ion binding affinity. The required quantities of $Al_2(SO_4)_3$ (I), $CaSO_4$ (VI) and their mixtures (II–V) to achieve zero zeta potential values, sorted by size, are shown in Table 2.

Pure salt of $Al_2(SO_4)_3$ and $CaSO_4$, proved to be the most effective in neutralizing the charge of pectin macromolecules (Table 2, I and VI). From the tested mixtures, compounds with the highest proportion of Al^{3+} (80% $Al_2(SO_4)_3$ + 20% $CaSO_4$), as expected, showed the highest affinity for binding ions. In order to reach zero zeta potential value, necessary amount was 234 mg_{mix}/g_{pectin} for P_1 and 180 mg_{mix}/g_{pectin} for P_2. This confirms earlier presented conclusions on the impact of Al^{3+} on the surface charge modification of colloidal particles. The charge inversion from negative to positive for the investigated concentrations in mixtures of $Al_2(SO_4)_3$ and $CaSO_4$ infers, that besides ionic exchange and decrease in the surface potential, ψ_0, caused by charge neutralization, marked specific adsorption of Al^{3+} occurs at active sites of pectin macromolecules (COO^-).

The most unfavourable proved to be a mixture with approximately equal shares of Al^{3+} and Ca^{2+} (Table 2, compounds III and IV). Lower strenght of bonding ions in this case, can be explained by the mutual competition of Ca^{2+} and Al^{3+} for the same adsorption site (COO^-) on the surface of pectine macromolecules. This is most likely because of phenomenon that occurs in the presence of salts which differ in their physical and chemical properties. This phenomenon is known in literature as “ion antagonism”, when the coagulation ability of the salt mixture is usually less than coagulation capabilities of individual components [37].

The effect of ion size ratio was observed at ion valence ≥ 2, most likely due to small concentrations of these ions and a small charge of pectin macromolecules.

As for the pure salts, also in the case of mixtures, the compound P_2 showed better cation-binding characteristics in relation to the product P_1 ($CBC_{T(P2)}$ = = 2.37×$CBC_{T(P1)}$). This is as expected, since the product P_2 has a higher content of galacturonic acid (72.24%), a lower degree of esterification (39.50) and a higher molar mass, *i.e.*, greater length of polygalacturonic chains (119048 g/mol).

Based on these studies it can be concluded that in the presence of a mixture of Al^{3+} and Ca^{2+}, binding mechanism of ions and mechanism of discharge of pectin macromolecules are more complex. In addition to the concentration, size, and charge of ions, the pH of the solution, the number of binding sites on the surface of pectin macromolecules and other factors play a role as well. These are, above all, ion competition for the same adsorption site, the possibility of partial dehydration of ions and the possibility of overlapping hydration layers of ions in the Stern part of the EDL.

In the case of mixtures, GCSG model was proposed to illustrate the accomodation and interactions of Ca^{+2}, Al^{+3} and H^+ in the EDL (Fig. 1.)

In the sugar industry in clarification stage of sugar beet juice, about 2.2%, w/w, CaO is used (calculated to the mass of juice). Extracted sugar beet juice contains about 14%, w/w, of dry matter or 15 g_{CaO}/100 g_{DM}. Calculated to the pectin mass that represents about 60% of dry matter, content of juice is about 9 $g_{CaO}/g_{pectins}$. This means that the amounts of $Al_2(SO_4)_3$ and $CaSO_4$, determined in this study, individually or in mixtures, are significantly lower (142–710 mg per g pectin) compared with the amount of conventional coagulant CaO.

CONCLUSION

Multivalent cation Al^{3+} exerts a greater influence on the zeta potential of pectin than divalent cation Ca^{2+}. The binding of Ca^{2+} and Al^{3+}, appeared to be regulated by following mechanisms:

– elctrostatic bonding with a small share of specific adsorption (Ca^{2+}),

– surface complexation, solely through the mechanisam of specific adsorption, with a small portion of electrostatic bonding (Al^{3+}) and

– competition of ions for adsorption sites (mixtures of Ca^{2+} and Al^{+3}).

Compared to conventional process where approximately 9 g CaO per g of pectin is used, the amount of $Al_2(SO_4)_3$ and $CaSO_4$ (in the form of mixtures or pure

salt) were significantly lower, ranging in the interval 142–710 mg per 1 g of pectin.

GCSG model has been proposed to illustrate the placement and interactions of Ca^{2+}, Al^{3+} and H^{+} on the surface of the pectin particles.

Control of the zeta potential and appropriate dosing of Ca^{2+} and Al^{3+}, could very efficiently remove the pectin from sugar beet juice. The significance of this method is that it achieves significantly higher cleaning efficiency of sugar beet juice compared to the conventional method. With certain improvement in techniques and methods of work and further study of the electrokinetical phenomenon, better results could be obtained.

However, reliable comparison between the proposed coagulants and traditional coagulant CaO, require additional testing under industrial conditions of sugar beet juice processing.

Acknowledgement

The authors gratefully acknowledge the financial support from the Ministry of Education, Science and Technological Development of the Republic of Serbia (Project TR-31055).

REFERENCES

[1] H. Haapala, N. Goltsova, V. Pitulko and M. Lodenius, The effects of simultaneous large acid and alkaline airborne pollutants on forest soil, Environ. Pollut. **94** (1996) 159–168.

[2] M.T.G. Cubero, G.G. Benito, J.B. Alonso, M.R. Holst, M.G. de Quevedo, F. Martín, Pilot plant installation for the purification of raw juices. Part II: Optimization of the operating parameters in the preliming and main liming units, Zuckerindustrie **125** (2000) 391–395.

[3] G. Schrevel, Separation of macromolecules in beet sugar processing, Zuckerindustrie **127** (2002) 197.

[4] F. Lipnizki, M. Carter, G. Trägårdh, Application of membrane processes in the beet and cane sugar production, Zuckerindustrie **131** (2006) 28–39.

[5] P.W. Poel, H. Schiweck, T. Schwarts, Sugar Technology – Beet and Cane Sugar Manufacture, Verlag Dr. A. Bartens, Berlin, 1998, p. 494.

[6] B.M. Yapo, Pectin quantity, composition and physicochemical behavior as influenced by the purification process, Food Res. Int. **42** (2009) 1197–1202.

[7] Lj. Lević, M. Tekić, M. Djurić, T. Kuljanin, $CaCl_2$, $CuSO_4$, $AlCl_3$ and $NaHCO_3$ as possible pectin precipitants in sugar juice clarification, Int. J. Food Sci. Tech. **42** (2007) 609–614.

[8] J. Duan, J. Gregory, Coagulation by hydrolyzing metal salts, Adv. Colloid Interf. Sci. **100–102** (2003) 475–502.

[9] R. Kohn, Binding of divalent cations to oligomeric fragments of pectin, Carbohydr. Res. **160** (1987) 343–353.

[10] V.M. Dronnet, C.M.G. Renard, M.A.V. Axelos, J.F. Thibault, Characterization and selectivity of divalent metal ions binding by citrus and sugar-beet pectins, Carbohyd. Polym. **30** (1996) 253–263.

[11] S.K. Wiedemer, A. Cassely, M. Hong, M.V. Novotny, M. Riekkola, Electrophoretic studies of polygalacturonate oligomers and their interactions with metal ions, Electrophoresis **21** (2000) 3212–3219.

[12] J. Duan, J. Wang, N. Graham, F. Wilson, Coagulation of humic acid by aluminum sulphate in saline water conditions, Desalination **150** (2002) 1–14.

[13] S. Pattabi, K. Ramasami, K. Selvam, Swaminathan, Influence of polyelectrolytes on sewage water treatment using inorganic coagulants, Indian. J. Environ. Prot. **20** (2000) 499–507.

[14] T. Kuljanin, N. Mišljenović, G. Koprivica, L. Jevrić, J. Grbić, Uticaj bakarnih jona, aluminijumovih jona i njihovih smeša na izdvajanje pektina iz soka šećerne repe, Hem. Ind. **67** (2012) 69–76

[15] D.G. Kinniburgh, W.H. Riemsdijk, L.K. Koopal, M. Borkovec, M.F. Benedetti, M. J. Avena, Ion binding to natural organic matter: competition, heterogeneity, stoichiometry and thermodynamic consistency, Colloids Surfaces, A **151** (1999) 147–166.

[16] T. Kuljanin, Lj, Lević, L. Jevrić, B. Ćurčić, J. Grbić, R. Jevtić-Mučibabić, Aluminium sulfate as ecological coagulant in phase of sugar beet juice clarification, XVI International Eco-Conference, Safe Food, 2012, Novi Sad, Serbia, Ecological Movement of Novi Sad, Procedings, pp. 427–435.

[17] Lj. Lević, J. Gyura, Influence of aluminium sulphate concentration on the change of electrokinetic potential of macromolecular compounds in molasses, Nahrung **43** (1999) 288–289.

[18] B. Sagripanti, P. Fontana, L'Industria saccarif. Ital. **1** (1992) 7–11.

[19] Lj. Lević, J. Gyura, M. Đurić and T. Kuljanin, Optimization of pH value and aluminum sulphate quantity in the chemical treatment of molasses, Eur. Food Res. Technnol. **220** (2005) 70–73.

[20] P. Pellerin, M. A. O'Neill, The interaction of pectin polysaccharide Rhamnogalacturonan II with heavy metals and lanthanides in wines and fruit juices, Analysis Magazine **26** (1998) M32–M39.

[21] P. Zhou, H. Yan, B. Gu, Competitive complexation of metal ions with humic substances, Chemosphere **58** (2005) 1327–1337.

[22] A.M. Molina, M.Q. Perez, F.G. Gonzales, R.H. Alvarez, Primitive models and electrophoresis: an experimental study, Colloids Surfaces, A **222** (2003)155–164.

[23] M. Alkan, O. Demirbas, M. Dogan, Electrokinetic properties of kaolinite in mono- and multivalent electrolyte solutions, Micropor. Mesopor. Mat. **83** (2005) 51–59.

[24] T. Kuljanin, Lj. Lević, N. Mišljenović, G. Koprivica, Electric double layer and electrokinetic potential of pectic macromolecules in sugar beet, APTEFF. **39** (2008) 21–27.

[25] G.J.M. Koper, An Introduction to Interfacial Engineering, VSSD, Delft, 2007.

[26] J. Lyklema, Electrokinetics after Smoluchowski, Colloids Surfaces, A **222** (2003) 5–14.

[27] AOAC – Methods of Analysis of Official Analytical Chemists, Washington, 2000.

[28] T. Kuljanin, N. Mišljenović, G. Koprivica, Lj. Lević, B. Filipčev, Influence of Cu^{2+} and Al^{3+} on Zeta potential

change of pectin and protein preparations extracted from sugar beet, Journal on processing and energy in agriculture **14** (2010) 141–144.

[29] F. Kar, N. Arslan, Effect of temperature and concentration on viscosity of orange peel pectin solutions and intrinsic viscosity-molecular weight relationship, Carbohyd. Polym. **40** (1999) 277–284.

[30] C. Garnier, M.A.V. Axelos, J.F. Thibault, Selectivity and cooperativity in the binding of calcium ions by pectins, Carbohydr. Res. **256** (1994) 71.

[31] Z. Reddad, C. Gerente, Y. Andres, M.-C. Ralet, J.-F. Thibault, P. Le Cloriec, Ni (II) and Cu (II) binding properties of native and modified sugar beet pulp, Carbohyd. Polym. **49** (2002) 23–31.

[32] M.T. Riddick, Zeta-Meter Manual (third ed.), New York, 1975.

[33] C. Schneider, M. Hanisch, B. Wedel, A. Jusufi, M. Ballauff, Experimental study of electrostatically stabilized colloidal particles: Colloidal stability and charge reversal, J. Colloid Interf. Sci. **358** (2011) 62–67.

[34] T.B. Kinraide, U. Yermiyahu, A scale of metal ion binding strengths correlating with ionic charge, Pauling electronegativity, toxicity and other physiological effects, J. Inorg. Biochem. **101** (2007) 1201–1213.

[35] N.A. Wall, G.R. Choppin, Humic acids coagulation: influence of divalent cations, Appl. Geochem. **18** (2003) 1573–1582.

[36] M. Ahmaruzzaman, Industrial wastes as low-cost potential adsorbents for the treatment of waste water laden with heavy metals, Adv. in Colloid and Interf. Sci. **166** (2011) 36–59.

[37] Lj. Đaković, Koloidna hemija, Tehnološki fakultet, Novi Sad, 1990.

IZVOD

VEZIVANJE ALUMINIJUMOVIH I KALCIJUMOVIH JONA SA PEKTININIMA SOKA ŠEĆERNE REPE – MODEL DVOJNOG ELEKTRIČNOG SLOJA

Tatjana A. Kuljanin[1], Lidija R. Jevrić[1], Biljana Lj. Ćurčić[1], Milica R. Nićetin [1], Vladimir S. Filipović[1], Jasna P. Grbić[2]

[1]*Tehnološki fakultet, Univerzitet u Novom Sadu, Srbija*

[2]*Naučni Institut za prehrambene tehnologije, Univerzitet u Novom Sadu, Srbija*

(Naučni rad)

U industriji šećera, u fazi čišćenja soka šećerne repe, najčešće se koristi CaO u obliku $Ca(OH)_2$. Količine upotrebljenog kreča su jako velike i iznose 1–3 mas.% na suvu masu šećerne repe. $Ca(OH)_2$ može prouzrokovati neželjen proces alkalizacije zemljišta u neposrednom okruženju fabrike šećera. Izneta je teorijska osnova nove metode čišćenja soka šećerne repe koja se bazira na primeni soli $Al_2(SO_4)_3$ i $CaSO_4$ kako čistih, tako i njihovih smeša u cilju smanjenja količine otpadnog materijala. Proučavana su dva model-rastvora pektina čija koncentracija odgovara srednjoj koncentraciji pektina u soku šećerne repe (0,1 mas.%). Koristeći elektroforetsku metodu merenja ceta potencijala, utvrđeno je da Al^{+3} imaju bolji afinitet vezivanja sa pektinskim makromolekulima u poređenju sa jonima Ca^{2+}. Utvrđeno je da čiste soli $Al_2(SO_4)_3$ i $CaSO_4$ poseduju bolje karakteristike vezivanja jona nego njihove smeše. Smanjena jačina vezivanja jona u slučaju smeša može se objasniti međusobnim takmičenjem Al^{+3} i Ca^{+2} za adsorpciono mesto (COO^-) na površini makromolekula pektina. Najnepovoljnije su se pokazale smeše sa približno jednakim udelima Ca^{+2} i Al^{+3} (antagonizam jona). U poređenju sa klasičnim postupkom čišćenja soka šećerne repe gde se koristi približno 9 g CaO po g pektina, ustanovljene količine $Al_2(SO_4)_3$ i $CaSO_4$ (u vidu smeša ili čistih soli) su znatno manje i kreću se u intervalu od 142–710 mg po g pektina. Korišćen je *Gouy–Chapman––Stern–Graham*-ov (GCSG) model dvojnog električnog sloja da bi se prikazala raspodela Al^{+3} i Ca^{+2} na površini makromolekula pektina. Ustanovljeni su sledeći mehanizmi razelektrisanja pektinskih makromolekula: elektrostatičko vezivanje (Ca^{+2}), površinska kompleksacija – isključivo preko mehanizma specifične adsorpcije (Al^{+3}) i kompeticija jona za adsorpciono mesto (smeša Ca^{+2} i Al^{+3}). Kontrolom zeta potencijala uz pravilno doziranje $Al_2(SO_4)_3$ i $CaSO_4$, moglo bi se postići efikasnije uklanjanje pektina iz soka šećerne repe u poređenju sa konvecionalnom metodom. Predloženi koagulanti su povoljni ne samo iz ekonomskih razloga, nego i zbog očuvanja životne sredine. Preporučuje se delimična ili potpuna zamena tradicionalnog koagulanta CaO sa predloženim koagulantima $Al_2(SO_4)_3$ i $CaSO_4$.

Ključne reči: Pektini • Šećerna repa • $Al_2(SO_4)_3$ • $CaSO_4$ • Zeta potencijal • Dvojni električni sloj

Rheological properties of dough and quality of bread supplemented with emulsifying polysaccharides

Tamara Dapčević Hadnađev[1], Ljubica Dokić[2], Milica Pojić[1], Miroslav Hadnađev[1], Aleksandra Torbica[1], Slađana Rakita[1]

[1]*University of Novi Sad, Institute of Food Technology, Novi Sad, Serbia*
[2]*University of Novi Sad, Faculty of Technology, Novi Sad, Serbia*

Abstract

The aim of present study was to evaluate the effects of emulsifying starches used as additives in breadmaking. In order to achieve this, the partial replacement (5-10%) of wheat flour with starch sodium octenyl succinate (OSA starch), pregelatinized starch sodium octenyl succinate (Pregel OSA starch) and hydrolyzed spray-dried starch sodium octenyl succinate (Hydrol OSA starch) was prepared. The quality characteristics of obtained bread were compared to control wheat flour bread and bread containing 0.5% hydroxypropyl methylcellulose (HPMC). The obtained results indicated that addition of Pregel and OSA starches influenced the increase in water absorption, whilst addition of Hydrol OSA starch exhibited the opposite effect. Moreover, the addition of all chosen starches influenced the decrease in dough stability. On the other hand, the positive effects of implementation of emulsifying starches on specific volume and texture were observed, where Pregel OSA and OSA starch have expressed the best effect.

Keywords: bread; emulsifying starches; HPMC; Mixolab simulator.

Available online at the Journal website: http://www.ache.org.rs/HI/

SCIENTIFIC PAPER

UDC 664.6/.7:66.022

Hem. Ind. **68** (1) 99–106 (2014)

doi: 10.2298/HEMIND130124033D

Wheat bread is a widely consumed product and staple food in many countries, especially in Serbia where bread consumption per capita is far above EU average. Recently it was found that in Serbia 25 tons of bread per day are discarded due to its reduced quality caused by staling [1]. Starch as a major component of flour (about 75–85%), significantly affects the textural properties and quality of dough and bread. Starch retrogradation during storage is responsible for bread staling and product texture changes, where both amylose and amylopectin behavior upon baking play important role. Unlike amylose, which is almost completely recrystallized after cooling, recrystallization of amylopectin requires more time and due to that it is considered the main reason for staling [2]. This phenomenon is a very complex process that involves physical and chemical changes such as loss and redistribution of water between crumb and crust, firming of crumbs and decrease in starch solubility [3–6].

Modified starches, initially developed to suppress undesirable properties of native starches, have found wide application in food processing as they are able to improve water retention capacity, texture, thickness, freeze-thaw stability, retardation of retrogradation, etc. [7,8]. Modification of starches with octenyl succinic anhydride (OSA) was firstly patented by Caldwell and Wurzburg [9]. OSA starch is obtained by esterification reaction between starch and anhydrous octenyl succinic acid under alkaline conditions. Due to its amphiphilic nature, containing both hydrophilic and hydrophobic groups, OSA starch could act as an effective emulsifier. Therefore, aqueous solutions of OSA starches have been successfully used to stabilize oil in salad dressings and food flavor concentrates in beverages, to encapsulate flavors and vitamins in sauces, puddings and baby foods [10]. Moreover, it has been reported that OSA starch exhibits resistance to digestive enzymes, so it could act as a functional dietary fiber. It implies that products supplemented with OSA starches have additional nutritional value, being significantly different to other additives commonly used in breadmaking [11].

Based on our knowledge and available literature, the utilization of OSA starches, as additives in breadmaking has not been studied so far. This study was performed to estimate the suitability of partial replacement of wheat flour with OSA starches in breadmaking, where the main focus was on improving bread texture and structure in order to reduce the impact of bread staling. Therefore, the quality characteristics of bread supplemented with OSA starches (starch sodium octenyl succinate, pregelatinized starch sodium octenyl succinate and spray-dried hydrolyzed starch sodium octenyl succinate) were compared to control bread and bread containing hydroxypropylmethylcellulose (HPMC), with already proven ability to improve bread volume, strengthen bread crumbs, increase crumb moisture and reduce crumb hardening rate [4,12].

Correspondence: Milica Pojić, Institute of Food Technology, University of Novi Sad, Bulevar cara Lazara 1, 21000 Novi Sad, Serbia.
E-mail: milica.pojic@fins.uns.ac.rs
Paper received: 24 January, 2013
Paper accepted: 10 May, 2013

MATERIALS AND METHODS

Materials

Wheat flour (moisture content 13.8%; protein content 12.0% d.m.; ash content 0.50% d.m.) was provided from Žitobačka, Kula, Serbia. Hydroxypropylmethylcellulose (HPMC) was purchased from Alfa Aesar Gmbh & Co KG, Germany and starch sodium octenyl succinate starhes (OSA) were donated by Cargill, France. Three types of OSA starches, obtained from waxy maize, were used: starch sodium octenyl succinate (C*EmTex 06328), pregelatinized starch sodium octenyl succinate (C*EmTex 12688) and hydrolyzed and spray-dried starch sodium octenyl succinate (C*EmCap 12633), which were referred to as OSA starch, Pregel OSA starch and Hydrol OSA starch, respectively. Salt and yeast were purchased from local market.

Methods

Rheological properties of dough

Rheological properties of dough made of wheat flour sample (control sample), wheat flour/HPMC mixture (benchmark sample) and wheat flour/OSA starch mixtures were investigated using Mixolab (Chopin Technologies, France). Measurements were performed in duplicates by Chopin Simulator protocol (Table 1) whose results correspond to values and units obtained by Brabender Farinograph. However, in contrast to Farinograph which operates with the constant flour mass (50 or 300 g), Mixolab flour mass depends on flour water absorption, where the parameter which is fixed is the dough mass (75 g) [13,14]. The obtained parameters from recorded curves were water absorption (Wabs), dough development time (min), dough stability (min), degree of softening (BU) and initial maximum consistency, C1 (Nm) which was used to determine the water absorption.

Table 1. Chopin simulator protocol

Setting	Value
Mixing speed, rpm	80
Dough weight, g	75
Tank temperature, °C	30
Dough temperature	30
Total analysis time, min	30

Breadmaking procedure

Dough formulation that consisted of different flour/flour mixtures, fresh yeast and salt is given in Table 2. The amount of water required to reach the consistency of 500 Brabender Units (BU) was determined by Mixolab Simulator protocol. After kneading, the dough was rounded, and rested in a fermentation cabinet for 60 min (T = 30 °C, *RH* 80–85%). Afterwards, the dough was divided (350 g), kneaded and mechanically sheeted and rolled. Cylinder-shaped dough pieces were placed into teflon pans ($L\times W\times H$: 240 mm×85 mm×65 mm, Tefal, France) and proofed up to the optimum volume increase at 35 °C and the relative humidity of 85% RH for final fermentation. The bread loaves (4 per formulation) were baked in MIWE deck baking oven (MIWE Condo, Germany) at 220 °C until the mass loss of 9% was reached. Finally, bread was cooled at room temperature for 2 h and stored (at 23 °C, 40% *RH*) for further bread quality evaluation.

Bread physicochemical characteristics

Bread volume was evaluated 24 h after baking by using the millet displacement method, while the specific volume was calculated as volume/weight (cm^3/g) of four loaves. Moisture content was monitored 24 h after baking according to ICC 110/1 [15]. Breadcrumb firmness was measured by TA.XTPlus Texture Analyzer (Stable Micro Systems, UK) according to standard method for determination of bread firmness AACC (74--09) [16] using a P/36 probe (HDP/P/36) and 5 kg load cell in compression mode. Bread loaves were sliced at 25 mm thickness and compressed up to 40% of strain at a test speed of 1.7 mm/s. Textural analyses were conducted after 6, 24 and 48 h, at 23 °C, in nine replicates per batch.

Statistical analysis

The obtained results for specific bread volume and crumb moisture were analyzed by one-way analysis of variance (ANOVA), whilst the effects of additives and storage time were analyzed by two-way ANOVA using software XLSTAT, version (2012.2.02). ANOVA was fol-

Table 2. Bread dough formulation

Sample	Wheat flour %	*HPMC* %	Pregel OSA starch	Hydrol OSA starch %	OSA starch %	Yeast %	Salt %
Control	100	–	–	–	–	2	2
Control+HPMC	99.5	0.5	–	–	–	2	2
Control+Pregel OSA starch	95	–	5	–	–	2	2
Control+Hydrol OSA starch	90	–	–	10	–	2	2
Control+OSA starch	90	–	–	–	10	2	2

lowed by Fisher's Least Significant Difference (LSD) test. The analysis of the differences between the categories was performed with a confidence interval of 95%.

RESULTS AND DISCUSSION

Rheological properties of dough

The monitoring of rheological properties of dough is of great importance for the whole processing chain in order to assess the mechanical properties of dough, molecular structure and composition of the material, to imitate behaviour during dough processing and to anticipate the quality of the final product [14].

In the last decade, HPMC addition to wheat dough was studied by many authors [4,12,17]. It has been proven that HPMC addition exhibits positive effects on water absorption, dough stability during processing, increasing bread volume, and prolonged freshness of bread. OSA starches used in this experiment were modified in three different ways, where different physical and chemical properties of added modified starches caused differences in the rheological behaviour of wheat dough (Figure 1).

The addition of selected additives caused the increase in water absorption of formulation containing 0.5% HPMC (benchmark sample), 5% Pregel OSA starch and 10% OSA starch, with the exception of formulation containing 10% Hydrol OSA starch which exhibited the decrease from 56.9 and 57.5 to 52.6% in relation to control and benchmark samples. The decrease in water absorption of system containing 10% Hydrol OSA starch was due to starch hydrolysis, which caused the decrease in amylopectin molecular weight and thus lowered the ability of Hydrol OSA starch granules to absorb water [18]. On the other hand, the increase in water absorption of Pregel OSA and OSA starch containing samples could be attributed to the structure of starch granules. Namely, starch modification process influences the increase in ratio of amorphous region of starch granule in relation to its crystal counterpart which resulted in increased water absorption of Pregel OSA and OSA starch granules. Therefore, they act as damaged starch granules which are able to bind more water than intact ones.

Regarding dough development time, only sample containing 10% Hydrol OSA starch exhibited the increase in dough development time from 2.0 to 4.5 min, whilst the addition of HPMC and OSA starch did not significantly influence the time required for dough to reach the maximum consistency. Namely, due to physical modification of spray-drying and hydrolysis, Hydrol OSA starch became cold water soluble and thus it dissolved in contact with water, while during mixing the uptake of water by diluted gluten was slow. On the contrary, Pregel OSA starch was only pregelatinized and not hydrolyzed, and thus itswelled even in cold water,

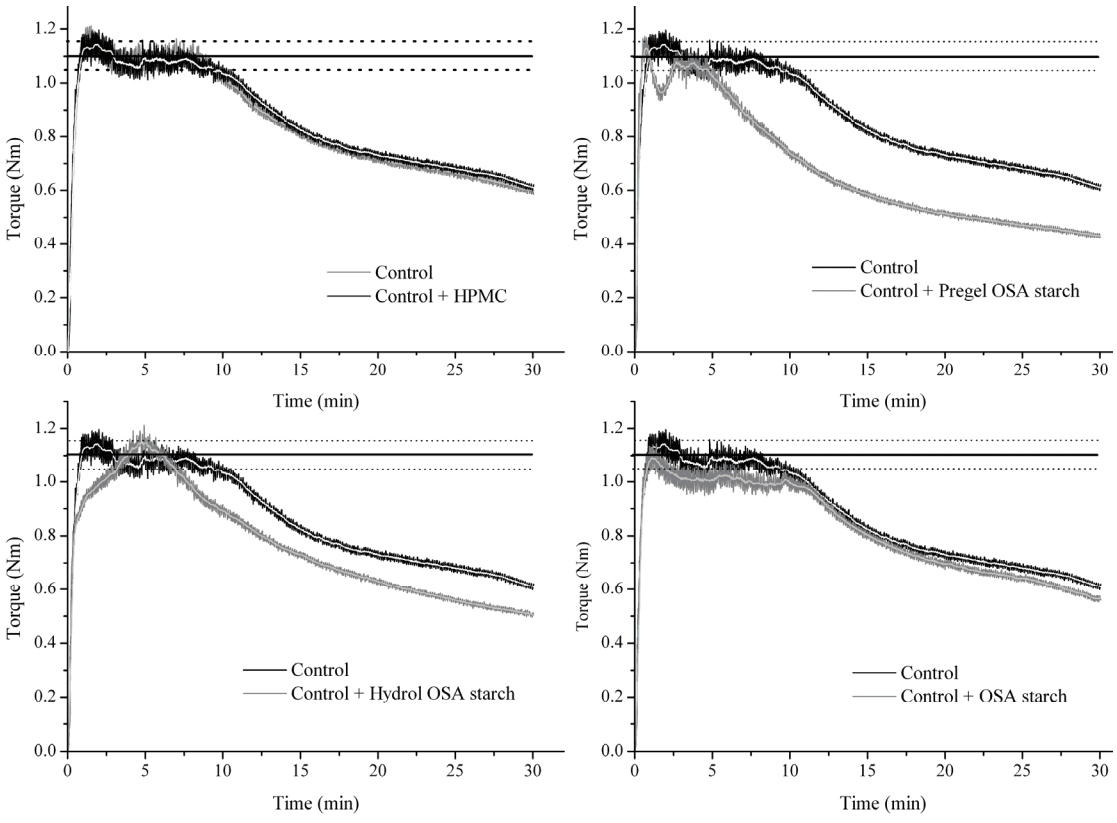

Figure 1. Dough rheological properties of wheat flour, wheat flour/HPMC as well as wheat flour/ emulsifying starch mixtures.

i.e., it had the ability to bind water. Therefore the Mixolab curve of dough supplemented with 5% of Pregel OSA starch was characterized by the presence of sharp peaks during dough development phase, which corresponded to modified starch water absorption, whilst the second peak corresponded to diluted gluten water absorption [19].

Dough stability of control and benchmark sample decreased from 9.0 and 9.5 to 2.0 min for 5% Pregel OSA starch formulation, 3.5 min for 10% Hydrol OSA starch formulation and 6.5 min for 10% OSA starch formulation, indicating that the inclusion of modified starches decreased the time during which the dough maintains maximum consistency. Moreover, softening degree was significantly influenced by the addition of 5% Pregel and 10% Hydrol OSA starches. However, the addition of 10% OSA starch did not significantly influence above mentioned parameter in comparison to control and benchmark sample. The physical properties of dough prepared with Pregel and Hydrol OSA starches could be attributed to their property of being soluble in water during dough formation phase, which increases dough extensibility, softness and stickiness [19]. Furthermore, during large mixing deformation Pregel OSA starch granules could not retain the absorbed water, which could not be taken up by diluted gluten either, and thus these systems expressed the lowest stability and the highest softening effect. On the other hand, the physical properties of dough prepared with OSA starch could be attributed to preserved crystalline structure of starch granules that act as a rigid filler contributing to the formation of starch-gluten network and thus making the stronger dough [19].

Bread quality characteristics

A white loaf of bread of good quality is characterized by having sufficient volume, an attractive appearance and evenly developed crumb that is soft enough for easy chewing and firm enough for thin slicing [20].

Specific bread volume

The volume and texture of the final baked product is dependent on the size, distribution, growth, and gas cells burst during proofing and baking [21,22]. The appearance of obtained bread loaves and bread crumb is shown in Figure 2. The obtained effect of selected additives on specific bread volume and crumb moisture is shown in Table 3. In general, the specific bread volume was significantly enhanced by addition of selected additives in comparison to the control, regardless of their type and concentration used ($P < 0.05$). The improved quality of HPMC to bread volume could be attributed to the formation of temporal HPMC network during baking, which strengthens the gas cells of the dough at the beginning of baking, improves the gas cells expansion during baking, and prevents the gas losses, thus affecting the bread volume increase [4]. On the other hand, the incorporation of OSA starches into bread formulation significantly improved specific bread volume in comparison to benchmarking bread ($P < 0.05$), with the exception of formulation with 10% Hydrol OSA starch, being at the same level as benchmark bread ($P > 0.05$).

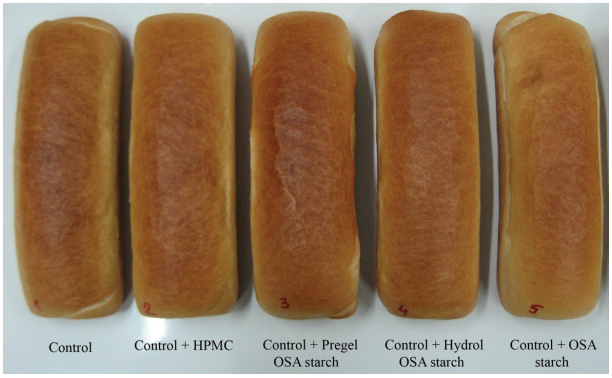

(a)

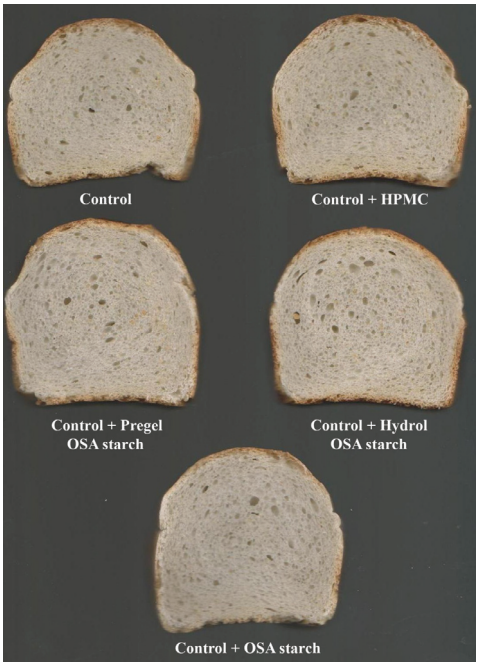

(b)

Figure 2. Appearance of a) bread loaves and b) bread crumbs made of wheat flour, wheat flour/HPMC as well as wheat flour/emulsifying starch mixtures.

The largest effect on specific bread volume was achieved by incorporation of 5% Pregel OSA starch. This phenomenon could be attributed to the nature of starch which has already been gelatinized and thus can easily develop dough structure and high bread volume [23]. The improving effect of OSA starches on the bread volume could be also attributed to the presence of hydrophobic groups affecting enhanced interfacial activity within dough during proofing, and gel network for-

Table 3. The effect of selected additives on specific loaf volume and crumb moisture; mean value ± standard deviation of three replicates; values followed by the different letter in the same column are significantly different (P < 0.05)

Sample	Specific volume, cm^3/g	Crumb moisture, %
Control	2.97±0.06[a]	41.96±0.10[a]
Control+HPMC	3.23±0.01[b]	42.48±0.01[b]
Control+Pregel OSA starch	3.50±0.03[c]	43.60±0.01[c]
Control+Hydrol OSA starch	3.20±0.01[b]	39.17±0.02[d]
Control+OSA starch	3.39±0.04[d]	43.36±0.08[e]

mation during breadmaking process [24]. Moreover, it was found that waxy starches, due to high amount of amylopectin, are more susceptible to α-amylase degradation during fermentation, where the products of enzymatic degradation such as water-soluble sugars and/or high DE value maltodextrin may improve the yeast fermentation [25–27]. Gas cells are incorporated during dough mixing and due to CO_2 release caused by yeast fermentation [22]. It was found that OSA substitution increased the air incorporation into dough as well as stabilized the air-incorporated texture that resulted in larger final cake volume [23,28].

Bread crumb moisture

Crumb water content determines the shelf life of bread, crumb softness, crumb hardening and crumbliness, influencing the overall consumer acceptance [29]. Bread crumb moisture significantly depended on the type of improver used (Table 3). After 24 h of storage, formulation with HPMC exhibited higher crumb moisture in comparison to the control bread ($P < 0.05$) due to higher water retention ability of HPMC resulting from its hydrophilic nature [4,12,17]. The significant increase in bread crumb moisture in comparison to those of control and benchmark bread was achieved by formulation with 5% Pregel OSA and 10% OSA starch, whilst incorporation of 10% Hydrol OSA starch exhibited the opposite effect, which is in agreement with the results of Mixolab water absorption (Table 3). The obtained results confirmed previous findings of Morita *et al.* [30] and Sabanis and Tzia [31] who reported that higher water absorption of flour resulted in higher crumb moisture. Hung *et al.* [32] reported that incurporation of waxy wheat starch affected the retention of moisture in breadcrumbs thus influencing the retardation of bread staling. Crumb moisture has the influence on the mechanical properties of crumb which are commonly used for monitoring of bread staling process. He and Hoseney [33] and Morita *et al.* [30] indicated that moisture content significantly affects bread firming, where higher crumb moisture affected slower firming rate and lower final firmness. However, there are certain conflicting reports which indicated that moisture content of bread crumb was not related to hardness [26].

Bread firmness

The firmness of bread crumb is an important bread feature because it directly affects the consumer preference. Firming of bread crumb is associated with bread staling which essentially means getting harder, more dry and crumbly. The changes in crumb firmness determined immediately after baking and over 48 h of storage are shown in Figure 3. The incorporation of OSA starches decreased initial crumb firmness in relation to the control sample. However, the addition of Pregel OSA starch and OSA starch yielded softer bread crumbs in comparison to that containing HPMC, whilst addition of Hydrol OSA starch did not exhibit a decrease in firmness in comparison to benchmark bread. The lower crumb firmness of all samples containing certain improver could be related to the higher crumb moisture content due to inverse relation between firmness and crumb moisture content that has been previously reported [4]. Moreover, firmness measurements are largely influenced by the volume and density of bread loaves, where the decrease in bread firmness may be attributed to an increase of total area of gas cells and consequently to decrease in the force needed to compress the sample [34,35]. Due to its emulsifying properties it is possible that added modified starches increased the strength and elasticity of gluten-starch matrix surrounding gas cells in dough, which affected the higher retention rate of CO_2 present in the gas cells, resulting in fine and homogeneous crumb texture as shown in Figure 2b [36]. Addition of emulsifying starches into wheat flour dough presumably reduced the gel forming properties of the amylose polymers, which led to weaker gel structure and, consequently, to a softer bread crumb. Regardless of the type of improver used, the firmness of all investigated crumbs increased rapidly over 48h of storage ($P < 0.05$). Firmness during storage is a result of moisture loss, moisture redistribution and starch retrogradation [37]. Firmness values of bread crumb prepared with OSA and Pregel OSA starch after 24 and 48 h of storage, remained significantly lower than those of control and benchmark bread, whilst the crumb firmness of bread prepared with Hydrol OSA was similar to that of benchmark bread. Two-way ANOVA indicated that both storage time and selected additives influenced changes in tex-

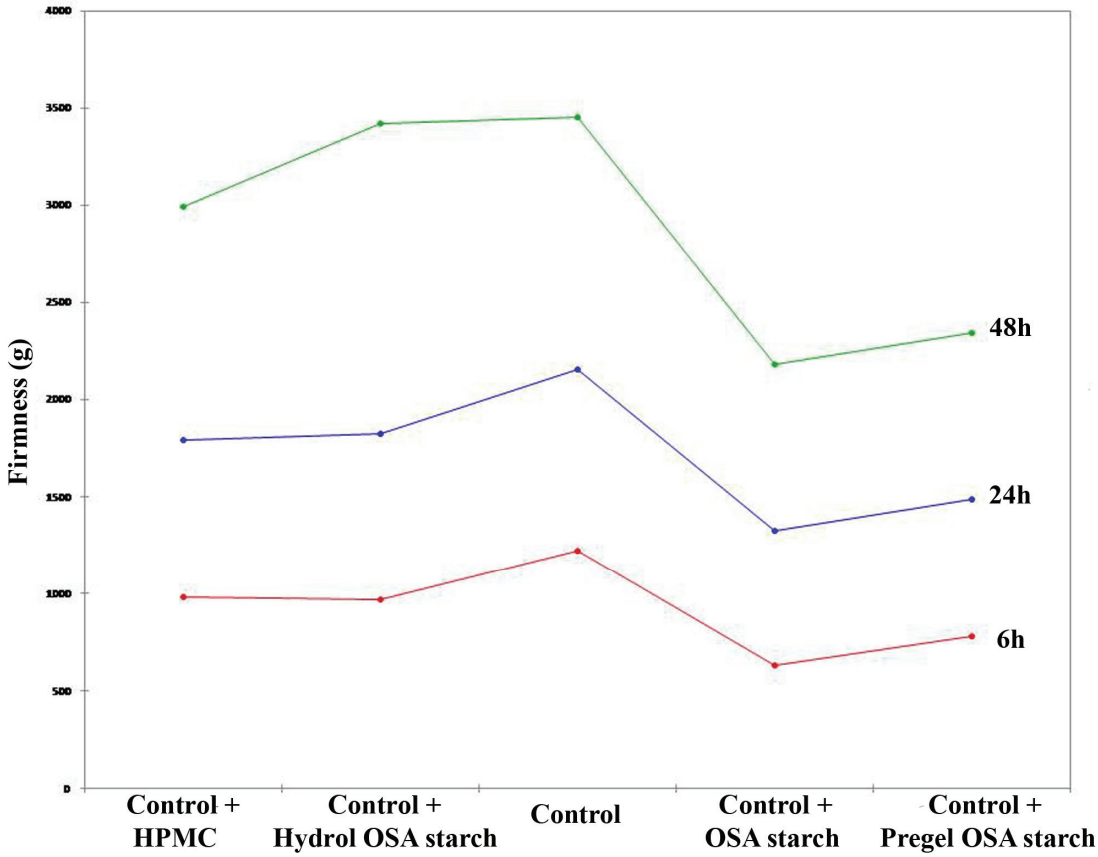

Figure 3. Influence of storage time and different additives on bread crumb firmness.

tural properties of bread crumb ($P < 0.05$) where storage time revealed dominant effect (Figure 3).

CONCLUSION

The results of this study revealed that emulsifying starches could be used as bread improvers, since their incorporation into wheat flour led to bread of similar or even improved quality in comparison to bread containing already well investigated bread improving emulsifier (HPMC). The investigated emulsifying starches (OSA starch, pregelatinized OSA starch and hydrolyzed spray-dried OSA starch) showed different impact on dough rheological properties depending on type of modification performed on starch granule structure. However, all investigated starches significantly improved bread specific volume and crumb texture, where the highest effect was observed for pregelatinized OSA starch due to its ability to incorporate and stabilize the gas cells formed during fermentation.

Acknowledgement

The authors gratefully acknowledge financial support of this work by the Ministry of Education, Science and Technological Development, Republic of Serbia, through Project TR 31007.

REFERENCES

[1] Z. Nježić, J. Živković, B. Cvetković, Possibilities of utilization of leftover bread, Chem. Ind. Chem. Eng. Q. **16** (2010) 399−403.

[2] V.A. Vaclavik, E.W. Christian, Essentials of Food Science, Springer, New York, 2008.

[3] P.V. Hung, N. Morita, Dough properties and bread quality of flours supplemented with cross-linked corn starch, Food Res. Int. **37** (2004) 461–467.

[4] M.E. Bárcenas, C.M. Rosell, Effect of HPMC addition on the microstructure, quality and aging of wheat bread, Food Hydrocolloid. **19** (2005) 1037–1043.

[5] M. Miyazaki, T. Maeda, N. Morita, Starch retrogradation and firming of bread containing hydroxypropylated, acetylated, and phosphorylated cross-linked tapioca starches for wheat flour, Cereal Chem. **82** (2005) 639––644.

[6] M. Miyazaki, P.V. Hung, T. Maeda, N. Morita, Recent advances in application of modified starches for breadmaking, Trends Food Sci. Tech. **17** (2006) 591–599.

[7] J. Singh, L. Kaurb, O.J. McCarthy, Factors influencing the physico-chemical, morphological, thermal and rheological properties of some chemically modified starches for food applications-A review, Food Hydrocolloids **21** (2007) 1–22.

[8] K.A. Abbas, S.K. Khalil, A.S.M. Hussin, Modified starches and their usages in selected food products: a review study, J. Agr. Sci. **2** (2010) 90–100.

[9] C. Caldwell, O. Wurzburg, Polysaccharide derivatives of substituted dicarboxylic acids, U.S. Patent, 2661349 (1953).

[10] R.L. Shogren, A. Viswanathan, F. Felker, R.A. Gross, Distribution of octenyl succinate groups in octenyl succinic anhydride modified waxy maize starch, Starch-Stärke **52** (2000) 196–204.

[11] R. Hui, C. Qi-He, F. Ming-Liang, X. Qiong, H. Guo-Qing, Preparation and properties of octenyl succinic anhydride modified potato starch, Food Chem. **114** (2009) 81––86.

[12] A. Guarda, C.M. Rosell, C. Benedito, M.J. Galotto, Different hydrocolloids as bread improvers and antistaling agents, Food Hydrocolloid. **18** (2004) 241–247.

[13] Mixolab applications handbook: Rheological and Enzymatic Analysis (2006).

[14] T. Dapčević Hadnađev, M. Pojić, M. Hadnađev, A. Torbica, The role of empirical rheology in flour quality control, in: I. Akyar (Ed.), Wide Spectra of Quality Control, InTech, Rijeka, 2011, pp. 335–360.

[15] ICC Standards (1996), Standard methods of the international association for cereal science and technology, International Association for Cereal Science and Technology, Vienna, ICC Standard No. 110/1.

[16] AACC International (2000), Approved Methods of Analysis, American Association of Cereal Chemists, St. Paul, MO, Method 74-09.

[17] Z. Kohajdová, J. Karovičová, Application of hydrocolloids as baking improvers, Chem. Pap. **63** (2009) 26–38.

[18] M. Miyazaki, T. Maeda N. Morita, Effect of various dextrin substitutions for wheat flour on dough properties and bread qualities, Food Res. Int. **37** (2004) 59–65.

[19] T.R. Dapčević Hadnađev, Lj.P. Dokić, M.S. Hadnađev, M.M. Pojić, A.M. Torbica, Rheological and breadmaking properties of wheat flours supplemented with octenyl succinic anhydride-modified waxy maize starches, Food Bioprocess Technol., DOI 10.1007/s11947-013-1083-y.

[20] N.L. Kent, A.D. Evers, Technology of Cereals, Elsevier Science Ltd., Oxford,1994.

[21] S.P. Cauvain, Breadmaking: Improving Quality, Woodhead, Cambridge, 2003.

[22] C.M. Rosell, The science of doughs and bread quality, in: V.R. Preedy, R.R. Watson, V.B. Patel (Eds.), Flour and Breads and their Fortification in Health and Disease Prevention, Elsevier, London, 2011, pp. 3–14.

[23] N. Seyhun, G. Sumnu, S. Sahin, Effects of different starch types on retardation of staling of microwave-baked cakes, Food Bioprod. Process. **83** (2005) 1–5.

[24] A. Lazaridou, D. Duta, M. Papageorgiou, N. Belc, C.G. Biliaderis, Effects of hydrocolloids on dough rheology and bread quality parameters in gluten-free formulations, J. Food Eng. **79** (2007) 1033–1047.

[25] M.R. Lee, B.G. Swanson, B.K. Baik, Influence of amylose content on properties of wheat starch and breadmaking quality of starch and gluten blends, Cereal Chem. **78** (2001) 701–706.

[26] Y. Hibi, Effect of retrograded waxy corn starch on bread staling, Starch-Stärke **53** (2001) 227–234.

[27] M. Witczak, J. Korus, R. Ziobro, L. Juszczak, The effects of maltodextrins on gluten-free dough and quality of bread, J. Food Eng. **96** (2010) 258–265.

[28] H.Y.L. Kim, H.W. Yeom, H.S. Lim, S.T. Lim, Replacement of shortening in yellow layer cakes by corn dextrins, Cereal Chem. **78** (2001) 267–271.

[29] J.P. Smith, D.P. Daifas, W. El-Khoury, Crc. Cr. Rev. Food. Sci. **44** (2004) 19–55.

[30] N. Morita, T. Maeda, M. Miyazaki, M. Yamamori, H. Miura, I. Ohtsuka, Effect of Substitution of Waxy-Wheat Flour for Common Flour on Dough and Baking Properties, Food Sci. Technol. Res. **8** (2002) 119–124.

[31] D. Sabanis, C. Tzia, Effect of hydrocolloids on selected properties of gluten-free dough and bread, Food Sci. Technol. Int. **17** (2011) 279–291.

[32] P.V. Hung, T. Maeda, N. Morita, Waxy and high-amylose wheat starches and flours-characteristics, functionality and application, Trends Food Sci. Tech. **17** (2006) 448––456.

[33] H. He, R.C. Hoseney, Changes in bread firmness and moisture during long term storage, Cereal Chem. **67** (1990) 603–608.

[34] H. Goesaert, P. Leman, J.A. Delcour, Model approach to starch functionality in bread making, J. Agr. Food Chem. **56** (2008) 6423–6431.

[35] A. Skendi, C.G. Biliaderis, M. Papageorgiou, M.S. Izydorczyk, Effects of two barley β-glucan isolates on wheat flour dough and bread properties, Food Chem. **119** (2010) 1159–1167.

[36] K. Autio, M. Salmenkallio-Marttila, Understanding microstructural changes in biopolymers using light and electron microscopy, in: G. Kaletunç, K.J. Breslauer (Eds.), Characterization of Cereals and Flours: Properties, Analysis, and Applications, Marcel Dekker, Inc., New York, 2003.

[37] C.G. Biliaderis, M.S. Izydorczyk, O. Rattan, Effect of arabinoxylans on breadmaking quality of wheat flours, Food Chem. **53** (1995) 165–171.

IZVOD

REOLOŠKA SVOJSTVA TESTA I KVALITET HLEBA PROIZVEDENIH SA DODATKOM EMULGUJUĆIH POLISAHARIDA

Tamara Dapčević Hadnađev[1], Ljubica Dokić[2], Milica Pojić[1], Miroslav Hadnađev[1], Aleksandra Torbica[1], Slađana Rakita[1]

[1]*Univerzitet u Novom Sadu, Naučni institut za prehrambene tehnologije, Novi Sad, Srbija*
[2]*Univerzitet u Novom Sadu, Tehnološki fakultet, Novi Sad, Srbija*

(Naučni rad)

Cilj ovoga rada je bio ispitivanje uticaja emulgujućih skrobova kao nove vrste aditiva u pekarstvu. U skladu sa tim, deo pšeničnog brašna je zamenjivan sa tri vrste emulgujućih skrobova (5-10%): skrob-natrijum-oktenilsukcinat (OSA starch), preželatinizirani skrob-natrijum-oktenilsukcinat (Pregel OSA starch) i hidrolizovani skrob-natrijum-oktenilsukcinat (Hydrol OSA starch). Reološka svojstva testa i kvalitet hleba dobijeni sa dodatkom emulgujućih skrobova su upoređena sa kontrolnim testom, odnosno hlebom proizvedenim bez dodataka, kao i sa testom odnosno hlebom proizvedenim sa dodatkom hidroksipropil-metilceluloze (0,5%) (HPMC), koja je u pekarstvu već dobro poznat aditiv. Dobijeni rezultati su pokazali da je dodatak preželatiniziranog skrob-natrijum-oktenilsukcinata (Pregel OSA *starch*) i skroba-natrijum-oktenilsukcinata (OSA *starch*) uticao na povećanje moći upijanja vode, dok je dodatak hidrolizovanog skrob-natrijum-oktenilsukcinata (Hydrol OSA *starch*) imao suprotan efekat. Međutim, pozitivan efekat upotrebe emulgujućih skrobova se ogleda u kvalitetnim karakteristikama krajnjeg proizvoda – hleba, i to povećanju specifične zapremine i poboljšanju teksturnih svojstava hleba, pri čemu je najveći uticaj pokazao dodatak preželatiniziranog skrob-natrijum-oktenilsukcinata (Pregel OSA *starch*) i skroba-natrijum-oktenilsukcinata (OSA *starch*).

Ključne reči: Hleb • Emulgujući skrobovi • HPMC • Miksolab simulator

Photostability of piroxicam in the inclusion complex with 2-hydroxypropyl-β-cyclodextrin

Vesna D. Nikolić[1], Snežana S. Ilić-Stojanović[1], Ljubiša B. Nikolić[1], Milorad D. Cakić[1], Aleksandar S. Zdravković[2], Agneš J. Kapor[3], Mirjana M. Popsavin[4]

[1]*University of Niš, Faculty of Technology, Leskovac, Serbia*
[2]*Vocational Hight School for Textiles, Leskovac, Serbia*
[3]*University of Novi Sad, Faculty of Sciences, Department of Physics, Novi Sad, Serbia*
[4]*University of Novi Sad, Faculty of Sciences, Department of Chemistry, Novi Sad, Serbia*

Abstract

The aim of this work is the protection of piroxicam from photodegradation by forming inclusion complex with 2-hydroxypropyl-β-cyclodextrin. Piroxicam:2-hydroxypropyl-β-cyclodextrin molecular inclusion complex was prepared by coprecipitation method with 1:1 molar ratio. Structural characterization of the complex, the corresponding physical mixture and complexing agents of piroxicam and 2-hydroxypropyl-β-cyclodextrin was carried out by X-ray diffraction (XRD), proton nuclear magnetic resonance (^{1}H-NMR) and Fourier transform infrared spectroscopy (FTIR). Photosensitivity to daylight of piroxicam and piroxicam:2-hydroxypropyl-β-cyclodextrin inclusion complex was investigated by FTIR. The investigations show that higher photostability of piroxicam was achieved in the complex than in non-complexed piroxicam.

Keywords: inclusion complex, piroxicam, 2-hydroxypropyl-β-cyclodextrin, photodegradation.

Available online at the Journal website: http://www.ache.org.rs/HI/

SCIENTIFIC PAPER

UDC 543.42:615:547.458.68

Hem. Ind. **68** (1) 107–116 (2014)

doi: 10.2298/HEMIND130306034N

Piroxicam (4-hydroxy-2-methyl-*N*-pyrido-2-yl-2*H*--1,2-benzothiazine-3-carboxamide-1,1-dioxide) is the first representative of the class of non-steroidal anti--inflammatory drugs of the oxicam group with analgesic, antipyretic and anti-inflammatory effects.

Piroxicam shows polymorphism and can exist in several conformations [1] and prototrophic shapes [2]. Different conformations are proposed for piroxicam in the basic state, in accordance with the ability of forming intramolecular hydrogen bonds between the enol hydroxyl group and amide carbonyl oxygen [3]. Due to zwitterion formation it is found that neutral form is its basic state. It is difficult to isolate this behavior spectroscopically, so neutral and zwitterionic forms together are called "globally neutral" [4]. Excited state intramolecular proton transfer (ESIPT) of piroxicam is very sensitive to solvent polarity [5]. Acid-base balance leads to the existence of different prototrophic forms of piroxicam, investigated during the complexation with cyclodextrins [6]. Similar spectroscopic behavior has been found between piroxicam and one of its precursors, *i.e.*, 4-hydroxy-2-methyl-1,2-l-benzothiazine--1,1-dioxide-3-methylcarboxilate, where pyridine ring and amide groups are absent [7].

Correspondence: V. Nikolić, University of Niš, Faculty of Technology, Bulevar oslobođenja 124, 16000 Leskovac, Serbia.
E-mail: nikolicvesna@tf.ni.ac.rs
Paper received: 06 March, 2013
Paper accepted: 08 May, 2013

Despite large pharmacological and therapeutic potential, piroxicam is hydrophobic and has low solubility in aqueous media, which limits its application. The tests showed enhanced release of piroxicam from granules with β-cyclodextrin [8]. Inclusion complexes of piroxicam and β-cyclodextrin can be obtained by various methods, such as physical mixing, coprecipitation, evaporation and heating under reflux [9,10]. Inclusion complex of piroxicam with 2-hydroxypropyl-β-cyclodextrin has a significantly improved solubility [11].

Piroxicam can cause skin sensitivity to sunlight and therefore is subject to photochemical tests [12–15]. The investigations of photostability of drugs and medicinal formulations are very important. Drug photodecomposition may result in loss of efficiency and development of product side effects due to the formation of photodegradation products during storage or use. Photostability depends on the light wavelength, intensity and time of exposure. Clinical tests have shown that irradiation of piroxicam produces ampiroxicam as a photodegradation product, which cannot be created by biotransformation of piroxicam [16]. Glass *et al.* have investigated the structure of the resulting photodegradation products and photostability of piroxicam and other drugs [17].

Cyclodextrins and their derivatives are specific drug carriers, because of their ability to alter the physical, chemical and biological properties of the molecules included in their cavities. They have a three-dimensional structure with OH groups on the outside and

inside are hydrogen atoms. In an aqueous solution nonpolar aliphatic and aromatic molecules of appropriate size may enter the hydrophobic cavities of cyclodextrins [18]. As complexing agents they are capable of enhancing solubility, photostability, volatility and bioavailability of various drugs, *e.g*., nifedipine [19], amlodipin besylate [20], atenolol [21] or allicin [22]. Because of better solubility at room temperature than β-cyclodextrin, in this study, 2-hydroxypropyl-β-cyclodextrin was chosen (Figure 1).

The aim of this work is to prepare a molecular inclusion complex of piroxicam:2-hydroxypropyl-β-cyclodextrin, to enhance the photostability of piroxicam within the complex. The results obtained for the inclusion complex by nuclear magnetic resonance (^{1}H-NMR), X-ray diffraction (XRD) and Fourier transform infrared spectrometry (FTIR) were compared with those of physical mixture of piroxicam and 2-hydroxypropyl-β-cyclodextrin.

EXPERIMENTAL

Materials and methods

Piroxicam was acquired from Megafine Pharma Ltd. (99.67% purity), while 2-hydroxypropyl-β-cyclodextrin. (97%) was supplied by Merck, Darmstadt. Other solvents and reagents used were p.a. purity.

Preparation of inclusion complex by co-precipitation

Piroxicam (1 mmol, 331.348 mg) and 2-hydroxypropyl-β-cyclodextrin (1 mmol, 1540 mg) were mixed and dissolved in 150 cm^3 of water. The solution was mixed at room temperature for 72 h. Due to poor solubility, the prepared solution was then subjected to ultrasound. The ultrasound device Sonic, Nis (YU) was used and a ultrasonic bath with dimensions *A*:*B*:*H* = 300 mm×151 mm×200 mm, 8 dm^3 volume, under the following conditions: temperature 30 °C, ultrasound wave frequency 40 kHz and power of 150 W, the total nominal power of 3×50 W and exposure time was 1 h. After treatment by ultrasound, this solution was evaporated in a vacuum evaporator at 50 °C, protected from the light, to volume of approximately 20 cm^3, and then dried in a desiccator above concentrated sulfuric acid at 25 °C. After drying, a yellow crystalline complex was obtained and used for further investigations.

Preparation of physical mixture

Physical mixtures were prepared by simple mixing of piroxicam with complex agents 2-hydroypropyl-β--cyclodextrin in 1:1 molar ratio.

Infrared Fourier transformation (FTIR)

FTIR spectra of samples were recorded in KBr tablet (0.2 mg of sample, 140 mg of KBr), wavelength range from 4000 to 400 cm^{-1} on the FTIR spectrophotometer of Bomem Hartmann & Braun MB-series.

X-Ray crystallography

X-Ray diffraction was performed on a Phillips PW 1030 powder diffractometer by exposing the samples to monochrome CuKα radiation, λ = 1.54178 Å and

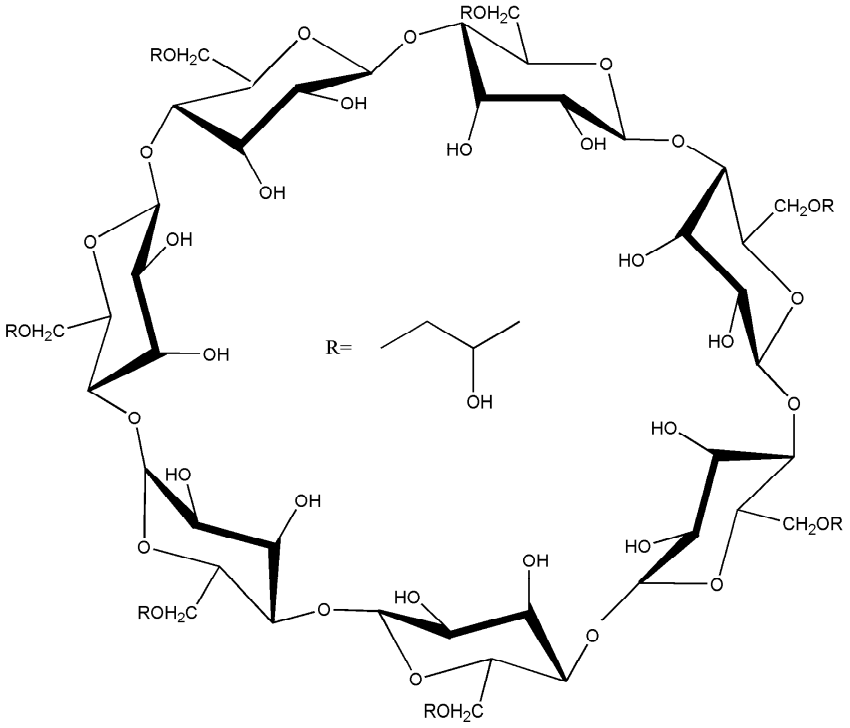

Figure 1. Structural formula of 2-hydroxypropyl-β-cyclodextrin.

analyzed for 2θ (5–45°) with 0.05° increments and recording time, τ = 5 s. The voltage and the strength of the electric current were 40 kV and 20 mA, respectively.

^{1}H-NMR Spectrometry

^{1}H NMR Spectra of the samples of inclusion complex piroxicam:2-hydroxypropyl-β-cyclodextrin, 2-hydroxypropyl-β-cyclodextrin and piroxicam were made on a Bruker AC 250 E NMR spectrometer with operating frequencies of 250 MHz, in a 5 mm diametar glass cuvette at room temperature. D_2O was used as the solvent.

RESULTS AND DISCUSSION

Structural characterization of the obtained molecular inclusion complex piroxicam:2-hydroxypropyl-β-cyclodextrin was performed by the methods: X-ray diffraction (XRD), proton nuclear magnetic resonance (^{1}H-NMR) and Fourier transform infrared spectroscopy (FTIR).

In Figure 2 given are the diffraction patterns of piroxicam, 2-hydroxypropyl-β-cyclodextrin, physical mixture and piroxicam:2-hydroxypropyl-β-cyclodextrin molecular inclusion complex.

High similarity between the diffraction pattern of the complex and the diffraction pattern of the complexing agent 2-hydroxypropyl-β-cyclodextrin is observed in Figure 2. Broad peaks at 11.6 and 18–19° in diffractogram of 2-hydroxypropyl-β-cyclodextrin, which are not structured, indicate an amorphous structure, which is partially retained in the piroxicam:2-hydroxypropyl-β-cyclodextrin complex. Piroxicam diffraction patterns (Figure 2c) have a number of sharp peaks at 8.6, 11.8, 14.4, 17.6, 21.6, 25.9 and 27.3° with clearly defined reflections, characteristic of an arranged crystal structure. Peaks of piroxicam are present in the diffractogram of physical mixtures (Figure 2a), while in the diffractogram of the complex (Figure 2b) there are none, probably due to the fact that they are protected in the cavity of 2-hydroxypropyl-β-cyclodextrin. The results of this analysis are consistent with published data [11].

In order to prove the formation of piroxicam:2-hydroxypropyl-β-cyclodextrin inclusion complex ^{1}H-NMR analysis was used and the results of these studies are presented in Table 1, and the markings of C-atoms containing protons of glucopyranose units (A) and piroxicam (B) are given in Figure 3.

^{1}H-NMR spectrum of the piroxicam:2-hydroxypropyl-β-cyclodextrin complex (Table 1), does not give signals in the region of chemical shift δ 7.11 to 8.89 ppm, usually assigned to pyridine and benzene ring of piroxicam. On the other hand, present are all typical signals of proton from 2-hydroxypropyl-β-cyclodextrin. Triplet assigning H_3 protons at δ 3.966 and 3.875 ppm assigning H_6 protons of 2-hydroxypropyl-β-cyclodextrin in the complex are shifted towards smaller values of δ units by –0.017 and –0.025, respectively. Small shifts in

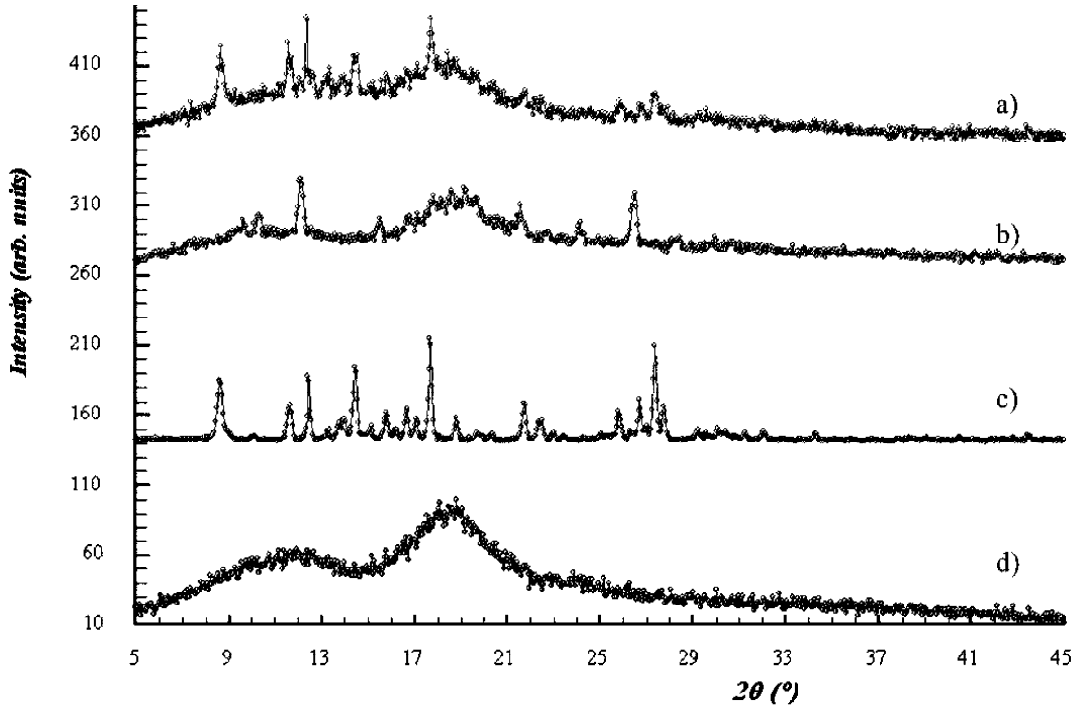

Figure 2. XRD Diffractograms of physical mixture of 2-hydroxypropyl-β-cyclodextrin and piroxicam (a); piroxicam:2-hydroxypropyl-β-cyclodextrin inclusion complex (b); piroxicam (c); 2-hydroxypropyl-β-cyclodextrin (d).

Table 1. Chemical shifts (δ) and variations in chemical shifts ($\Delta\delta$) of protons in ^{1}H-NMR spectra of piroxicam, 2-hydroxypropyl-β-cyclodextrin and piroxicam:2-hydroxypropyl-β-cyclodextrin complex

C-atom	δ/ ppm (piroxicam)	C-atom	δ/ ppm		$\Delta\delta$/ ppm
			HP-β-CD	Complex	
3'	7.22–8.11 (*m*, 1H)	1	5.083 (*d*, 1H)	5.083 (*d*, 1H)	–
4'	8.33–8.89 (*m*, 1H)	2	3.633 (*t*, 1H)	3.633 (*t*, 1H)	–
5	7.22–8.11 (*m*, 1H)	3	3.966 (*t*, 1H)	3.959 (*t*, 1H)	–0.017
5'	7.11 (*t*, 1H)	4	3.45–3.53 (*m*, 1H)	3.45–3.53 (*m*, 1H)	–
6	7.22–8.11 (*m*, 1H)	5	–	–	–
6'	8.33–8.89 (*m*, 1H)	6	3.875 (*s*, 2H)	3.85 (*s*, 2H)	–0.025
7	7.22–8.11 (*m*, 1H)	7	–	–	–
8	8.18–8.25 (*m*, 1H)	8	–	–	–
9	3.00 (*s*, 3H)	9	1.15 (*d*, 3H)	1.15 (*d*, 3H)	–

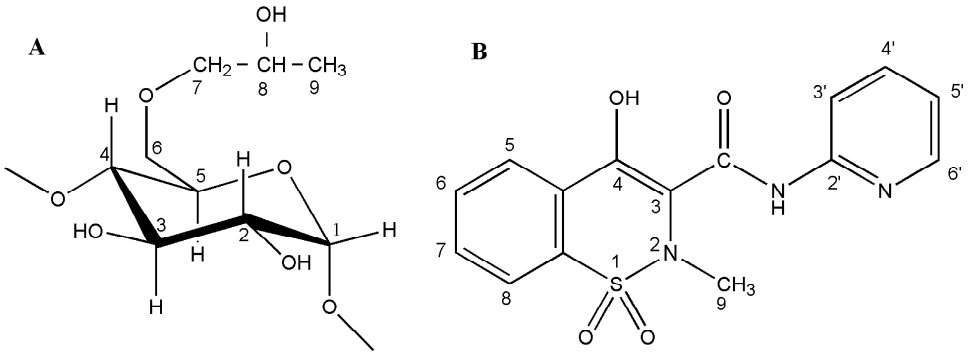

Figure 3. Numeration of C-atoms in the glucopyranose unit of 2-hydroxypropyl-β-cyclodextrin (A) and piroxicam (B).

the spectra of the complexes indicate that the H_3 and H_6 protons are involved in a noncovalent interaction with the guest molecule, piroxicam, *i.e.*, that there was an inclusion in the cavity of 2-hydroxypropyl-β-cyclodextrin.

The FTIR spectra of piroxicam (A), 2-hydroxypropyl-β-cyclodextrin (B), physical mixture (C) and piroxicam:2-hydroxypropyl-β-cyclodextrin complex (D) are shown in Figure 4.

In the FTIR spectrum of piroxicam (Figure 4A) a sharp medium intensity band with a maximum at 3338 cm^{-1} is the result of valence vibrations of OH groups, ν(OH), and a low intensity band with a maximum absorbance at 3393 cm^{-1} corresponds to the valence vibration of NH group, secondary amide, ν(NH) [8,23]. Absorption bands from the conjugated benzene ring and pyridine are located in the range from 1650-1550 cm^{-1} [11]. In the FTIR spectrum of piroxicam (Figure 4A) there are bands at 1574 and 1435 cm^{-1} originating from valence vibrations ν(C=C) of benzene and pyridine. Medium intensity absorption band at 1630 cm^{-1} is the result of valence vibrations ν(C=O) of the secondary amides, and the high intensity band at 1530 cm^{-1} is the result of deformation vibrations of NH group, δ(NH). The presence of SO_2 group in piroxicam is confirmed by bands at 1351 and 1181 cm^{-1} originating from the asymmetric and symmetric valence vibrations, respectively. The area from 660–900 cm^{-1} is characteristic of deformation vibrations in the plane δ(C-H) of aromatic structures, which exist in the spectrum of piroxicam, and occur at 875, 830 and 775 cm^{-1}.

The FTIR spectrum of 2-hydroxypropyl-β-cyclodextrin (Figure 4B) is characterized by an intensive broad band at 3431 cm^{-1}, which is the result of OH group valence vibrations, ν(OH). In the range of 2970–2930 cm^{-1} expected are the bands from C–H valence vibrations that exist in the spectrum, occurring at 2927 cm^{-1}. Asymmetric and symmetric C–H deformation vibrations in the plane give bands at 1458 and 1374 cm^{-1}, respectively. The complex band (Figure 4B) in the range from 1200–1000 cm^{-1} with maxima at 1155, 1083 and 1036 cm^{-1} is defined as coupled vibration of C–O, C–O–C, C–C–O and C–C–C asymmetric valence vibrations. In the range from 700–1000 cm^{-1} appear bands of valence and deformation vibrations of glukopyranose units. The presence of glucopyranose units of 2-hydroxypropyl-β--cyclodextrin in C1 chair conformation is confirmed by bands at 950 and 855 cm^{-1}, which are present in the spectrum (Figure 4B).

Comparative analysis of the FTIR spectra of piroxicam and 2-hydroxypropyl-β-cyclodextrin and the spectrum of physical mixtures (Figure 4C) shows the

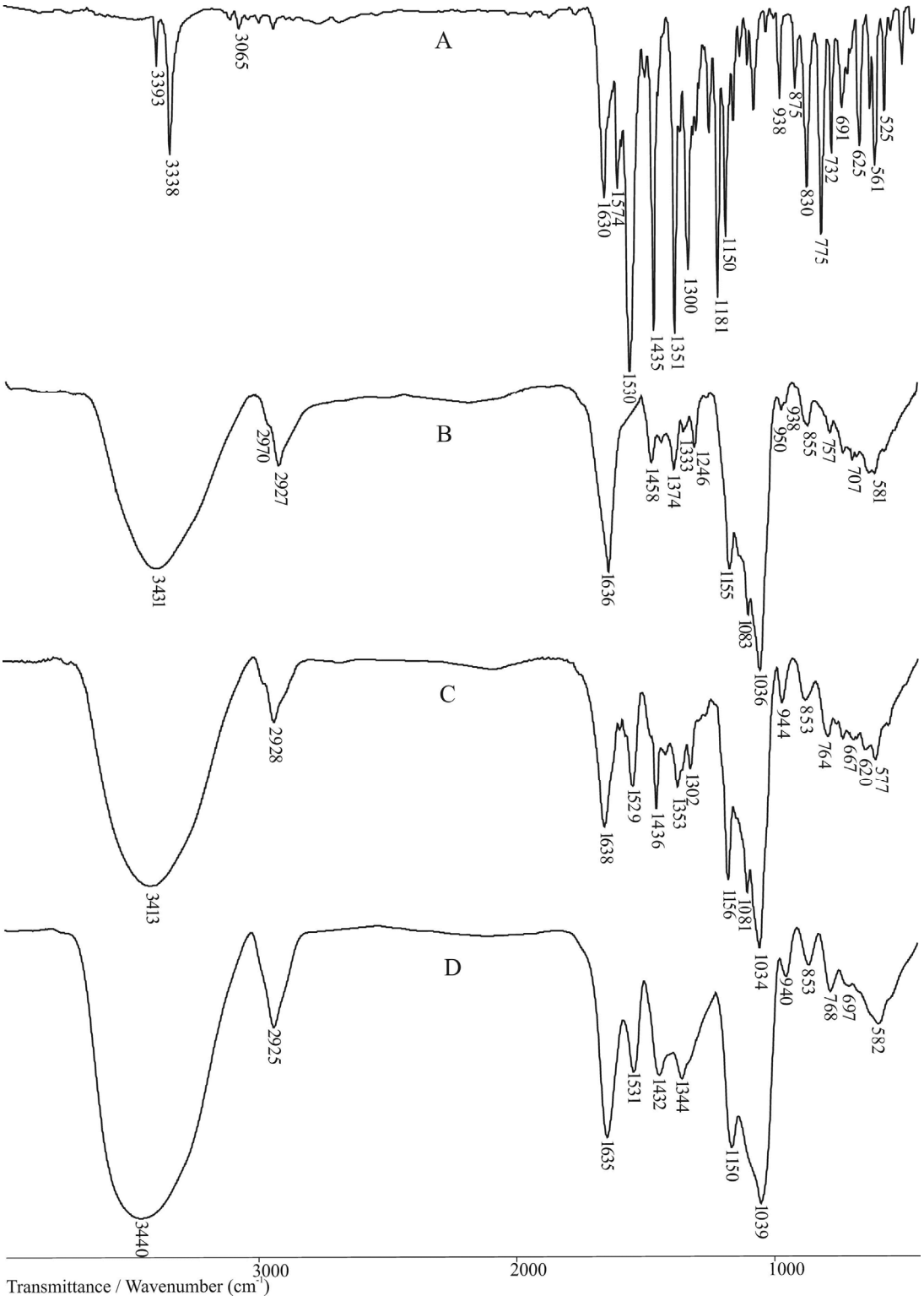

Figure 4. FTIR spectra of piroxicam (A), 2-hydroxypropyl-β-cyclodextrin (B), physical mixture of piroxicam and 2-hydroxypropyl-β-cyclodextrin (C) and piroxicam:2-hydroxypropyl-β-cyclodextrin inclusion complex (D).

presence of both components, as expected since there was no interaction in the mixture.

FTIR spectrum of piroxicam:2-hydroxypropyl-β-cyclodextrin complex (Figure 4D) was modified in relation to the spectra of piroxicam and 2-hydroxypropyl-β-cyclodextrin. In the complex spectrum, intensive band in the range of OH group valence vibrations, which occurs at 3431 cm^{-1} in 2-hydroxypropyl-β-cyclodextrin is shifted by 9 units toward the higher values of wavelength and occurs at 3440 cm^{-1}. In the same range for

the complex there are no bands present at 3338 and 3393 cm^{-1}, which are characteristic of the ν(OH) and ν(NH) of piroxicam. Also, there are no bands in the complex indicative of ν(C=C) from the aromatic structures and bands ν(C=O) from the secondary amide groups present in piroxicam. CH valence vibrations, which occur at 2927 cm^{-1} in the spectrum of 2-hydroxypropyl-β-cyclodextrin are shifted towards lower values of wavelength in the spectrum of the complex and appear at 2925 cm^{-1}. These shifts may indicate the interaction of these groups from 2-hydroxypropyl-β--cyclodextrin with the corresponding groups from piroxicam. A band of C–O valence vibrations from 2-hydroxypropyl-β-cyclodextrin at 1155 cm^{-1} in the complex is shifted to 1150 cm^{-1}, which also supports the hypothesis of piroxicam inclusion in the cavities of the host. C1 conformation of glucopyranose unit of host molecules in the complex is not affected because there are bands present at 940 and 853 cm^{-1} which are also present in the spectrum of 2-hydroxypropyl-β-cyclodextrin.

These studies are consistent with the results of XRD and ^{1}H-NMR analyses and indicate a molecular encapsulation of piroxicam.

Piroxicam is a photosensitive molecule and under the influence of light it can degrade whereby the pharmacological activity and safety of its use are reduced, and on the other hand, the adverse effect of the products formed is increased. There are data in the literature on photostability and possible degradation products of piroxicam [11,17]. Kochevar *et al.* examined the sensitivity of patients to piroxicam photodegra-

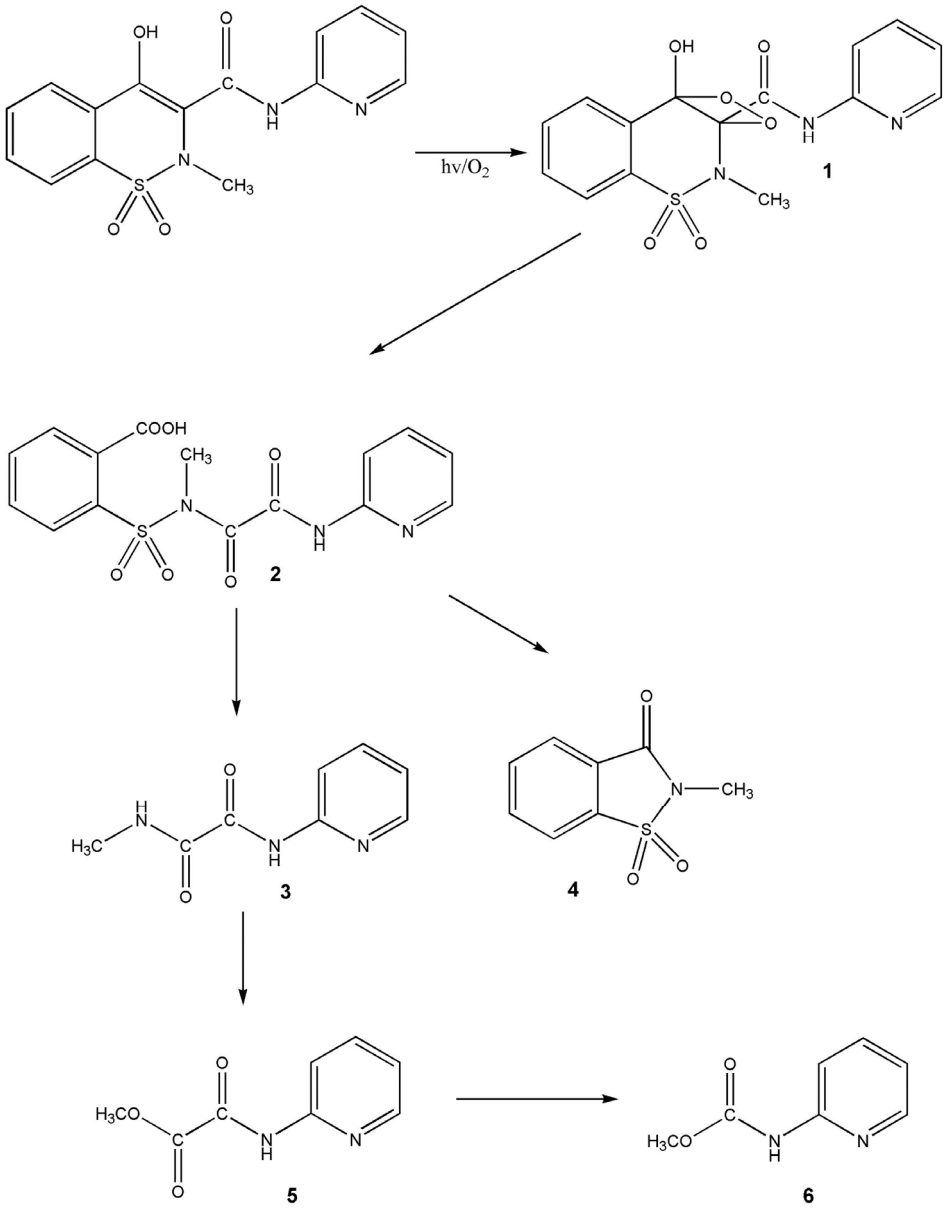

Figure 5. Photodegradation products of piroxicam.

dation products [11], also Glass *et al.* studied photodegradation products (Figure 5) [17].

In the process of oxidation the first derivative of piroxicam produced is dioxiethane (**1**), which is converted to carboxylic acid through the ring cleavage (**2**). In transacylation reaction 2-methyl-1,2-benzisothiazol-3(2*H*)-one-1,1-dioxide (**4**) and *N*-(2-pyridyl)-methoxyformylamides (**5**) are formed. By subsequent carbonylation of the products (**5**) *N*-(2-pyridyl)-methoxyamide (**6**) are produced. The compound *N*-methyl-*N'*-(2-pyridyl)-ethane-diamide (**3**), is obtained by splitting the bond between nitrogen and sulfur in the structure (**2**). According to the research literature [17], among the resulting photodegradation products the main product is 2-methyl-1,2-benziso-thiazol-3(2*H*)-one-1,1-dioxide (**4**).

Stability of piroxicam exposed to daylight was monitored by changes in FTIR spectra for 30 days in our investigations. FTIR spectra of piroxicam not exposed to light (A) and continuously exposed to daylight for 5 days (B) are shown in Figure 6.

In the spectrum of piroxicam which has been exposed to daylight for 5 days (Figure 6B) changes in the position and intensity of the individual bands can be observed in relation to initial piroxicam (Figure 6A). OH group (3338 cm^{-1}) and NH group (3393 cm^{-1}) valence vibration bands in the FTIR spectrum of piroxicam which has been exposed to daylight for 5 days have a significantly lower intensity and appear in the domain of noise. This indicates a change in the structure of piroxicam. Also, in the spectrum of piroxicam which has been continuously exposed to daylight for 5 days (Figure 6B) there is a loss of band at 688 cm^{-1} and a decrease of the band intensity at 734 cm^{-1}, resulting from C–H deformation vibrations outside the plane of the aromatic rings. This may indicate a degradation of the pyridine ring. On the other hand, bands at 1353 and 1182 cm^{-1} indicate the presence of SO_2 group in the piroxicam subjected to photodegradation. In the degradation product the benzene ring was retained as indicated by the bands at 1576 and 1436 cm^{-1} from ν(C=C). The appearance of a new medium intensity band at 1600 cm^{-1} (Figure 6B) may be assigned to a cyclic amide which, depending on the size of the ring, can be expected around 1700 cm^{-1}. Shifting of this band towards lower wavelengths can be associated with the presence of SO_2 group in the cyclic amide ring. Based on the above analysis of FTIR spectra and the degradation products structure shown [17] it is considered that 2-methyl-1,2-benzisothiazol-3(2*H*)-one--1,1-dioxide (**4**) had most likely been formed as a degradation product which, according to the literature [17], is the most common (60%).

For determination of piroxicam photostability in the complex, FTIR spectroscopy was also applied. In Figure

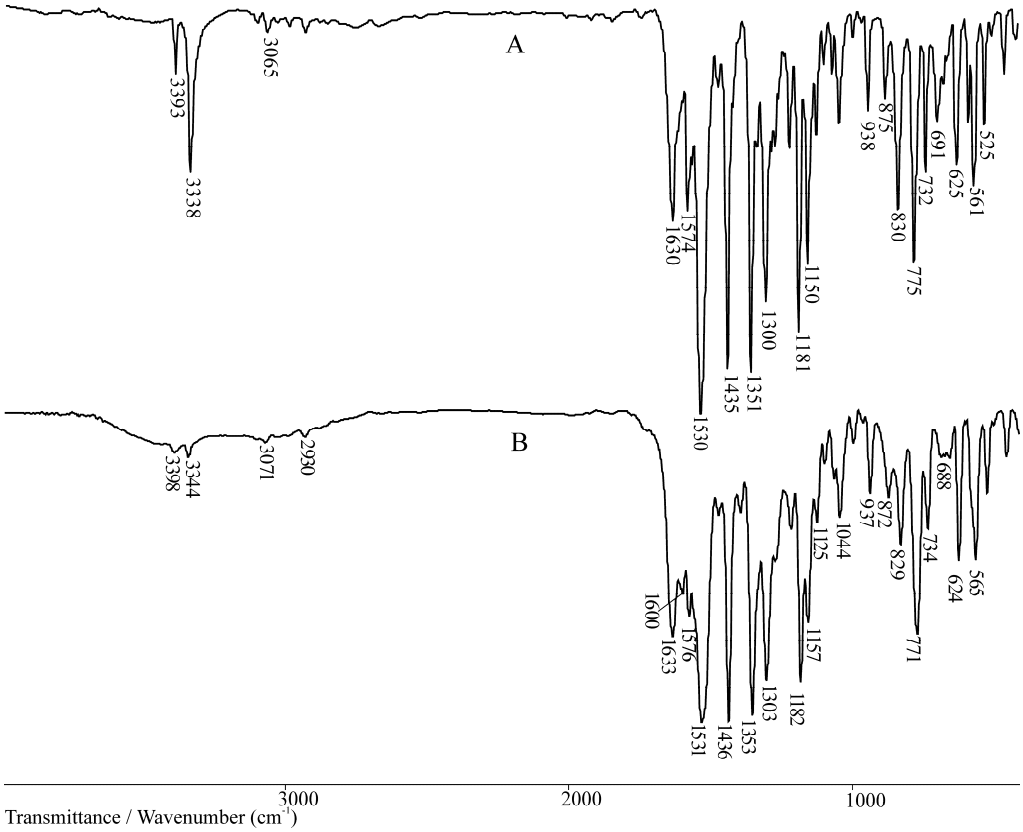

Figure 6. FTIR spectrum of piroxicam, which has not been exposed (A) and which has been exposed to daylight for 5 days (B).

7, A and B are shown the FTIR spectra of piroxicam:2-hydroxypropyl-β-cyclodextrin complexes exposed and not exposed to daylight for more than 30 days, respectively.

Based on the above FTIR spectra (Figure 7A and B) it can be noted that piroxicam in the complex is stable under the influence of daylight up to 30 days. After this period of time the complex begins to decompose as evidenced by the change of position, intensity and number of bands in its FTIR spectrum (Figure 7B). In this spectrum the bands at 1351 and 1081 cm^{-1} occur as a result of SO_2 group valence vibrations, which are not present in the initial complex (Figure 7A). The band at 1344 cm^{-1} (Figure 7A) is not present in a complex that has been exposed to daylight for more than 30 days, but there appeared a band at 1302 cm^{-1}. There is also a band shift from ν(OH) vibrations of the initial complex by 26 units toward smaller wavelengths. Band occured at 3414 cm^{-1} in the spectrum of the complex that has been exposed to daylight, which may indicate a change in noncovalent interactions within the inclusion complex, *i.e*., its decomposition.

The results of this analysis show that the photostability of piroxicam in the piroxicam:2-hydroxypropyl-β-cyclodextrin inclusion complex is increased compared to that of the uncomplexed piroxicam during one month of exposure. Therefore, this formulation protects piroxicam from photodegradation and increases the safety of its application.

CONCLUSIONS

Molecular inclusion complex of piroxicam with 2-hydroxypropyl-β-cyclodextrin as complexing agent was prepared by coprecipitation method in solid state. Complex diffractograms show that the inclusion of piroxicam in the cavities of 2-hydroxypropyl-β-cyclodextrin retains the amorphous structure of the complexing agent with the characteristic low intensity peaks at 11.6 and 18–19°. Diffraction peaks of piroxicam disappear in the diffractogram of the complex, indicating its inclusion. Analysis of the results obtained by nuclear magnetic resonance (^{1}H-NMR) indicates that the H_3 and H_6 protons are involved in the noncovalent interaction with piroxicam. By analyzing FTIR spectrum of the complex piroxicam:2-hydroxypropyl-β-cyclodextrin the absence of characteristic peaks of piroxicam is observed (valence vibration bands of NH and OH groups, aromatic parts of the structure and the secondary amide), and shifts of bands typical of the complexing agent, indicating formation of supramolecular structures by inclusion. Testing photostability by FTIR method shows that by inclusion of piroxicam in the cavities of 2-hydroxypropyl-β-cyclodextrin is protected

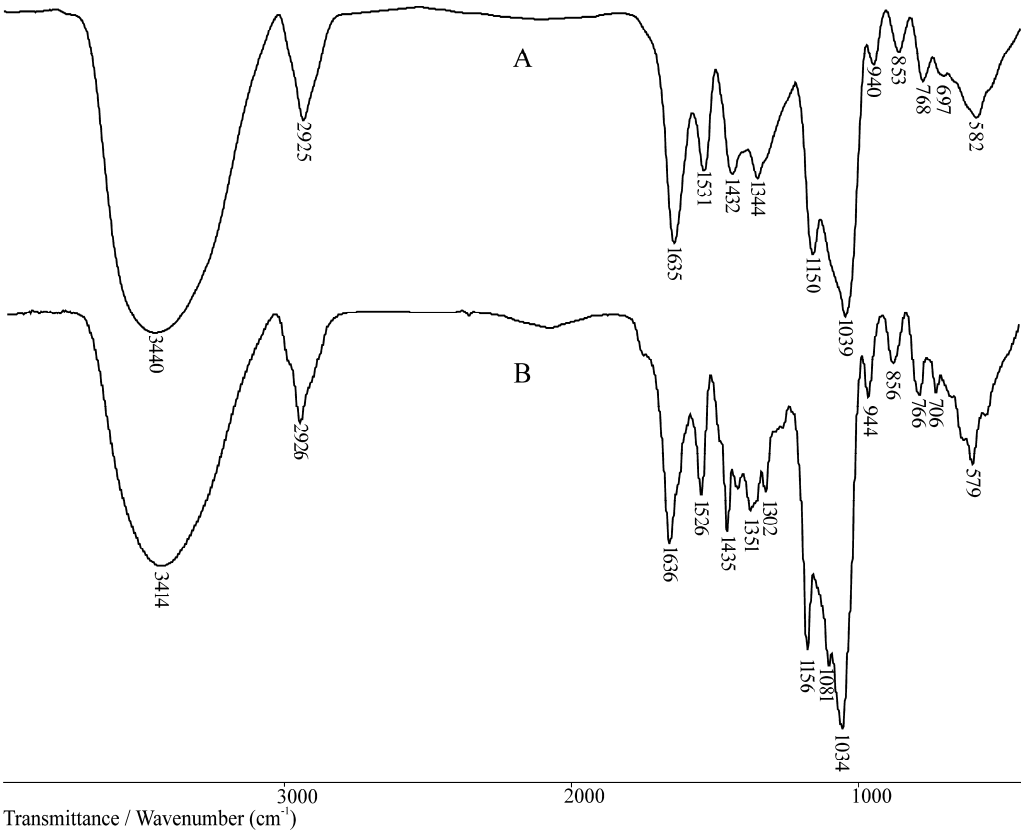

Figure 7. FTIR Spectrum of the piroxicam:2-hydroxypropyl-β-cyclodextrin inclusion complex, which has not been exposed to daylight (A), and which has been exposed to daylight for 30 days (B).

from daylight for a period of up to 30 days, while piroxicam that had not been complexed showed considerably lower stability when exposed to daylight.

Acknowledgements

Financial support provided by the Ministry of Education, Science and Technological Development, Republic of Serbia (project No. TR 34012) is gratefully acknowledged.

REFERENCES

[1] J. Bordner, P.D. Hammen, E.B. Whipple, Deuterium isotope effects on carbon-13 NMR shifts and the tautomeric equilibrium in N-substitued pyridyl derivatives of Piroxicam, J. Am. Chem. Soc. **111** (1989) 6572–6578.

[2] R.S. Tsai, P.A. Carrupt, N. El Tayar, Y. Giroud, P. Andrade, B. Testa , Physicochemical and structural properties of non-steroidal anti-inflammatory oxicams, Helv. Chim. Acta **76** (1993) 842–854.

[3] Y.H. Kim, D.W. Cho, S.G. Kang, M. Yoon, D. Kim, Excited-state intramolecular proton transfer emission of Piroxicam in aqueous β-cyclodextrin solutions, J. Lumin. **59** (1994) 209–217.

[4] R. Banerjee, H. Chakraborty, M. Sarkar, Photophysical studies of oxicam group of NSAIDs: piroxicam, meloxicam and tenoxicam, Spectrochim. Acta, A **59** (2003) 1213–1222.

[5] S.M. Andrade, S.M.B. Costa, Hydrogen bonding effects in the photophysics of a drug. Piroxicam, in homogeneous media and dioxane–water mixtures, Phys. Chem. Chem. Phys. **1** (1999) 4213–4218.

[6] J.E. Hansen, E. Pines, G.R. Fleming, Excited-state proton transfer of protonated 1-aminopyrene complexed with beta-cyclodextrin, J. Phys. Chem., B **96** (1992) 6904––6910.

[7] M. Yoon, H.N. Choi, H.W. Kwon, K.H. Park, Solvent dependence of absorption and fluorescence spectra of Piroxicam. A possible intramolecular proton transfer in the excited state, Bull. Korean Chem. Soc. **9** (1988) 171––175.

[8] C. Cavallari, B. Albertini, M.L. González-Rodríguez, Rodriguez L, Improved dissolution behaviour of steam-granulated piroxicam, Eur. J. Pharm. Biopharm. **54** (2001) 65–73.

[9] P.O. Osadebe, L.E. Onugwu, A.A. Attama, Energetics of the interaction between piroxicam and beta-cyclodextrin (β-CD) in inclusion complexes, Sci. Res. Essay **3** (2008) 86–93.

[10] T. Van Hees, G. Piel, S.H. de Hassonville, B. Evrard, L. Delattre, Determination of the free / included piroxicam ratio in cyclodextrin complexes: comparison between UV spectrophotometry and differential scanning calorimetry, Eur. J. Pharm. Sci. **15** (2002) 347–353.

[11] X. Zhang, D. Wu, J. Lai, Y. Lu, Z. Yin, W. Wu, Piroxicam/2-hydroxypropyl-β-cyclodextrin inclusion complex prepared by a new fluid-bed coating technique, J. Pharm. Sci. **98** (2009) 665–675.

[12] L. Mammen, C.P. Schmidt, Photosensitivity reactions: a case report involving NSAIDs, Am. Fam. Physician **52** (1995) 575–584.

[13] E. Kochevar, M.L. Morison, J.L. Lamm, D.J. Mc Auliffe, A. Western, and A.F. Hood, Possible mechanisms of piroxicam-induced photosensitivity, Arch. Dermatol. **122** (1986) 1283–1287.

[14] S.M. Andrade, S.M.B. Costa, R. Pansu, The influence of water on the photophysical and photochemical properties of piroxicam in AOT/isooctane/water reversed micelles, Photochem. Photobiol. **71** (2000) 405–412.

[15] D.E. Moore, Drug-induced cutaneous photosensitivity: incidence, mechanism, prevention and management, Drug Safety **25** (2002) 345–372.

[16] T. Sasaki, H. Shimizu, S. Tokuyama, T. Hariya, I. Soh, H. Sueki, M. Iijima, T. Yamamoto, Y. Kuroiwa, Antigenic characterization in ampiroxicam-induced photosensitivity using an *in vivo* model of contact hypersensitivity, J. Dermatol. Sci. **21** (1999) 170–175.

[17] B.D. Glass, M.E. Brown, S. Daya, M.S. Worthington, P. Drummond, E. Antunes, M. Lebete, S. Anoopkumar-Dukie, D. Maharaj, Influence of cyclodextrins on the photostability of selected drug molecules in solution and the solid-state, Int. J. Photoenergy **3** (2001) 205––211.

[18] F. Manakker, T. Vermonden, C.F. Nostrum, E.H Wim, Cyclodextrin-based polymeric materials, synthesis, properties, and pharmaceutical/biomedical applications, Biomacromolecules **10** (2009) 3156–3159.

[19] V. Nikolić, D. Ilić, Lj. Nikolić, M. Stanković, M. Cakić, Lj. Stanojević, A. Kapor, M. Popsavin, The protection of nifedipin from photodegradation due to complex formation with β-cyclodextrin, Cent. Eur. J. Chem. **8** (2010) 744–749.

[20] A. Kapor, V. Nikolić, Lj. Nikolić, M. Stanković, M. Cakić, Lj. Stanojević, D. Ilić, Inclusion complexes of amlodipine besylate and cyclodextrins, Cent. Eur. J. Chem. **8** (2010) 834–841.

[21] V. Nikolić, Lj. Nikolić, M. Stanković, A. Kapor, M. Popsavin, D. Cvetković, A molecular inclusion complex of atenolol with 2-hydroxypropyl-β-cyclodextrin; production and characterization thereof, J. Serb. Chem. Soc. **72** (2007) 737–746.

[22] V. Nikolić, Synthesis of allicin, its derivatives and inclusion complexes, Ph.D. Thesis, Faculty of Technology, Leskovac, 2003 (in Serbian).

[23] L.Y. Lyn, H.W. Sze, A. Rajendran, G. Adinarayana, K. Dua, S. Garg, Crystal modifications and dissolution rate of piroxicam, Acta Pharm. **61** (2011) 391–402.

IZVOD

FOTOSTABILNOST PIROKSIKAMA U INKLUZIONOM KOMPLEKSU SA 2-HIDROKSIPROPIL-β-CIKLODEKSTRINOM

Vesna D. Nikolić[1], Snežana S. Ilić-Stojanović[1], Ljubiša B. Nikolić[1], Milorad D. Cakić[1], Aleksandar S. Zdravković[2], Agneš J. Kapor[3], Mirjana M. Popsavin[4]

[1]*Univerzitet u Nišu, Tehnološki fakultet, Leskovac, Srbija*
[2]*Visoka strukovna škola za tekstil, Leskovac, Srbija*
[3]*Univerzitet u Novom Sadu, Prirodno-matematički fakultet, Departman za Fiziku, Novi Sad, Srbija*
[4]*Univerzitet u Novom Sadu, Prirodno-matematički fakultet, Departman za Hemiju, Novi Sad, Srbija*

(Naučni rad)

Cilj ovog rada je zaštita piroksikama od fotodegradacije formiranjem inkluzionog kompleksa sa 2-hidroksipropil-β-ciklodekstrinom. Piroksikam je fotoosetljiva supstanca iz grupe nesteroidnih antiinflamatornih lekova. Ciklodekstrini i njihovi derivati kao specifični nosači mogu lekovitim supstancama da menjaju fizičko–hemijska svojstva, tako da je njihova primena aktuelna u farmaceutskoj industriji. Molekulski inkluzioni kompleks piroksikam:2-hidroksipropil-β-ciklodekstrin pripremljen je metodom koprecipitacije u molskom odnosu 1:1. Strukturna karakterizacija kompleksa, odgovarajuće fizičke smeše i kompleksirajućih agenasa piroksikama i 2-hidroksipropil-β-ciklodekstrina izvršena je difrakcijom rendgenskih zraka (XRD), protonskom nuklearno magnetnom rezonancom (^{1}H-NMR) i infracrvenom spektroskopijom sa Furijeovom (*Fourier*) transformacijom (FTIR). Pikovi koji potiču od piroksikama (8,6; 11,8; 14.4º; 17,6; 21,6; 25,9 i 27,3°) nisu prisutni u difraktogramu kompleksa piroksikam:2-hidroksipropil-β-ciklodekstrin i ukazuju na to da je lek zaklonjen u šupljine domaćina. Da je došlo do kompleksacije pokazuje i analiza FTIR spektara gde u spektru kompleksa ne postoje trake od valencionih vibracija NH i OH grupa, aromatičnih delova strukture i sekundarnog amida piroksikama. ^{1}H-NMR analiza piroksikama i kompleksa takođe pokazuje da je ostvarena nekovalentna interakcija pirosikama sa glukopiranoznim jedinicama ciklodekstrina i da su najveća pomeranja zapažena kod H_3 i H_6 protona. Fotoosetljivost na dnevnoj svetlosti za piroksikam i inkluzioni kompleks piroksikam:2-hidroksipropil-β--ciklodekstrin ispitivana je metodom FTIR. Rezultati pokazuju da piroksikam koji je kompleksiran po tipu inkluzije zadržava stabilnost na dnevnu svetlost 30 dana u odnosu na piroksikam koji nije kompleksiran i koji pokazuje fotostabilnost unutar 5 dana. Kompleksacijom, piroksikam se štiti od fotodegradacije, čime se obezbeđuje sigurnost njegove primene i farmakološka aktivnost.

Ključne reči: Inkluzioni kompleks • Piroksikam • 2-Hidroksipropil-β-ciklodekstrin • Fotodegradacija

Immobilization of chemically modified horseradish peroxidase within activated alginate beads

Dragica Spasojević[1], Miloš Prokopijević[1], Olivera Prodanović[1], Marilen Gabriel Pirtea[2], Ksenija Radotić[1], Radivoje Prodanović[3]

[1]*Institute for multidisciplinary studies, University of Belgrade, Belgrade, Serbia*
[2]*Multidisciplinary research platform „Nicholas Georgescu-Roegen", West University of Timisoara, Timisoara, Romania*
[3]*Faculty of Chemistry, University of Belgrade, Belgrade, Serbia*

Abstract

Immobilization of horseradish peroxidase (HRP) within alginate beads was enabled by chemical modification of the enzyme and polysaccharide chains. HRP and alginate were oxidized by periodate and subsequently modified with ethylenediamine. Highest specific activity of 0.43 U/ml of gel and 81% of bound enzyme activity was obtained using aminated HRP and alginate oxidized by periodate. Immobilized enzyme retained 75% of its original activity after 2 days of incubation in 80% (v/v) dioxane and had increased activity in basic solutions compared to native enzyme. During repeated use in batch reactor for pyrogallol oxidation immobilized peroxidase retained 75% of its original activity.

Keywords: periodate, ethylene diamine, peroxidase, immobilized.

Available online at the Journal website: http://www.ache.org.rs/HI/

SCIENTIFIC PAPER

UDC 66.094.3.097:547.313.2:547.415.1

Hem. Ind. **68** (1) 117–122 (2014)

doi: 10.2298/HEMIND121122036S

Horseradish peroxidase (HRP) is one of the most studied peroxidases from plants that can be used for organic synthesis of chemicals like DOPA and bisphenols [1], for removal of polutants such as phenol and aniline from wastewaters [2] and for manufacturing of biosensors [3].

In order to be used in industry, it is necessary to decrease the cost of the enzyme. This can be achieved by repeated use of the same enzyme batch for prolonged period of time. In order to do so, it is necessary to develop efficient method for enzyme immobilization that will facilitate easy removal of the catalyst from reaction mixture without leaking or losing activity [4]. Immobilization within alginate is one of the most common methods for enzyme and cell immobilization since it does not require expensive chemicals or complicated setup [5]. Since alginate macromolecular gel has large pore diameter, low molecular weight enzymes like peroxidases, can easily diffuse out [6]. In order to overcome this problem several approaches were tried including coating with polylysine or chitosan [7]. Chemical modification of polymers or enzymes can introduce new functional groups that also promote enzyme immobilization and adsorption to the gel [8].

Alginate was used previously for immobilization of soybean peroxidase [9], turnip peroxidase [10] and horseradish peroxidase [6,11] but in most cases, due to low molecular weight, approximately 45 kDa, leakage of the peroxidase from alginate gel was significant.

In the presented research article we developed a novel method for peroxidase immobilization within alginate hydrogel by chemically modifying enzyme molecules and introducing new functional groups into alginate through periodate oxidation.

MATERIALS AND METHODS

Immobilization of native HRP within native alginate

Sodium alginate was dissolved in the reagent grade water for preparing a 2% (w/v) solution. The gel was stored at 4 °C till further use. Solution of enzyme in water (concentration 1 mg/ml) was added to alginate gel to yield final concentration of 0.01 mg/ml. To perform matrix beading, a needle syringe was filled with the solution and the beads were obtained by dripping the bead-forming solution into a solution of $CaCl_2$ (5.5%) and mildly stirring for 1 h to allow beads hardening. The beads were then washed with the same solution of $CaCl_2$ (20 ml) and stored in HEPES buffer (10 mM, pH 7) with 5mM $CaCl_2$ at 4 °C.

Activation of alginate by oxidation

Sodium alginate (1 g) was added to 100 ml of sodium periodate solution (50 mM) at 4 °C in the dark for activation. The reaction was stopped after 24 h by adding an equimolar amount of glycerol. NaCl (2 g) was then added to the mixture, in order to facilitate the subsequent precipitation in the excess of ethanol (3 volumes). The precipitate was collected, redissolved in distilled water (10 ml) and dialyzed for 24 h to remove completely the sodium periodate and other chemicals

Correspondence: R. Prodanović, Faculty of Chemistry, University of Belgrade, Studentski trg 12, Belgrade, Serbia.
E-mail: rprodano@chem.bg.ac.rs
Paper received: 22 November, 2012
Paper accepted: 27 March, 2013

or byproducts. After that, the polymer was precipitated and washed three times in 100% (v/v) ethanol, filtered, then dried with pure acetone. The obtained activated alginate product was conserved at room temperature.

Immobilization of native HRP within periodate oxidized alginate

Activated alginate was dissolved in 0.2 M $NaHCO_3$, pH 8.0, to yield final concentration of 2% (w/v), while stirring. After dissolving, HRP was added to the alginate solution, final concentration 0.01 mg/ml. Enzyme immobilization was continued for 24 h at 4 °C. Finally, 50 mM Tris buffer pH 7.0 (up to 1/4 of the final volume), was introduced drop by drop into the solution to quench the remaining noncoupled (if any) carbonyl groups. The bead forming solution was obtained by addition of 2% (w/v) of native alginate at 1:1 ratio to the alginate-HRP conjugate solution. Additional non--modified alginate is essential to improve the mechanical properties of beads, because the structure of activated alginate was altered during periodate oxidation. The same procedure was employed for alginate matrix beading as described previously for native alginate.

Modification of HRP with etylenediamine

Peroxidase (1 mg) was dissolved in 2 ml of 50 mM $NaHCO_3$ buffer, pH 8.0, followed by adding 200 µL of 50 mM sodium periodate. The solution was left at 4 °C in the dark for 6 h, stirring occasionally. After 6 h, 10 µL of glycerol was added to the final solution and allowed to settle for 30 min. Finally, the solution was placed for dialysis against distilled water.

Periodate oxidized HRP was mixed with ethylenediamine (50 mM final concentration, pH 8.0) for 2 h, followed by addition of $NaBH_4$ in 0.1 M NaOH,final concentration being 1 mg/ml, for 60 min at 4 °C. Unreacted ethylenediamine was removed by dialysis against 0.1 M sodium phosphate buffer, pH 7.0, and after that, against distilled water. Obtained HRP was kept in a freezer.

Immobilization of aminated HRP in periodate oxidized alginate was performed as previously described for immobilization of native HRP within periodate oxidized alginate.

Modification of periodate oxidized alginate with ethylenediamine

Periodate oxidized alginate (0.4 g) was dissolved in 10 ml of $NaHCO_3$ buffer (pH 8.0), then 10 ml of 0.1 M ethylenediamine was added and the mixture was left in the dark for 30 min. After that 0.05 g $NaBH_3$ (CN) was added and left overnight. This solution was placed for dialysis against distilled water.

Immobilization of periodate oxidized HRP in aminated alginate was performed as previously described for immobilization of native HRP within periodate oxidized alginate.

Enzyme activity

Pyrogallol solution (13 mM) in 10 mM HEPES buffer (pH 7.0) was prepared. Enzyme immobilized beads (50––80 mg) were added to 3 ml of thus prepared solution along with 30 µl of 0.97 M H_2O_2. The mixture was kept for constant stirring on magnetic stirrer and aliquots were taken at 0, 5, 10 and 15 min post-incubation. Absorbance was measured at 420 nm.

Unbound activity was measured in a solution of $CaCl_2$ after gel beading. "Leakage" was measured after 24, 48 h and 5 days, and retained specific activity was measured after 5 days.

RESULTS AND DISCUSSION

Immobilization of HRP

In order to efficiently immobilize HRP within alginate beads, different methods of enzyme and alginate modification were tried. Three types of alginate were used: native one, alginate oxidized by periodate and alginate modified with ethylene diamine after periodate oxidation. Three types of HRP were also used, native enzyme, enzyme oxidized by periodate and enzyme modified with ethylene diamine after periodate oxidation. Enzyme concentration used for immobilization was fixed at 0.01 mg/mL, alginate concentration was 2% (w/v) and in order to have better mechanical properties, modified alginate was mixed in 1:1 ratio with 2% (w/v) native form, just before immobilization. Ionotropic gelation with $CaCl_2$ gave beads with average diameter of 1.5 mm (Figure 1).

Four different combinations of native and modified enzyme and alginate were tried. First, native HRP was immobilized within native alginate and in the second experiment within periodate oxidized alginate. Third, periodate oxidized HRP, according to the protocol we previously developed [12] in order to introduce aldehyde groups, was immobilizied within alginate modified with ethylenediamine after periodate oxidation. Forth experimental setup was HRP modified with ethylenediamine after periodate oxidation immobilized within periodate oxidized alginate.

Based on analysis of enzyme activity after immobilization, it can be concluded that modified alginate and modified enzyme exhibited higher amount of activity compared to the classical method for HRP immobilization within alginate beads (Table 1).

Highest activity of 0.43 U/g was obtained by encapsulation of aminated HRP within oxidized alginate. The same conjugate showed also highest retention of activity after 5 days of washing, which is indicative that enzyme was not only entrapped within alginate matrix, but also covalently bound via aldehyde groups present in oxidized alginate. Aminated HRP immobilized within oxidized alginate was further characterized with res-

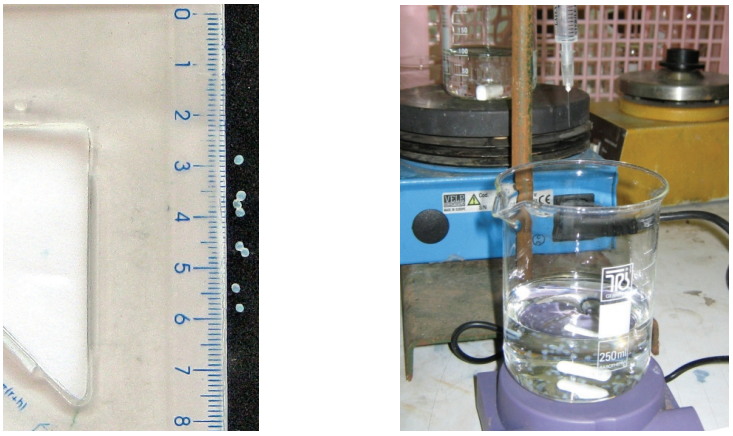

(a) (b)

Figure 1. Beads with immobilized enzyme after gelation in $CaCl_2$ solution (a) and setup used for bead formation (b).

pect to pH optimum, stability in organic solvent and kinetic properties.

pH Influence on activity

pH Optimum was determined using acetate, HEPES and glycine buffer. Compared to native HRP, aminated form immobilized within oxidized alginate showed pH optimum shift towards low values (pH < 7), as in Figure 2.

While in previous studies of peroxidase immobilization within nonmodified alginate, pH optimum was not changed [11], in our case change in pH optimum was probably result of introduced charged groups

Table 1. Specific activity, bound activity, percentage of binding, immobilization yield and residual activity within alginate beads for different immobilization methods. Percentage of binding is defined as a ratio of bound activity and activity that was added per gram of alginate gel during immobilization. Immobilization yield is defined as a ratio of specific and bound activity. Residual activity is defined as a ratio of specific activity immediately after immobilization and specific activity after 5 days of rinsing in buffer

Immobilization method	Specific activity, U/g	Bound activity, U/g	Percentage of binding, %	Immobilization yield, %	Residual activity, U/g	Residual activity, %
Alginate + HRP	0.15	0.80	9.69	18.4	0.063	42.6
Oxidized alginate + HRP	0.13	1.11	9.69	11.7	0.081	62.3
Aminated alginate + oxidized HRP	0.15	1.73	14.1	8.92	0.074	48.0
Oxidized alginate + aminated HRP	0.43	5.76	81.4	7.43	0.409	95.6

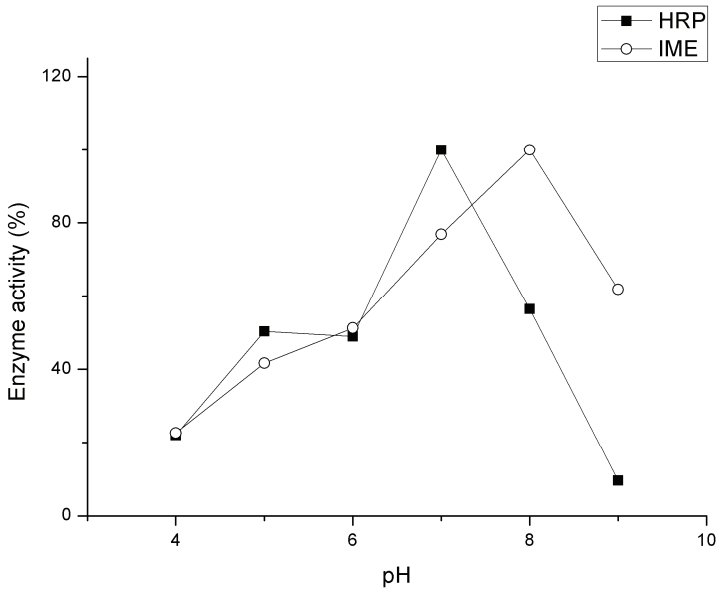

Figure 2. Influence of pH on activity of free (filled square) and immobilized HRP (open circle).

within alginate due to chemical modification. Wider pH optimum and higher activity at more basic pH values of immobilized HRP makes it more suitable for industrial application since it is less sensitive to changes in pH.

Stability in the presence of dioxane

Since HRP is also used for polymer synthesis in organic solvents, stability in these media is important for its application. Stability of our immobilized HRP was measured in 80% (v/v) dioxane at room temperature (25 °C). After incubation in dioxane water mixture, immobilized enzyme was washed with buffer and residual activity was measured in water solution (Figure 3).

Stability of immobilized enzyme in the presence of dioxane increased substantially. While free enzyme was losing 90% of its original activity after 1 day of incubation, immobilized enzyme retained more than 75% of the original activity after 2 days of incubation in 80% (v/v) dioxane.

Determination of K_m and V_{max}

K_m value for pyrogallol of free enzyme is 2.24 mM, while our immobilized enzyme showed K_m value of 4.86 mM (Figure 4).

These results were in good agreement with previous reports for enzymes immobilized within alginate gels and they appear to be a result of diffusional limitations that occur within alginate beads.

Repeated cycle testing in batch reactor

At the end aminated HRP immobilized within beads made from oxidized alginate was tested in a batch reactor for repeated use during pyrogallol oxidation.

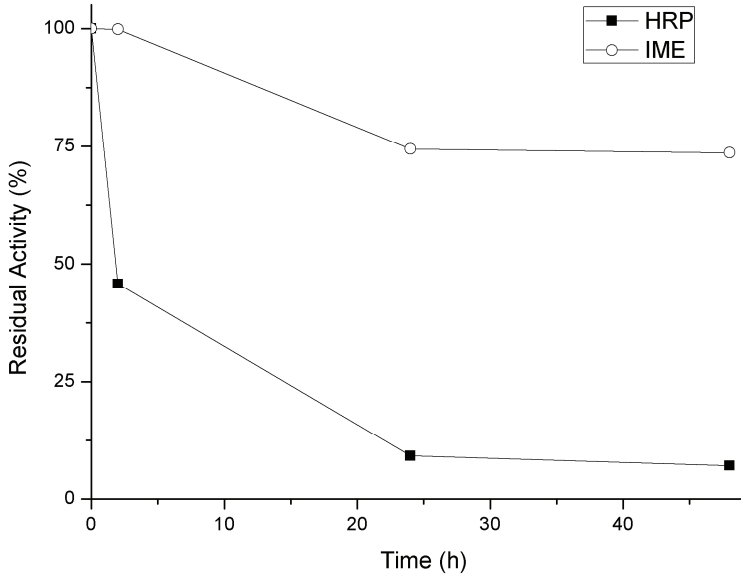

Figure 3. Influence of incubation time in 80% (v/v) dioxane on residual activity of free and immobilized HRP.

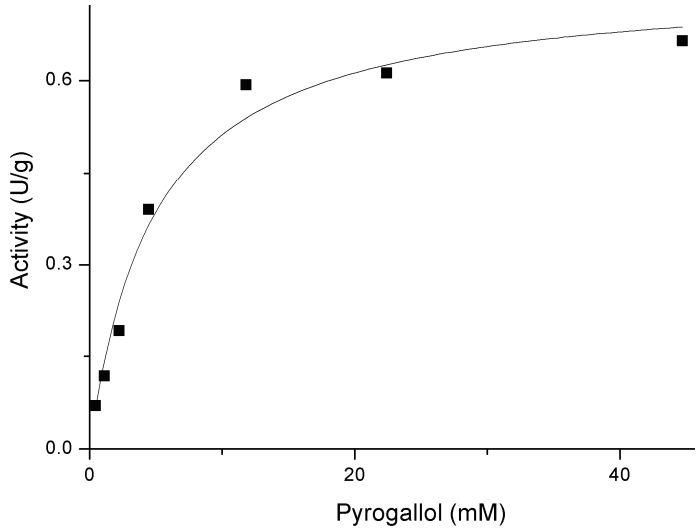

Figure 4. Michaelis–Menten curve for immobilized HRP.

Each cycle lasted for 6 h and afterwards, amount of oxidized pyrogallol was determined spectrophotometrically while beads were washed and reused (Figure 5).

After first cycle, immobilized enzyme lost some of the activity, but later activity remained unchanged through 5 cycles of repeated use. This was a better result than previously reported for HRP immobilized within native alginate [6] where activity after 5 cycles dropped below 40 % of the original value. This makes our immobilized HRP a suitable candidate for application in industry where operational stability is of the utmost importance.

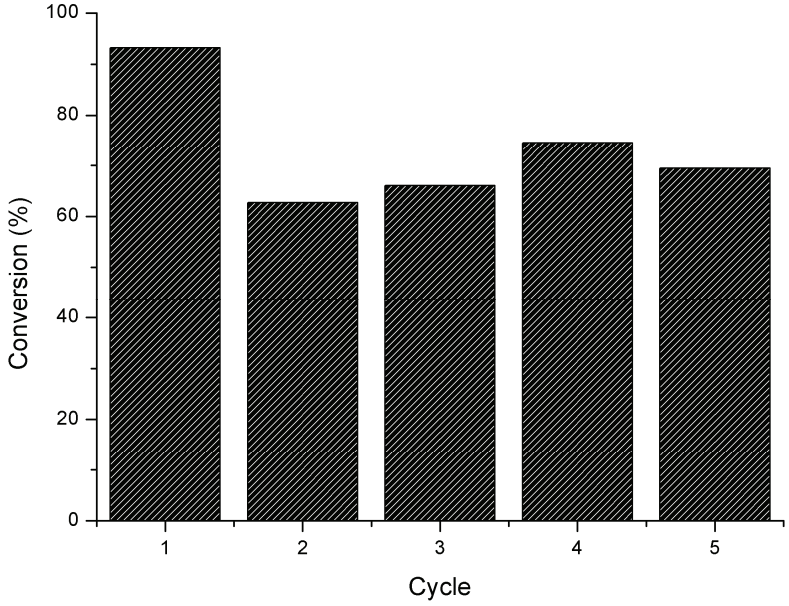

Figure 5. Activity of immobilized HRP during repeated batch run.

CONCLUSION

We have developed the protocol for efficient immobilization of HRP within alginate beads. In order to improve immobilization efficiency, HRP was modified with ethylenediamine and at the same time alginate was oxidized with sodium periodate to introduce reactive aldehyde groups into polysaccharide backbone. Due to those modifications enzyme was covalently bound to the alginate beads and could not be released after subsequent washing or repeated use in batch reactor. Immobilized enzyme also showed high stability in the presence of organic solvents and increased tolerance to pH changes. In a batch reactor it could be used in 5 consecutive rounds for pyrogallol oxidation without significant loss of enzymatic activity. Therefore, thus prepared immobilized HRP is a suitable candidate for industrial application in phenol removal or polymer synthesis in monophasic organic solvent and aqueous solutions.

Acknowledgment

This work was supported by Grant No. ON173017 and Grant No. ON172049 sponsored by the Ministry of Education, Science and Technological Development, Republic of Serbia.

REFERENCES

[1] A.M. Klibanov, Z. Berman, B.N. Alberti, Preparative hydroxylation of aromatic compounds catalyzed by peroxidase. J. Am. Chem. Soc. **103** (1981) 6263–6264.

[2] Q. Husain, R. Ulber, Immobilized Peroxidase as a Valuable Tool in the Remediation of Aromatic Pollutants and Xenobiotic Compounds, Review. Crit. Rev. Env. Sci. Tec. **41** (2011) 770–804.

[3] G.V. Presnova, M.Y. Rybcova, A.M. Egorov, Electrochemical biosensors based on horseradish peroxidase, Russ. J. Gen. Chem. **78** (2008) 2482–2488.

[4] D. Brady, J. Jordaan, Advances in enzyme immobilisation, Biotechnol. Lett. **31** (2009) 1639–1650.

[5] J.K. Park, H.N. Chang, Microencapsulation of microbial cells, Biotechnol. Adv. **18** (2000) 303–319.

[6] S.V. Mohan, K.K. Prasad, N.C. Rao, P.N. Sarma, Acid azo dye degradation by free and immobilized horseradish peroxidase (HRP) catalyzed process, Chemosphere **58** (2005) 1097–1105.

[7] Y.J. Hong, M.S. Lee, J.C. Kim, pH-dependent release of alginate beads coated with polylysine, J. Ind. Eng. Chem. **17** (2011) 410–414.

[8] R.C. Rodrigues, A. Berenguer-Murcia, R. Fernandez-Lafuente, Coupling Chemical Modification and Immobilization to Improve the Catalytic Performance of Enzymes, Adv. Synth. Catal. **353** (2011) 2216–2238.

[9] U.J. Trivedi, A.S. Bassi, J. Zhu, Investigation of phenol removal using sol-gel/alginate immobilized soybean seed hull peroxidase, Can. J. Chem. Eng. **84** (2006) 239–247.

[10] F. Quintanilla-Guerrero, M.A. Duarte-Vazquez, B.E. Garcia-Almendarez, R. Tinoco, R. Vazquez-Duhalt, C. Regalado, Polyethylene glycol improves phenol removal by immobilized turnip peroxidase, Bioresource Technol. **99** (2008) 8605–8611.

[11] I. Alemzadeh, S. Nejati, Removal of Phenols with Encapsulated Horseradish Peroxidase in Calcium Alginate, Iran. J. Chem. Chem. Eng. **28** (2009) 43–49.

[12] O. Prodanovic, M. Prokopijevic, D. Spasojevic, K. Radotic, Z. Knezevic-Jugovic, R. Prodanovic, Improved Covalent Immobilization of Horseradish Peroxidase on Macroporous Glycidyl Methacrylate-Based Copolymers, App. Biochem. Biotechnol. **168** (2012) 1288–1301.

IZVOD

IMOBILIZACIJA HEMIJSKI MODIFIKOVANE PEROKSIDAZE IZ RENA UNUTAR AKTIVIRANIH ALGINATNIH KUGLICA

Dragica Spasojević[1], Miloš Prokopijević[1], Olivera Prodanović[1], Marilen Gabriel Pirtea[2], Ksenija Radotić[1], Radivoje Prodanović[3]

[1] *Institut za multidisciplinarna istraživanja,Univerzitet u Beogradu, Beograd, Srbija*
[2]*Multidisciplinary research platform „Nicholas Georgescu-Roegen“, West University of Timisoara, Timisoara, Romania*
[3] *Hemijski fakultet,Univerzitet u Beogradu, Beograd, Srbija*

(Naučni rad)

Imobilizacija peroksidaze iz rena unutar alginatnih kuglica je poboljšana hemijskom modifikacijom enzima i polisaharidnih lanaca. Peroksidaza i alginat su oksidovani perjodatom i naknadno modifikovani etilendiaminom. Najveća specifična aktivnost od 0,43 U/ml gela i 81% vezane aktivnosti je dobijeno korišćenjem aminovane peroksidaze i alginata oksidovanog perjodatom. Imobilizovani enzim je zadržao 75% originalne aktivnosti nakon 2 dana inkubacije u 80% (v/v) dioksanu i imao je povećanu aktivnost pri baznim pH vrednostima u poređenju sa nativnim enzimom. Tokom višestruke upotrebe u šaržnom reaktoru za oksidaciju pirogalola imobilizovana peroksidaza je zadržala 75% početne aktivnosti.

Ključne reči: Perjodat • Etilendiamin • Peroksidaza • Imobilizovan

Review of techological methods and experimental determination of thermodynamic and transport properties of reagents for carbon dioxide removal from flue gases

Vuk D. Spasojević[1], Slobodan P. Šerbanović[2], Predrag Stefanović[1], Mirjana Lj. Kijevčanin[2]

[1]*Institute for Nuclear Sciences „Vinča", University of Belgrade, Mike Petrovića Alasa 12-14, Belgrade, Serbia*
[2]*Faculty of Technology and Metallurgy, University of Belgrade, Karnegijeva 4, Belgrade, Serbia*

Abstract

In this work a review of the currently available methods for carbon dioxide removal from flue gasses is given. Some of them are commercially available, while others are still under development. Special attention is given to detailed description of the methods based on hemi sorption by aqueous solutions of alkanolamines, which found wide commercial use in industry. Selection of appropriate absorbent, process equipment, methods, working parameters, combustion processes, etc., are some of the key points that will be reviewed within this work in order to present advantages and limitations of carbon dioxide removal methods. In the experimental section we have provided data on density, viscosity and refractive index of insufficiently investigated carbon dioxide removal agents, such as monoisopropanolamine (MIPA), diisopropanolamine (DIPA), triisopropanolamine (TIPA) and currently widely used dietanolamine (DEA). The data obtained are crucial for the equipment design and process optimization.

Keywords: density, viscosity, refractive index, carbon dioxide removal, hemisorption, flue gases, alkanolamines.

Available online at the Journal website: http://www.ache.org.rs/HI/

SCIENTIFIC PAPER

UDC 66.081.4:66.07:502/504

Hem. Ind. **68** (1) 123–134 (2014)

doi: 10.2298/HEMIND130312039S

In order to reduce the green house gases (GHG) emission, it is necessary to use adequate prevention measures, which have to comprise efforts in energy sector, industry, commerce and transport. In general, it could be assumed that over 40% of the worldwide carbon dioxide (CO_2) emissions are caused by electricity generation in fossil fuel power plants. Climate changes are affecting weather systems causing negative impacts on human health, agriculture, and global economy. This resulted in serious environmental concerns and the need to reduce GHG emissions from industrial resources. CO_2 has the largest ratio in the world's annual emissions of GHG's. Reduction of CO_2 emissions from industrial waste gases have become major target. Before laboratory applications or industrial equipment installation, it is a common practice nowadays that process simulation is carried out using software specially designed for these purposes. However, majority of process simulators such as ChemCad, ASPEN PLUS and computational fluid dynamic software (Fluent, ANSYS, etc.) use constant values of pure component properties, independent of temperature and concentration. This leads toward the use of this data in narrow temperature or concentration range. If a real process exceeds these ranges, significant calculation errors can occur, thus providing false overall process equipment design. In order to contribute to the requirements of realistic and reliable thermodynamic and transport property data, the series of experiments were conducted using four pure alkanolamines. Alkanolamines, as weak bases, are usually used for acid gasses absorption. In this paper, densities, refractive indices and viscosities of monoisopropanolamine (MIPA), diisopropanolamine (DIPA, triisopropanolamine (TIPA) and diethanolamine (DEA), were measured in the temperature range 288.15–333.15 K and at atmospheric pressure. Obtained data is important for understanding the nature of chemical bonds within alkanolamines and their mixing effects, but also relevant for the process design and optimization. Fortunately, all software packages previously mentioned offer possibilities for the implementation of experimental data, introducing different parameters through custom built-in user defined functions.

REVIEW OF CARBON DIOXIDE CAPTURE TECHNOLOGIES

Primary goals for the carbon dioxide capture technologies were actually established for the use in other industries, rather than for the mitigation of green house gases. Nevertheless its contribution to carbon capture field development is undisputable. Industrial implementation of these technologies was set mainly

Correspondence: M.Lj. Kijevčanin, Faculty of Technology and Metallurgy, University of Belgrade, Karnegijeva 4, Belgrade, Serbia.
E-mail: mirjana@tmf.bg.ac.rs
Paper received: 12 March, 2013
Paper accepted: 8 May, 2013

on the purification of gases emitted from petrochemical and oil industries or, on the generation of derivates that can be synthesized and effectively used for other purposes. In early 1990's the first pilot plants and large laboratory installations emerged with the task of CO_2 removal from flue gases. As worldwide attention increased with clear connection between negative effects on climate change and increase of the concentration of CO_2 in atmosphere, international community set main rules and emission quotas for different gases that contribute to the green house effect. This key point opened up opportunities for the commercialization of emission quotas trading system followed by increase of investments in development of CO_2 removal technologies. During the past ten years, full scale industrial units were implemented in USA and Germany as the world leaders in this field.

Nowadays, there are numerous technologies for treatment of flue gases. Currently, there are three main routes for the development of the CO_2 removal process that are presented in Figure 1. The first process includes CO_2 capture from the flue gas stream after combustion (Post-combustion). The other process includes the CO_2 capture from the reformed synthesis gas of an upstream gasification unit (Pre-combustion). The newly developed technique for combustion uses nearly pure oxygen instead of air thus increasing the CO_2 concentration within flue gases stream (Oxyfuel). All the main principles of the above mentioned techniques are presented in Figure 2.

Listed processes require additional energy input for gas separation, regeneration of absorbents, capture, conditioning, storage and transportation of the CO_2. It is clear that the negative side effect of the CO_2 removal is the decrease of energy efficiency of power plants from 10 to 14%. In the post-combustion process the efficiency loses are from 10 to 12% [1], while they reach 10% for the oxyfuel process [1]. There is signi-

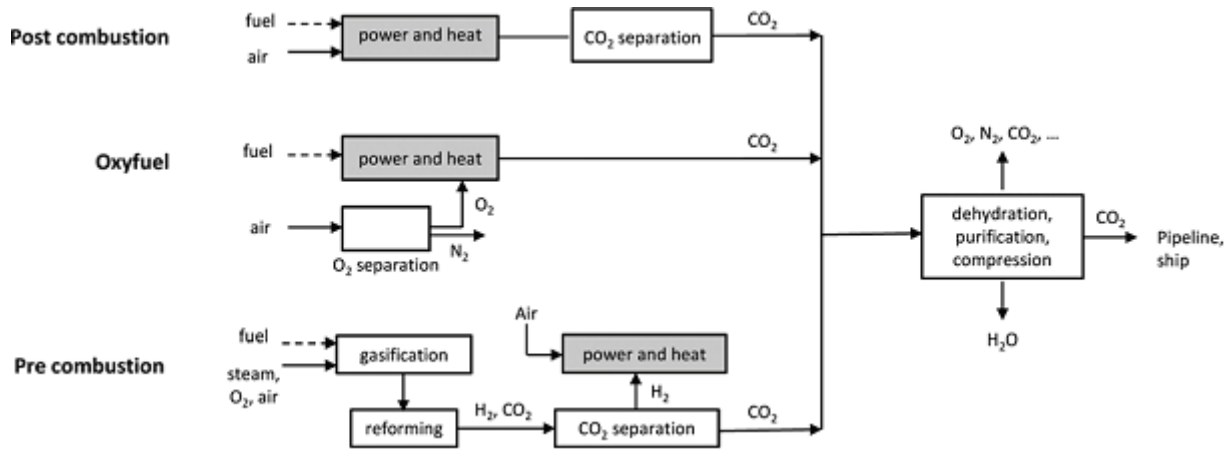

Figure 1. Main routes of development of the CO_2 removal technologies.

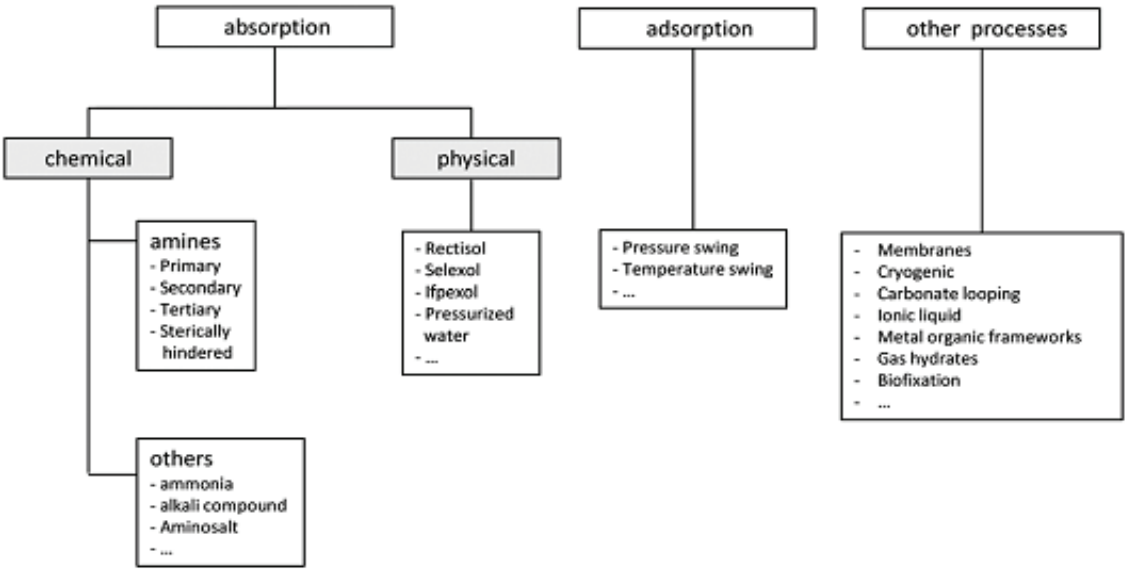

Figure 2. Main principles of carbon dioxide capture in use or under development.

ficant potential for reduction in energy requirements for the carbon dioxide removal. The largest amounts of energy are needed for the absorbent regeneration (around 60% of overall energy requirement) and additional 20–30% are spent for the compression, storage and transportation of CO_2. In this respect, new research data show promising results for the use of so-called sterically hindered amines and their blends characterized by increased loading capacity for CO_2 and simultaneous decrease in energy requirements for their regeneration [2,3]. Additional savings could be made by the use of waste heat (heat loses from cooling of flue gases before the entry point into CO_2 removal plant, but also heat gains from the exothermic reactions between absorbents and flue gases). Efficiency loses of 8% are feasible and could be easily achieved in the near future.

Pre-combustion processes

Two dominant pre-combustion technologies are the production of synthesis gas and pressure swing adsorption (PSA). The first process includes partial oxidation of fuel in gasification unit and the generation of CO rich stream. After the gasification, through the catalytic CO-shift reaction, CO reacts with steam as oxidant where CO_2 and H_2 rich stream is generated. Since such generated fuel gas is under high pressure and has a high content of H_2, CO_2 removal methods based on physical adsorption become advantageous.

This process requires additional cleaning of synthesis gas (from ash particles, alkali and sulfur components and other impurities). That could be accomplished using air separator unit prior gasification unit. The CO_2 capture takes place after the conversion of CO into CO_2 and H_2 and generation of fuel gas. Such decarbonized fuel gas is then directed to the combined gas and steam turbine cycle for generation of electricity. Overall process of integrated gas coal cycle (IGCC) plant with CO_2 capture is given in Figure 3.

Pressure swing adsorption method uses physical adsorbents such as carbon, zeolites or alumina [4], which selectively absorb CO_2 while flue gas passes through layers of beds. Process consists of two step cycles. In the first step, adsorbent selectively adsorbs CO_2 from feed gas, under high pressure conditions, while in the second step, CO_2 is removed from adsorbent by reduction of pressure, thus enabling regeneration of adsorbent and its use in the next cycle. Beside the production of synthesis gas and PSA methods, scrubbing procedure with physical sorbents can be used, offering the possibility for simultaneous removal of H_2S and COS. Methanol based solvents could be effectively used for scrubbing of fuel gases and easily regenerated using nitrogen and applying temperature change. Positive side of the scrubbing process is that CO_2 can be removed together with H_2S and COS. Disadvantage is the necessity for high pressure operating conditions which limits the use of the aforementioned technologies in pulverized coal power plants, operating at lower pressures.

Evaluation of the use of IGCC technology shows some clear advantages and disadvantages regarding the CO_2 removal. Advantages are: high efficiency potential and generation of electricity and hydrogen. Synthesis gas could be effectively used for the production of other chemicals and fuels (methanol, hydrogen for fuel cells), leading to greater flexibility, higher plant utilization and reduction of operating costs. Huge

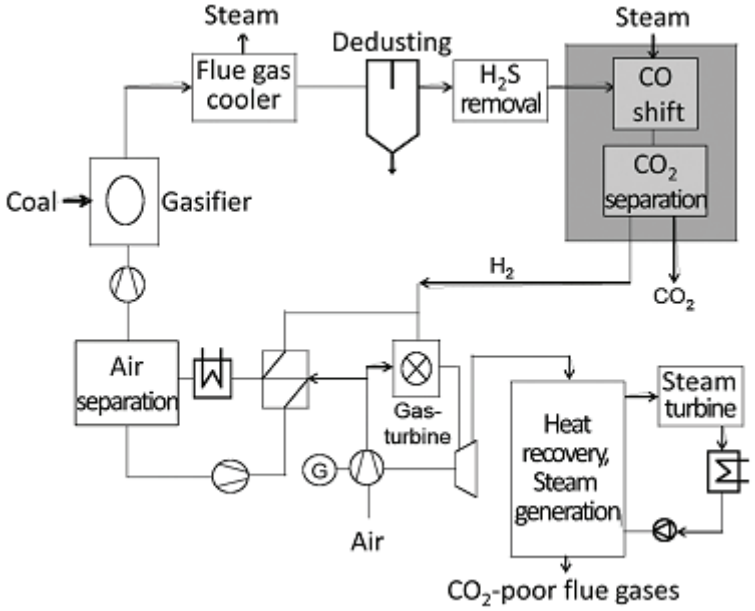

Figure 3. IGCC power plant with carbon dioxide capture.

investments, operational and maintenance cost followed by technical shortfalls manifested through long startup periods are some of the disadvantages, which drove much of the current research attention. With 5 operational IGCC power plants in the world [5] and plans for construction of new power plants in England and Canada based on oxyfuel combustion technology, significant contributions are made towards improving the process efficiency and reduction of operational costs.

Oxyfuel process

The oxyfuel process uses stream of pure oxygen for combustion of coal. Flue gases, after cleaning and washing, consist of high CO_2 concentration (around 90 vol.%), compared to the conventional power plants (7––15 vol.%). Such pure CO_2 stream could be easily compressed and transported to storage site after being demoisturized. Supply of pure oxygen stream is achieved by "gas to liquid" cryogenic air separation units (at temperatures around –180 °C). Currently, the largest planned unit for generation of pure oxygen can supply about 800000 m^3/h [6]. Taking into account that 500 MW unit with efficiency of 43% requires about 270000 m^3/h of pure oxygen according to stoichiometry, great attention must be given to the development of new methods that will assure steady and continuous supply of pure oxygen with reasonable operating costs.

The combustion process with stream of pure oxygen causes the altering of temperature within steam generator unit. Change in temperature must be limited due to the limitations in properties of applied materials in combustion chamber. In order to achieve this, large portion of CO_2 rich stream (around two-thirds of flue gases volume flow) is directed back to combustion chamber. The entire process is presented in Figure 4.

The problems yet to be solved include several improvements: of air separation method and units, of the steam generator and of the processes of denitrification and desulfurization. Air separation unit consumes the largest portion of energy (from overall 10% energy consumption, 7% is required for the process of air separation and additional 3% for the CO_2 compression and storage). Current and future development [7] in this field is set on the usage of the mixed ion electron conducting membrane technology and chemical looping technology. Main concept behind the membrane separation technique is the application of ceramic or other advanced materials that show the selective permeability towards different gas components. Air stream at high temperature (above 700 °C) passes through the membrane. Membrane selectivity allows only transport of oxygen, preventing other components to pass through it. Present limitations of wider usage of these membranes on large scale industrial units are temperature stability of the membrane and its mechanical strength.

The chemical looping process includes the use of metal oxides for combustion with fuel, instead of pure oxygen. After combustion, these metal oxides are regenerated in another reactor using air, limiting input of nitrogen from air. Current laboratory and pilot scale tests have asset a main goal to identify the most suitable materials as metal oxygen carriers. At this point, these oxygen generation methods are still in early stage of development and can be classified as second generation carbon capture and storage technologies.

Advantages of oxyfuel technology are low environmental impact with high potential for further energy requirements reduction through implementation of new separation methods. On the other hand, different heat and flow conditions require new design of heat exchangers, burner's modification, etc., are clear disadvantages of this technology.

Post-combustion process

The post-combustion process includes treatment of flue gases after combustion. Most widely used process includes the so-called chemical washing with amine based solvents. Main process includes two columns (an absorber and a stripper column). Flue gases, after pre-

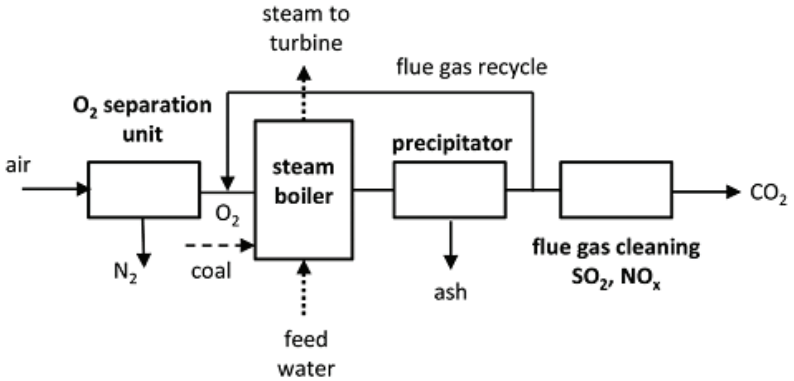

Figure 4. Process flow diagram of carbon dioxide capture with oxyfuel combustion.

cipitator, are cooled to temperature between 40 °C and 60 °C. Subsequently, they are introduced into the bottom of the absorption column. Amine based solvent is introduced at the top of the column. Gas-liquid contact is achieved either by tray or packed columns. Bonding of CO_2 with amine solvent is accompanied by release of heat. This heat must be effectively removed because of decrease of CO_2 solubility in amine solvent with the increase of temperature. CO_2 rich stream at the bottom of absorber column is carried to stripper column where, at elevated temperatures around 120 °C, the process of solvent regeneration and release of CO_2 takes place. Steam used for this process is taken from low pressure power plant steam, thus reducing the potential for generation of electricity. The chemical bonds between CO_2 and amine solvent are broken, thus leaving pure stream of CO_2 (99.9%) which is taken from stripper column, dried, compressed and transported to storage. Regenerated amine solvent is returned to absorption column after passing through heat exchanger used for preheating of CO_2 rich stream. The amine based chemical washing method has some constraints that require additional research efforts. Originally, chemical washing was designed and effectively used for scrubbing of the flue gases from petrochemical industries. High levels of oxygen in the flue gases from power plants can cause amine solvent degradation, which could be prevented by chemical inhibitors. Furthermore, high efficiency of precipitator units must be achieved due to the problems regarding blocking of packed column, which disable the effective operation of process equipment. Levels of gases NO_x and SO_x have to be reduced due to solvent degradation, since they can react with them by salt formation. For example, 10 ppm SO_x is the target concentration upon which the salt formation is avoided [8]. The most challenging problem yet to be resolved is reduction of the energy requirements of stripper column since almost 50 % of overall energy needed for the CO_2 capture goes to the process of solvent regeneration. The optimization of the entire process is required so that the thermodynamic limits can be achieved. Recent development offers solvents with significant increase in loading capacity of CO_2 and with decrease in energy requirements for its regeneration [9]. Moisture content must also be reduced, since it can cause negative effects on process equipment such as corrosion problems. Integrated system that compensates for all of those effects is presented in Figure 5.

In 2010, post combustion unit started to operate in Germany (Niederaussem site). It is planned to remove 99% CO_2 with less than 10% energy efficiency loses [10]. Process flow diagram for this unit is presented in Figure 6.

In conclusion, the post combustion carbon dioxide capture process offers some clear advantages such as highest purity of CO_2 (99.9%) that can be achieved. No fundamental changes of the original power plant process are required, which enables retrofit of the existing power plants. There is also high potential for further improvements and reduction in energy loses by utilization of advanced solvents and overall process optimization. Still, high costs and flexibility of such plants that yet need to be tested, limit the wider use of this method for CO_2 removal.

DETERMINATION OF THERMODYNAMIC AND TRANSPORT PROPERTIES OF CARBON DIOXIDE REMOVAL AGENTS

Determination of transport, physical and chemical properties is crucial in investigation of suitable absorbents for the CO_2 removal from flue gases. Data on density, viscosity, vapor pressure, solubility of gases in liquid phases, heat capacities, heat of generations, etc., are some of the data needed for efficient and accurate development of the process and process equipment design. The absorption processes are complex and almost always are followed by multiphase heat, mass and fluid flow transfer. Due to its complexity and variety of potential chemicals that could be used as CO_2 absorbents, it is impossible to collect all necessary data

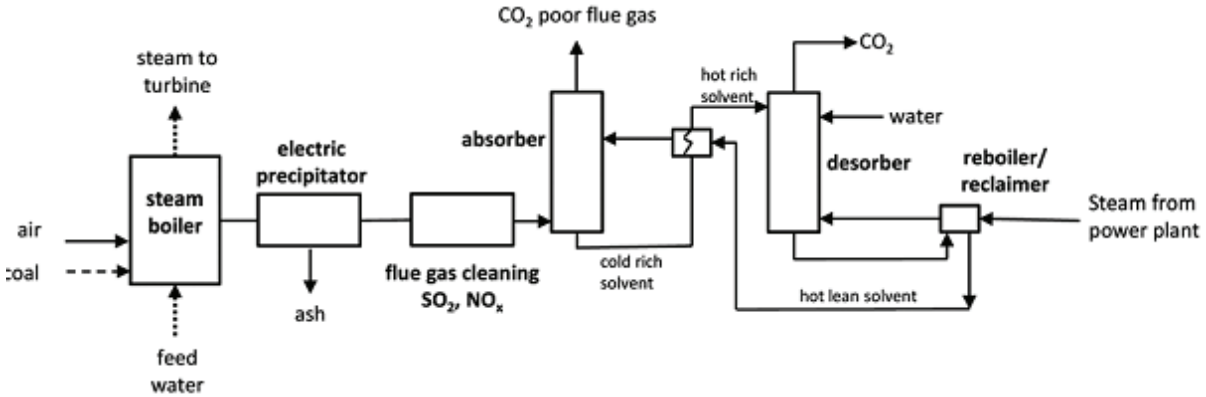

Figure 5. Integrated system for post combustion CO_2 capture using amine washing

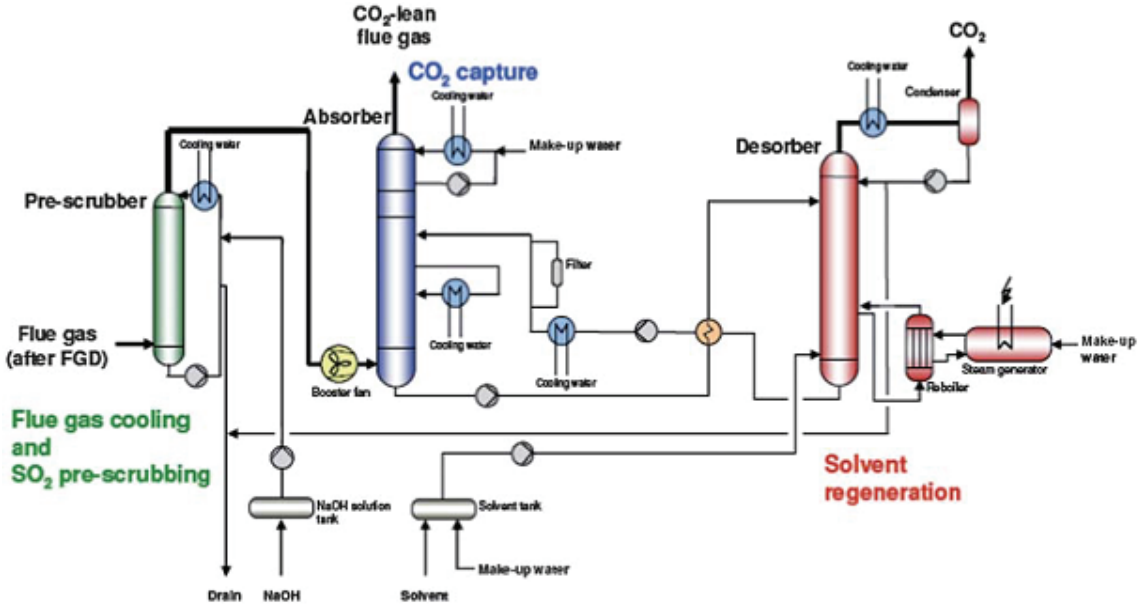

Figure 6. Niederaubem carbon dioxide capture facility.

from laboratory experiments. Large effort is being made toward determination of these properties, yet the correlation data is often used in design of process equipment.

In order to have accurate and reliable data for pure components, measurements of density and viscosity as the most important properties, and monitoring of their changes with temperature, were carried out herein.

Understanding of these properties is important from several points of view. Density and viscosity data and their changes with temperature have significant role in all balance equations. Accurate data can improve understanding of necessary requirements for industrial equipment, thus providing significant capital cost savings which may emerge from the reduction of used absorbents, height of absorber and striper columns, heat for sorbent regeneration etc.

Within the experimental section, thermodynamic and transport properties of four pure alkanolamines were investigated. The following pure chemicals were used: 1-amino-2-propanol (MIPA) (98%), diisopropanolamine (DIPA) (98%), diethanolamine (DEA) (99.5%) all supplied by Merck and used without further purification. TIPA was supplied by Sigma Aldrich with purity higher than 95%. Density measurements were performed using Anton Paar DMA 5000 digital vibrating U-tube densimeter (with automatic viscosity correction) and instrument accuracy $\pm 5\times10^{-3}$ kg m^{-3}. Refractive index measurements were carried out using Anton Paar RXA 156 refractometer. Viscosities, η, of pure alkanolamines were measured using a digital Stabinger viscometer (model SVM 3000/G2). Detailed description of calibration, solution preparation, working methods of selected measuring equipment and information about measuring uncertainty, repeatability and reproducibility are given in our previous work [11–14].

RESULTS AND DISCUSSION

Experimental measurements were carried out in the temperature range from 288.15 to 333.15 K with temperature step of 5 K. The density, refractive index and viscosity of MIPA, DIPA, TIPA and DEA alkanolamines were measured and compared with literature data, showing good agreement as presented in Table 1. Experimental data of the measured properties of four studied pure alkanolamines are presented in Figures 7–9.

Table 1. Review of the literature data for densities, refractive indices and viscosities of 1-amino-2-propanol (MIPA), diisopropanolamine (DIPA), triisopropanolamine (TIPA) and Diethanolamine (DEA)

T / K	ρ / kg m^{-3}		n_D		η / mPa·s	
	This work	Literature	This work	Literature	This work	Literature
			MIPA			
293.15	960.625	961.223 [15], 960.38 [16], 959.46 [17]	1.44792	1.4461 [18], 1.44609 [19]	–	–
298.15	956.644	957.114 [15], 956.40 [16], 956.3 [18], 956.51 [20], 956.972 [21]	1.44590	1.44604 [22]	23.259	24.234 [18], 26.685 [19], 26.685 [20], 23.00 [21]

Table 1. Continued

T / K	ρ / kg m^{-3}		n_D		η / mPa·s	
	This work	Literature	This work	Literature	This work	Literature
			MIPA			
303.15	952.641	952.980 [15], 952.39 [16], 952.52 [20]	–	–	17.702	20.314 [20]
308.15	948.608	948.828 [15], 948.36 [16]	–	–	–	–
313.15	944.543	944.656 [15], 944.30 [16], 944.42 [20]	–	–	10.869	12.514 [20]
318.15	940.449	940.462 [15], 940.20 [16]	–	–	–	–
323.15	936.322	936.244 [15], 936.08 [16], 936.19 [20]	–	–	7.1156	7.543 [20]
333.15	–	–	–	–	4.9475	5.220 [20]
			DIPA			
313.15	992.460	991.99 [21]	–	–	–	–
323.15	984.835	984.90 [23]	–	–	123.21	125.73 [23], 125.20 [24]
328.15	980.973	981.40 [25]	–	–	81.793	82.02 [24]
333.15	977.040	976.98 [21], 977.30 [23]	–	–	55.954	57.98 [23], 55.91 [24]
338.15	973.048	973.90 [25]	–	–	39.370	39.39 [24]
343.15	969.008	969.58 [23]	–	–	28.572	29.55 [23], 28.08 [24]
			DEA			
293.15	1096.424	1097.250 [15]	–	–	–	–
298.15	1093.221	1094.019 [15], 1093.70 [26], 1093.52 [27]	1.47640	1.4747 [21]	566.57	566.30 [28]
303.15	1089.989	1090.778 [15], 1090.89 [28], 1089.4 [29], 1089.84 [30]	–	–	384.84	380.0 [31]
308.15	1086.712	1087.508 [15], 1087.41 [26], 1086.7 [29]	–	–	–	–
313.15	1083.429	1084.199 [15], 1084.3 [25], 1083.95 [27], 1084.7 [32], 1083.8 [33], 1084.6 [34], 1084.01 [35]	–	–	189.86	188.80 [28]
318.15	1080.221	1080.862 [15]	–	–	–	–
323.15	1076.968	1077.491 [15], 1077.8 [25], 1077.01 [27], 1077.4 [32], 1077.1 [33], 1078.1 [34], 1077.32 [35]	–	–	–	–
328.15	1073.670	1073.54 [27]	–	–	–	–
333.15	1070.338	1071.4 [25], 1070.3 [32], 1070.0 [33], 1071.6 [34], 1070.74 [35]	–	–	58.407	57.69 [28]

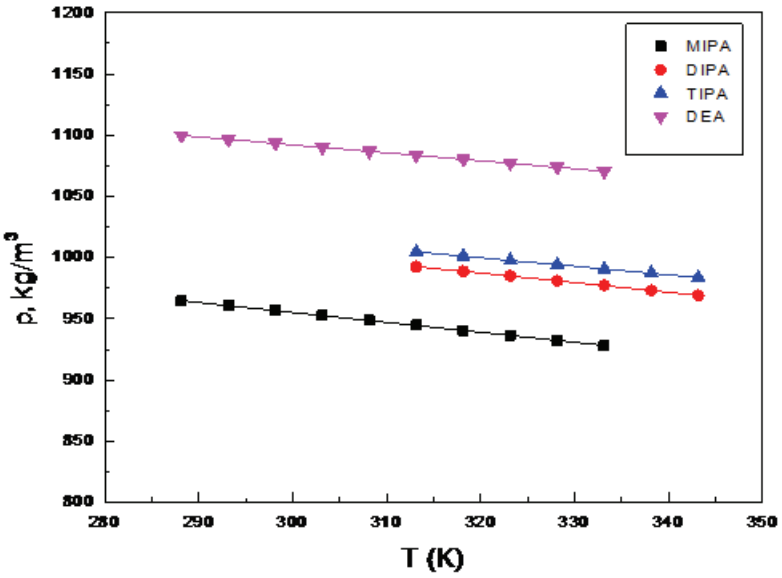

Figure 7. Densities of pure MIPA, DIPA, TIPA, and DEA at different temperatures and atmospheric pressure.

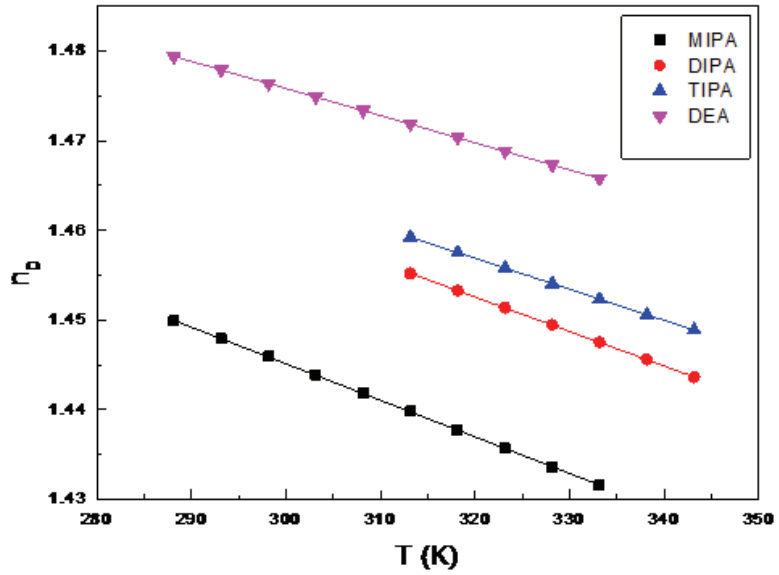

Figure 8. Refractive indices of pure MIPA, DIPA, TIPA, and DEA at different temperatures and atmospheric pressure.

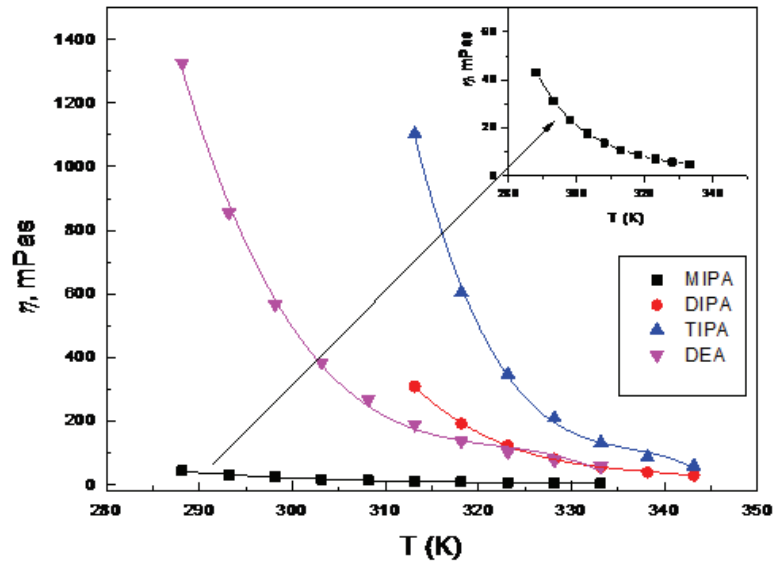

Figure 9. Viscosity of pure MIPA, DIPA, TIPA, and DEA at different temperatures and atmospheric pressure.

Density. Densities of four pure components were measured in temperature range from 288.15 to 333.15 K. Measured data shows linear temperature dependence of densities.

Refractive indices. The refractive indices almost linearly decrease with increase in temperature. The measured values of refractive index for all pure components are presented in Table 3.

Table 2. Densities (ρ / kg m^{-3}) of pure MIPA, DIPA, TIPA and DEA at atmospheric pressure

T / K	Compound			
	MIPA	DIPA	TIPA	DEA
288.1	964.573	–	–	1099.611
293.15	960.625	–	–	1096.424
298.15	956.644	–	–	1093.221
303.15	952.641	–	–	1089.989
308.15	948.608	–	–	1086.712
313.15	944.543	992.460	1004.59	1083.429

Table 2. Continued

T / K	Compound			
	MIPA	DIPA	TIPA	DEA
318.15	940.449	988.611	1001.11	1080.221
323.15	936.322	984.835	997.605	1076.968
328.15	932.160	980.973	994.057	1073.670
333.15	927.961	977.040	990.616	1070.338
338.15	–	973.048	987.139	–
343.15	–	969.008	983.626	–

Table 3. Refractive indices, n_D, of pure MIPA, DIPA, TIPA and DEA at atmospheric pressure

T / K	Compound			
	MIPA	DIPA	TIPA	DEA
288.15	1.44992	–	–	1.47939
293.15	1.44792	–	–	1.47788
298.15	1.44590	–	–	1.47640
303.15	1.44386	–	–	1.47489
308.15	1.44185	–	–	1.47340
313.15	1.43980	1.45517	1.45927	1.47188
318.15	1.43774	1.45330	1.45754	1.47035
323.15	1.43568	1.45139	1.45581	1.46883
328.15	1.43361	1.44946	1.45405	1.46730
333.15	1.43162	1.44753	1.45233	1.46578
338.15	–	1.44559	1.45061	–
343.15	–	1.44363	1.44890	–

Viscosity. Viscosities of pure components decrease with increase in temperature. Experimental data are presented in Table 4.

CONCLUSIONS

Experimental determination of density, viscosity and refractive index of four alkanolamine reagents was carried out. CO_2 capture technologies early developed for petrochemical industries application, are still in early phase of development regarding the treatment of flue gases in power plants. This paper presents main routes for the treatment of carbon capture with clear advantages, but also reveals the technical problems that need to be resolved. Due to economic limitations, it is clear that the focus in near future will be on increase of efficiency of already built power plants with

Table 4. Viscosities (η / mPa·s) of pure MIPA, DIPA, TIPA and DEA at atmospheric pressure

T / K	Compound			
	MIPA	DIPA	TIPA	DEA
288.15	43.032	–	–	1326.7
293.15	31.238	–	–	855.25
298.15	23.259	–	–	566.57
303.15	17.702	–	–	384.84
308.15	13.750	–	–	267.51
313.15	10.869	308.54	1103.4	189.86
318.15	8.7213	191.68	604.38	137.48
323.15	7.1156	123.21	348.18	101.45
328.15	5.8798	81.793	210.04	76.189
333.15	4.9475	55.954	132.30	58.407
338.15	–	39.370	86.697	–
343.15	–	28.572	59.186	–

further delay in construction of new power plant units (IGCC). Concerning this, the amine based washing of flue gases will remain dominant technology in treatment of flue gases. Pre combustion processes, although effective, are still too expensive. Bearing in mind that number of currently installed units based on IGCC technology are below 10, their contribution in reduction of total CO_2 emission is low. In order to have "less expensive" CO_2 removal technologies, storage of CO_2 should be gradually replaced with further utilization of the removed CO_2. New developments in the field of selective membranes, physical absorption and new energy efficient advanced absorbents, will further lower costs of flue gases treatment. Increase in energy demand will undoubtedly contribute to the emission of CO_2, so implementation of all measures that are presented within this paper as standalone concept will not be sufficient.

Acknowledgment

The authors gratefully acknowledge the financial support received from the Research Fund of Ministry of Education, Science and Technological Development, Serbia, and the Faculty of Technology and Metallurgy, University of Belgrade (Project no. 172063).

REFERENCES

[1] IPCC, Carbon Dioxide Capture and Storage-Special Report of the Intergovernmental Panel on Climate Change, Cambridge University Press, Cambridge, 2005.

[2] J.Y. Park, S.J. Yoon, H. Lee, Effect of steric hindrance on carbon dioxide absorption into new amine solutions, Environ. Sci. Tecnol. **37** (2003) 1670–1675.

[3] A. Adisorn, V. Amornvadee, Characterization and comparison of the CO_2 absorption performance into single and blended alkanolamines in a packed column, Ind. Eng. Chem. Res. **43** (2004) 2228–2237.

[4] K. Ariga, S. Ishihara, H. Abe, M. Li, P. Hill, Materials nanoarchitectonics for environmental remediation and sensing, J. Mater. Chem. **22** (2012) 2369–2377.

[5] M. Wietschel, M. Arens, C. Duotsch, S. Herkel, W. Krewitt, P. Markewitz, D. Muost, M. Scheufen, Energietechnologie 2050: Schwerpunkte fur Forschung und Entwicklung. Fraunhofer Verlag, Stuttgart, 2010.

[6] A. Kather, M. Klostermann, In Efficient Carbon Capture for Coal Power Plants, D. Stolten and V. Scheerer, Eds., Wiley-VCH Verlag, Weinheim, 2011, pp. 271–292.

[7] E. Kourosh, E. Zanganeh, A. Shafeen, C. Salvador, CO_2 Capture and Development of pilot scale cryogenic separation and compression unit, Energy Procedia. **1** (2009) 247–252.

[8] B.A. Rao, S.E. Rubin, A technical, economic and environmental assessment of amine based CO_2 capture technology for power plant greenhouse gas control, Environ. Sci. Technol. **36** (2002) 4467–4475.

[9] J. Rorkel, M. Seiler, Industrial progress: New energy efficient absorbents for the CO_2 separation from natural gas, syngas and flue gas, Adv. Chem. Eng. Sci. **1** (2011) 280–288.

[10] P. Moser, S. Schmidt, G. Sieder, H. Garcia, I. Ciattaglia, H. Klein, Enabling post combustion capture optimization-the pilot plant project at Niederaussem, Energy Procedia. **1** (2009) 807–814.

[11] V.D. Spasojević, S.P. Šerbanović, B.D. Djordjević, M.Lj. Kijevčanin, Densities, viscosities and refractive indices of aqueous alkanolamine solutions as potential carbon dioxide removal reagents, J. Chem. Eng. Data **58** (2013) 84–92.

[12] S.P. Šerbanović, M.Lj. Kijevčanin, I.R. Radović, B.D. Djordjević, Effect of temperature on the excess molar volumes of some alcohol + aromatic mixtures and modeling by cubic EOS mixing rules, Fluid Phase Equilib. **239** (2006) 69−82.

[13] M.Lj. Kijevčanin, M.M. Djuris, I.R. Radović, B.D. Djordjević, S.P. Šerbanović, Volumetric properties of the binary methanol + chloroform and ternary methanol + chloroform + benzene mixtures at 288.15, 293.15, 298.15, 303.15, 308.15 and 313.15 K, J. Chem. Eng. Data **52** (2007) 1136−1140.

[14] [14] M. Lj. Kijevčanin, I. R. Radović, E. M. Živković, B. D. Djordjević, S. P. Šerbanović, Influence of chain length and degree of branching of alcohol+chlorobenzene mixtures on determination and modelling of V^E by CEOS and CEOS/G^E mixing rules, Fluid Phase Equilib. 263 (2008) 205−213.

[15] E. Alvarez, F. Cerdeira, D. Gomez-Diaz, M. Navaza, Density, speed of sound, isentropic compressibility, and excess volume of binary mixtures of 1-amino-2-propanol or 3-amino-1-propanol with 2-amino-2-methyl-1-propanol, diethanolamine, or triethanolamine from 293.15 to 323.15 K. J. Chem. Eng. Data **55** (2010) 2567–2575.

[16] S. Mokraoui, A. Valtz, C. Coquelet, D. Richon, Volumetric properties of the isopropanolamine-water at atmospheric pressure from 283.15 to 353.15 K, Thermochim. Acta **440** (2006) 122–128.

[17] H. Herba, G. Czechowski, B. Zywucki, M. Stockhausen, J. Jadzyn, Molar Excess Volumes of Binary Mixtures of Amino Alcohols with 1,4-Dioxane, J. Chem. Eng. Data. **40** (1995) 214–215.

[18] D. Gomez-Diaz, M. Dolores La Rubia, A. Lopez, J. Navaza, R. Pacheco, S. Sanchez, Density, Speed of sound, refractive index, and viscosity of 1-amino-2-propanol {or bis(2-hydroxypropyl)amine} + triethanolamine + water from t = 288.15 to 333.15 K, J. Chem. Eng. Data **57** (2012) 1104−1111.

[19] Y. Maham, N. C. Liew, E. A. Mather, Viscosities and excess properties of aqueous solutions of ethanolamines from 25 to 80 °C, J. Solution Chem. **31** (2002) 743−756.

[20] V. Rayer, S. Kadiwala, K. Narayanaswamy, A. Henni, Volumetric properties, viscosities and refractive indices for aqueous 1-amino-2-propanol (monoisopropanolamine (mipa)) solutions from 298.15 to 343.15 K, J. Chem. Eng. Data **55** (2010) 5562−5568.

[21] The Alkanolamines Handbook, Dow Chemical Company, Midland, MI, 1981.

[22] R.R. Dreisbach, Physical properties of chemical compounds III, American Chemical Society, Washington D.C., 1961.

[23] A. Henni, J. Hromek, P. Tontiwachwuthikul, A.Chakma, Volumetric properties and viscosities for aqueous diisopropanolamine solutions from 25 °C to 70 °C, J. Chem. Eng. Data **48** (2003) 1062–1067.

[24] J.J. Ko, T.C. Tsai, C.Y. Lin, H.M. Wang, M.H. Li, Diffusivity of nitrous oxidein aqueous alkanolamine solutions, J. Chem.Eng. Data **46** (2001) 160–165.

[25] W.Y. Wang, S. Xu, D.F. Otto, E.A. Mather, Solubility of N_2O in alkanolamines and in mixed solvents, Chem. Eng. J. **48** (1992) 31–40.

[26] B. Hawrylak, E.S. Burke, R. Palepu, Partial molar and excess volumes and adiabatic compressibilities of binary mixtures of ethanolamines with water, J. Solution Chem. **29** (2000) 575–594.

[27] F. Murrieta-Guevara, A.T. Rodriguez, Liquid density as a function of temperature of five organic solvents, J. Chem. Eng. Data **29** (1984) 204–209.

[28] T.T. Teng, Y. Maham, L.G. Hepler, A.E. Mather, Viscosity of aqueous solutions of n-methyldiethanolamine and of diethanolamine, J. Chem. Eng. Data **39** (1994) 290–293.

[29] J. Aguila-Hernandez, A. Trejo, E.B. García-Flores, R. Molna, Viscometric and volumetric behaviour of binary mixtures of sulfolane and *N*-methylpyrrolidone with monoethanolamine and diethanolamine in the range 303–373 K, Fluid Phase Equilib. **267** (2008) 172–180.

[30] J.A. Riddick, W.B. Bunger, Organic Solvents: Physical Properties and Methods of Purification, 3rd ed., Wiley Interscience, New York, 1970.

[31] Ethanolamines, Product Data, Olin Chemicals, Stamford, CT, 1980.

[32] J. Aguila-Hernandez, R. Gomez-Quintana, F. Murrieta--Guevara, A. Romero-Martınez, A. Trejo, Liquid density of aqueous blended alkanolamines and *N*-methylpyrrolidone as a function of concentration and temperature, J. Chem. Eng. Data **46** (2001) 861–867.

[33] F. Murrieta-Guevara, A. Trejo, Liquid density as a function of temperature of five organic solvents, J. Chem. Eng. Data **29** (1984) 204–206.

[34] M.R. DiGuilio, J.R. Lee, T.S. Schaeffer, L.L. Brasher, S.A. Teja, Densities and viscosities of the ethanolamines, J. Chem.Eng. Data **37** (1992) 239–242.

[35] Y. Maham, T.T. Teng, G.L. Hepler, E.A. Mather, Densities, excess molar volumes, and partial molar volumes for binary mixtures of water with monoethanolamine, diethanolamine, and triethanolamine from 25 to 80 °C, J. Solution Chem. **23** (1994) 195–205.

IZVOD

PREGLED TEHNOLOŠKIH POSTUPAKA I EKSPERIMENTALNO ODREĐIVANJE TERMODINAMIČKIH I TRANSPORTNIH SVOJSTAVA REAGENSA ZA UKLANJANJE UGLJEN-DIOKSIDA

Vuk D. Spasojević[1], Slobodan P. Šerbanović[2], Predrag Stefanović[1] , Mirjana Lj. Kijevčanin[2]

[1]*Institut za nuklearne nauke „Vinča“, Univerzitet u Beogradu, Mike Petrovića Alasa 12–14, Beograd, Srbija*
[2]*Tehnološko–metalurški fakultet, Univerzitet u Beogradu,Karnegijeva 4, Beograd, Srbija*

(Naučni rad)

Intezivna naučna istraživanja u proteklih dvadeset godina pružaju jasne dokaze da su klimatske promene, kao i porast koncentracije gasova koji izazivaju efekat staklene bašte u atmosferi, prouzrokovane čovekovim delovanjem. Energetski sektor igra ključnu ulogu u ukupnoj emisiji ugljen-dioksida sa udelom između 60 i 70%, obaveza po pitanju smanjenja emisije gasova staklene bašte. Pored toga, povećanje potrošnje energije iz godine u godinu, kao i očekivano povećanje industrijske proizvodnje, dovešće do povećanja potrošnje fosilnih goriva, a samim tim i do povećanja emisije gasova staklene bašte. Navedene činjenice impliciraju da će energetski sektor biti ključan sektor u kome je potrebno ostvariti implementaciju svih mera i aktivnosti koje kao glavni cilj imaju smanjenje emisije gasova staklene bašte. Ovaj rad daje pregled tehnoloških postupaka za uklanjanje ugljen-dioksida od kojih su neki već našli komercijalnu upotrebu, dok su drugi još uvek u fazi razvoja. Posebna pažnja je posvećena opisu metoda zasnovanih na hemisoprpciji rastvora alkanolamina, koji su našli široku komercijalnu upotrebu. Izbor odgovarajućeg rastvarača, procesne opreme, radnih parametara, procesa sagorevanja itd. su samo neki od ključnih tačaka koje su prikazane u okviru ovog rada sa ciljem pružanja jasnije slike o mogućnostima i ograničenjima metoda za uklanjanje ugljen-dioksida. U okviru eksperimentalnog dela rada dati su rezultati merenja transportnih svojstava, nedovoljno ispitanih jedinjenja monoizopropanolamina (MIPA), diizopropanolamina (DIPA), triizopropanolamina (TIPA) i dietanolamina (DEA) kao potencijalnih reagensa za uklanjanje ugljen-dioksida. Od posebnog interesa su svojsta gustine, indeksa refrakcije i viskoznosti kao i promena ovih svojstava čistih jedinjenja sa temperaturom. Navedeni parametri su ključni za projektovanje procesne opreme kao i za optimizaciju samog procesa uklanjanja ugljen-dioksida.

Ključne reči: Gustina • Viskoznost • Indeks refrakcije • Uklanjanje ugljen-dioksida • Hemisorpcija • Dimni gasovi • Alkoholamini

DOKTORSKE DISERTACIJE I MAGISTARSKE TEZE HEMIJSKO–TEHNOLOŠKE STRUKE ODBRANJENE NA UNIVERZITETIMA U SRBIJI U 2013. GODINI

TEHNOLOŠKO–METALURŠKI FAKULTET, UNIVERZITET U BEOGRADU

Ime i prezime	Tema	Mentor
	Doktorske disertacije	
1. ČOLOVIĆ BOŽANA	BIOMIMIČNO DIZAJNIRANJE NOSAČA NA BAZI HIDROKSIAPATITA U CILJU INKAPSULACIJE ANTIBIOTIKA SA KONTROLISANIM OTPUŠTANJEM	Dr Branko Bugarski
2. CVIJOVIĆ ALAGIĆ IVANA	OTPORNOST PREMA OŠTEĆENJU I LOMU LEGURA TITANA ZA PRIMENU U MEDICINI	Dr Marko Rakin
3. VUKČEVIĆ MARIJA	UTICAJ MORFOLOGIJE I POVRŠINSKIH GRUPA NANOPOROZNIH UGLJENIČNIH MATERIJALA NA ADSORPCIJU PESTICIDA IZ VODE	Dr Mila Laušević
4. MARJANOVIĆ VESNA	PROUČAVANJE SORPCIJE HROMA (IV) IZ VODENIH RASTVORA NA FUNKCIONALIZOVANIM SEPIOLITIMA	Dr Rada Petrović
5. GAJIĆ-KVAŠČEV MAJA	NEDESTRUKTIVNA KARAKTERIZACIJA ARHEOLOŠKIH KERAMIČKIH ARTERFAKATA I UTVRĐIVANJE NJIHOVOG POREKLA STATISTIČKIM METODAMA PREPOZNAVANJA OBLIKA	Dr Radmila Jančić Heineman
6. DOSTANIĆ JASMINA	PROUČAVANJE FOTODEGRADACIJE ARILOZO PIRIDONSKIH BOJA	Dr Dušan Mijin
7. BANJAC NEBOJŠA	SINTEZA, STRUKTURA I SOLVATOHROMIZAM POTENCIJALNO FARMAKOLOŠKI AKTIVNIH DERIVATA SUKCIONIMIDA	Dr Gordana Ušćumlić
8. TRIVUNAC KATARINA	SEPARACIJA JONA METALA KOMBINOVANOM KOMPLEKSIRAJUĆE MIKROFILTRACIONOM METODOM	Dr Slavica Stevanović
9. SMILJANIĆ SLAVKO	PROUČAVANJE TRETMANA, FIZIČKO-HEMIJSKIH SVOJSTAVA CRVENOG MULJA I PARAMETARA SORPCIJE NA EFIKASNOST UKLANJANJA JONA NIKLA IZ VODENIH RASTVORA	Dr Dušan Antonović
10. ABDUNNASER HAMZA FADEL	RAZLAGANJE AUSTENITA U SREDNJEUGLJENIČNIM MIKROLEGIRANIM ČELICIMA: MEHANIZAM, STRUKTURA I SVOJSTVA	Dr Nenad Radović
11. KNEŽEVIĆ STEVANOVIĆ ANĐELA	EKSPERIMENTALNO ODREĐIVANJE I MODELOVANJE VOLUMETRIJSKIH SVOJSTAVA, INDEKSA REFRAKCIJE I VISKOZNOSTI VIŠEKOMPONENTNIH SISTEMA ORGANIH RASTVARAČA	Dr Mirjana Kijevčanin
12. SALAH SALEM MUSBAH	OPTIČKA I MEHANIČKA SVOJSTVA HIBRIDNIH NANOKOMPOZITNIH SVETLOVODNIH VLAKANA	Dr Radoslav Aleksić
13. ADEL S. ALIMMARI	SINTEZA, STRUKTURA I SOLVATOHROMIZAM NOVIH 5-(4-SUPSTITUI-SANIH FENILAZA)-4-(4-SUPSTITUISANIH FENIL)-6-HIDROKSI-3--CIJANO-2-PIRIDONA	Dr Gordana Ušćumlić
14. POŠARAC MARKOVIĆ MILICA	SINTEZA I KARAKTERIZACIJA KOMPOZITNOG KERAMIČKOG MATERIJALA NA BAZI SILICIJUM KARBIDA I KORDIJERITA	Dr Tatjana Holkov Husović
15. GLIŠIĆ DRAGOMIR	STRUKTURA I LOM U SREDNJEUGLJENIČNIM MIKROLEGIRANIM ČELICIMA	Dr Nenad Radović
16. ŽIVOJINOVIĆ DRAGANA	RAZVOJ I PRIMENA HEMOMETRIJSKIH METODA ZA KLASIFIKACIJU I PROCENU KVALITETA VODE	Dr Ljubinka Rajaković
17. BUČKO MIHAEL	ELEKTROHEMIJSKO TALOŽENJE I KARAKTERIZACIJA ZAŠTITNIH PREVLAKA Zn-Mn LEGURA	Dr Jelena Bajat
18. STOILJKOVIĆ ZORA	ODREĐIVANJE AMLODIPINA I NIFEDIPINA ELEKTROHEMIJSKIH I DRUGIM ANALITIČKIM METODAMA	Dr Slobodan Petrović
19. ERAKOVIĆ SANJA	ELEKTROFORETSKO TALOŽENJE I KARAKTERIZACIJA HIDROKSIAPATIT/LIGNIN I SREBRO/HIDROKSIAPATIT/LEGNIN PREVLAKA NA TITANU	Dr Vesna Mišković-Stanković
20. ARSENOVIĆ MILICA	OPTIMIZACIJA I PREDVIĐANJE KVALITETA MATERIJALA, PROCESA I KRAJNJIH OSOBINA OPEKARSKIH PROIZVODA MATEMATIČKIM MODELOVANJEM KARAKTERISTIČNIH PARAMETARA	Dr Slavka Stanković

Ime i prezime	Tema	Mentor
	Doktorske disertacije	
21. DIMITRIJEVIĆ MARIJA	MORFOLOŠKA ANALIZA OŠTEĆENJA VATROSTALNIH MATERIJALA IZLOŽENIH TERMOŠOKU	Dr Radmila Jančić Heinemann
22. ĐOKIĆ VELJKO	SINTEZA, KARAKTERIZACIJA I PRIMENA NEDOPIRANIH I DOPIRANIH NANOSTRUKTURNIH FOTOKATALIZATORA NA BAZI TITAN(IV)-OKSIDA	Dr Đorđe Janaćković
23. NOZHAT MOFTAH EL BUAISHI	PROUČAVANJE SINTERABILNOSTI KORDIJERITNIH PRAHOVA SINTETIZOVANIH SOL-GEL POSTUPCIMA	Dr Rada Petrović
24. ĐORĐEVIĆ TIJANA	UTICAJ FERMENTACIJE NA DEGRADACIJU OSTATAKA PESTICIDA U FERMENTISANIM PROIZVODIMA OD ŽITA	Dr Slavica Šiler-Marinković
25. LUKIĆ JELENA	PROCESI DEGRADACIJE PAPIRNO-ULJNE IZOLACIJE ENERGETSKIH TRANSFORMATORA I RAFINACIJA DEGRADIRANIH MINERALNIH IZOLACIONIH ULJA EKSTRAKCIJOM TEČNO-TEČNO SA N-METIL-2 PIROLIDONOM	Dr Dušan Antonović
26. RANČIĆ MILICA	STRUKTURA, SOLVATOHROMIZAM I ELEKTROFILNOST DERIVATA 5-ARILIDEN-2,4-TIAZOLIDINDIONA	Dr Aleksandar Marinković
27. SLOVIĆ ZORAN	TERMODINAMIČKI PRISTUP DESULFURACIJI PRI VANPEĆNOJ OBRADI KISEONIČNO-KONVERTORSKOG ČELIKA	Dr Karlo Raić
28. NAJDENOV IVAN	UPRAVLJANJE PROCESIMA TOPLJENJA I RAFINACIJE BAKRA U FUNKCIJI UNAPREĐENJA ENERGETSKE EFIKASNOSTI I EKONOMSKE OPRAVDANOSTI	Dr Karlo Raić
29. JOVIĆ MIHAJLO	ISPITIVANJE MOGUĆNOSTI PRIMENE NEKIH MORSKIH ORGANIZAMA KAO BIOINDIKATORA ZAGAĐENJA TEŠKIM METALIMA VODE ZALIVA BOKA KOTORSKA	Dr Slavka Stanković
30. ĐUKIĆ VUKOVIĆ ALEKSANDRA	PROIZVODNJA MLEČNE KISELINE I PROBIOTSKE BIOMASE NA DESTILERIJSKOJ DŽIBRI	Dr Ljiljana Mojović
31. SEMENČENKO VALENTINA	ISPITIVANJE RAZLIČITIH HIBRIDA KUKURUZA KAO SIROVINE ZA PROIZVODNJU BIOETANOLA, SKROBA I HRANE ZA ŽIVOTINJE	Dr Ljiljana Mojović
32. VELIČKOVIĆ ZLATE	MODIFIKACIJA I PRIMENA VIŠESLOJNIH UGLJENIČNIH NANOCEVI ZA IZDVAJANJE ARSENA IZ VODE	Dr Mirjana Ristić
33. BOŽIĆ BOJAN	SINTEZA, STRUKTURA I SVOJSTVA POTENCIJALNO BIOLOŠKI AKTIVNIH DERIVATA PROPANSKE KISELINE	Dr Gordana Ušćumlić
34. RADIŠIĆ MARINA	RAZVOJ I PRIMENA METODE TEČNE HROMATOGRAFIJE-TANDEM MASENE SPEKTROMETRIJE ZA ODREĐIVANJE PESTICIDA U VOĆU I VOĆNIM SOKOVIMA	Dr Mila Laušević
35. LOJPUR VESNA	SINTEZA I SVOJSTVA IZVORA SVETLOSTI NA BAZI ITRIJUM-OKSIDA DOPIRANIH JONIMA RETKIH ZEMALJA	Dr Radoslav Aleksić
36. ALI RAMADAN ELKAIS	UTICAJ PREVLAKA POLIANILINA NA KOROZIJU MEKOG ČELIKA U RAZLIČITIM SREDINAMA	Dr Branimir Grgur
37. DERVIŠEVIĆ IRMA	IZDVAJANJE METALA IZ ELEKTRONSKOG OTPADA I ZAMENA ZLATA, OLOVA I ARSENA U ELEKTRONSKOJ OPREMI TROKOMPONENTNIM LEGURAMA	Dr Mirjana Ristić
	Magistarske teze	
1. STANISAVLJEV ANA	PROCENA I OPTIMIZACIJA ODZIVNIH KARAKTERISTIKA POTENCIOMET-RIJSKIH SENZORA ZA ANALIZU POVRŠINSKI AKTIVNIH MATERIJA	Dr Aleksandra Perić-Grujić
2. ĐUKANOVIĆ ZORAN	MODELOVANJE I SIMULACIJA PROCESA HIDROOBRADE SMEŠE GASNOG ULJA I LAKOG CIKLIČNOG ULJA	Dr Aleksandar Orlović

TEHNOLOŠKI FAKULTET, UNIVERZITET U NOVOM SADU

	Doktorske disertacije	
1. POPOVIĆ SEKA	ISTRAŽIVANJE DOBIJANJA I KARAKTERIZACIJA BIORAZGRADIVIH KOMPOZITNIH FILMOVA NA BAZI BILJNIH PROTEINA	prof. dr Draginja Peričin
2. NAĐALIN VESNA	ISPITIVANJE EKSTRAKCIJE I EKSTRAKATA GAJENE LAVANDE (*Lavandula officinalis* L.)	prof. dr Žika Lepojević
3. IKONIĆ PREDRAG	RAZVOJ PROCESA SUŠENJA I ZRENJA TRADICIONALNE FERMENTISANE KOBASICE (PETROVSKA KLOBASA) U KONTROLISANIM USLOVIMA.	prof. dr Ljiljana Petrović
4. MARKOVIĆ MILICA	PRIMENA TRITIKALEA U FERMENTACIONIM PROCESIMA KAO DOPRINOS ODRŽIVOM RAZVOJU	prof. dr Siniša Markov

Ime i prezime	Tema	Mentor
	Doktorske disertacije	
5. FILIPOVIĆ VLADIMIR	UTICAJ PROCESA OSMOTSKE DEHIDRATACIJE NA PRENOS MASE I KVALITET MESA SVINJA	prof. dr Ljubinko Lević
6. VITAS JASMINA	ANTIOKSIDATIVNA AKTIVNOST FERMENTISANIH MLEČNIH PROIZVODA DOBIJENIH POMOĆU KOMBUHE	prof. dr Radomir Malbaša
7. JOKANOVIĆ MARIJA	KARAKTERIZACIJA KVALITETA MESA I IZNUTRICA SVINJA ČISTIH RASA ODGAJANIH U VOJVODINI	prof. dr Vladimir Tomović
8. ČOLOVIĆ RADMILO	UTICAJ DODATKA BILJNIH PROTEINSKIH KONCENTRATA U HRANU ZA ŽIVOTINJE NA KVALITET PELETA	prof. dr Ljubinko Lević
9. PEJIĆ BILJANA	KVALITET FERMENTISANOG MLEČNOG NAPITKA PAKOVANOG U RAZLIČITIM USLOVIMA	prof. dr Spasenija Milanović
10. HADNAĐEV-KOSTIĆ MILICA	STRUKTURNA I FOTOKATALITIČKA SVOJSTVA SISTEMA NA BAZI MODIFIKOVANIH SLOJEVITIH HIDROKSIDA I OKSIDA TITANA	prof. dr Tatjana Vulić
11. VASIĆ VESNA	PREČEŠĆAVANJE OTPADNE VODE IZ PROCESA PROIZVODNJE BIOETANOLA MIKROFILTRACIJOM	dr Marina Šćiban i doc. dr Aleksandar Jokić
12. JANKOVIĆ MILOVAN	MATEMATIČKI MODEL REAKCIONOG SISTEMA ZA IN SITU EPOKSIDOVANJE SOJINOG ULJA PERSIRĆETNOM KISELINOM	prof. dr Snežana Sinadinović-Fišer
13. ŠIMURINA OLIVERA	OPTIMIZACIJA KONCENTRACIJE ORGANSKIH KISELINA I ENZIMSKIH PREPARATA U BIOHEMIJSKOM MATRIKSU SUPSTANDARDNOG KVALITETA	prof. dr Stevan Popov i dr Bojana Filipčev
14. KOPRIVICA GORDANA	NUTRITIVNI PROFIL I SENZORSKI KVALITET VOĆA I POVRĆA OSMOTSKI DEHIDRIRANOG U MELASI ŠEĆERNE REPE I RASTVORIMA SAHAROZE	prof. dr Ljubinko Lević
15. DAPČEVIĆ-HADNAĐEV TAMARA	UTICAJ DODATKA EMULGUJUĆIH SKROBOVA NA TEHNOLOŠKE KARAKTERISTIKE TESTA I KVALITET HLEBA	prof. dr Ljubica Dokić
16. JANKOVIĆ V. VESNA	PROMENE PARAMETARA ZDRAVSTVENE ISPRAVNOSTI PETROVAČKE KOBASICE TOKOM PROIZVODNJE U TRADICIONALNIM KONTROLISANIM USLOVIMA	prof. dr Ljiljana Petrović
17. ŠOJIĆ BRANISLAV	ISPITIVANJE LIPOLITIČKIH I OKSIDATIVNIH PROMENA U TRADICIONALNOJ FERMENTISANOJ KOBASICI (PETROVAČKA KOBASICA) TOKOM STANDARDIZACIJE BEZBEDNOSTI I KVALITETA	prof. dr Ljiljana Petrović
18. LONČAREVIĆ IVANA	UTICAJ LECITINA RAZLIČITOG POREKLA NA KRISTALIZACIONA SVOJSTVA MASNE FAZE I KVALITET MAZIVNOG KREM PROIZVODA SA DODATKOM FUNKCIONALNIH BILJNIH ULJA	prof. dr Biljana Pajin
	Magistarske teze	
1. DIMITRIJEVIĆ DEJAN	ANTIOKSIDATIVNA AKTIVNOST MEDA I MEDA SA DODATKOM SUVIH ŠLJIVA	prof. dr Sonja Đilas
2. MOLNAR ELVIRA	UTICAJ TEMPERATURE PEČENJA NA FIZIČKO-MEHANIČKE KARAKTERISTIKE GLINENOG CREPA	prof. dr Jonjaua Ranogajec

TEHNOLOŠKI FAKULTET U LESKOVCU, UNIVERZITET U NIŠU

	Doktorske disertacije	
1. МИЛИЦА СОВРЛИЋ	ОПТИМИЗАЦИЈА УСЛОВА СИНТЕЗЕ АЛКИЛТИОНКАРБАМАТА ОКСИДАТИВНОМ ХЕТЕРОЛИЗОМ ПЕРСУЛФИДНЕ ВЕЗЕ АЛКИЛДИКСАНТОГЕНАТА	Сандра Константиновић
2. СНЕЖАНА ИЛИЋ СТОЈАНОВИЋ	СИНТЕЗА И КАРАКТЕРИЗАЦИЈА ХИДРОГЕЛОВА НА БАЗИ КОПОЛИМЕРА *N*-ИЗОЛПРОПИЛАКРИЛАМИДА И 2-ХИДРОКСИПРОПИЛМЕТАКРИЛАТА ЗА ПОТЕНЦИЈАЛНУ ПРИМЕНУ У ФОРМУЛАЦИЈАМА СА ЛЕКОВИТИМ СУПСТАНЦАМА	Љубиша Николић
	Magistarske teze	
1. ЗОРАН ТОДОРОВИЋ	СИНТЕЗА И КАРАКТЕРИЗАЦИЈА ПОРОЗНИХ ПОЛИМЕРА НА БАЗИ МЕТИЛМАТАКРИЛАТА И АКРИЛАМИДА И МОГУЋНОСТИ ЊИХОВЕ УПОТРЕБЕ ЗА ИМОБИЛИЗАЦИЈУ	Љубиша Николић
2. БОЈАН ЂОРЂЕВИЋ	КИНЕТИКА ХИДРОДЕСТИЛАЦИЈЕ, ХЕМИЈСКИ САСТАВ И АНТИОКСИДАТИВНА АКТИВНОСТ ЕТАРСКОГ УЉА РИЗОМА ЂУМБИРА (*ZINGIBER OFFICINALIS* L.)	Миодраг Лазић

TEHNIČKI FAKULTET U BORU, UNIVERZITET U BEOGRADU

Ime i prezime	Tema	Mentor
	Doktorske disertacije	
1. МИЛАН РАДОВАНОВИЋ	УТИЦАЈ ОРГАНСКИХ ИНХИБИТОРА НА КОРОЗИОНО ПОНАШАЊЕ МЕСИНГА У РАТСВОРУ НАТРИЈУМ-СУЛФАТА	др Милан Антонијевић, ред. професор
2. МР ЗОРАН СТЕВАНОВИЋ	ЛУЖЕЊЕ ТЕШКИХ МЕТАЛА ИЗ ФЛОТАЦИОНЕ ЈАЛОВИНЕ	др Милан Антонијевић, ред. професор
3. МИЛИЦА АРСИЋ	МОДЕЛОВАЊЕ ПРОЦЕСА СТВАРАЊА ПРИЗЕМНОГ ОЗОНА И ЊЕГОВЕ ДИСТРИБУЦИЈЕ У УРБАНИМ СРЕДИНАМА	др Живан Живковић, ред. професор
4. ПРЕДРАГ ЂОРЂЕВИЋ	МОДЕЛОВАЊЕ ДИСТРИБУЦИЈЕ БАКРА И ПРАТЕЋИХ ЕЛЕМЕНАТА У ПРОЦЕСУ ТОПЉЕЊА СУЛФИДНИХ КОНЦЕНТРАТА БАКРА	др Живан Живковић, ред. професор
5. МР ЗОРАН АВРАМОВИЋ	ИСПИТИВАЊЕ ПРОЦЕСА КОРОЗИЈЕ МЕСИНГА У РАСТВОРУ НАТРИЈУМ СУЛФАТА	др Милан Антонијевић, ред. професор
6. ИВАНА БЕРИЋ	АНАЛИЗА ПРИМЕНЕ КВАНТИТАТИВНИХ И КВАЛИТАТИВНИХ МЕТОДА ЗА СЕЛЕКЦИЈУ И ОПТИМИЗАЦИЈУ ПОРТФОЛИО ПРОЈЕКТА	др Иван Михајловић, ван. професор
7. ЉУБИША БАЛАНОВИЋ	КОМПАРАТИВНА ТЕРМОДИНАМИЧКА АНАЛИЗА И КАРАКТЕРИЗАЦИЈА ЛЕГУРА У СИСТЕМУ GA-ZN-ME(ME=AL,SN)A	др Драгана Живковић, ред. професор
8. ДРАГАНА ВИДАКОВИЋ	ВИШЕКРИТЕРИЈУМСКА АНАЛИЗА КВАЛИТЕТА ВАЗДУХА У УРБАНИМ СРЕДИНАМА У ЗАВИСНОСТИ ОД ВРЕМЕНСКИХ ФАКТОРА	др Милован Вуковић, ван. професор
	Magistarske teze	
1. ЕМИЛИЈА ЦЕКИЋ ЈОВИЧИЋ	УТИЦАЈ ОРГАНИЗАЦИОНИХ РЕСУРСА НА ЗАДОВОЉСТВО КОРИСНИКА УСЛУГА СПЕЦИЈАЛНЕ БОЛНИЦЕ ЗА ПСИХИЈАТРИЈСКЕ БОЛЕСНИКЕ ДР ЛАЗА ЛАЗАРЕВИЋ	др Снежана Урошевић, ван. професор
2. БРАНКО СТЕФАНОВИЋ	ИМПЛЕМЕНТАЦИЈА МАРКЕТИНГ КОНЦЕПЦИЈЕ И СТРАТЕГИЈЕ У ПОСЛОВАЊУ УСЛУЖНИХ ПРЕДУЗЕЋА	др Дејан Ризнић, ван. професор